

September 28, 2004

**CALIFORNIA REGIONAL PM10/PM2.5
AIR QUALITY STUDY (CRPAQS)
INITIAL DATA ANALYSIS
OF CLEAN AIRSHIP I
MEASUREMENTS
(TASK 6.4)**

CARB Contract No. 2002-01PM

Prepared By:

TRACER ENVIRONMENTAL SCIENCES & TECHNOLOGIES, INC.
970 Los Vallecitos Boulevard, Suite 100
San Marcos, California 92069
Voice: (760) 744-9611 / Fax: (760) 744-8616
www.tracer-est.com

Project No. 1451

DISCLAIMER

The statements and conclusions in this report are those of Tracer ES&T and not necessarily those of the California Air Resources Board, the San Joaquin Valleywide Air Pollution Study Agency, or its Policy Committee, their employees or their members. The mention of commercial products, their source, or their use in connection with material reported herein is not to be construed as actual or implied endorsement of such products.



TABLE OF CONTENTS

<u>SECTION</u>		<u>PAGE</u>
LIST OF FIGURES		iii
LIST OF TABLES		iv
1.0 INTRODUCTION.....		1-1
2.0 FIELD MEASUREMENT PROGRAM		2-1
2.1 STACK EMISSION SOURCE.....		2-3
2.2 CLEAN AIRSHIP I		2-7
2.3 METEOROLOGICAL DATA.....		2-9
2.4 DATA FILES.....		2-10
3.0 DATA ANALYSIS		3-1
3.1 FLIGHT CHARACTERISTICS		3-1
3.2 CONCENTRATIONS		3-3
3.3 SIGMA-Y		3-6
3.4 SIGMA-Z		3-10
3.5 PLUME RISE		3-14
3.6 PLUME INFILTRATION		3-17
4.0 CONCLUSIONS		4-1
REFERENCES.....		R-1
APPENDICES		
A FLIGHT PATH POSITION GRAPHS		A-1
B FLIGHT PATH DISTANCE & ANGLE GRAPHS.....		B-1
C SF ₆ CONCENTRATION TIME GRAPHS		C-1
D SF ₆ CONCENTRATION DISTANCE GRAPHS		D-1
E SF ₆ CONCENTRATION ANGLE GRAPHS		E-1
F SF ₆ CONCENTRATION ALTITUDE GRAPHS		F-1
G ALTITUDE TIME GRAPHS		G-1
H ALTITUDE TEMPERATURE GRAPHS		H-1
I SIGMA-Y GRAPHS.....		I-1
J SIGMA-Z GRAPHS		J-1

LIST OF FIGURES

<u>FIGURE</u>	<u>PAGE</u>
2-1 Plume Measurement Schematic.....	2-1
2-2 Clean Airship I – Pre-Flight.....	2-2
2-3 Clean Airship I – In-Flight.....	2-2
2-4 Field Measurement Program Location – Regional	2-5
2-5 Field Measurement Program Location – Local	2-6
2-6 Clean Airship I Navigation, Sensing, and Telemetry System	2-8
2-7 Clean Airship I Real-Time SF ₆ Instrument.....	2-8
3-1 $\chi u/Q$ Comparison.....	3-4
3-2 $\chi u/Q$ Comparison By Downwind Distance	3-5
3-3 Sigma-Y (σ_y) Comparison	3-9
3-4 Sigma-Y (σ_y) Comparison by Downwind Distance	3-10
3-5 Sigma-Z (σ_z) Comparison.....	3-12
3-6 Sigma-Z (σ_z) Comparison By Downwind Distance	3-13
3-7 Plume Height Comparison	3-15
3-8 Plume Height Comparison By Downwind Distance	3-16
3-9 Flight 6 Plume Infiltration	3-18
3-10 Flight 10 Plume Infiltration	3-19
3-11 Flight 11 Plume Infiltration	3-20
3-12 Flight 21 Plume Infiltration	3-21
3-13 Flight 28 Plume Infiltration	3-22

LIST OF TABLES

<u>TABLE</u>	<u>PAGE</u>
1-1 Flight Range of Clean Airship I During Field Program	1-1
2-1 Stack Description.....	2-3
2-2 SF ₆ Release Rates	2-4
2-3 Clean Airship I Design Features.....	2-7
2-4 Flight Summary	2-9
2-5 Meteorological Station.....	2-10
3-1 Flight Characteristic Graphs	3-1
3-2 Delta Temperature Stability Class Determination Method.....	3-1
3-3 Flight Stability Class by Altitude.....	3-2
3-4 Sigma-Y (σ_y) Comparison	3-8
3-5 Sigma-Z (σ_z) Comparison.....	3-11
3-6 Plume Height Comparison.....	3-14
3-7 Plume Infiltration into Stable Layer	3-17

1.0 INTRODUCTION

Tracer Environmental Sciences & Technologies, Inc. (Tracer ES&T) has prepared this report to summarize the analyses conducted under CARB Contract No. 2002-01PM for the California Regional PM₁₀/PM_{2.5} Air Quality Study (CRPAQS) Initial Data Analysis of Field Program Measurements Task 6.4. The goals of this project were to evaluate plume dispersion and diffusion characteristics under low wind speed, low visibility conditions in the San Joaquin Valley using atmospheric data previously collected by Clean Airship I (a 30 foot helium filled remotely piloted mini-blimp). Clean Airship I measured latitude, longitude, altitude, temperature, and sulfur hexafluoride (SF₆) concentration during 28 flights conducted over the South Belridge Oil Field (west of Bakersfield, California) between December 2000 and February 2001. During each flight, SF₆ tracer gas was released from a 50 foot stack while a ground based meteorological station measured wind speed, wind direction, and temperature. Table 1-1 indicates the flight range of the blimp during this study. Section 2 of this report summarizes the previous field measurement program while Section 3 details the data analyses conducted for this study. Section 4 then presents conclusions while the appendices provide supporting information.

TABLE 1-1 Flight Range of Clean Airship I During Field Program

Data Value	2-Dimensional Distance Between Stack and Clean Airship I		Altitude of Clean Airship I	
	(ft)	(m)	(ft)	(m)
Minimum	0	0	0	0
Maximum	4,432	1,351	1,577	481

2.0 FIELD MEASUREMENT PROGRAM^[1, 2]

In 1998, the U.S. Department of Energy (DOE) funded a feasibility study to investigate various methods for sampling air quality plumes from fossil energy sources during low and near zero visibility conditions (i.e. fog). As part of the research program, Tracer ES&T developed the Remotely Piloted Airship for Atmospheric Tracer Sampling (RPATS). RPATS, also known as Clean Airship I, consisted of a real-time sulfur hexafluoride (SF_6) tracer gas analyzer, on-board instrumentation for measuring GPS location and ambient temperature, and a telemetry system for communicating with the ground station. From December 2000 to February 2001, 28 flights were conducted where SF_6 was released from a stack and then nearby ambient air concentrations of SF_6 were measured using Clean Airship I (see Figures 2-1 through 2-3). During each flight, a ground based meteorological station measured wind speed, wind direction, and temperature. The following summarizes the stack, blimp, and meteorological station used during the field measurement program.

FIGURE 2-1 Plume Measurement Schematic

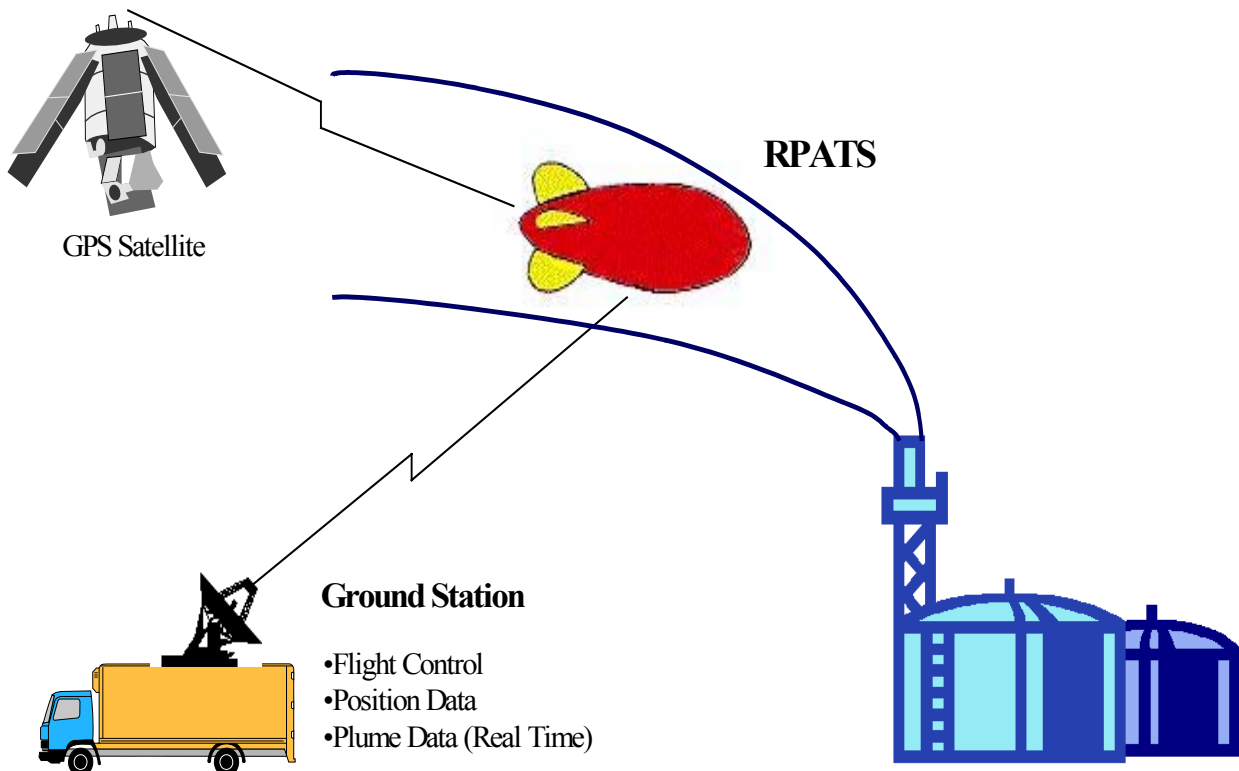


FIGURE 2-2 Clean Airship I – Pre-Flight



FIGURE 2-3 Clean Airship I – In-Flight



2.1 STACK EMISSION SOURCE

A stack at the AERA Energy Belridge Oil Field facility (located in the South Belridge Oil Field west of Bakersfield) was used to release the SF₆ tracer gas during each Clean Airship I flight. Table 2-1 provides a description of the stack while Table 2-2 lists the SF₆ release rate during each flight. See Figures 2-4 and 2-5 for the location of the test area and stack.

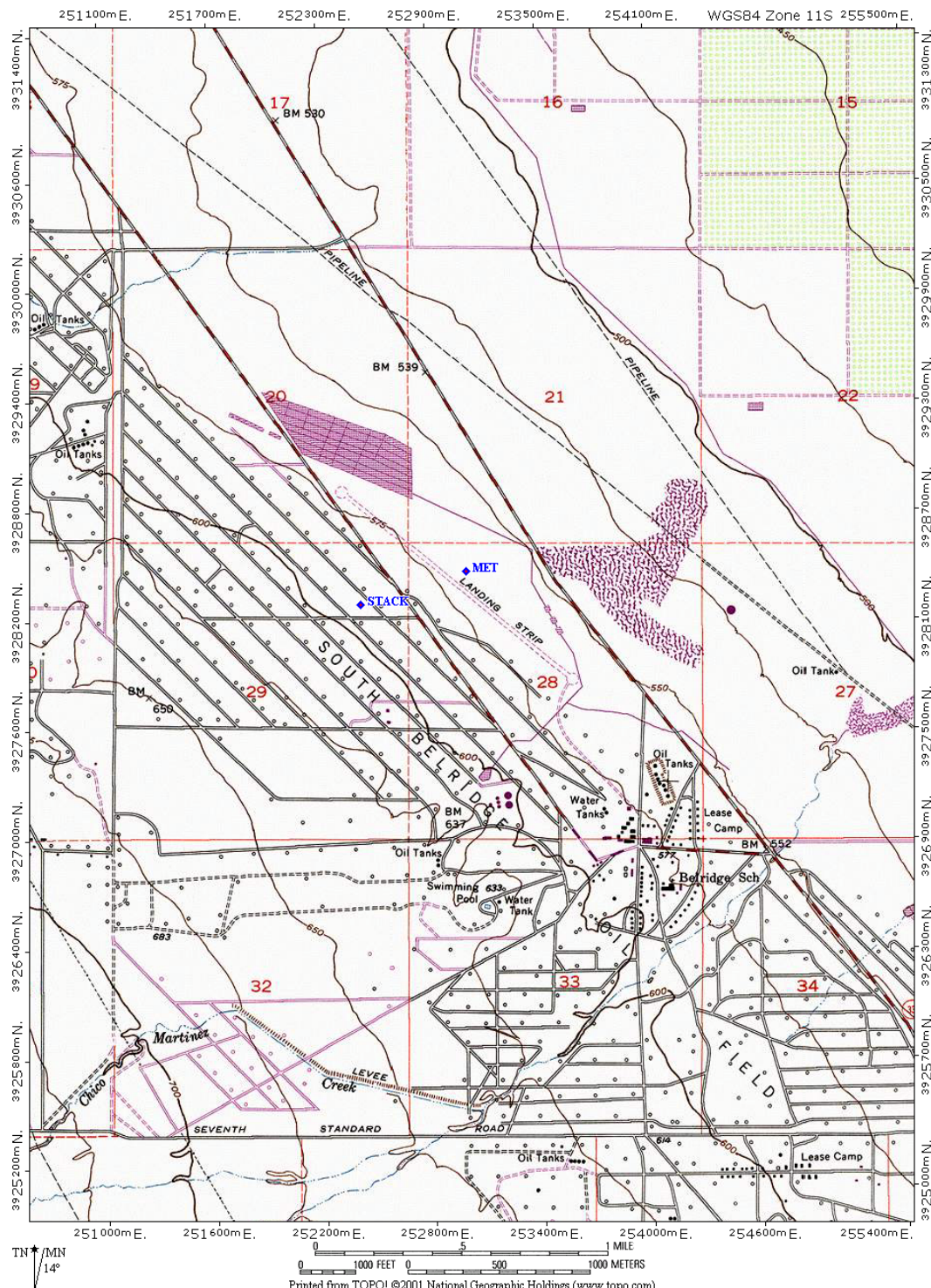
TABLE 2-1 Stack Description

Item	Description
Location - Latitude, Longitude (deg.deg)	35.46700 N, 119.72794 W
Location - UTM Easting, Northing (m)	252463, 3928254
Location – County	Kern
Location – Range	21E
Location – Section	NE29
Location – Township	28S
Height (m)	15.24
Diameter (m)	2.35
Temperature (K)	333.2
Gas Velocity (m/s)	2.64

TABLE 2-2 SF₆ Release Rates

Flight No.	SF ₆ Release Rate (lb/hr)
1	5.4
2	5.4
3	5.4
4	5.4
5	5.4
6	1.0
7	3.2
8	3.2
9	2.0
10	2.0
11	2.0
12	2.0
13	2.0
14	2.0
15	2.0
16	3.1
17	3.7
18	3.7
19	3.7
20	3.7
21	4.3
22	4.3
23	4.3
24	3.2
25	3.2
26	3.2
27	3.2
28	3.2

FIGURE 2-4 Field Measurement Program Location - Regional

FIGURE 2-5 Field Measurement Program Location - Local

2.2 CLEAN AIRSHIP I

Clean Airship I collected atmospheric data during 28 flight tests. See Table 2-3, Figure 2-6, and Figure 2-7 for the design features of the blimp. See Table 2-4 for a summary of the flights conducted.

TABLE 2-3 Clean Airship I Design Features

Item	Description
Purpose	<ul style="list-style-type: none"> • Sample plumes at lower altitudes • Sample plumes in low/zero visibility (e.g. fog)
Flight limitations	<ul style="list-style-type: none"> • Less than two miles from base station • Winds less than 12 mph • Altitudes less than 2,000 feet • Payload 7 pounds or less • 10-15 mph cruising speed • 20 mph top speed
Dimensions	<ul style="list-style-type: none"> • 30 foot length • 7.5 foot diameter at mid-section
Navigation System	<ul style="list-style-type: none"> • Trimble Navigation Lassen LP GPS receiver • USGS topographic map of region • accuracy less than 10 meters
Altitude	<ul style="list-style-type: none"> • Solid state pressure transducer • Range –200 to 5,000 feet (\pm 7 feet)
Heading, Attitude, and Temperature	<ul style="list-style-type: none"> • Precision Navigation TCM2 module • Precision Thermister
Detection System	<ul style="list-style-type: none"> • Real-time SF₆ monitor (Tracer ES&T) • Range 75 – 5,000+ ppt
Data Acquisition	<ul style="list-style-type: none"> • Multi-function data acquisition system (DAS) board
Data Telemetry	<ul style="list-style-type: none"> • Free Wave Technologies high speed spread spectrum radio frequency modems • 115,000 baud (upgraded from 9,600 baud for flights)
Power	<ul style="list-style-type: none"> • 7 nickel metal hydride (NiMH) batteries • 8.4 volts • 3.7 amp-hour capacity
Data collected	<ul style="list-style-type: none"> • GPS latitude and longitude • Altitude • Temperature • SF₆ concentration

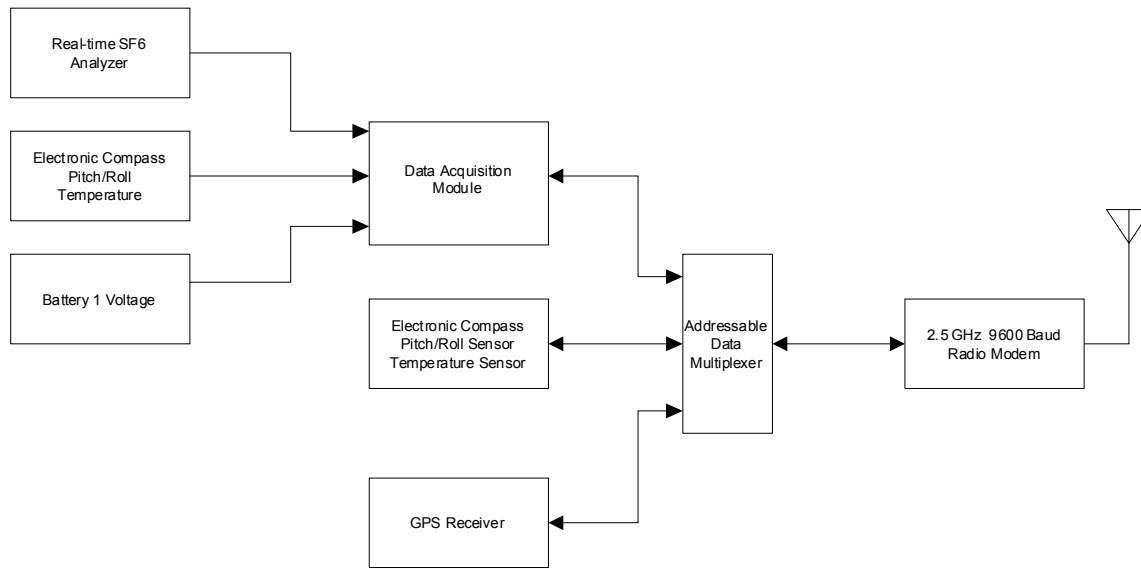
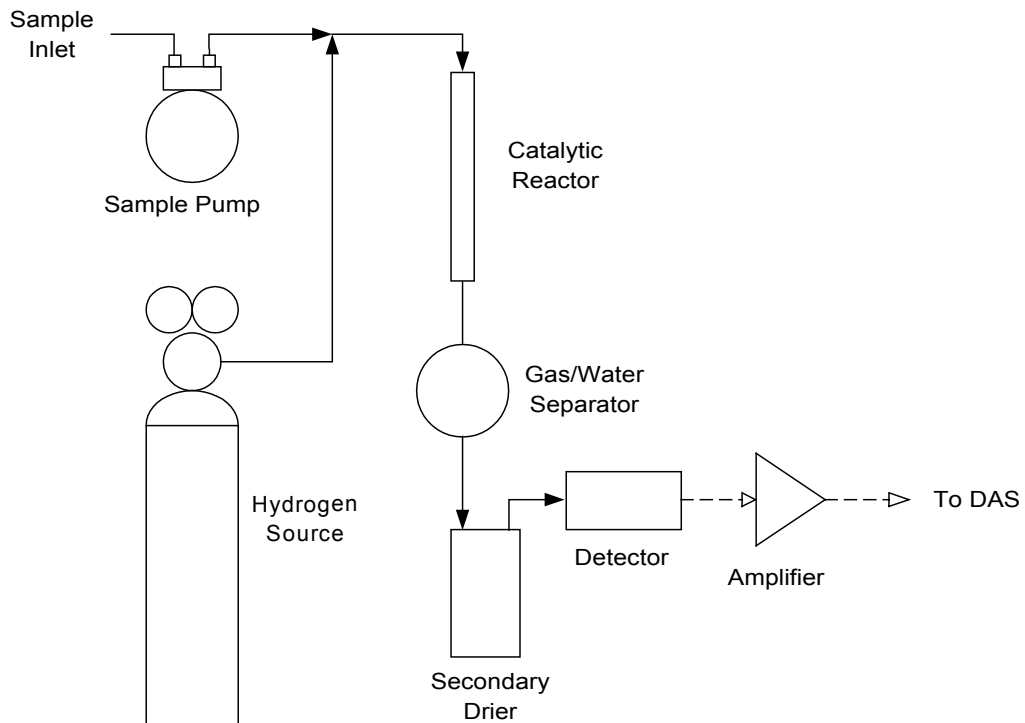
FIGURE 2-6 Clean Airship I Navigation, Sensing, and Telemetry System**FIGURE 2-7 Clean Airship I Real-Time SF₆ Instrument**

TABLE 2-4 Flight Summary

Flight No.	Date	Start Time	End Time	Comments
1	12/16/00	10:18:48 AM	10:24:33 AM	Flight terminated due to high winds. GPS system failed (no latitude longitude data).
2	12/16/00	3:13:08 PM	3:27:15 PM	
3	12/16/00	3:56:14 PM	4:16:43 PM	
4	12/17/00	8:51:05 AM	9:07:18 AM	
5	12/17/00	9:26:38 AM	9:32:57 AM	SF ₆ detection system saturated
6	12/17/00	10:15:10 AM	10:35:14 AM	
7	12/17/00	11:24:07 AM	11:49:50 AM	
8	12/18/00	7:11:16 AM	7:22:52 AM	SF ₆ detection system saturated
9	01/04/01	8:45:02 AM	8:55:12 AM	Flight terminated due to loose GPS antenna
10	01/04/01	9:12:34 AM	9:36:07 AM	
11	01/04/01	10:18:08 AM	10:42:56 AM	
12	01/04/01	11:12:01 AM	11:29:57 AM	
13	01/04/01	11:44:49 AM	12:05:49 PM	
14	01/04/01	12:34:31 PM	12:53:12 PM	Sounding at end of flight
15	01/05/01	9:14:40 AM	9:33:18 AM	
16	01/05/01	12:34:03 PM	12:58:00 PM	Sounding at beginning of flight
17	01/05/01	2:47:40 PM	3:05:22 PM	Sounding 1,000 feet over source
18	01/05/01	4:15:30 PM	4:34:19 PM	
19	01/06/01	8:53:49 AM	9:16:58 AM	Sounding at beginning of flight
20	01/06/01	9:37:58 AM	9:56:52 AM	Sounding at beginning of flight
21	01/06/01	2:24:20 PM	2:39:06 PM	
22	01/06/01	3:05:41 PM	3:19:31 PM	Flight terminated due to high winds
23	01/07/01	8:35:47 AM	8:37:32 AM	Flight terminated due to engine failure
24	01/31/01	9:23:03 AM	9:31:54 AM	Flight terminated due to gimble failure
25	01/31/01	2:45:53 PM	3:06:11 PM	
26	02/01/01	8:05:33 AM	8:26:49 AM	Sounding done at end of flight
27	02/01/01	9:04:06 AM	9:20:51 AM	
28	02/01/01	10:01:30 AM	10:20:07 AM	

2.3 METEOROLOGICAL DATA

A ground based meteorological station measured wind speed, wind direction, and temperature during each flight. See Table 2-5 for a description of the station and Figure 2-5 for its location.

TABLE 2-5 Meteorological Station

Item	Description
Location - Latitude, Longitude (deg.deg)	35.46866 N, 119.72153 W
Location - UTM Easting, Northing (m)	253050, 3928422
Manufacturer	Davis Instruments
Model	Weather Monitor II
Tower Height (m)	6
Temperature Range & Accuracy	-50° to 140° F ± 1° F
Wind Direction Resolution & Accuracy	16 compass points (22.5°) ± 7°
Wind Speed Range & Accuracy	2 to 175 mph ± 5%

2.4 DATA FILES

The flight and meteorological data collected during the field program were submitted electronically to the California Air Resources Board (ARB) in accordance with the ARB data transmittal policies and procedures.

3.0 DATA ANALYSIS

3.1 FLIGHT CHARACTERISTICS

Analysis of the field data began by preparing various graphs to illustrate the basic flight path and plume characteristics. Table 3-1 summarizes the graphs generated.

TABLE 3-1 Flight Characteristic Graphs

Appendix	Graph Description
A	Flight path in UTM coordinates
B	Flight path 2-dimensional distance and angle to stack by time
C	SF ₆ concentration by time
D	SF ₆ concentration by distance
E	SF ₆ concentration by angle
F	SF ₆ concentration by altitude
G	Altitude by time
H	Temperature by altitude

In addition, the stability class was estimated for each flight using the Delta Temperature method shown in Table 3-2^[3]. The stability class profiles were developed to facilitate dispersion modeling simulations of the plumes using ISCST, provide a basis for comparing observed and theoretical values (e.g. sigma-Y (σ_y), sigma-Z (σ_z), etc.), and investigate plume infiltration above stable layers. Table 3-3 displays the results by altitude.

TABLE 3-2 Delta Temperature Stability Class Determination Method^[3]

Stability Class	Delta Temp (°C per 100m)	Definition
A	Less than -1.9	Extremely unstable
B	-1.9 to -1.7	Unstable
C	-1.7 to -1.5	Slightly unstable
D	-1.5 to -0.5	Neutral
E	-0.5 to 1.5	Slightly stable
F	1.5 to 4.0	Stable
G	Greater than 4.0	Extremely stable

TABLE 3-3 Flight Stability Class By Altitude

Flight No.	Altitude (ft)	Altitude (m)	Stability Class
1	0 – 100	0 – 30	A
	100 – 363	30 – 111	D
2	0 – 514	0 – 157	D
3	0 – 867	0 – 264	D
4	0 – 906	0 – 276	E
5	0 – 100	0 – 30	B
	100 – 430	30 – 131	D
6	0 – 100	0 – 30	A
	100 – 517	30 – 158	E
7	0 – 795	0 – 242	D
8	0 – 100	0 – 30	E
	100 – 300	30 – 91	F
	300 – 500	91 – 152	E
	500 – 548	152 – 167	G
9	0 – 1000	0 – 305	E
	1000 – 1243	305 – 379	F
10	0 – 125	0 – 38	A
	125 – 500	38 – 152	F
	500 – 830	152 – 253	E
11	0 – 100	0 – 30	B
	100 – 200	30 – 61	A
	200 – 507	61 – 155	E
12	0 – 200	0 – 61	A
	200 – 400	61 – 122	D
	400 – 800	122 – 244	F
	800 – 1071	244 – 326	E
13	0 – 300	0 – 91	A
	300 – 573	91 – 175	D
	573 – 671	175 – 205	G
14	0 – 526	0 – 160	D
	526 – 1039	160 – 317	E
15	0 – 89	0 – 27	D
	89 – 354	27 – 108	E
	354 – 512	108 – 156	F
	512 – 1044	156 – 318	E
16	0 – 684	0 – 208	D
	684 – 1061	208 – 323	E
17	0 – 870	0 – 265	D
18	0 – 741	0 – 226	D
19	0 – 200	0 – 61	E
	200 – 400	61 – 122	G
	400 – 1027	122 – 313	F
20	0 – 30	0 – 9	A
	30 – 200	9 – 61	E
	200 – 483	61 – 147	F
21	0 – 100	0 – 30	A

Flight No.	Altitude (ft)	Altitude (m)	Stability Class
	100 – 581	30 – 177	E
22	0 – 1022	0 – 312	D
23	0 – 75 75 – 191	0 – 23 23 – 58	F E
24	0 – 45 45 – 484	0 – 14 14 – 148	A D
25	0 – 200 200 – 1577	0 – 61 61 – 481	A D
26	0 – 400 400 – 637	0 – 122 122 – 194	F E
27	0 – 150 150 – 430	0 – 46 46 – 131	E F
28	0 – 200 200 – 744	0 – 61 61 – 227	B E

3.2 CONCENTRATIONS

For the significant peaks from each flight, the measured SF₆ concentration was converted to $\chi u/Q$ (in units of 1/m²) where:

$$\begin{aligned}\chi &= \text{SF}_6 \text{ concentration (g/m}^3\text{)} \\ u &= \text{wind speed (m/s)} \\ Q &= \text{SF}_6 \text{ emission rate (g/s)}\end{aligned}$$

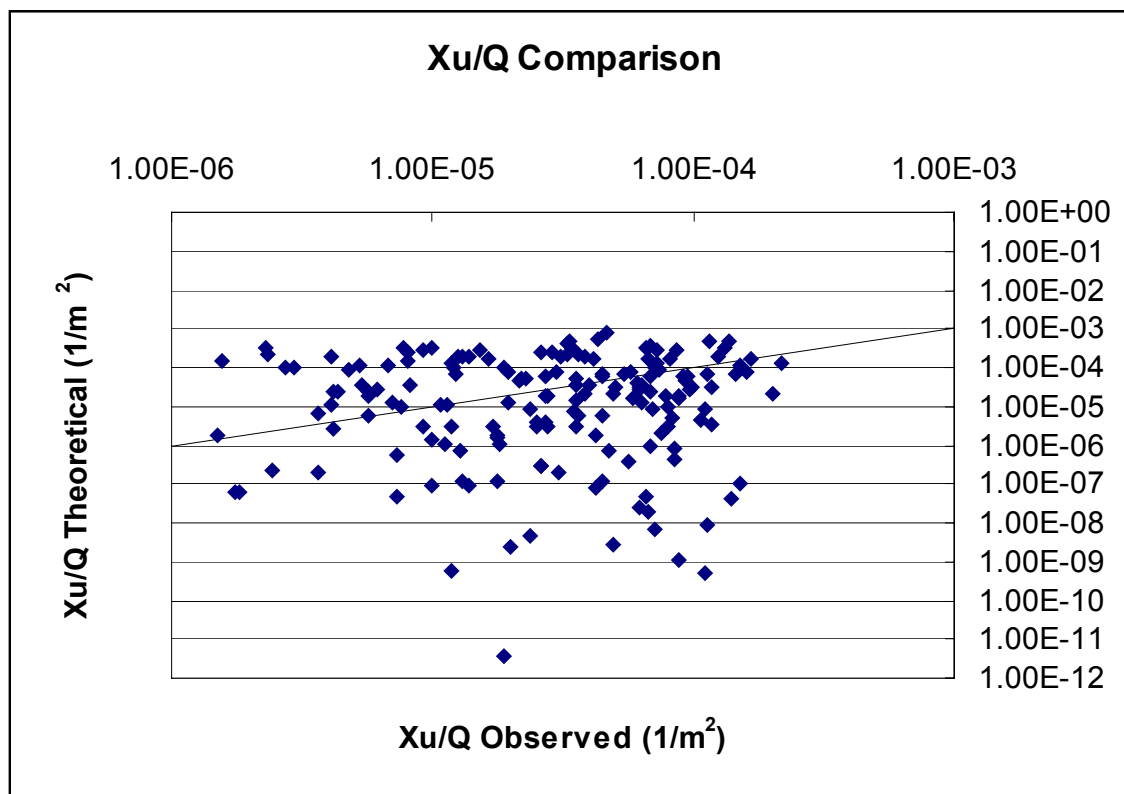
Next, each observed $\chi u/Q$ value was compared to the theoretical $\chi u/Q$ value predicted by the ISCST dispersion model for the atmospheric conditions encountered by the blimp. The ISCST model was configured to calculate a three-minute average $\chi u/Q$ value based upon flat terrain, in rural conditions, using the stack parameters listed in Table 2-1 and Table 2-2. For the meteorological data file, the following information was used:

- Mixing height: Assumed to be infinitely high (otherwise model predicted zero for any concentration where the receptor height was above the mixing height).
- Stability Class: Stability at the elevation of the blimp.
- Temperature: Average temperature of data collected by the local meteorological station during the flight. For flights 12-14, 18, and 24, there was no meteorological data collected so temperatures from the blimp were used.
- Wind Speed: Average wind speed of data collected by the local meteorological station during the flight. For flights 12-14, 18, and 24, there was no meteorological data collected so estimated wind speeds from the flight logs were used.

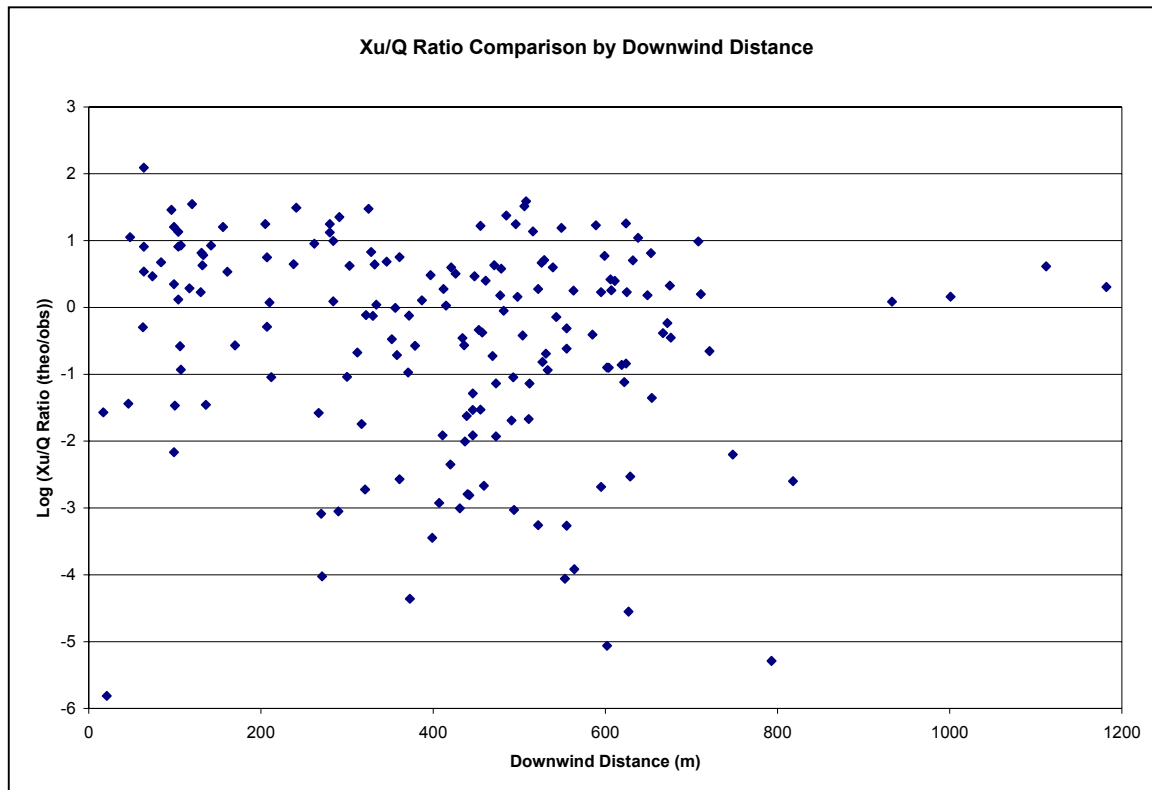
- Wind Direction: Blimp was assumed to be directly downwind of the stack when comparing plume peaks to modeled values.

Figure 3-1 displays the $\chi u/Q$ comparison using a log-log plot. The diagonal line drawn on the graph represents a slope of one meaning that the $\chi u/Q$ theoretical value equals the $\chi u/Q$ observed value. Figure 3-2 then displays a ratio of χuQ theoretical to $\chi u/Q$ observed as a function of downwind distance.

FIGURE 3-1 $\chi u/Q$ Comparison



Overpredictions by the ISCST model may indicate that the observed value was off-axis relative to the true plume centerline. Underpredictions by the ISCST model may indicate that the model estimated a plume height significantly different than that measured. Note, 24 data points were omitted from Figures 3-1 and 3-2 because the ISCST model predicted $\chi u/Q$ values of zero and such values can not be displayed on a log-log plot.

FIGURE 3-2 $\chi u/Q$ Comparison By Downwind Distance

3.3 SIGMA-Y (σ_y)

For the highest SF₆ peak from each flight, the plume's sigma-y (σ_y) value was estimated by:

- graphing concentrations measured against the blimp's angle relative to the stack just before, during, and after the peak;
- using analytical tools to generate the best curves to fit the data plotted (e.g. Gaussian, high order polynomial, etc.);
- calculating the distance from the plume centerline such that the area under the curve was represented one standard deviation; and
- converting the calculated sigma-theta (σ_θ) into sigma-y (σ_y) using:

$$\sigma_y = r * \tan(\sigma_\theta)$$

where r was the downwind distance of the blimp. See Appendix I for the data points plotted for the analysis. Note, this process was complicated by the following factors:

- While each peak was being recorded, the blimp was typically moving in all three-dimensions (r, θ , z) and not perpendicular to the plume centerline in a horizontal manner.
- The accuracy of the blimp's GPS position was within 10 meters which introduces a significant error when dealing with observed sigma-y ranging from 1.2 to 56.4 meters (see Table 3-4).
- Some data points near each peak had to be eliminated in order for the curve fitting tools to generate a solution (most likely required by the two contributing factors above). Since the elimination process was subjective, the choice of points eliminated could have a significant impact on the calculated results for sigma-y observed.
- In some cases, data points selected for analysis were only sufficient to analyze one-half of the standard Gaussian bell shaped curve.

For comparison, the Pasquill-Gifford model detailed in the EPA's User's Guide for the Industrial Source Complex (ISC3) Dispersion Models^[4] was used to predict the theoretical values for the atmospheric conditions encountered by the blimp. Table 3-4, Figure 3-3, and Figure 3-4 display the comparison of observed and theoretical sigma-y values.

The model over predicted the sigma-y values for all peaks with D stability conditions except for two cases (Flights 7 and 16). In Flight 7, the stability class was estimated to be D, although the

temperature – altitude slope was at the low end of range approaching the C stability class. Had the Flight 7 peak been modeled as C stability, the statistical agreement between the observed and theoretical sigma-y values would have increased with the theoretical sigma-y slightly over predicted as the trend suggests. In Flight 16, the model under prediction was most likely a result of the airship’s downwind distance of only 46 meters. Thus, stability class and impact downwind distance both play a crucial role in the model’s under prediction for D stability class impacts.

For flights with E stability, the comparison showed several cases of both over and under predicting the observed value. The differences appeared to be the result of either poor distribution of the data points measured (e.g. blimp may have drifted laterally or vertically while transecting the plume resulting in a non-Gaussian distribution) or the data points were near a stability transition layer. In every flight with F stability class conditions (Flights 12, 26, and 27), the model under predicted the observed sigma-y value. For these three cases, the difference in values was the greater closest to the stack (Flights 26 and 27) than further downwind (Flight 12).

Based upon the analysis, the statistical agreement between the theoretical and observed sigma-y values varied depending upon the stability class and downwind distance. It is important to note that the closest downwind measurement to the source was 46 meters and the furthest downwind measurement was 933 meters.

TABLE 3-4 Sigma-Y (σ_y) Comparison

Flight No. *	Blimp Downwind Distance (m)	Stability Class at Blimp Elevation	Observed Sigma-Y (σ_y) (m)	Theoretical Sigma-Y (σ_y) (m)	Ratio σ_y Theoretical / σ_y Observed
1	-	-	-	-	-
2	207	D	10.65	16.06	1.5
3	312	D	21.85	23.44	1.1
4	104	E	23.33	6.35	0.3
5	210	E	1.21	12.16	10.0
6	317	E	17.4	17.77	1.0
7	347	D	35.01	25.85	0.7
8	-	-	-	-	-
9	523	E	9.1	28.15	3.1
10	421	E	31.31	23.07	0.7
11	563	E	56.38	30.12	0.5
12	575	F	21.36	20.42	1.0
13	595	D	34.24	42.39	1.2
14	555	D	19.69	39.77	2.0
15	933	E	28.24	47.81	1.7
16	46	D	22.1	4	0.2
17	604	D	27.2	42.98	1.6
18	793	D	15.55	55.13	3.5
19	-	-	-	-	-
20	-	-	-	-	-
21	361	E	7.4	20.03	2.7
22	-	-	-	-	-
23	-	-	-	-	-
24	284	D	16.5	21.5	1.3
25	91	D	2.24	7.51	3.4
26	64	F	36.59	2.69	0.1
27	117	F	22.47	4.71	0.2
28	446	E	11.08	24.33	2.2

* Flights 1, 8, 22, 23: concentration data was either not measured or invalid
 Flights 19, 20: Sigma-y value not calculated due to poor distribution of data points.

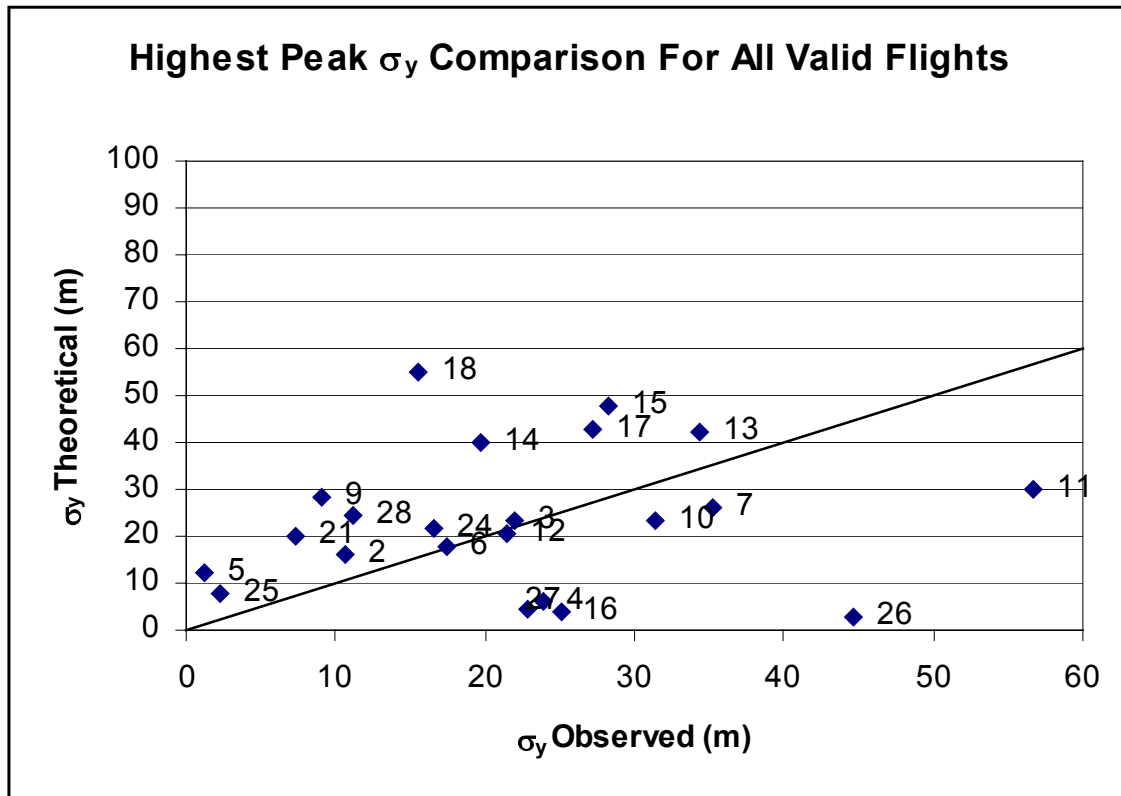
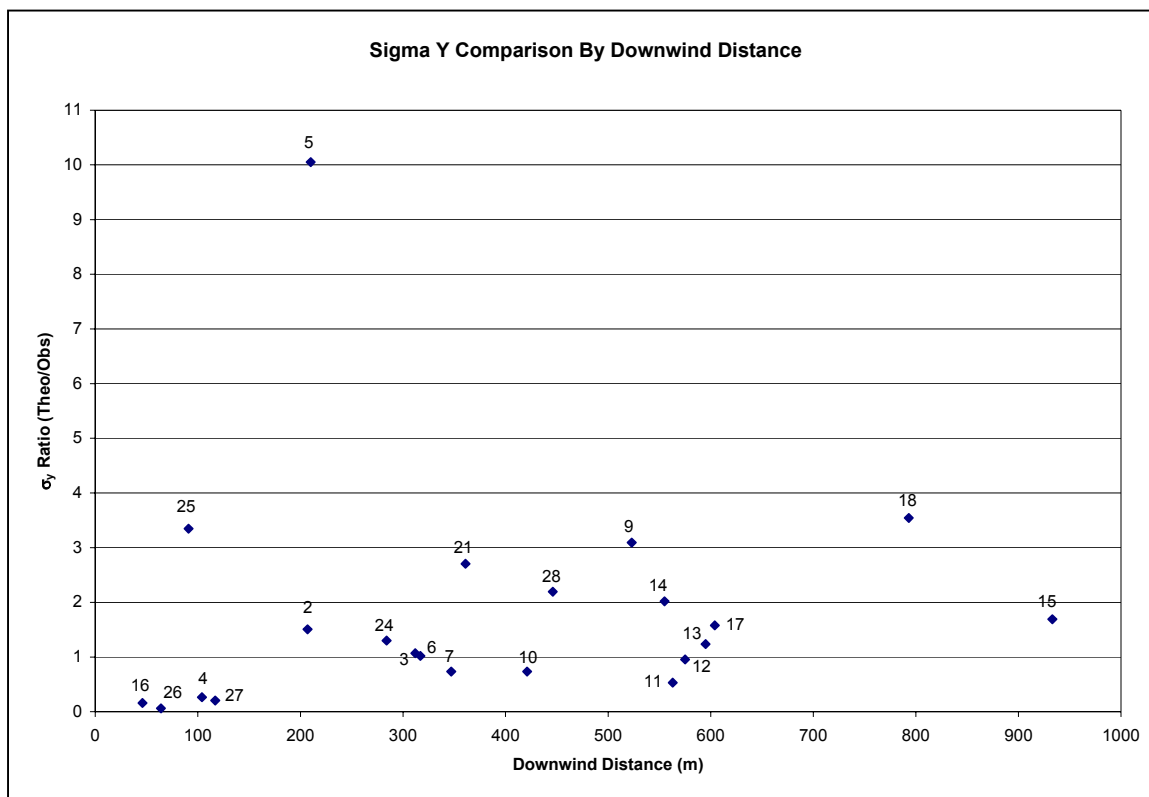
FIGURE 3-3 Sigma-Y (σ_y) Comparison

FIGURE 3-4 Sigma-Y (σ_y) Comparison By Downwind Distance

3.4 SIGMA-Z (σ_z)

Analysis of the sigma-z (σ_z) values for the highest SF₆ peak from each flight was conducted using the same methodology and assumptions as used for the sigma-y (σ_y) analysis. The only change being that the SF₆ concentration data for each peak was plotted against altitude instead of angle. See Appendix J for the analysis graphs.

For comparison, the Pasquill-Gifford model detailed in the EPA's User's Guide for the Industrial Source Complex (ISC3) Dispersion Models^[4] was used to predict the theoretical values for the atmospheric conditions encountered by the blimp. Table 3-5, Figure 3-5, and Figure 3-6 display the comparison of observed and theoretical sigma-z values. In almost all cases, the model under predicted the observed values. This was most likely due to poor-to-fair Gaussian distribution of the data points measured. In many cases, the blimp moved significantly in the x and y dimensions as opposed to just vertically in the z dimension. This caused greater difficulty in analyzing the data than experienced during the sigma-y analysis. Therefore, caution should be taken when making any conclusions in light of the accuracy of the data comparisons.

TABLE 3-5 Sigma-Z (σ_z) Comparison

Flight No. *	Blimp Downwind Distance (m)	Stability Class at Blimp Elevation	Observed Sigma-Z (σ_z) (m)	Theoretical Sigma-Z (σ_z) (m)	Ratio σ_z Theoretical / σ_z Observed
1	-	-	-	-	-
2	207	D	4.87	8.75	1.8
3	312	D	2.72	12.48	4.6
4	104	E	1.14	3.65	3.2
5	210	E	0.95	6.49	6.8
6	317	E	1.34	9.07	6.8
7	347	D	3.45	13.61	3.9
8	-	-	-	-	-
9	523	E	6.94	13.24	1.9
10	421	E	2.99	11.24	3.8
11	563	E	1.43	14.00	9.8
12	575	F	1.70	9.37	5.5
13	595	D	4.08	21.07	5.2
14	555	D	2.47	19.91	8.1
15	933	E	1.41	20.52	14.6
16	46	D	1.41	2.37	1.7
17	604	D	1.71	21.33	12.5
18	793	D	6.58	26.59	4.0
19	131	G	2.01	2.94	1.5
20	100	F	1.56	2.33	1.5
21	361	E	1.55	10.01	6.5
22	-	-	-	-	-
23	-	-	-	-	-
24	284	D	0.94	11.53	12.3
25	91	D	2.01	4.28	2.1
26	64	F	1.86	1.62	0.9
27	117	F	2.30	2.64	1.1
28	446	E	9.22	11.74	1.3

* Flights 1, 8, 22, 23: concentration data was either not measured or invalid

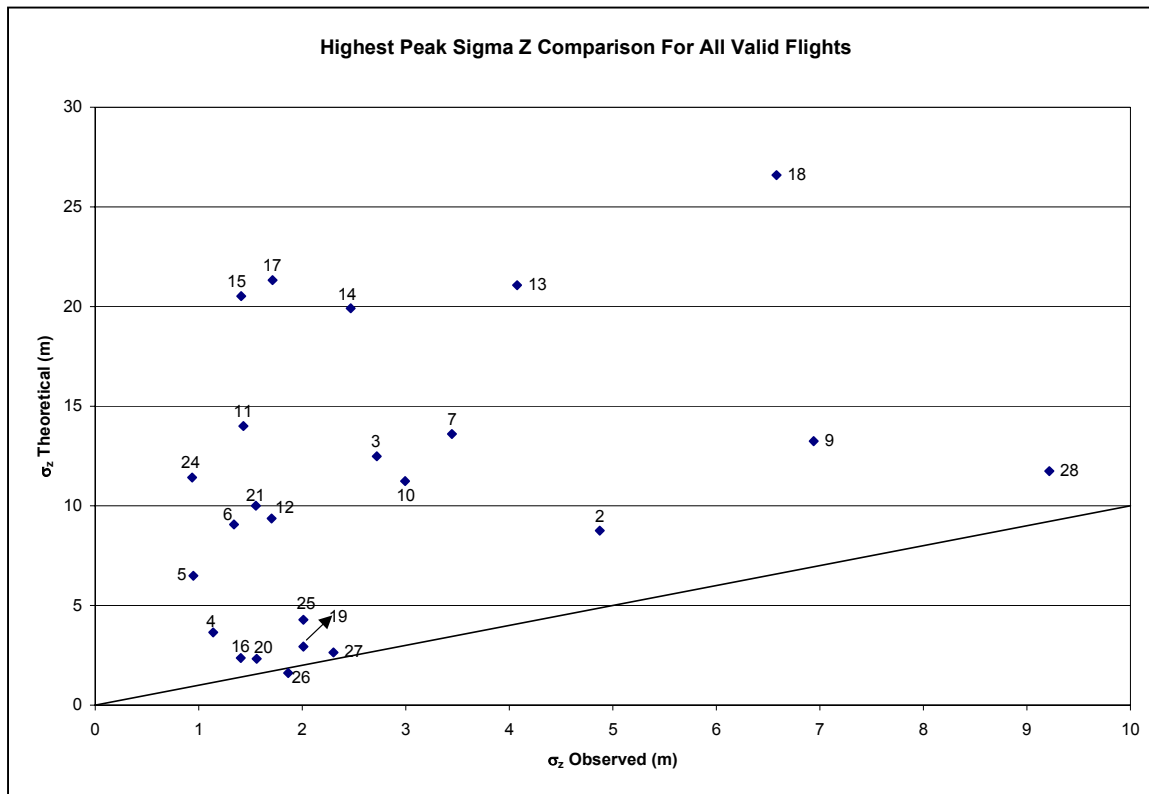
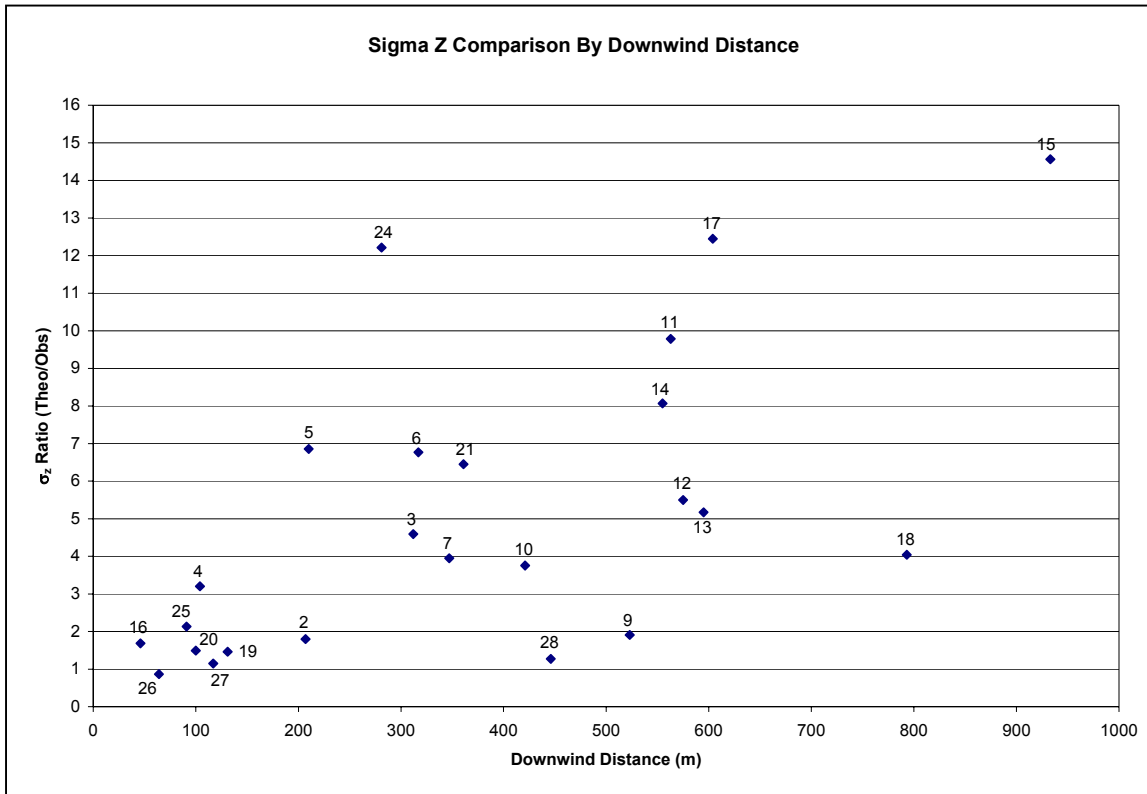
FIGURE 3-5 Sigma-Z (σ_z) Comparison

FIGURE 3-6 Sigma-Z (σ_z) Comparison By Downwind Distance

3.5 PLUME RISE

The plume height of the highest peak from each flight was compared against the values predicted by the EPA ISCST3 model^[4] and Holland's equation^[5]. Table 3-6, Figure 3-7, and Figure 3-8 display the results of the comparison. In most cases, ISC model did a better job of estimating the plume heights measured. This may be due to the fact that the Holland equation does not take stability into account.

TABLE 3-6 Plume Height Comparison

Flight No. *	Stability Class at Blimp Elevation	Highest Peak Plume Height		Holland's Predicted Plume Height		ISC Model Effective Plume Height		Plume Height Ratio (ISC / Observed)
		(ft)	(m)	(ft)	(m)	(ft)	(m)	
1	-	-	-	-	-	-	-	-
2	D	366	112	129	39	411	125	1.1
3	D	474	144	134	41	443	135	0.9
4	E	432	132	157	48	268	82	0.6
5	D	369	112	344	105	1504	458	4.1
6	E	340	104	79	24	191	58	0.6
7	D	591	180	81	25	203	62	0.3
8	-	-	-	-	-	-	-	-
9	E	987	301	189	58	281	86	0.3
10	F	158	48	82	25	168	51	1.1
11	E	242	74	84	26	196	60	0.8
12 &	F	567	173	75	23	158	48	0.3
13 &	D	424	129	73	22	158	48	0.4
14 &	D	485	148	78	24	182	55	0.4
15	E	315	96	146	45	258	79	0.8
16	D	402	123	121	37	391	119	1.0
17	D	547	167	105	32	307	94	0.6
18 &	D	703	214	86	26	221	67	0.3
19 #	F	210	64	290	88	283	86	1.3
20	F	322	98	122	37	205	62	0.6
21	E	384	117	82	25	189	58	0.5
22	-	-	-	-	-	-	-	-
23	-	-	-	-	-	-	-	-
24 &	D	255	78	88	27	238	73	0.9
25	D	879	268	95	29	268	82	0.3
26	F	251	77	899	274	412	126	1.6
27	F	203	62	75	23	162	49	0.8
28	E	301	92	73	22	179	55	0.6

* Flights 1, 8, 22, 23: concentration data was either not measured or invalid

Modeled as F stability in the ISC model

& No data recorded by meteorological station. Wind speed estimated taken from flight log.

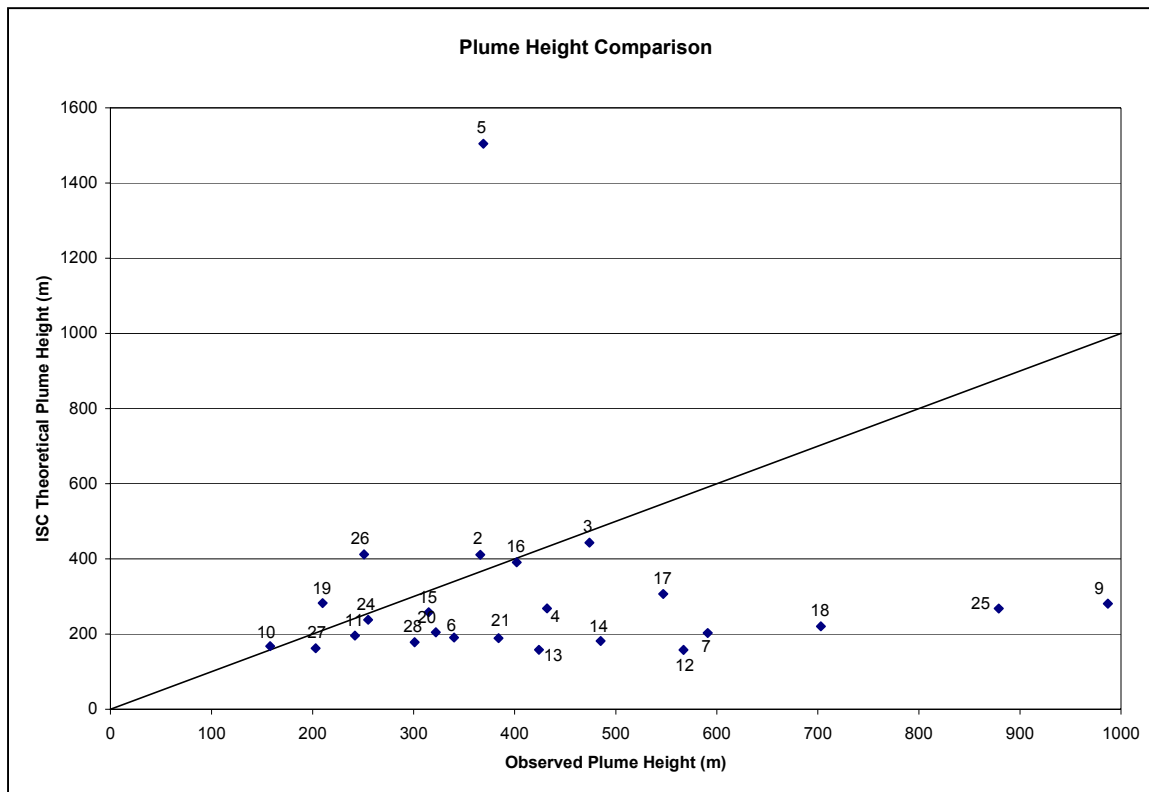
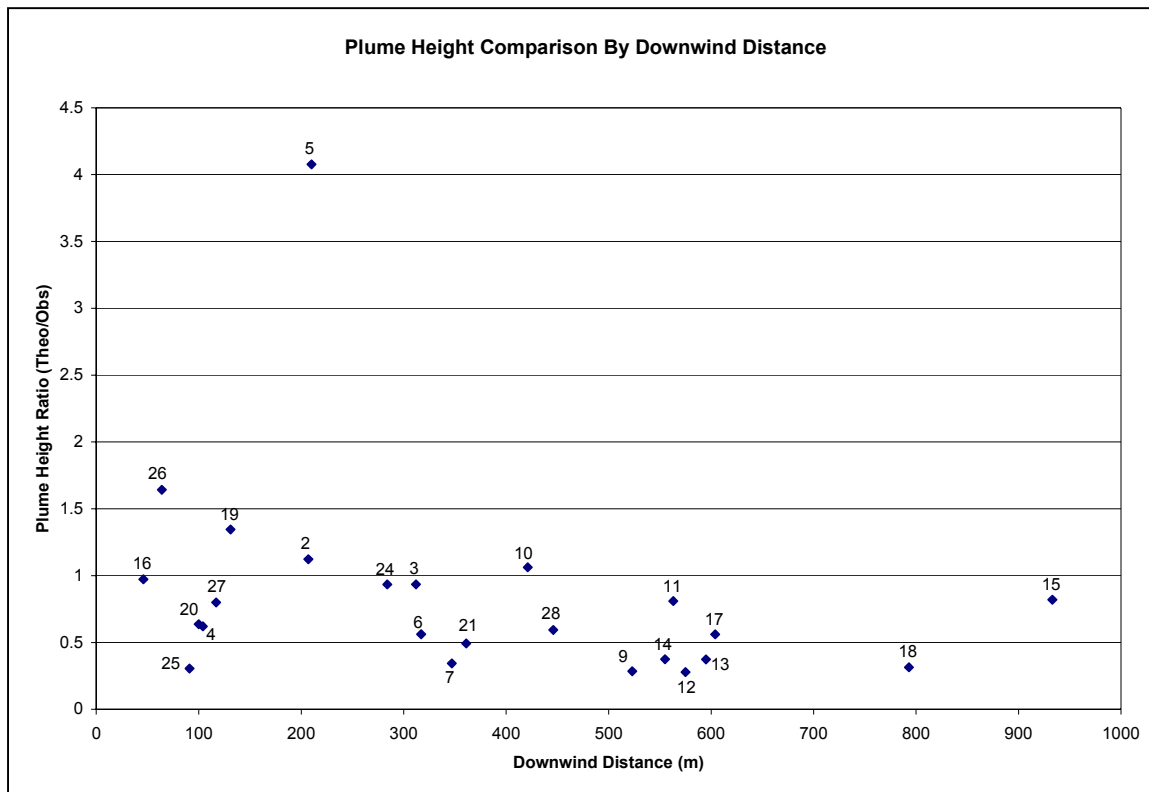
FIGURE 3-7 Plume Height Comparison

FIGURE 3-8 Plume Height Comparison By Downwind Distance

3.6 PLUME INFILTRATION

Based upon Table 3-3, several flights indicate an abrupt transition from unstable (e.g. stability class A-B) to stable (e.g. stability class E-G) conditions. For these flights, Table 3-7 demonstrates the plume infiltration into the stable layer by comparing the maximum SF₆ concentration measured above and below the estimated transition height. See Figures 3-9 to 3-13 which display the SF₆ concentration by altitude with the estimated stable layer height and ISC model predicted plume height superimposed for reference.

TABLE 3-7 Plume Infiltration into Stable Layer

Flight No.	Stability Class Transition (See Table 3-3)	Stable Layer Altitude (See Table 3-3) (ft)	Stable Layer Altitude (See Table 3-3) (m)	Maximum SF ₆ Concentration at or Below Stable Layer Altitude (ppt)	Maximum SF ₆ Concentration Above Stable Layer Altitude (ppt)
6	A to E	100	30	0	2,519
10	A to F	125	38	0	3,494
11	A to E	200	61	3,374	4,599
21	A to E	100	30	0	5,025
28	B to E	200	61	3,593	11,249

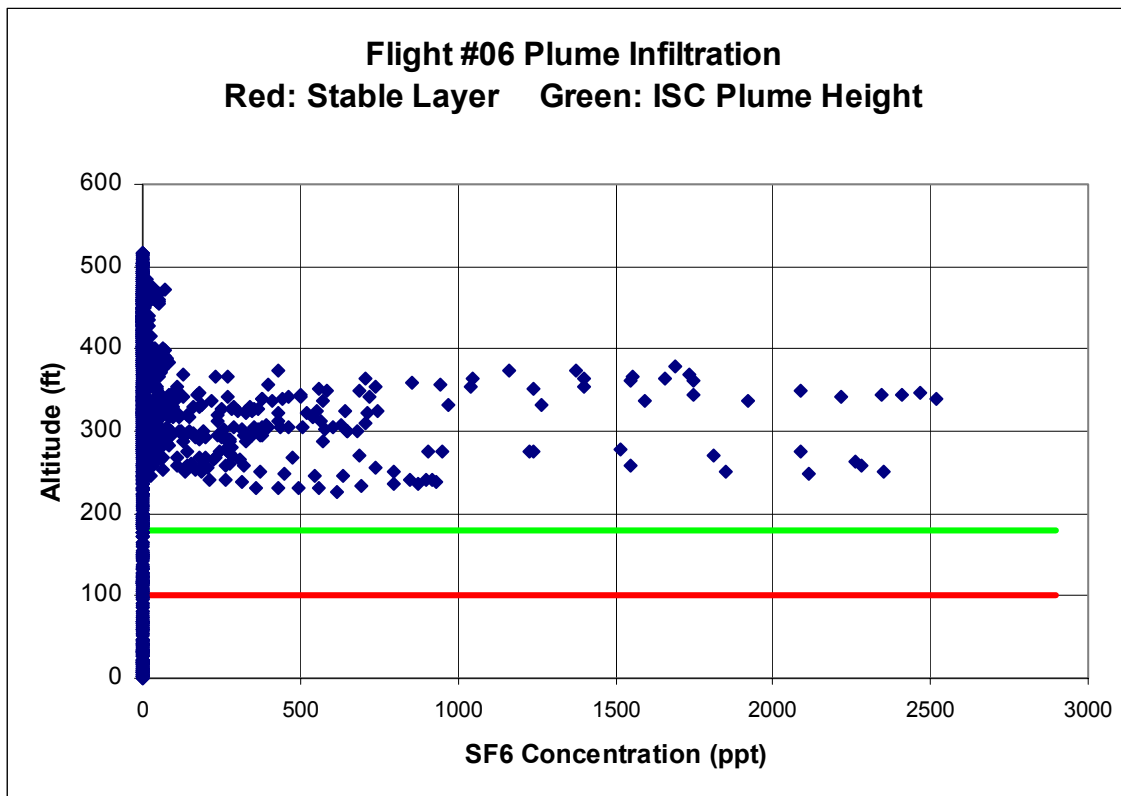
FIGURE 3-9 Flight 6 Plume Infiltration

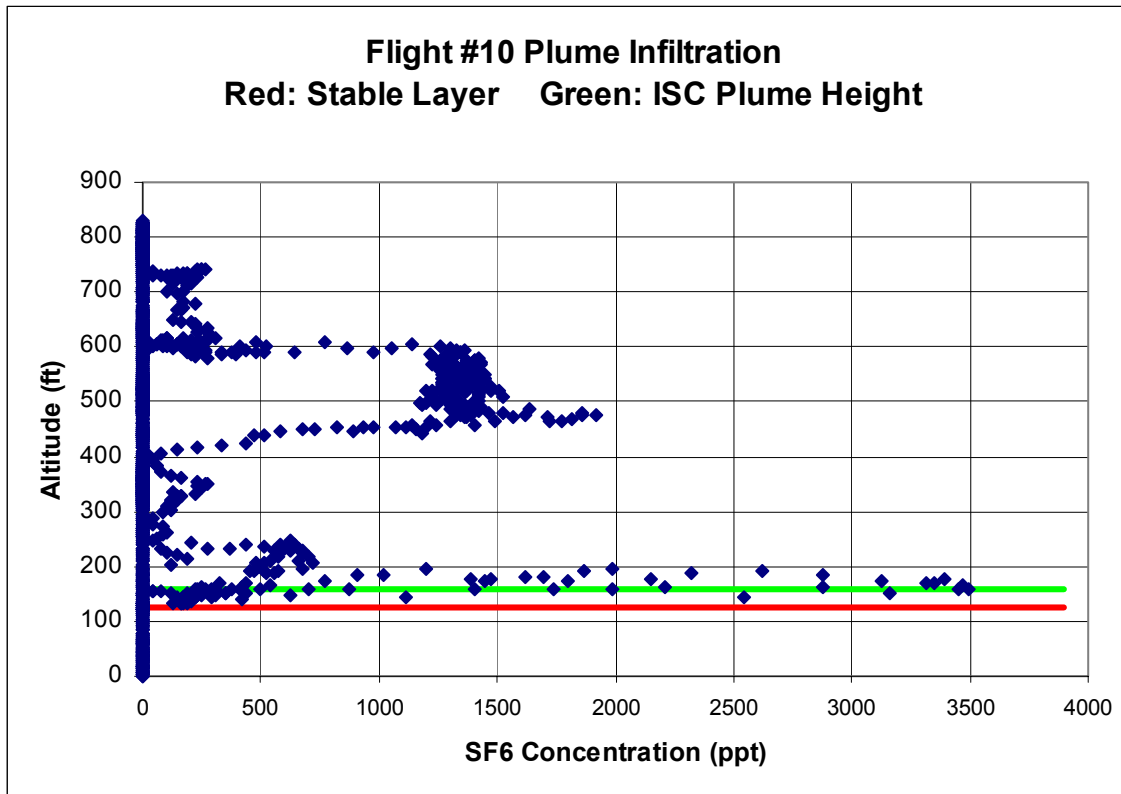
FIGURE 3-10 Flight 10 Plume Infiltration

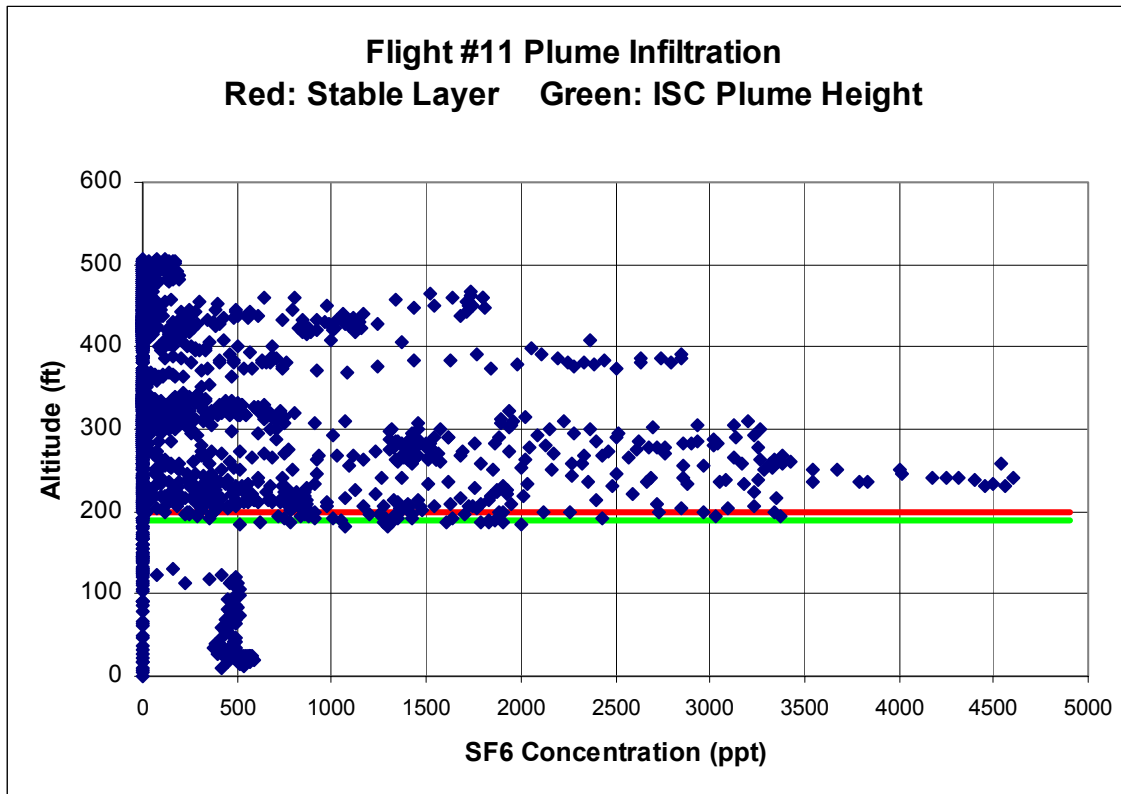
FIGURE 3-11 Flight 11 Plume Infiltration

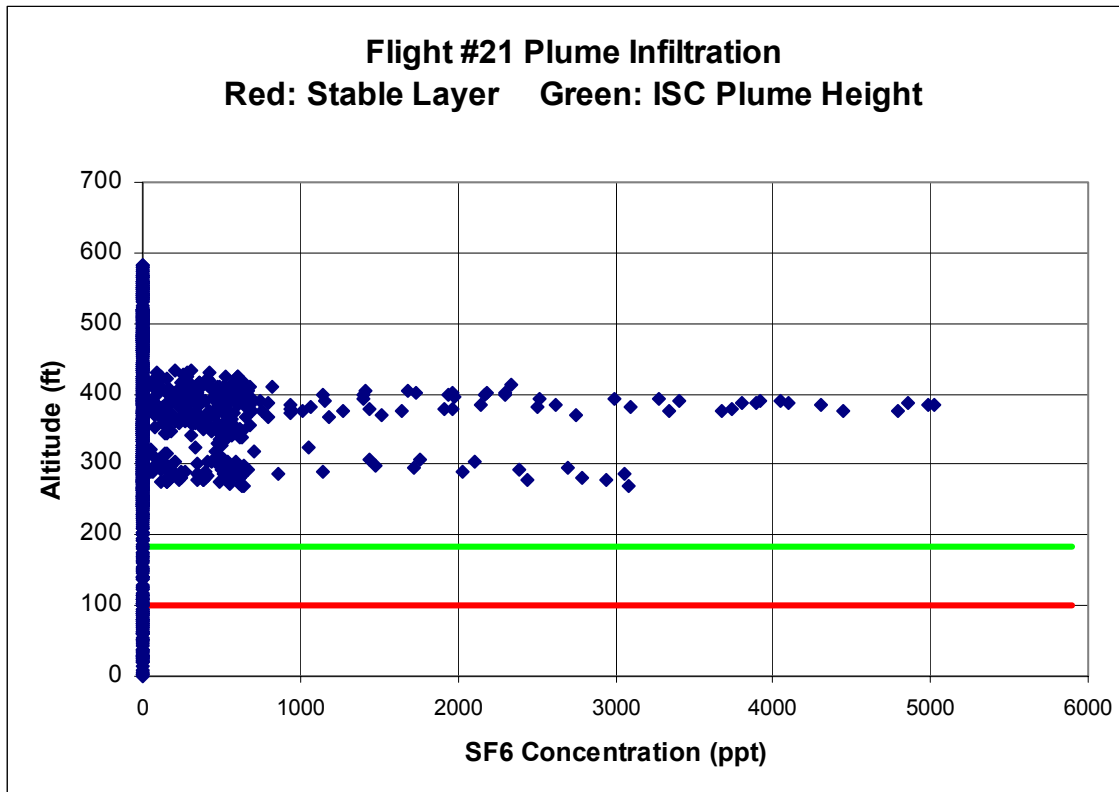
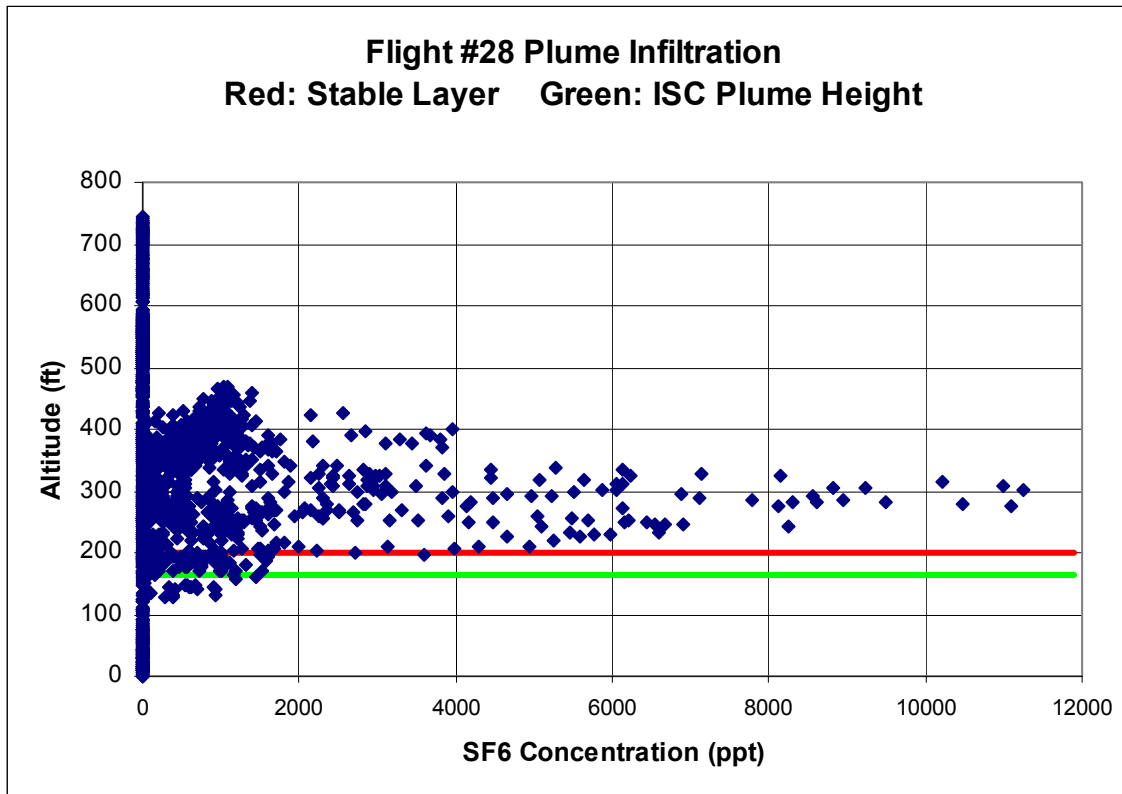
FIGURE 3-12 Flight 21 Plume Infiltration

FIGURE 3-13 Flight 28 Plume Infiltration

4.0 CONCLUSIONS

Based upon the data analyses conducted, the following conclusions are presented for short term averaging periods:

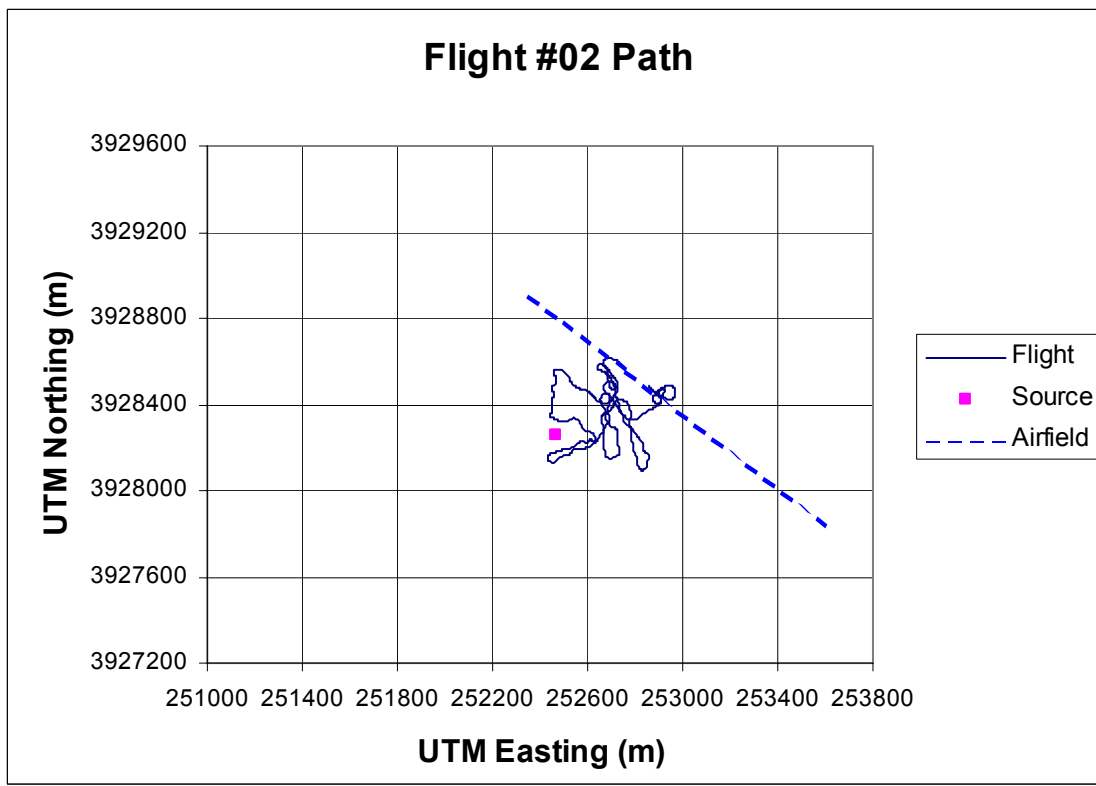
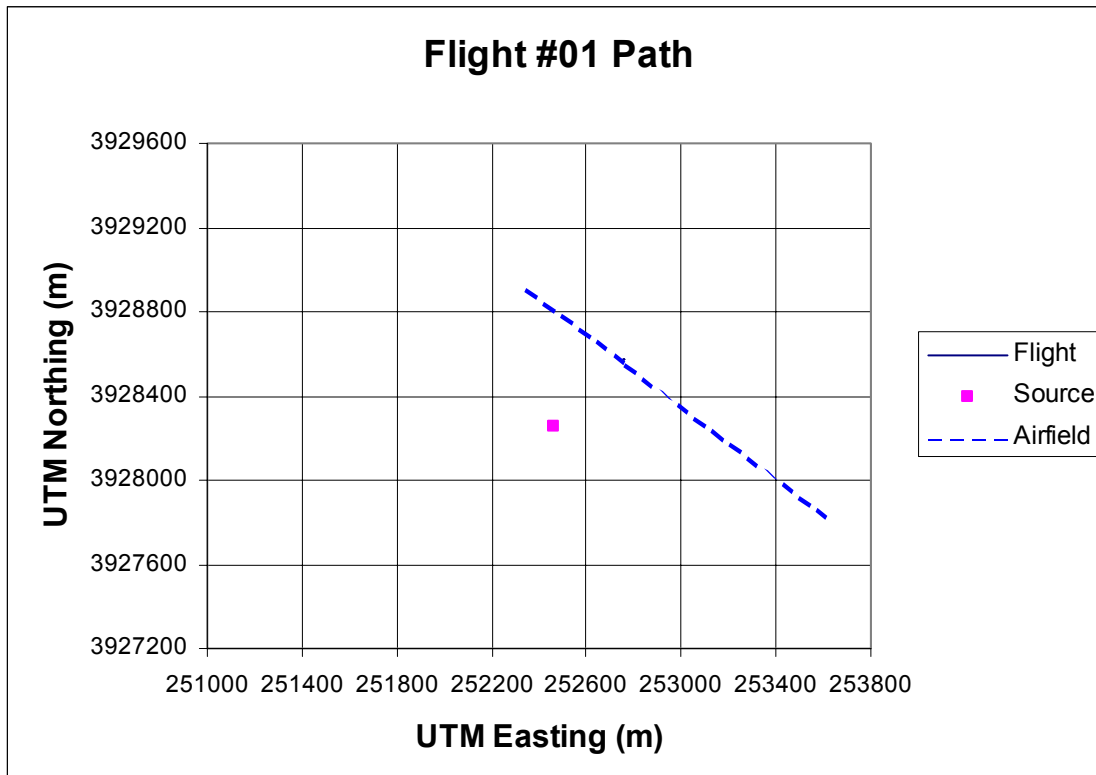
- Observations show that the tracer plume is entrained significantly into stable layers aloft, well above the ISCST model predictions.
- In the downwind zone of 50 meters to one kilometer, ISCST3 predictions demonstrate a bias to over predict during unstable and neutral conditions and seem to reverse this trend for very stable conditions.
- While vertical dispersion rates of plumes are over predicted by models, actual plume heights are significantly under predicted by ISCST3, especially in the presence of a low lifted inversion.

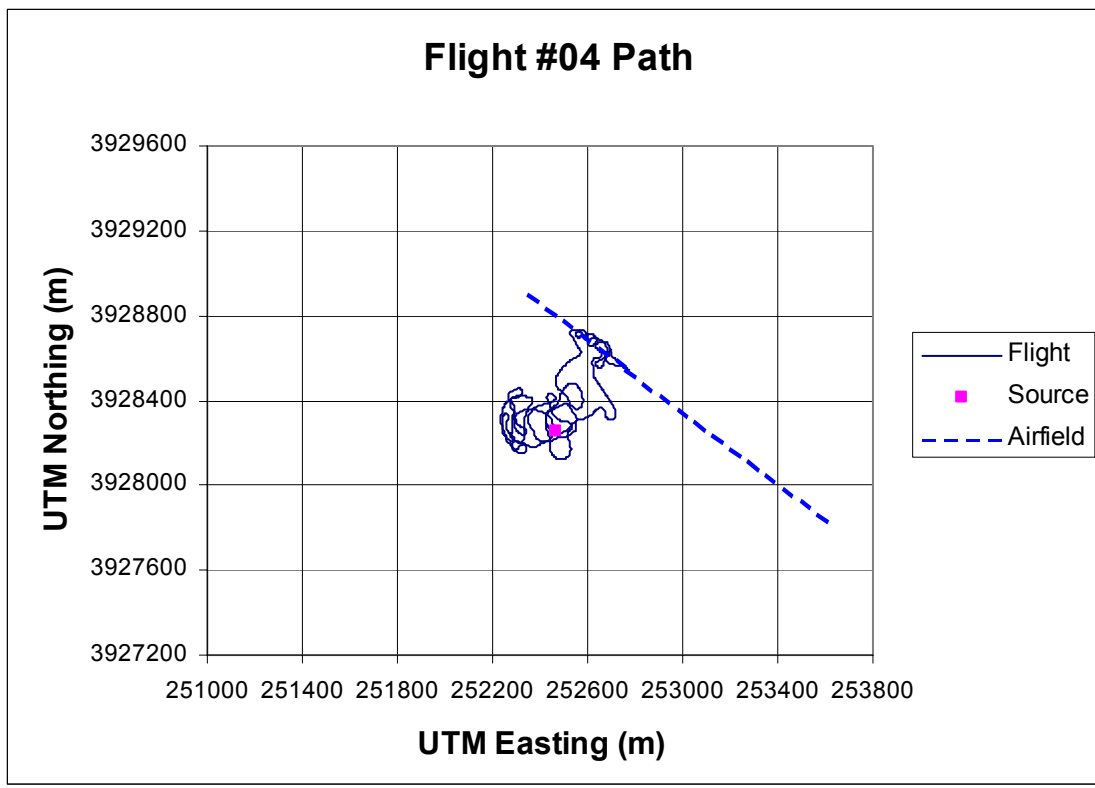
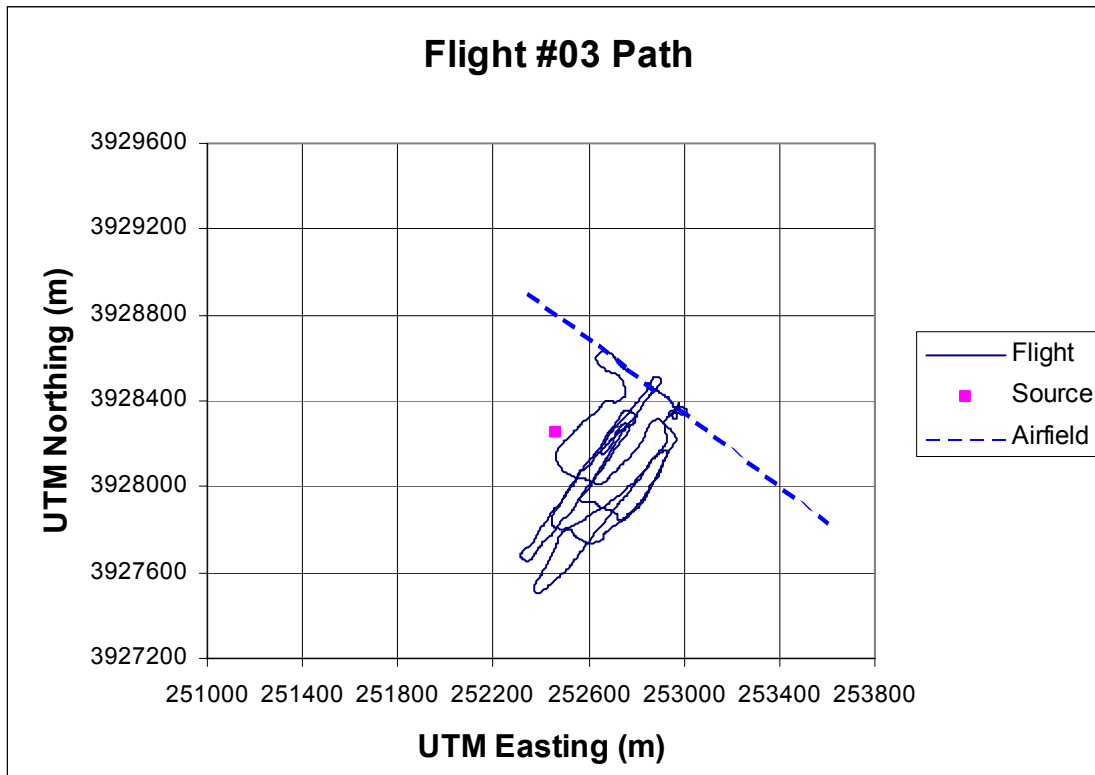
REFERENCES

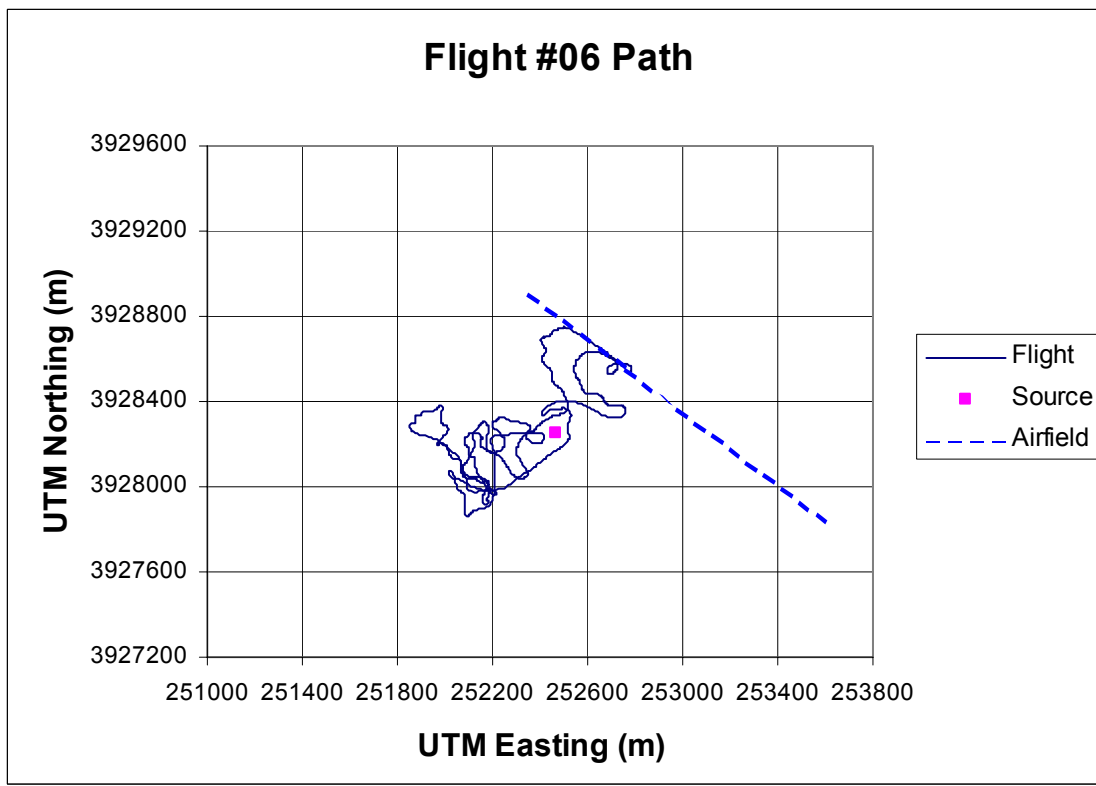
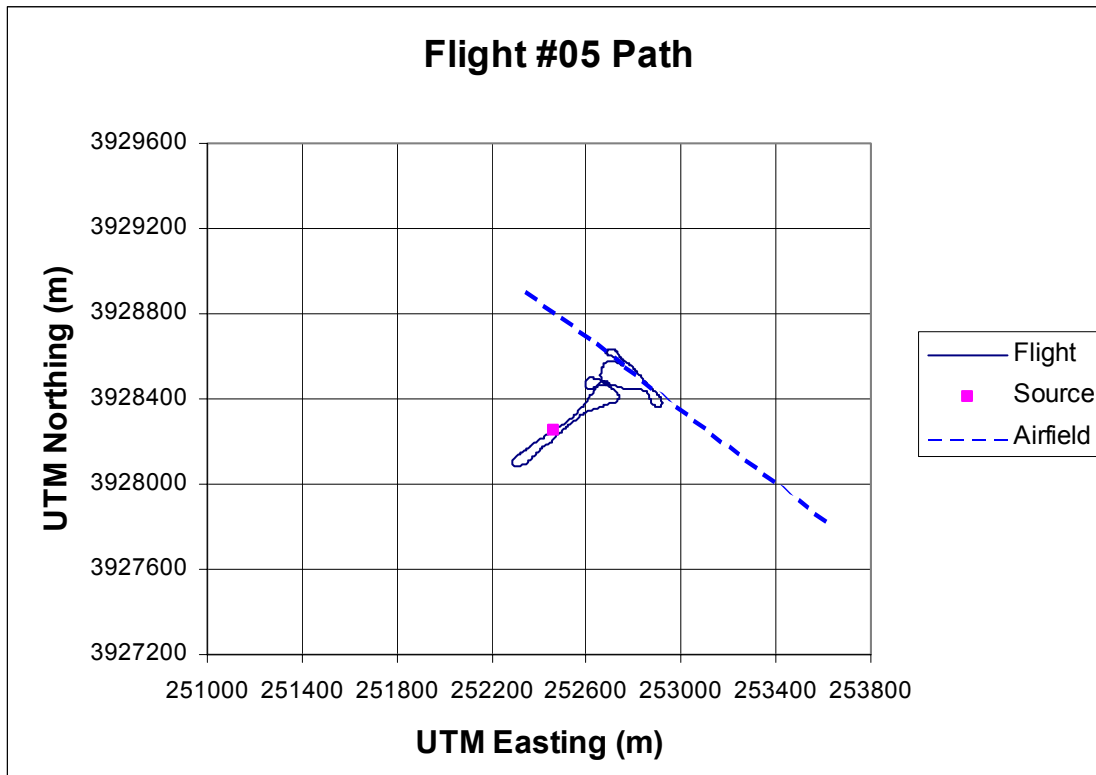
1. Rappolt, Thomas J. (Tracer ES&T), Kerrin, Stephen L. (Tracer ES&T), Hochheiser, William (U.S. Department of Energy), Ziman, Steven (Chevron Research and Technology Company), Reheis, Catherine (Western States Petroleum Association), “Mapping Air Quality Plumes from Fossil Energy Sources to Assess the Impacts of Secondary Aerosol Development”, SPE 66502, Society of Petroleum Engineers, Inc., Richardson, TX, 2001.
2. Remotely Piloted Airship for Atmospheric Tracer Sampling (RPATS) Development and Flight Readiness, U.S. Department of Energy contract DEAC-75-99-AP-47519, Tracer ES&T, San Marcos, CA, June 1, 2000.
3. “Meteorological Programs in Support of Nuclear Power Plants”, U.S. Nuclear Regulatory Commission, Office of Standards Development, Washington, DC, 1972 (Docket Reference No. II-P-II).
4. User’s Guide for the Industrial Source Complex (ISC3) Dispersion Models Volume II – Description of Algorithms, United States Environmental Protection Agency, Office of Air Quality Planning and Standards, Emissions, Monitoring, and Analysis Division, Research Triangle Park, North Carolina, September 1995.
5. Turner, D. Bruce, Workbook of Atmospheric Dispersion Estimates, United States Environmental Protection Agency, Office of Air Programs, Research Triangle Park, North Carolina, Publication AP-26, Revised 1970.

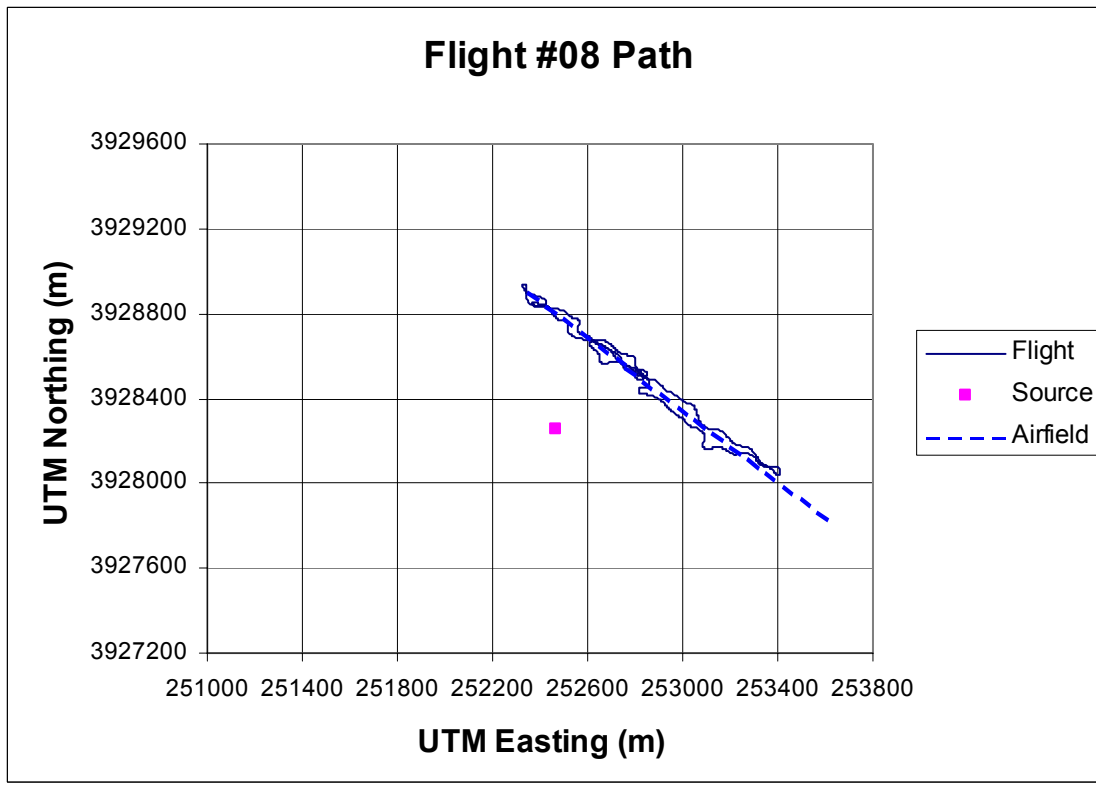
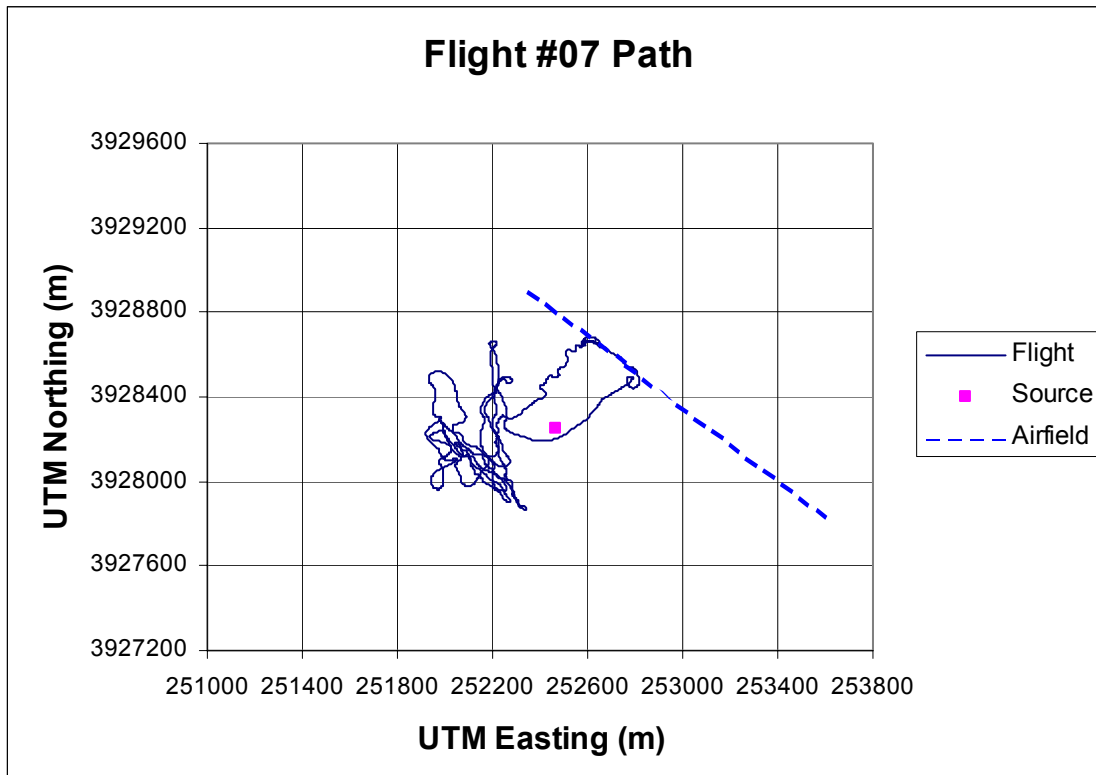
APPENDIX A

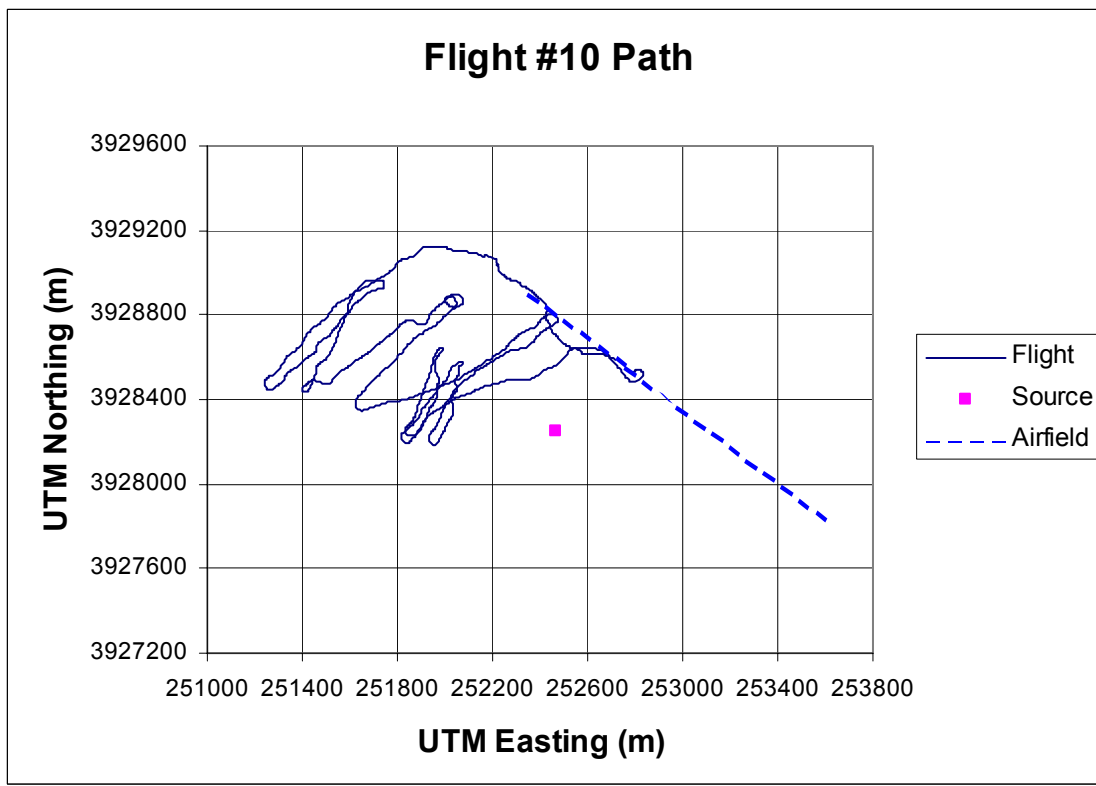
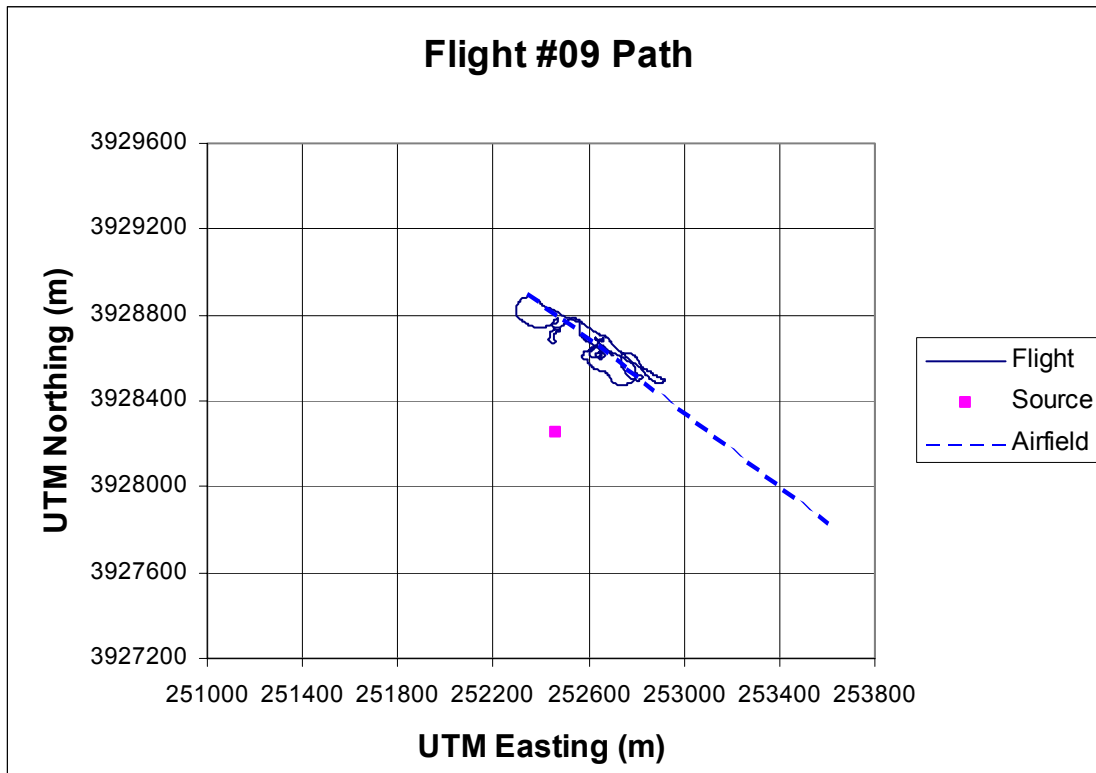
FLIGHT PATH POSITION GRAPHS

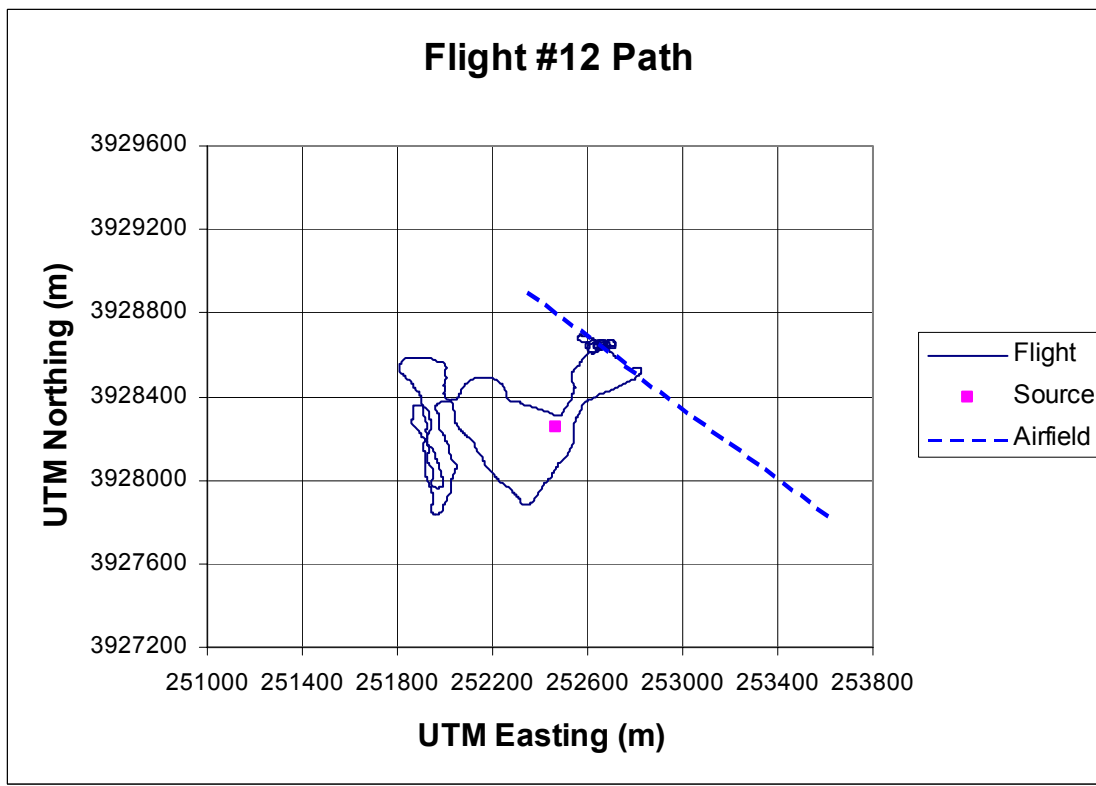
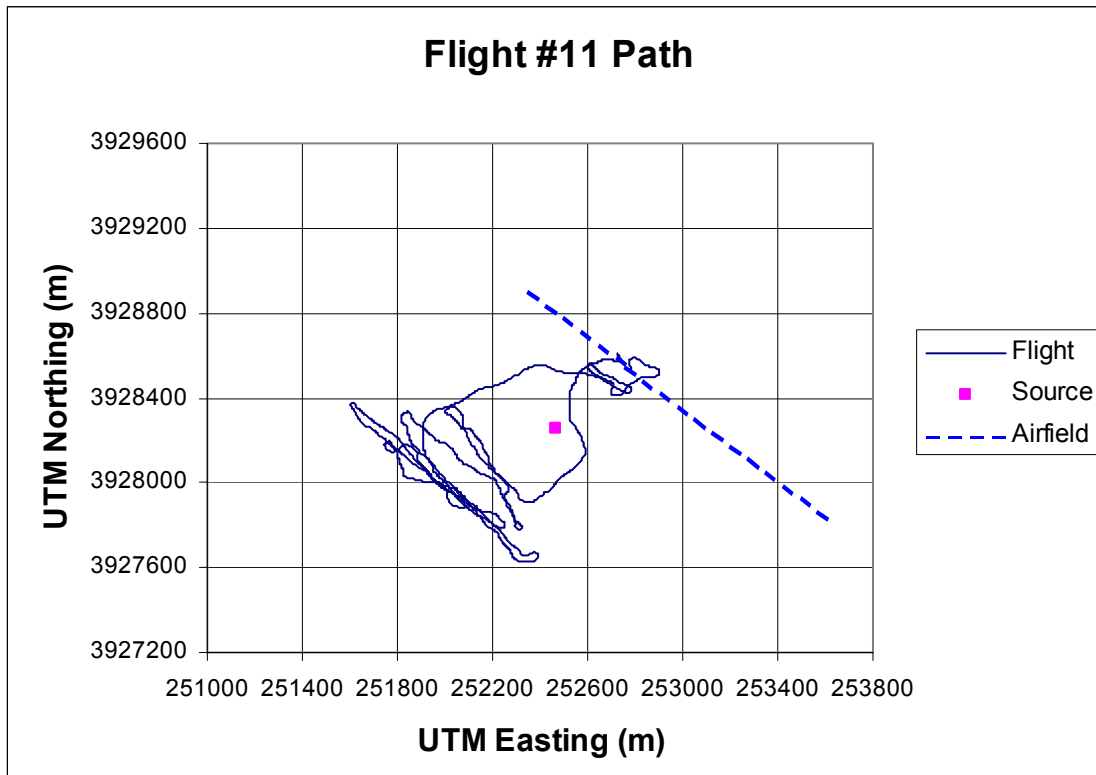


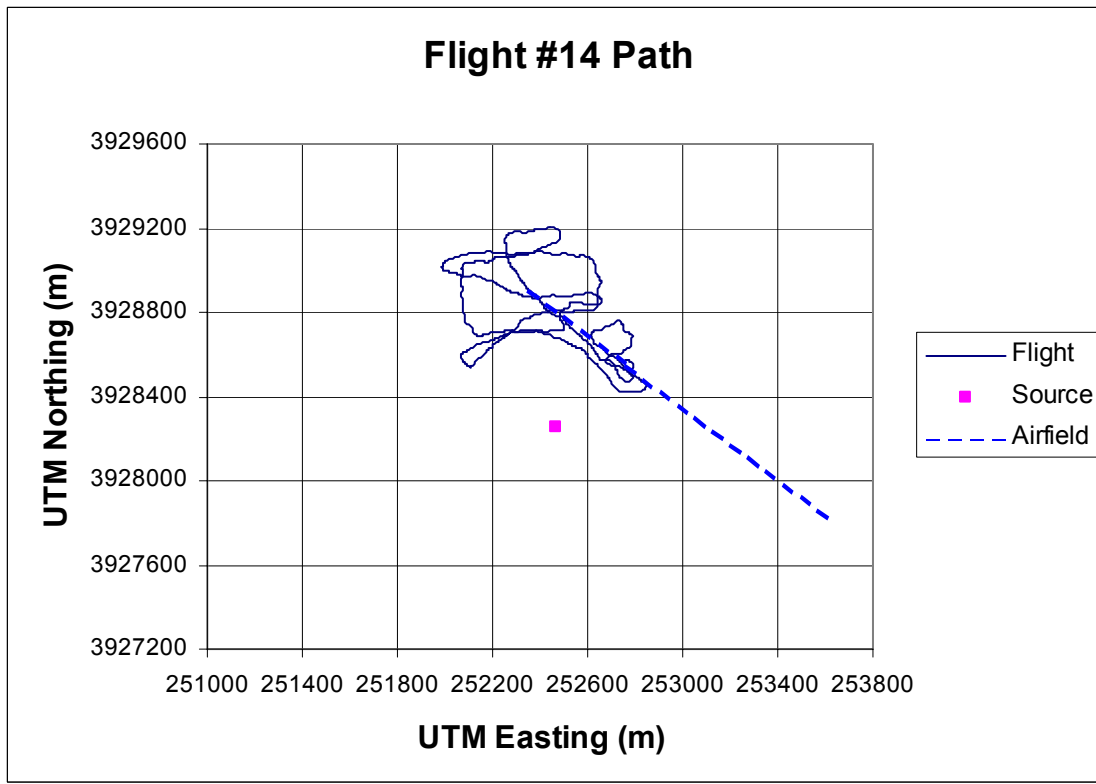
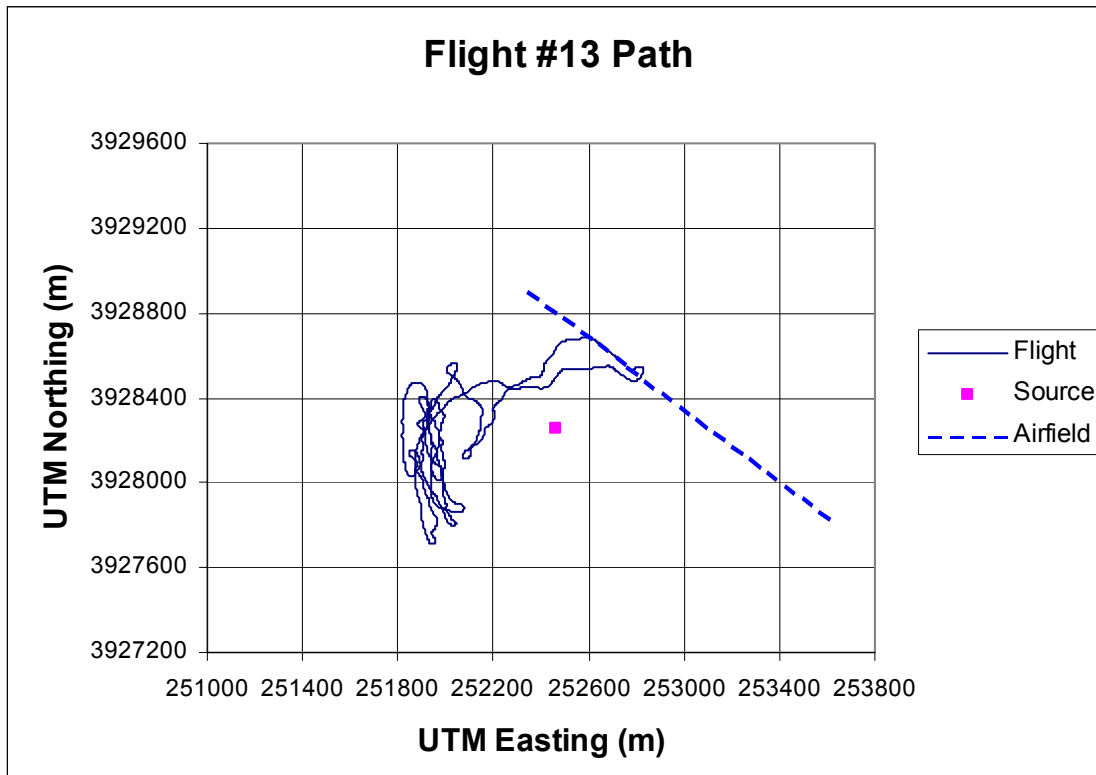


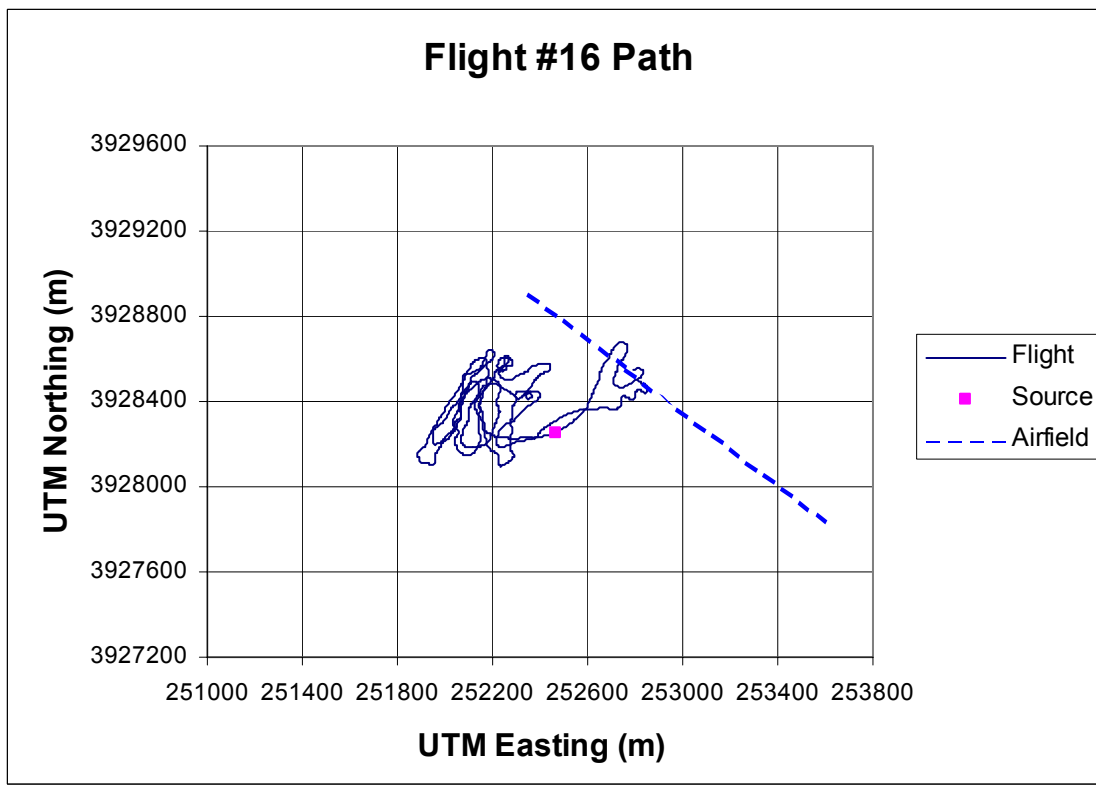
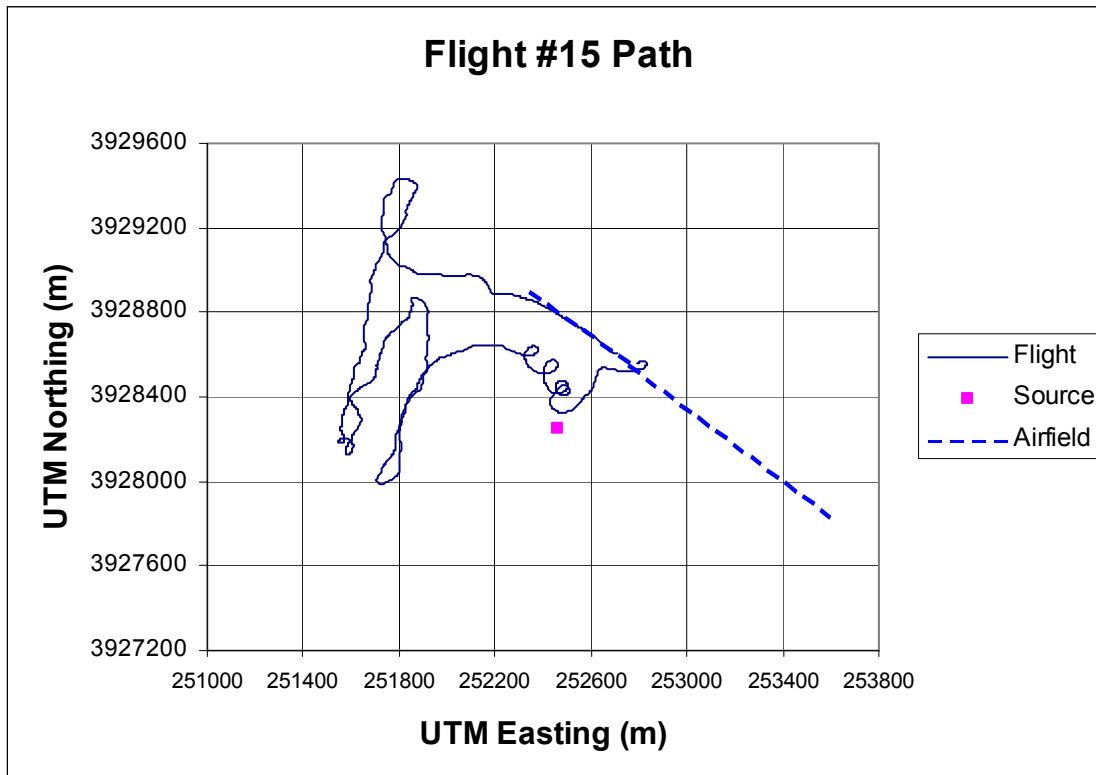


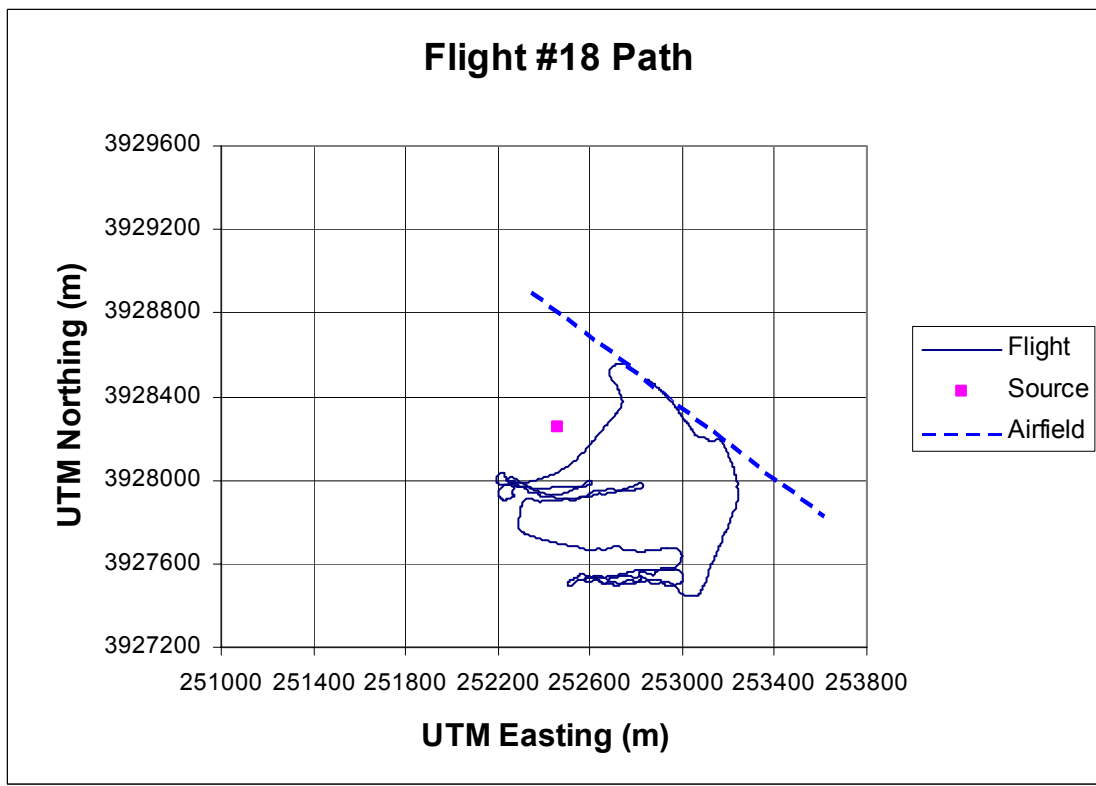
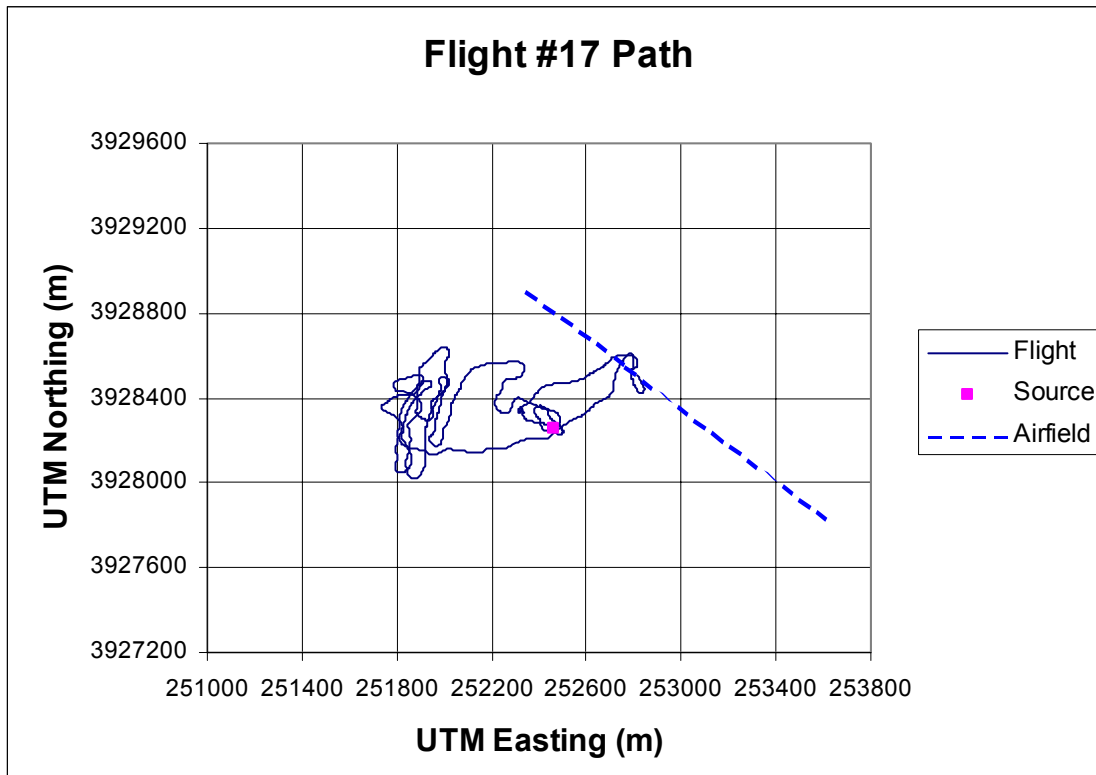


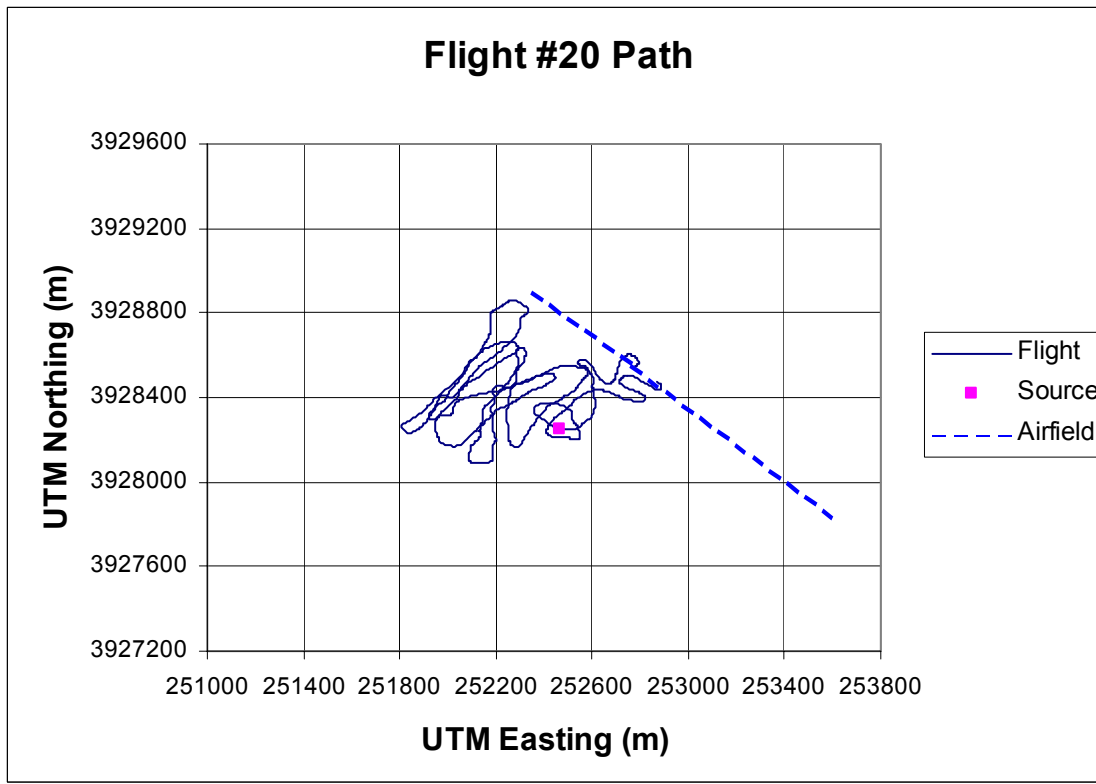
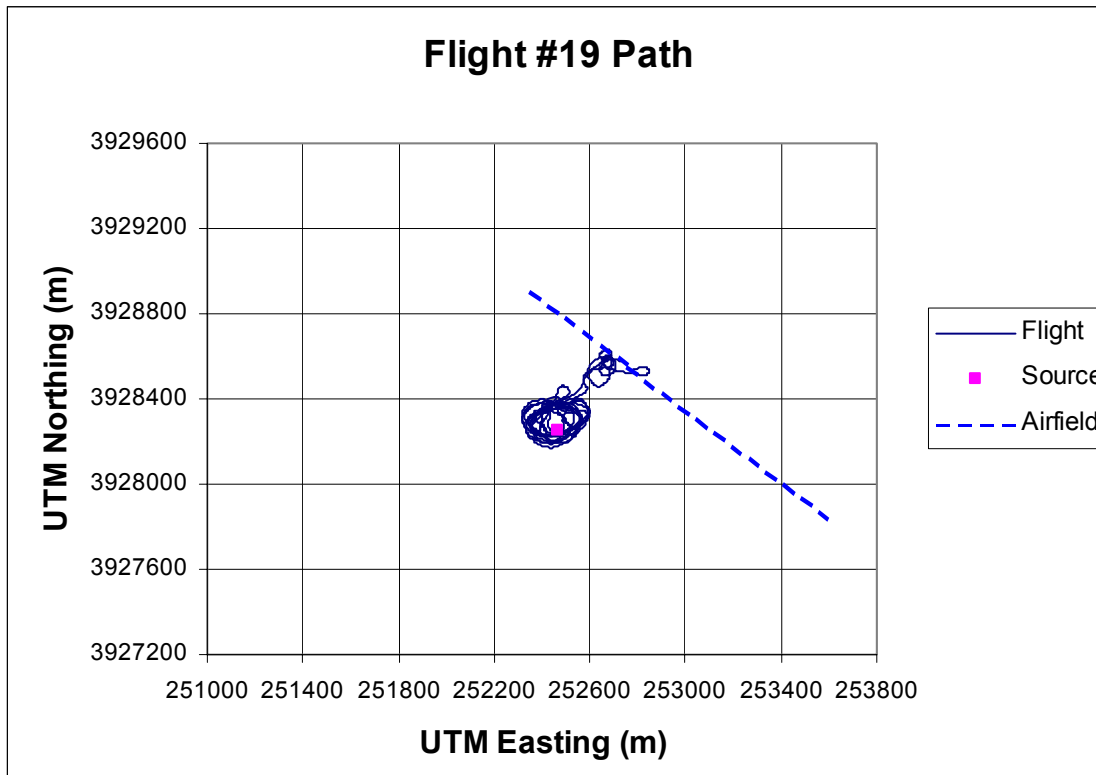


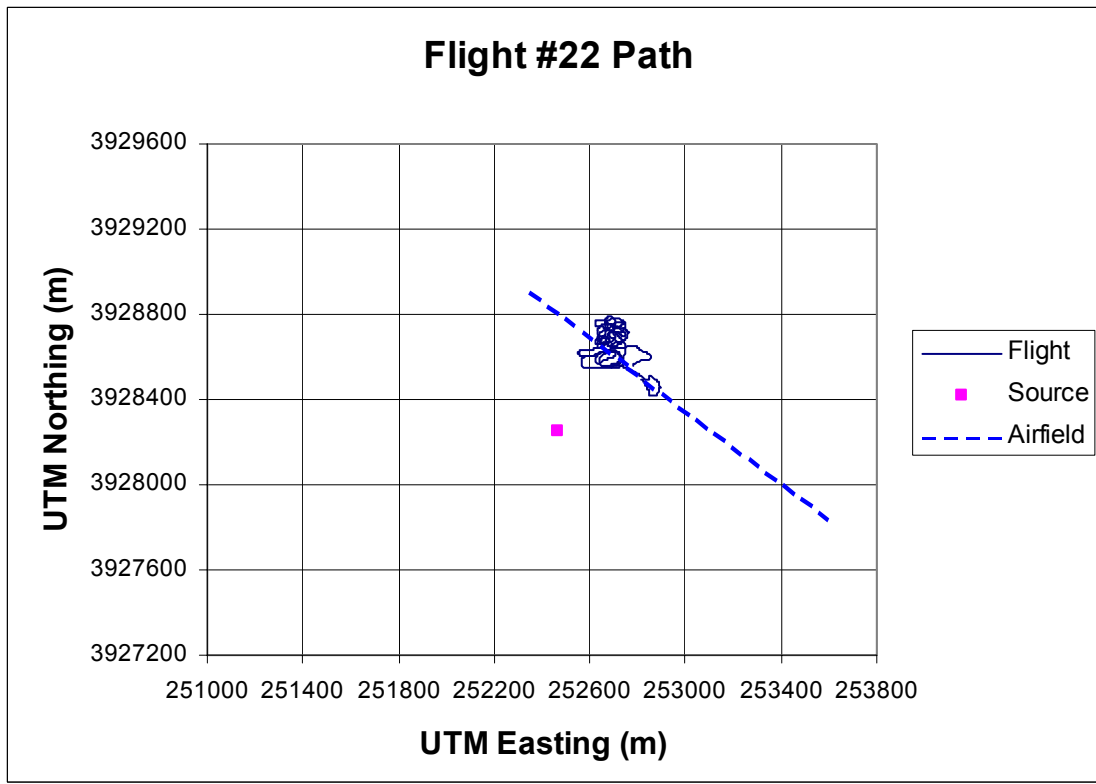
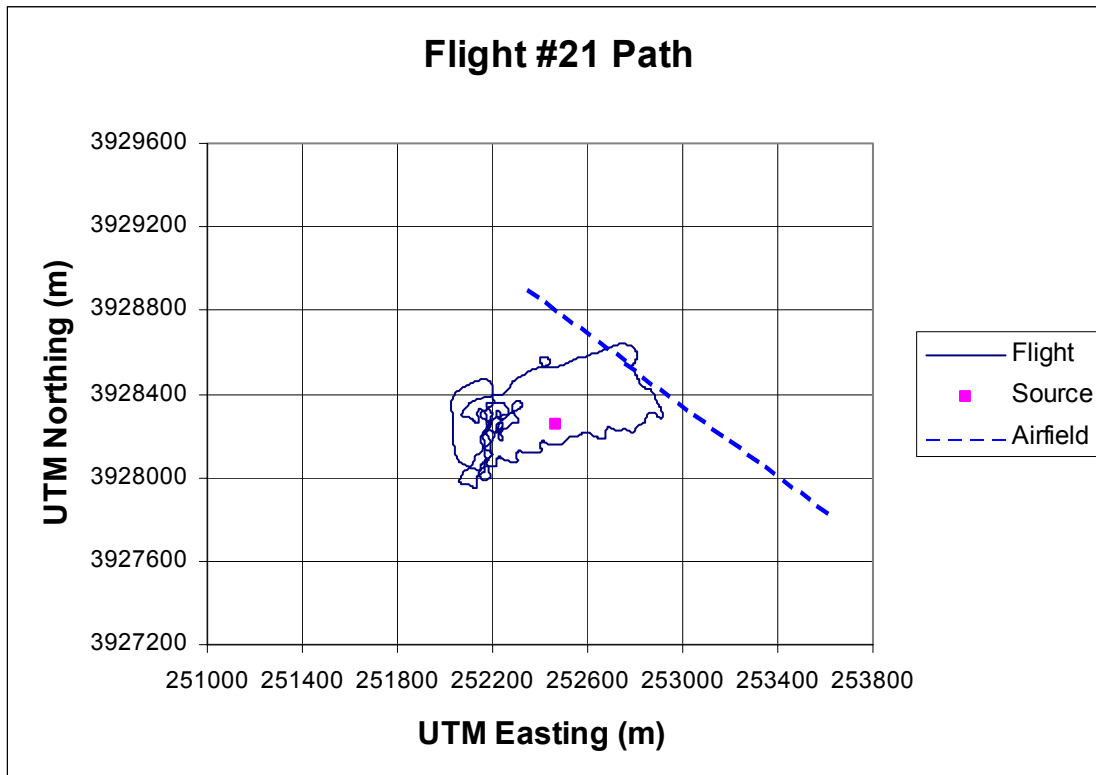


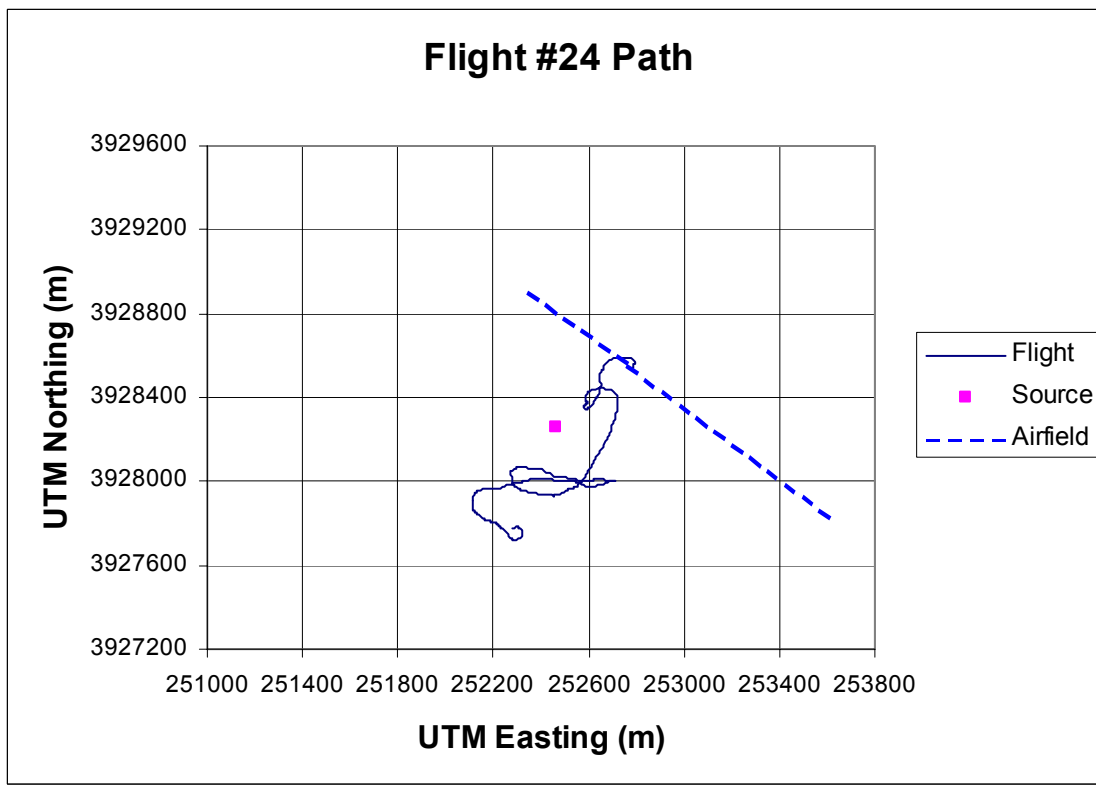
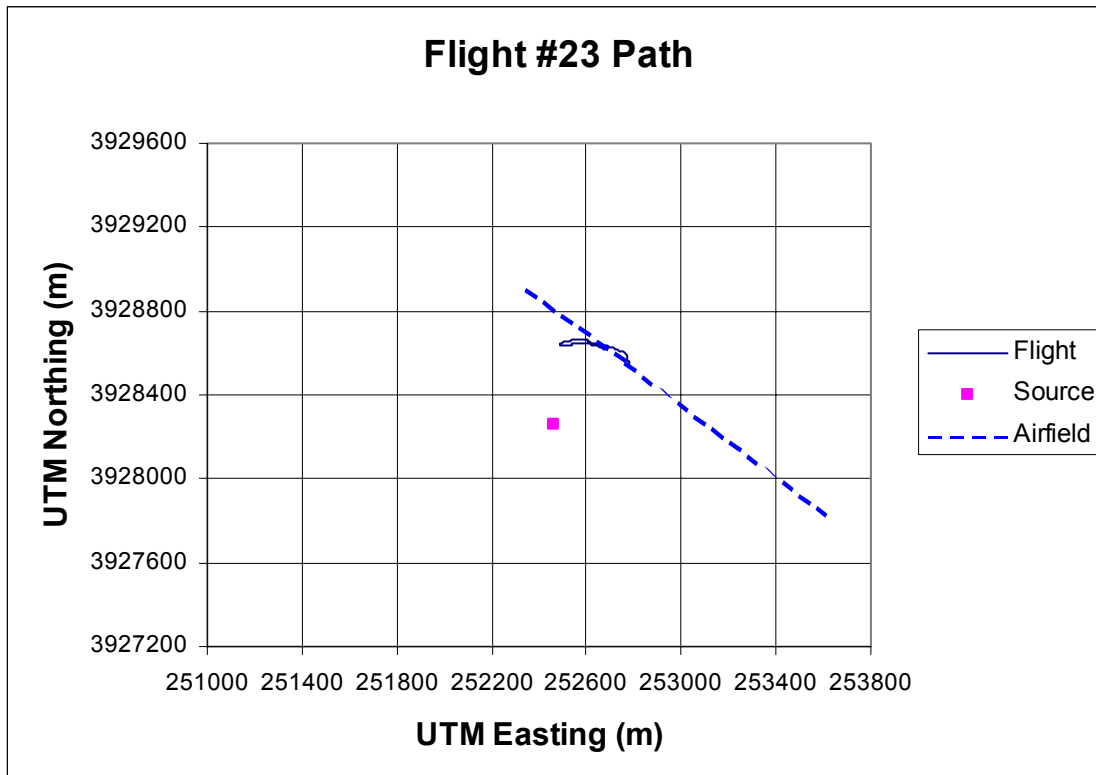


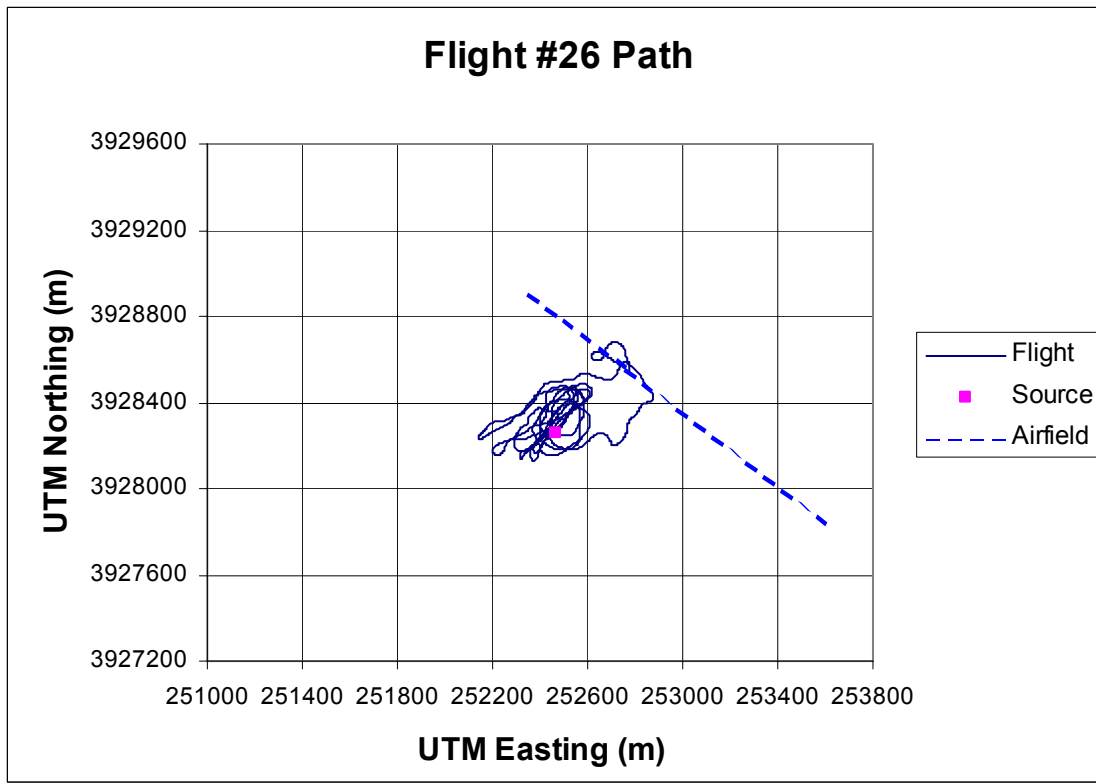
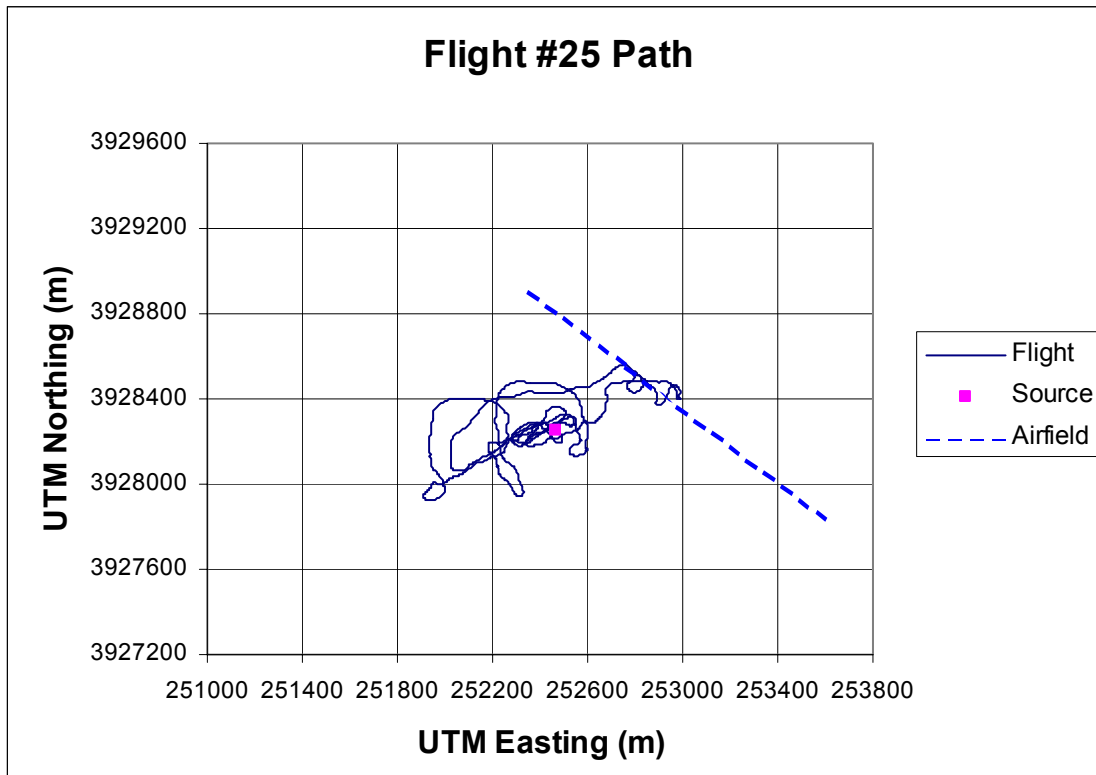


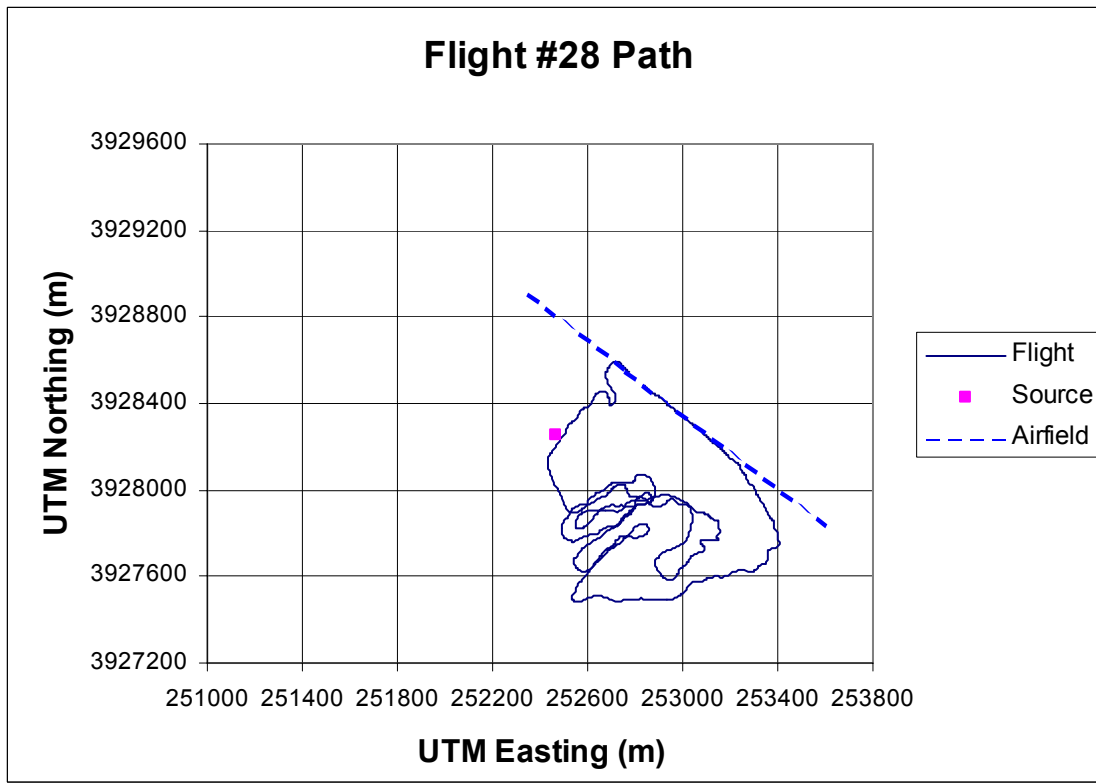
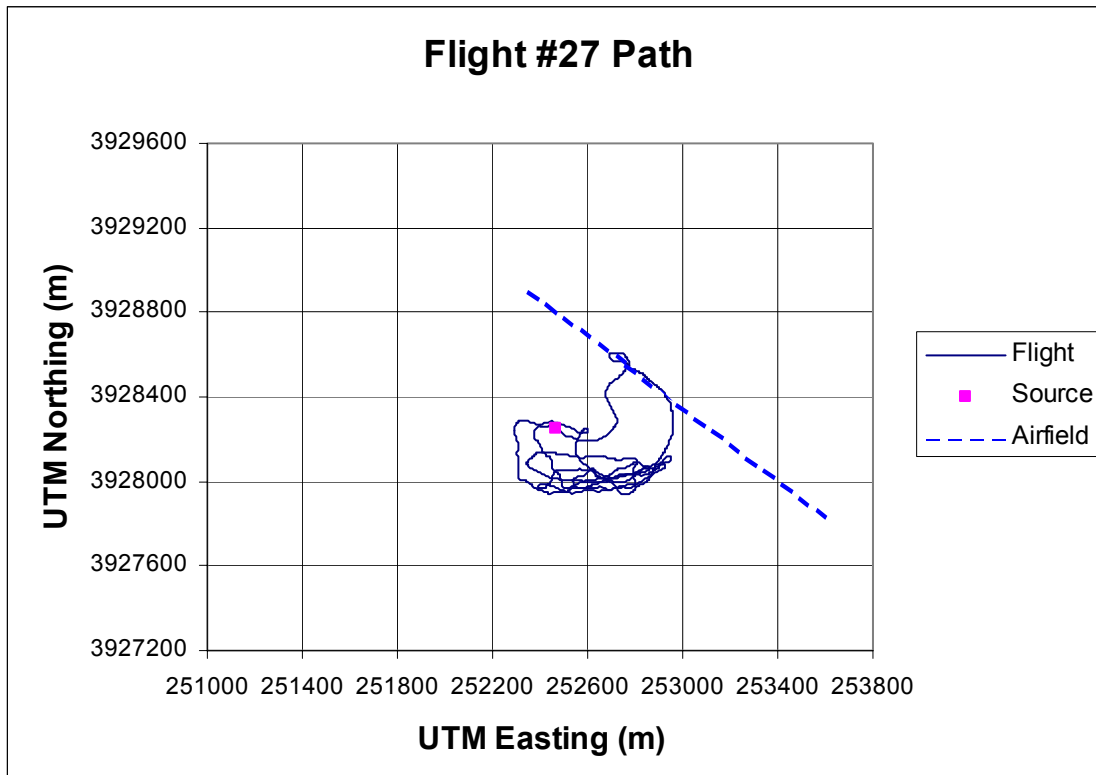






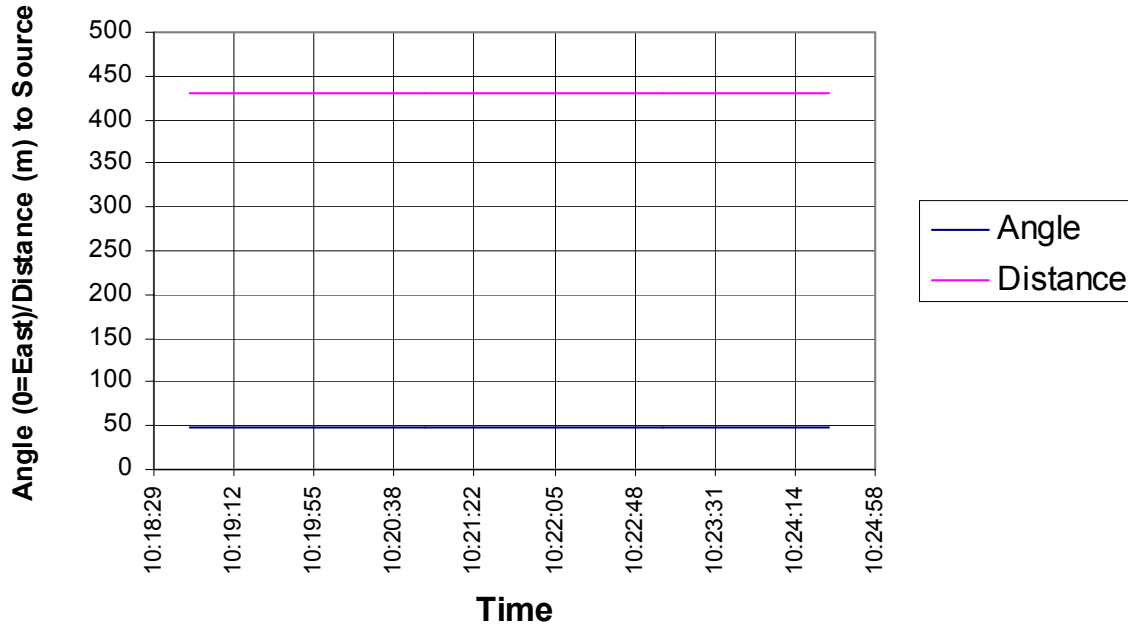
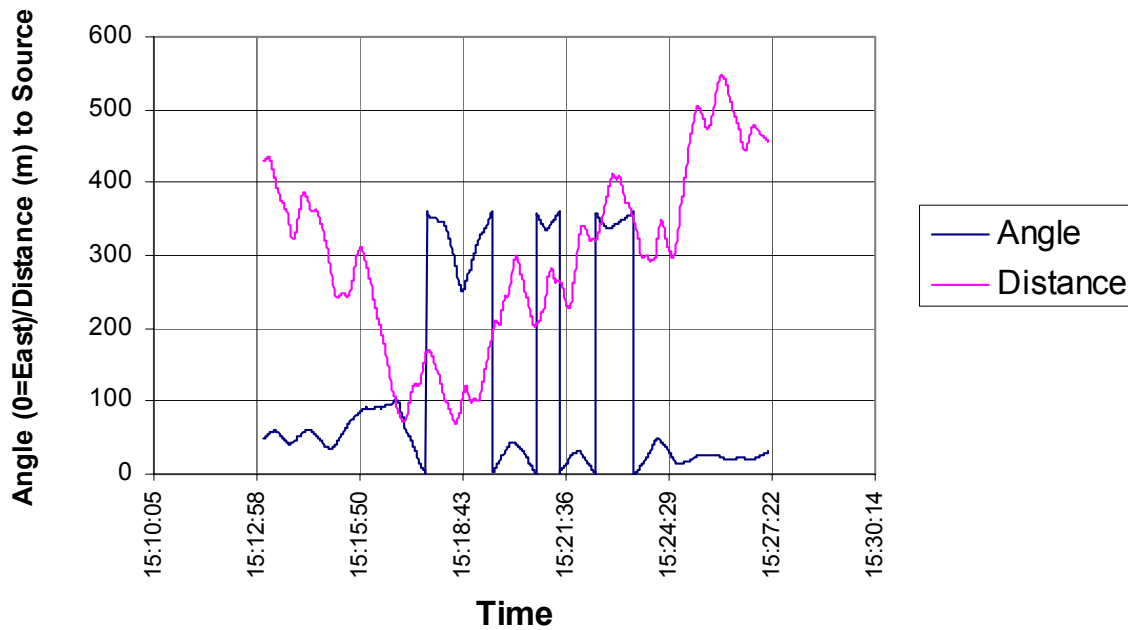


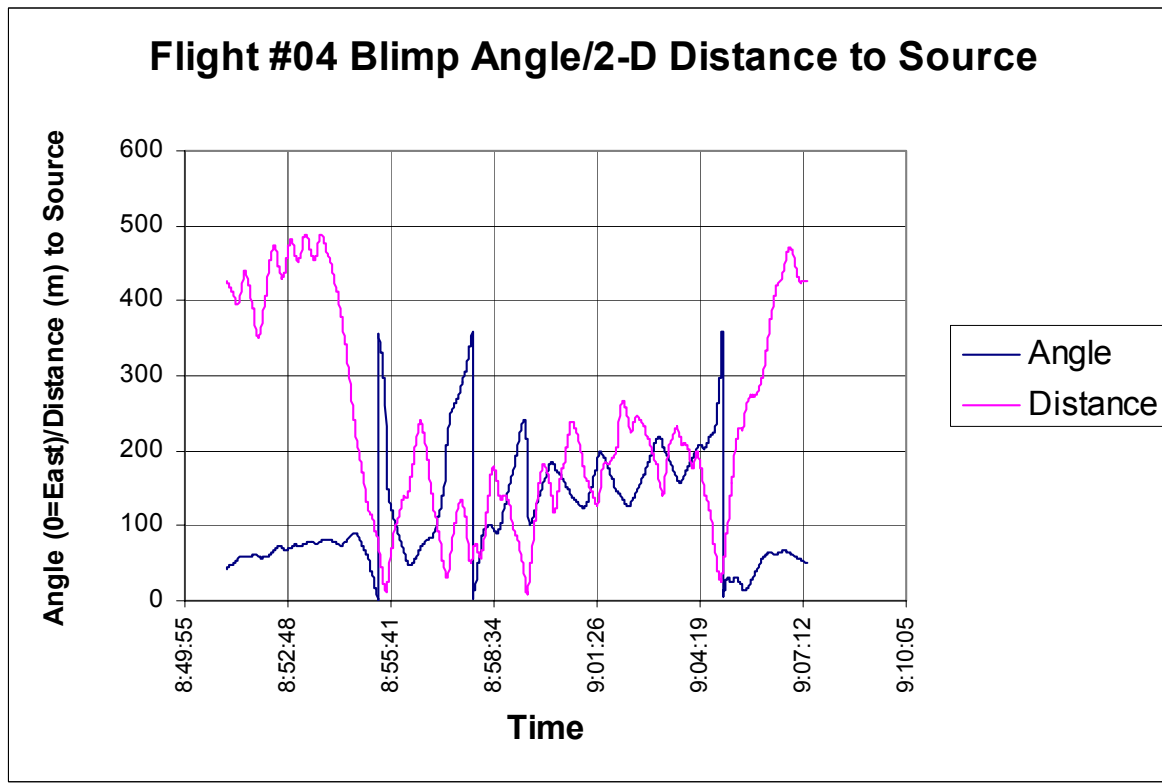
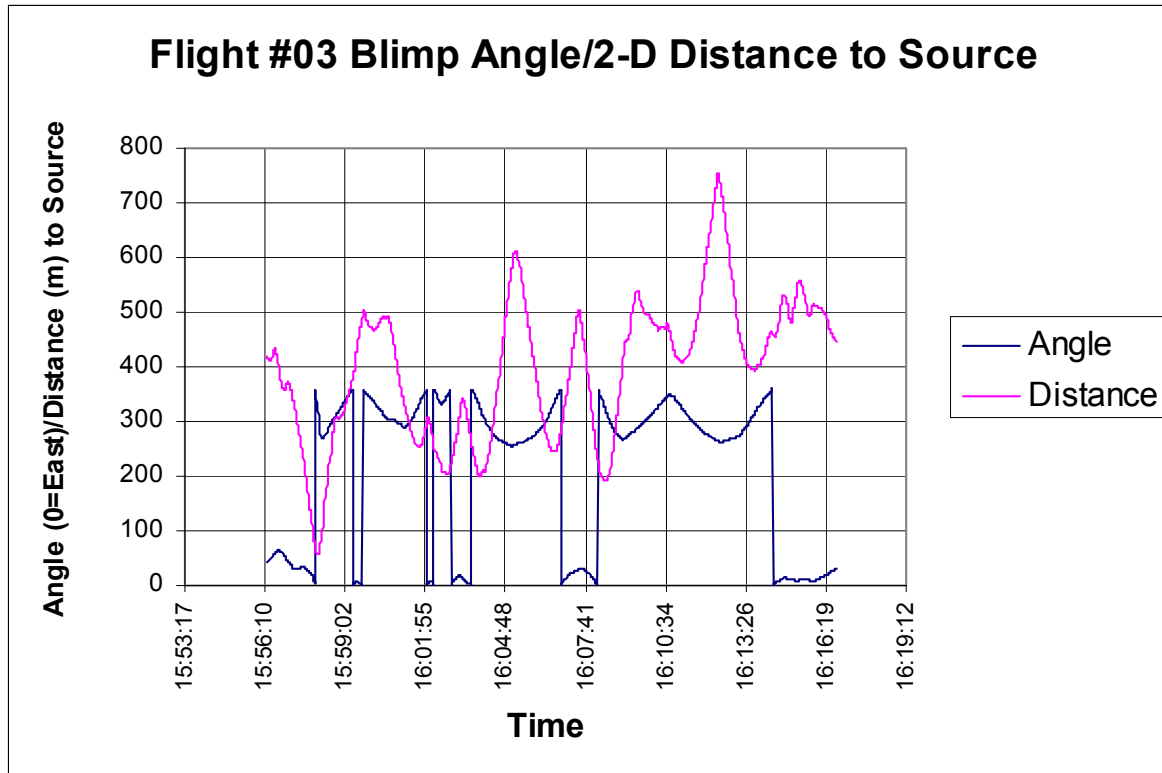




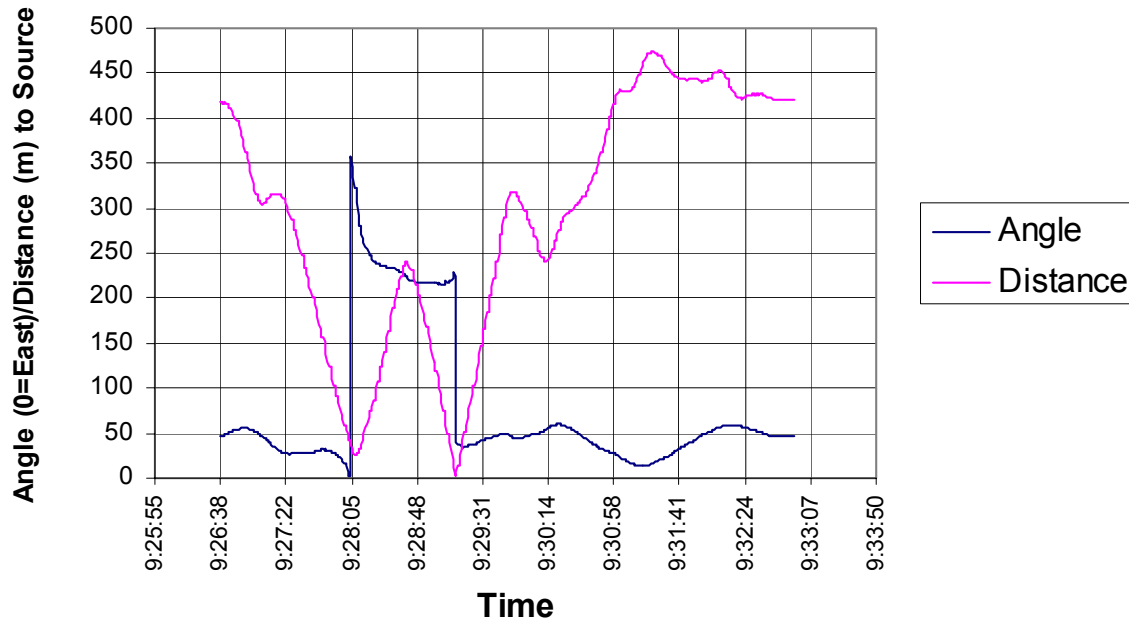
APPENDIX B

FLIGHT PATH DISTANCE & ANGLE GRAPHS

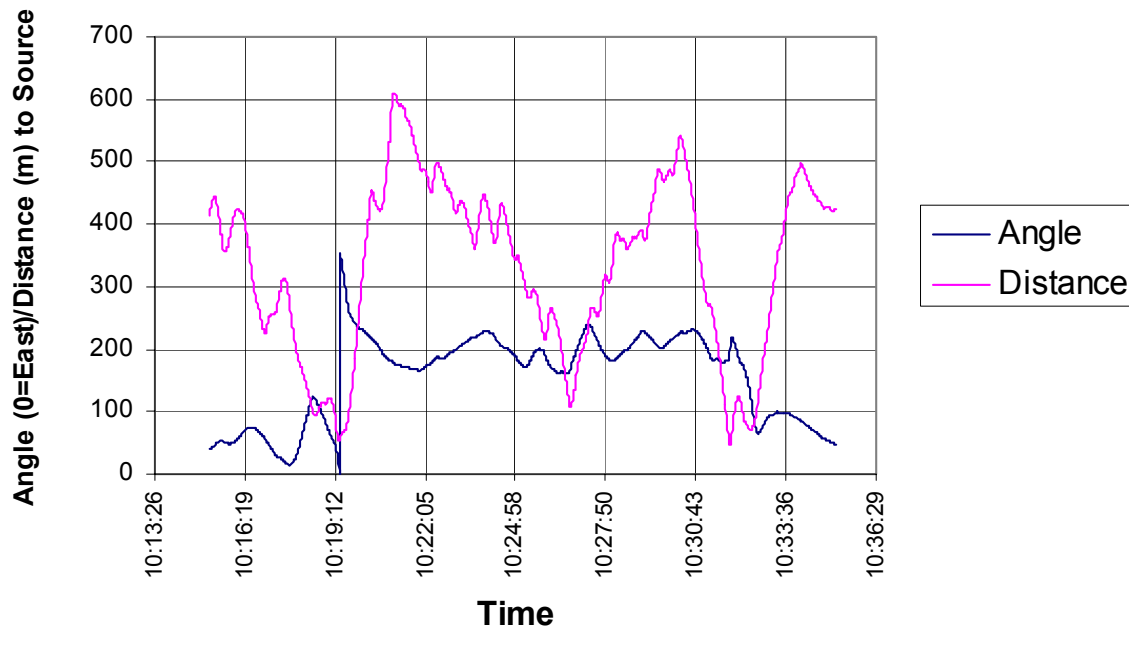
Flight #01 Blimp Angle/2-D Distance to Source**Flight #02 Blimp Angle/2-D Distance to Source**



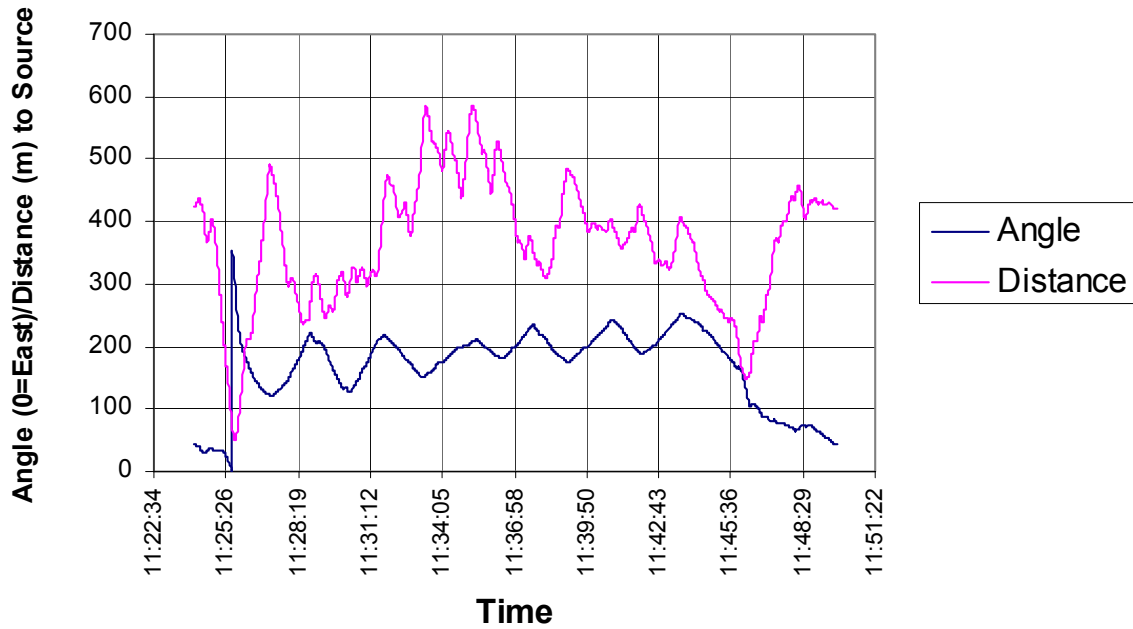
Flight #05 Blimp Angle/2-D Distance to Source



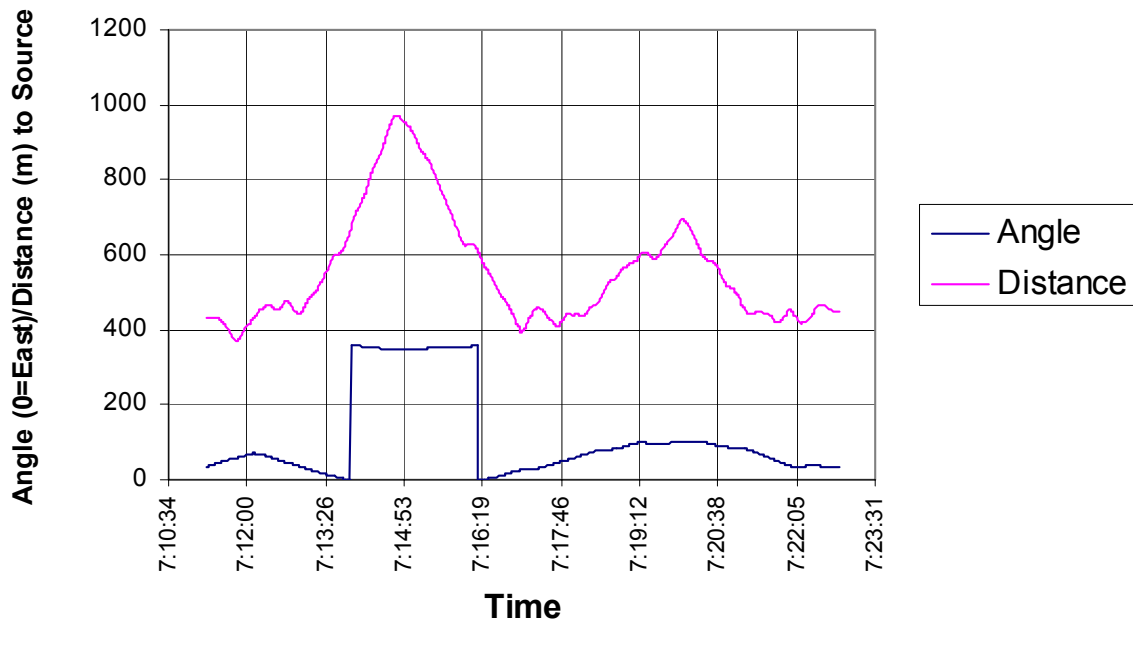
Flight #06 Blimp Angle/2-D Distance to Source



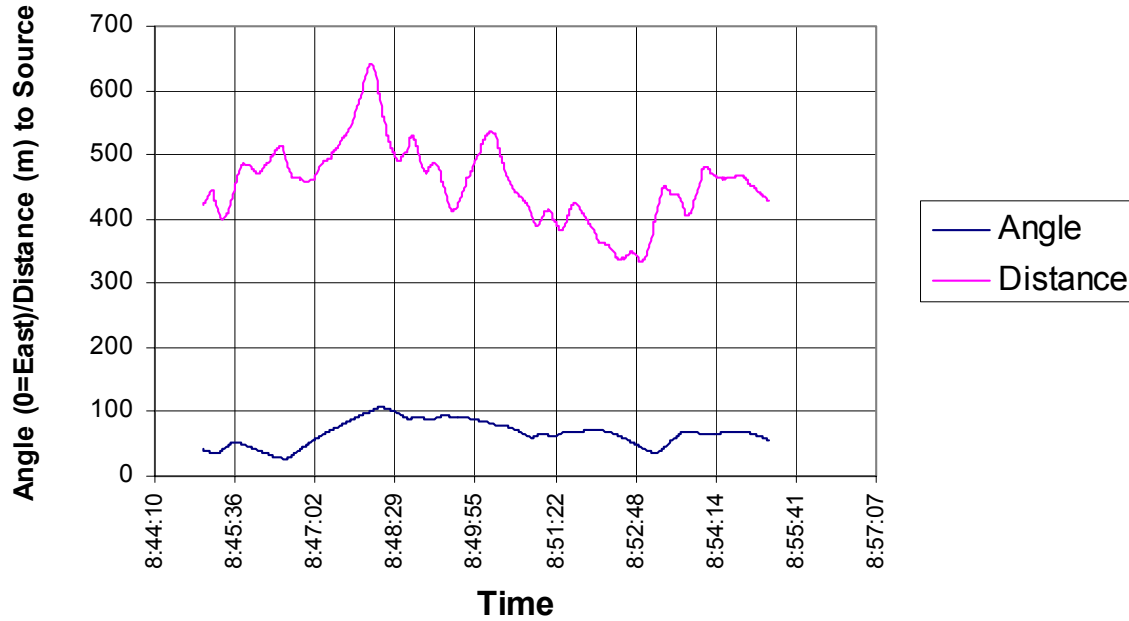
Flight #07 Blimp Angle/2-D Distance to Source



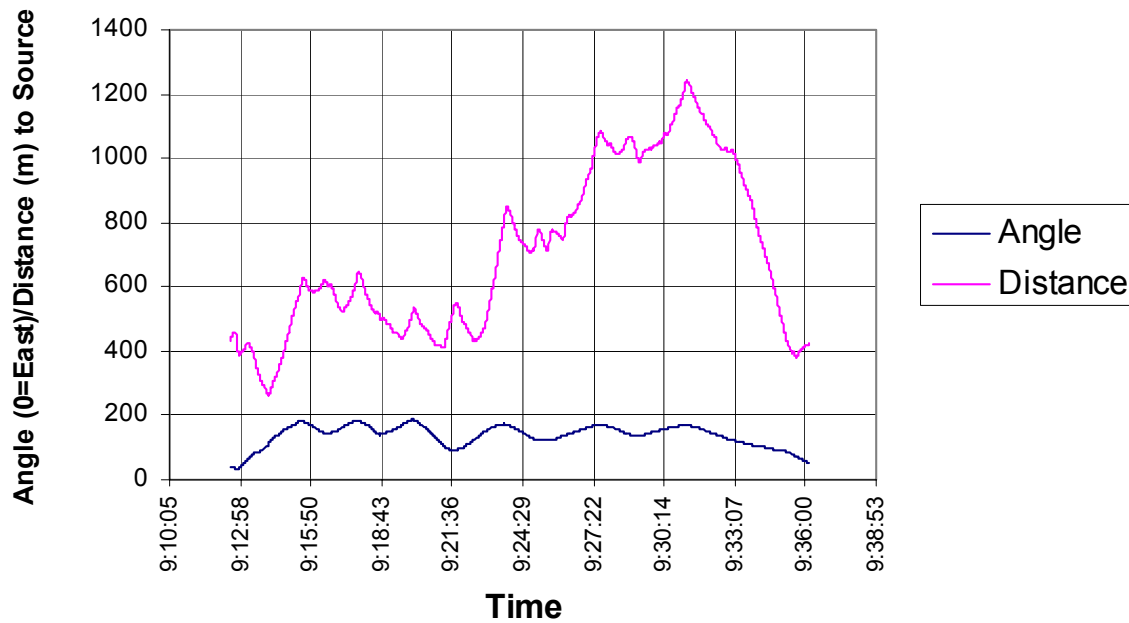
Flight #08 Blimp Angle/2-D Distance to Source



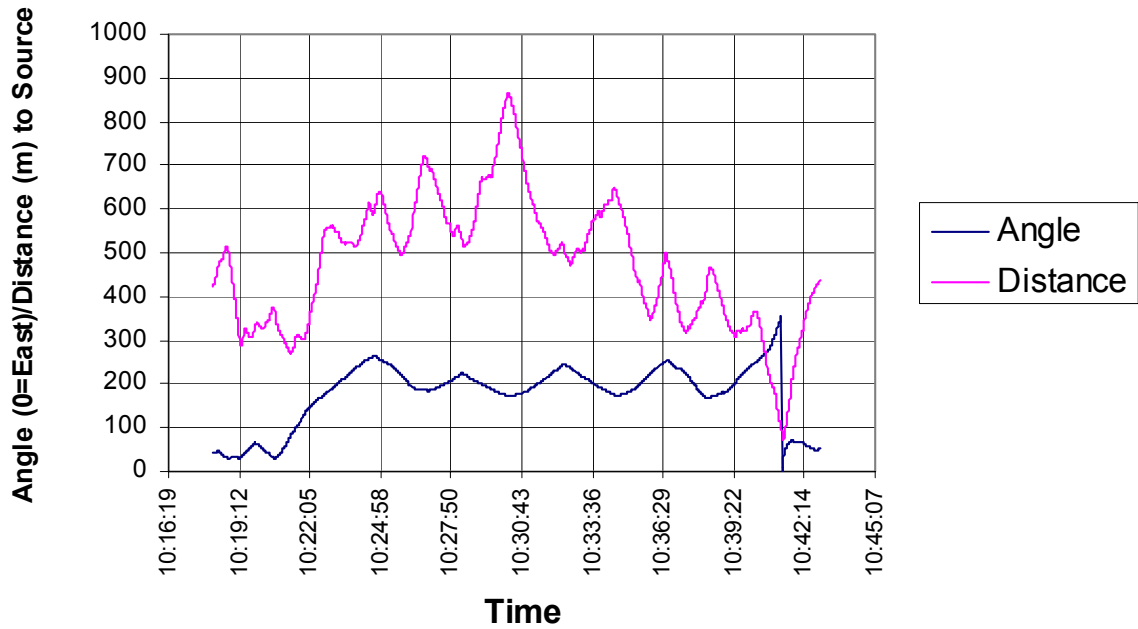
Flight #09 Blimp Angle/2-D Distance to Source



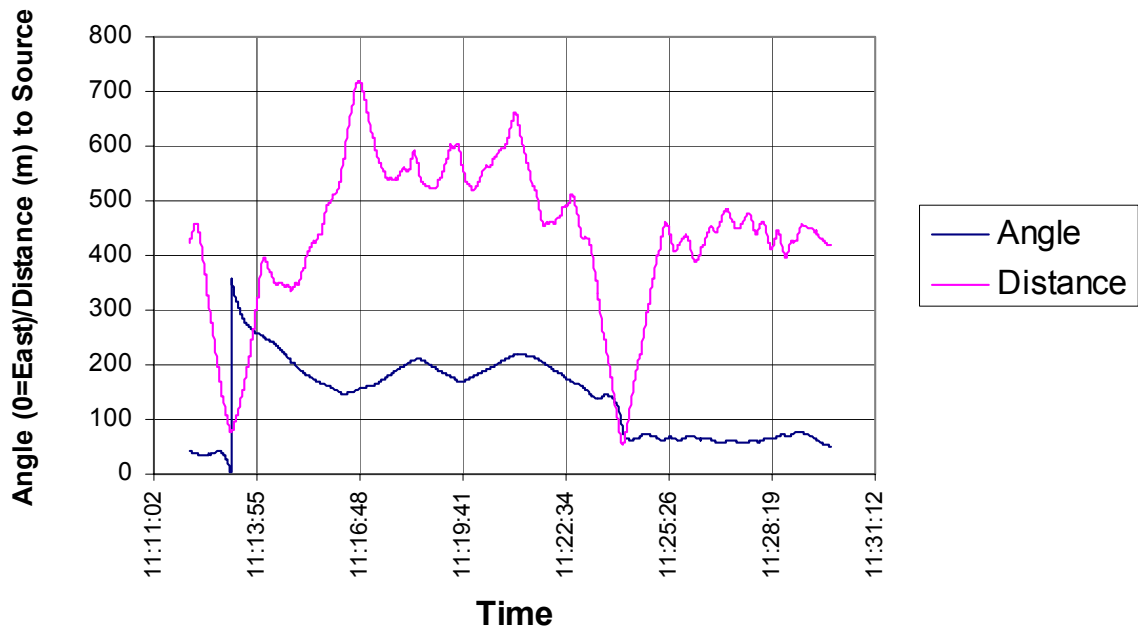
Flight #10 Blimp Angle/2-D Distance to Source



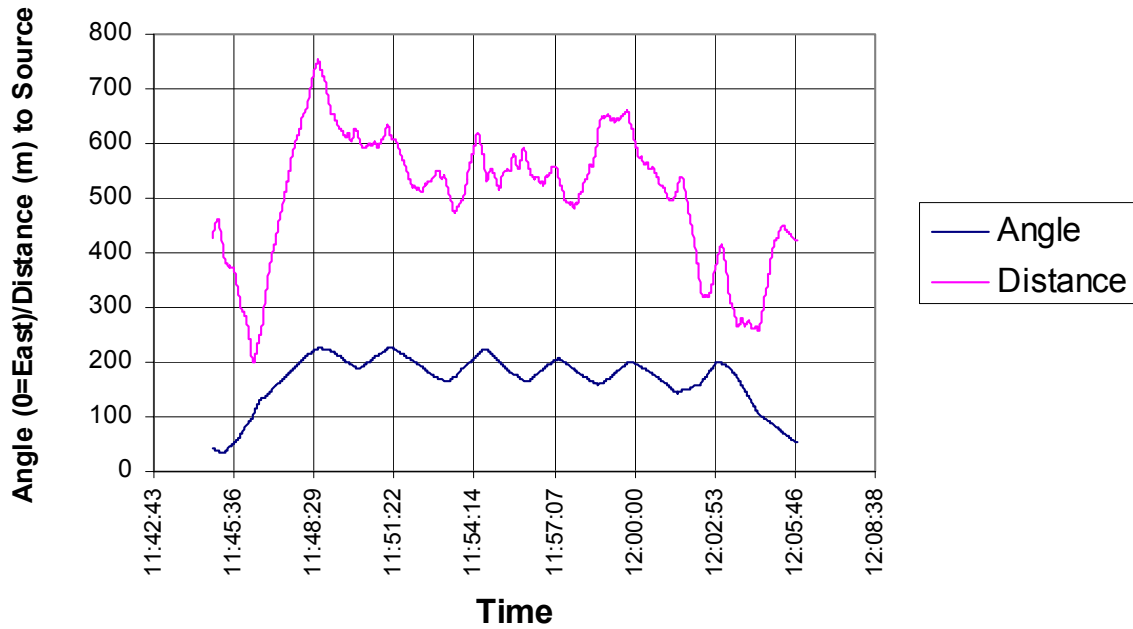
Flight #11 Blimp Angle/2-D Distance to Source



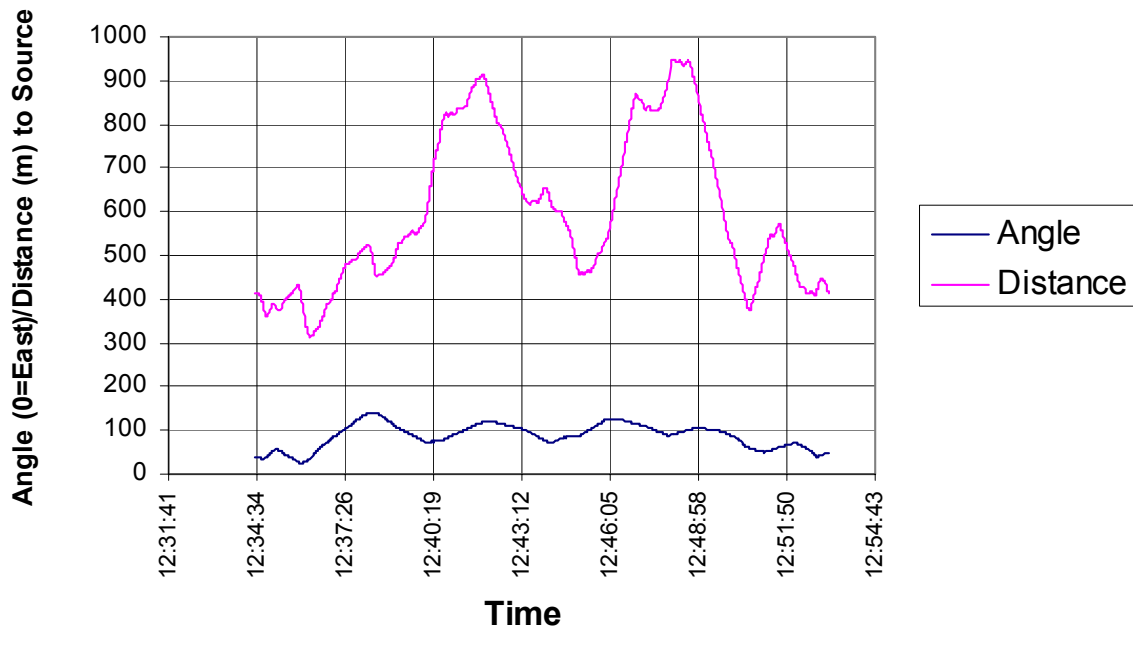
Flight #12 Blimp Angle/2-D Distance to Source



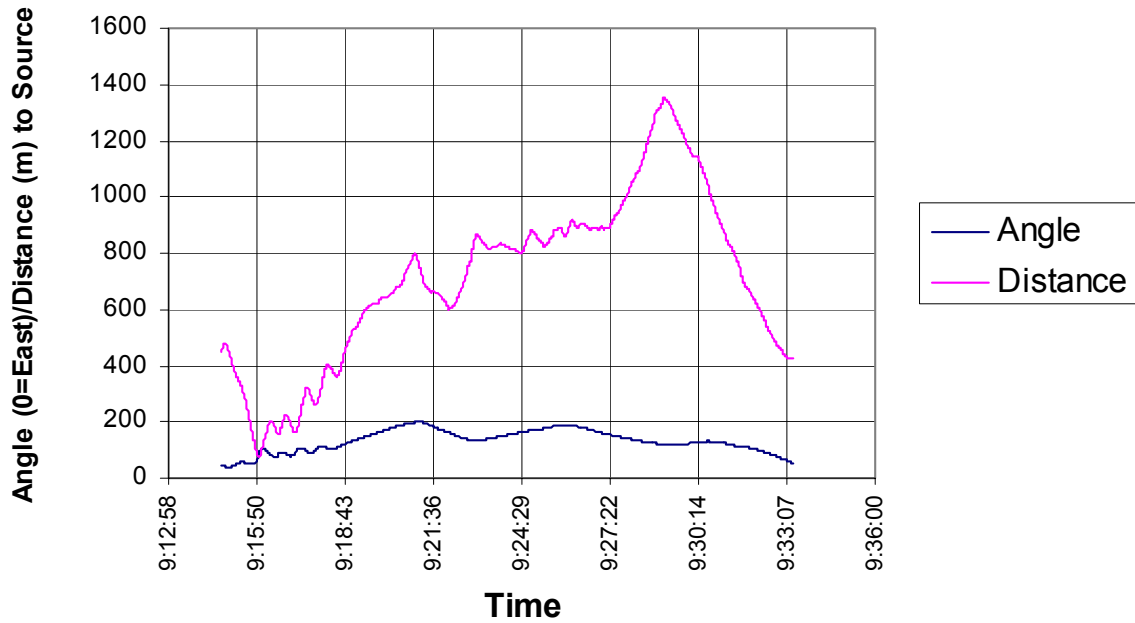
Flight #13 Blimp Angle/2-D Distance to Source



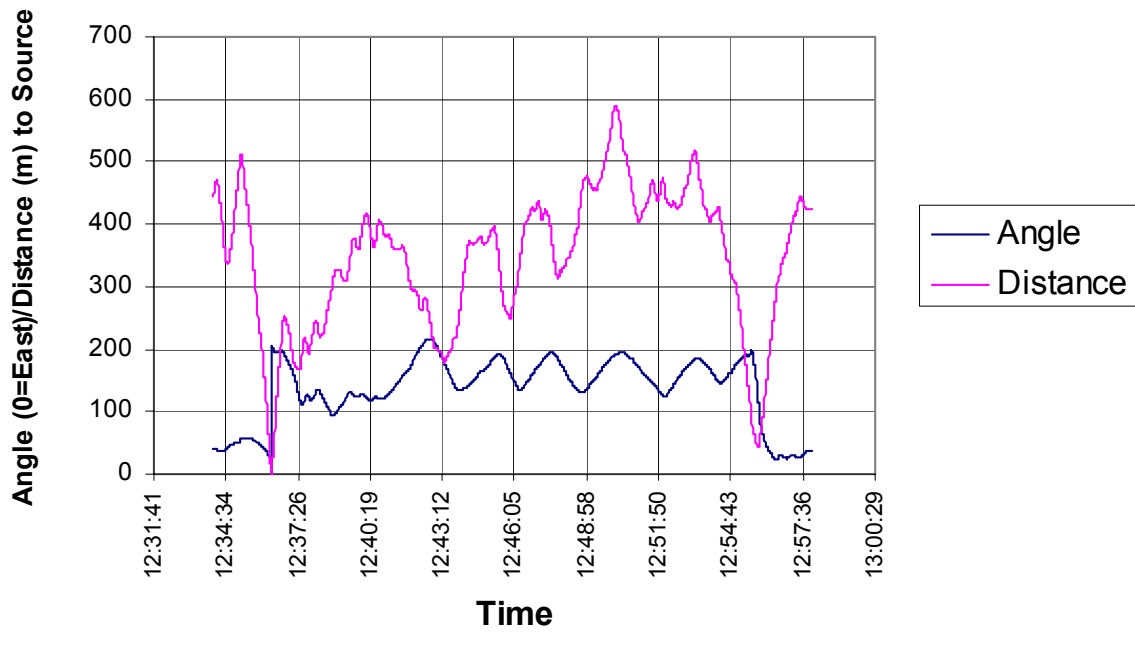
Flight #14 Blimp Angle/2-D Distance to Source

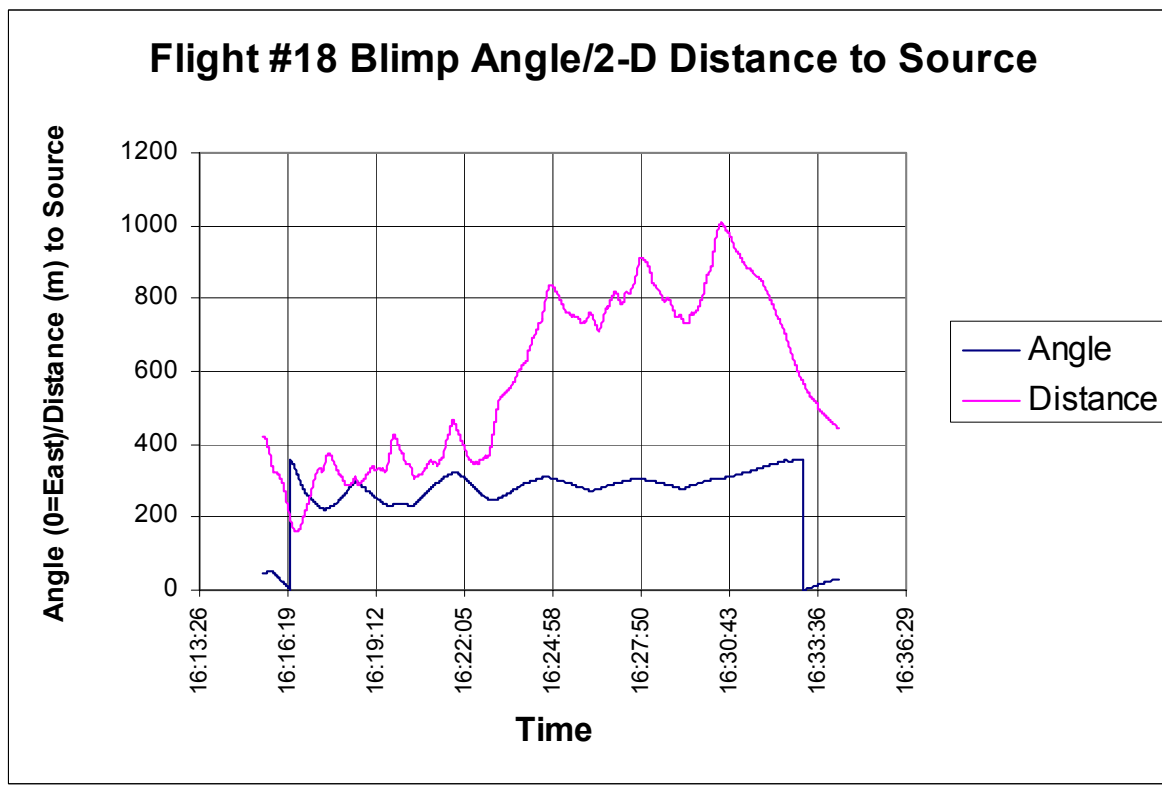
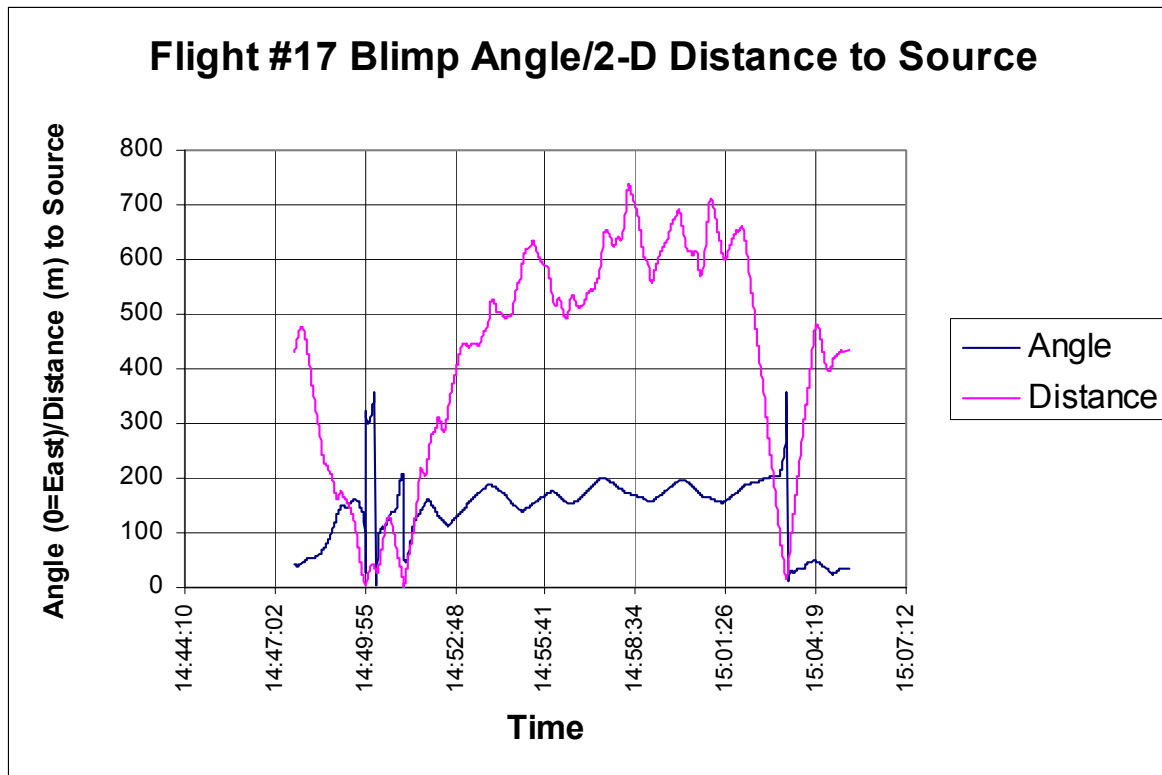


Flight #15 Blimp Angle/2-D Distance to Source

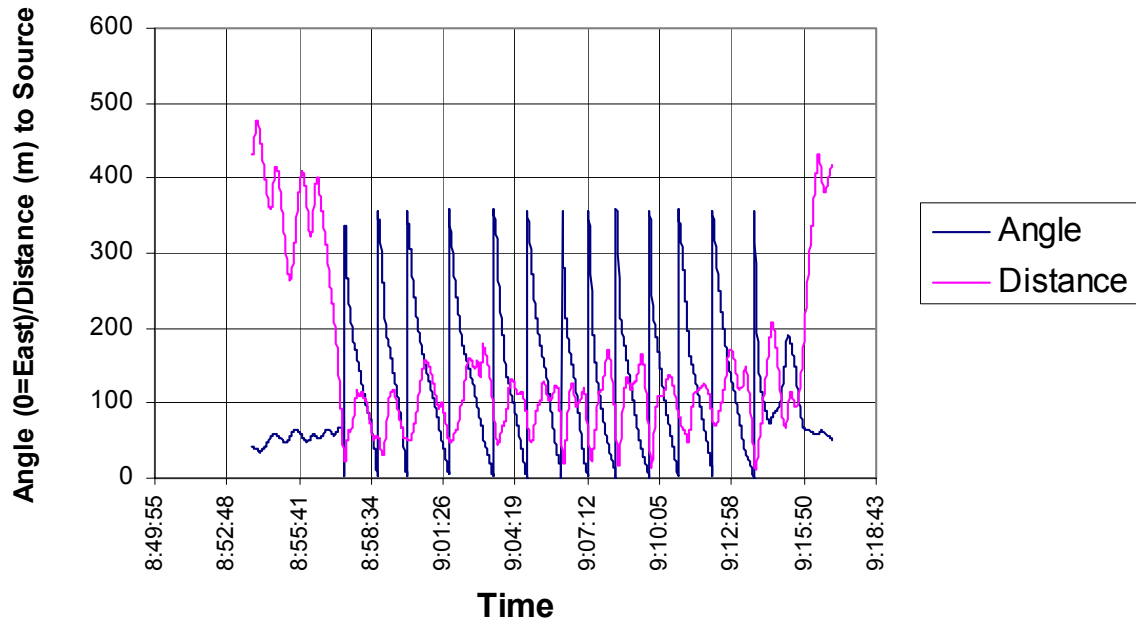


Flight #16 Blimp Angle/2-D Distance to Source

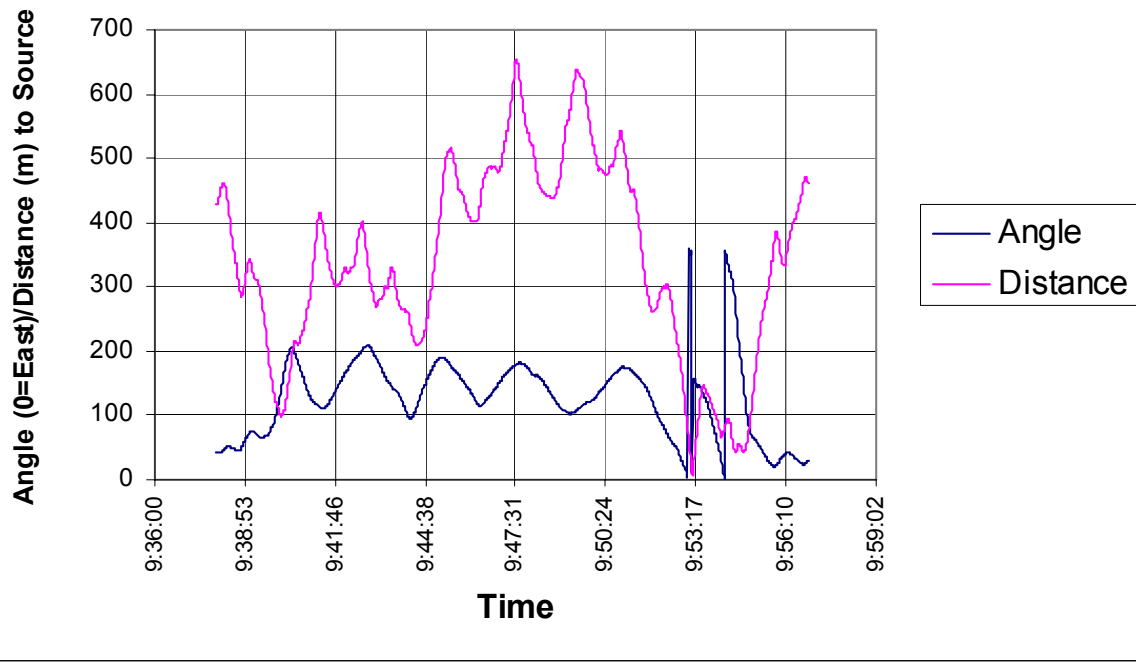


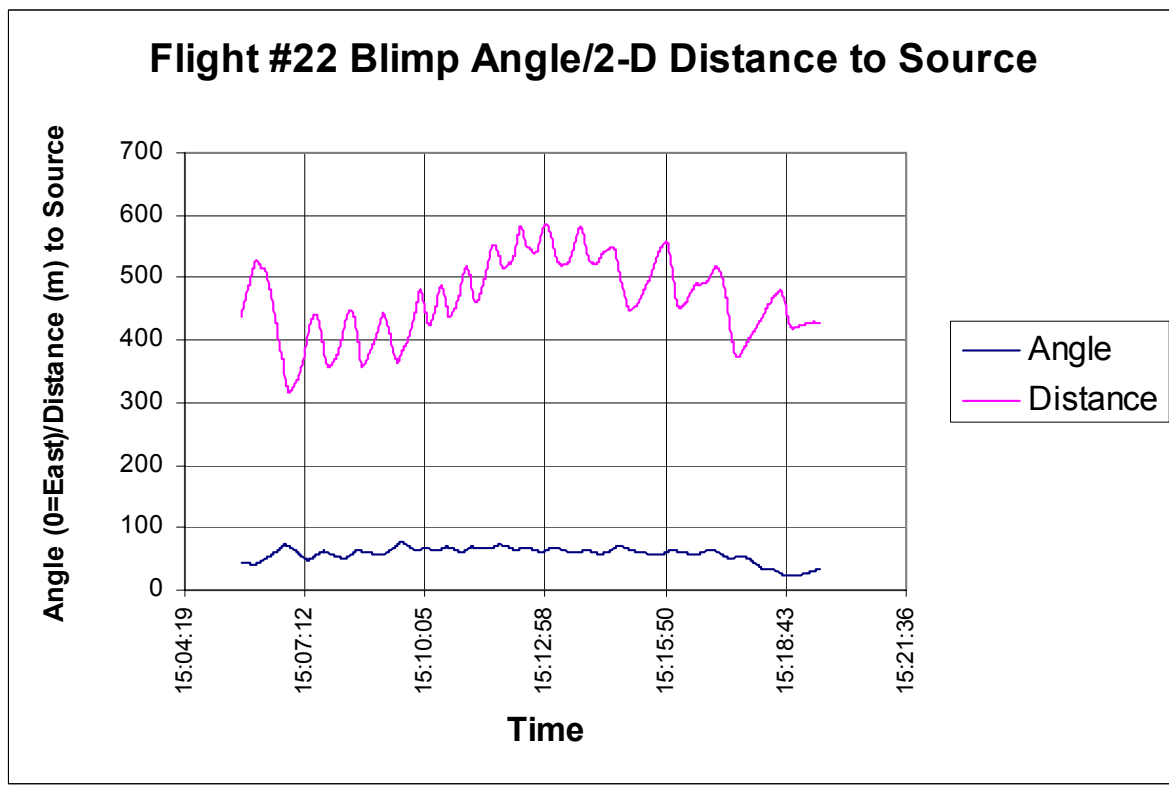
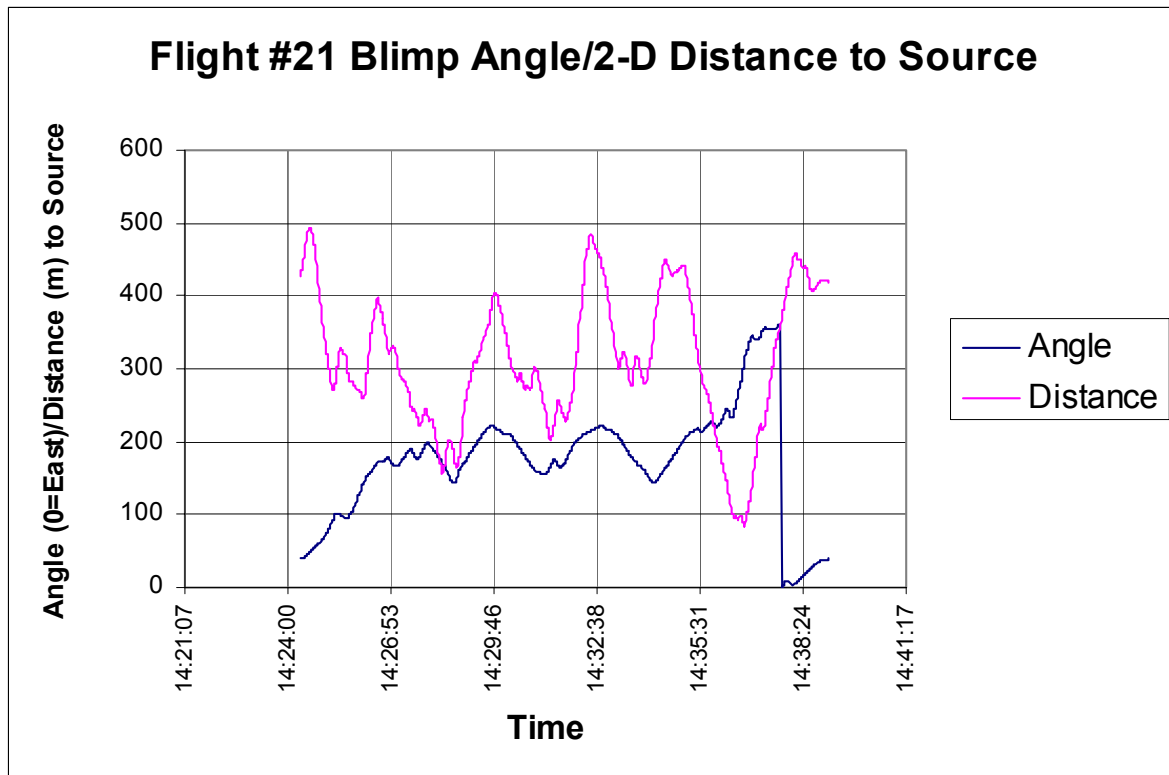


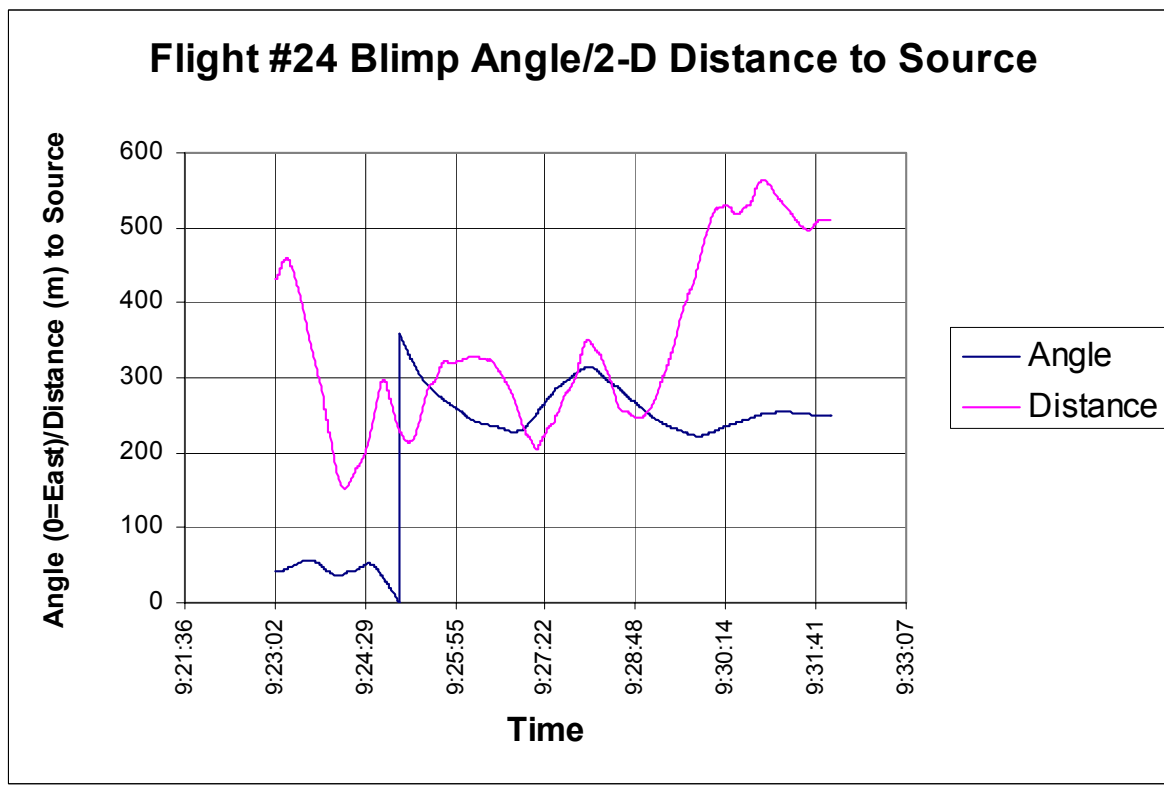
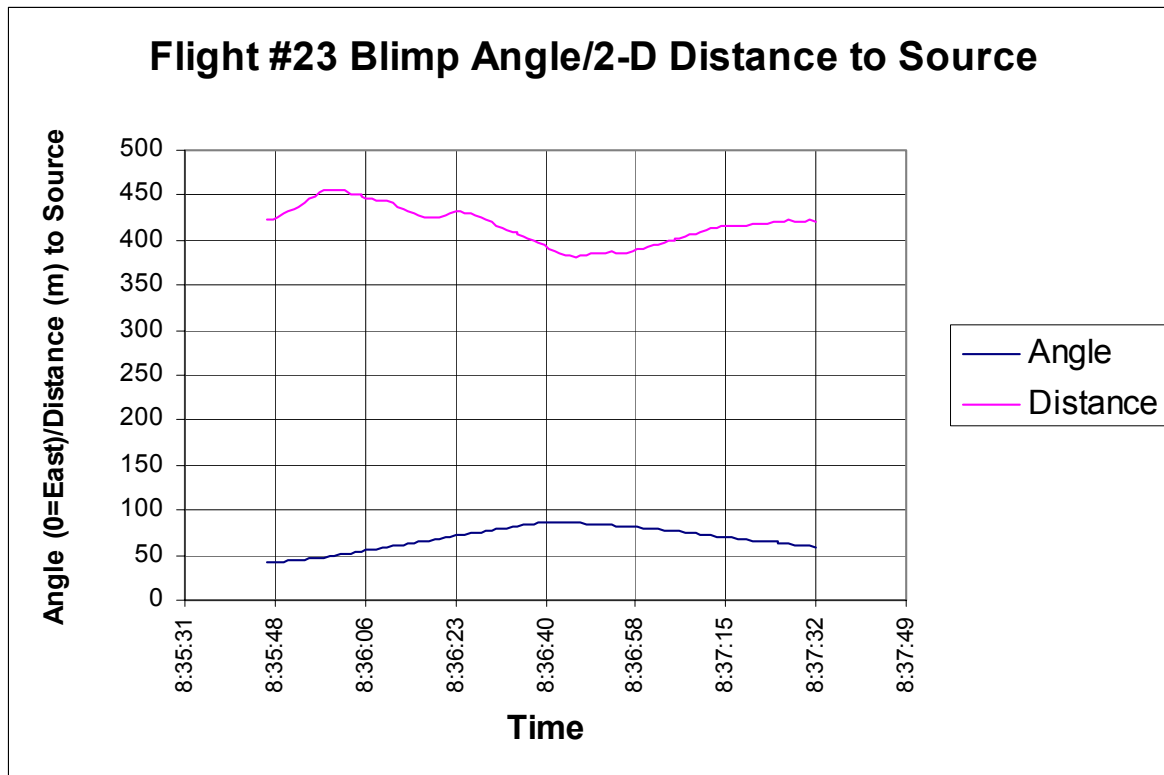
Flight #19 Blimp Angle/2-D Distance to Source

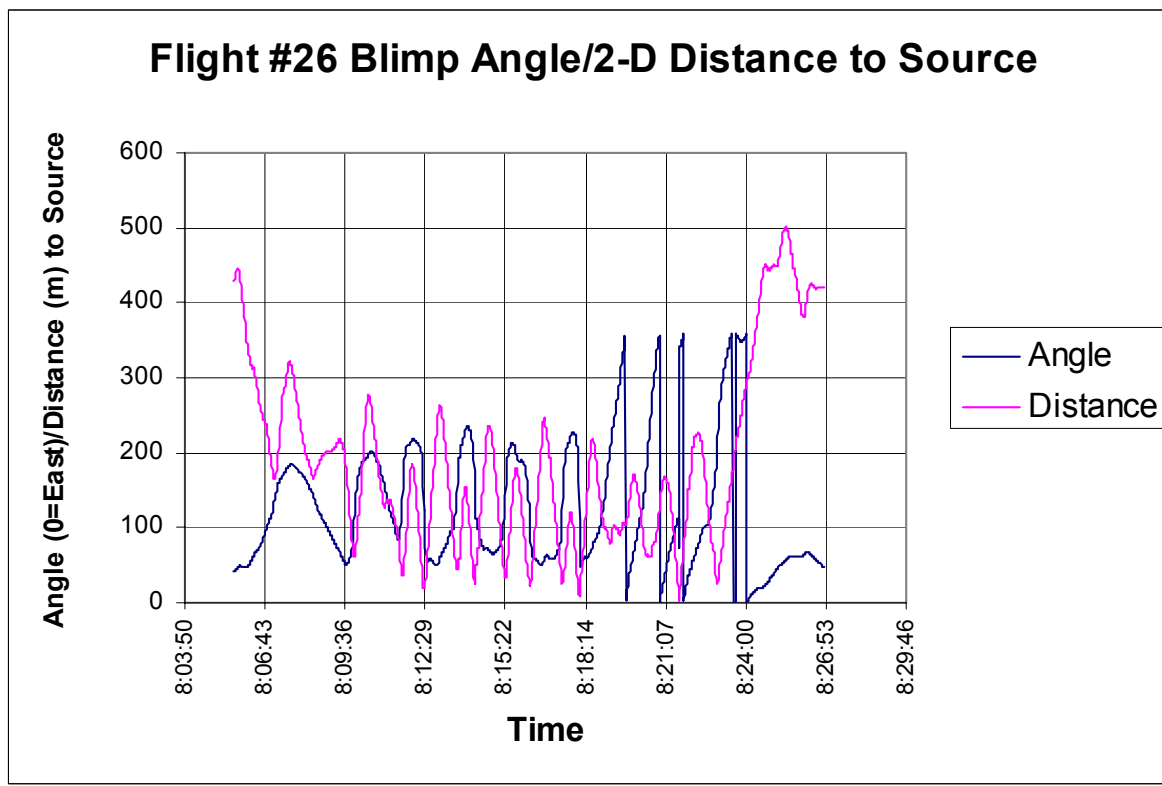
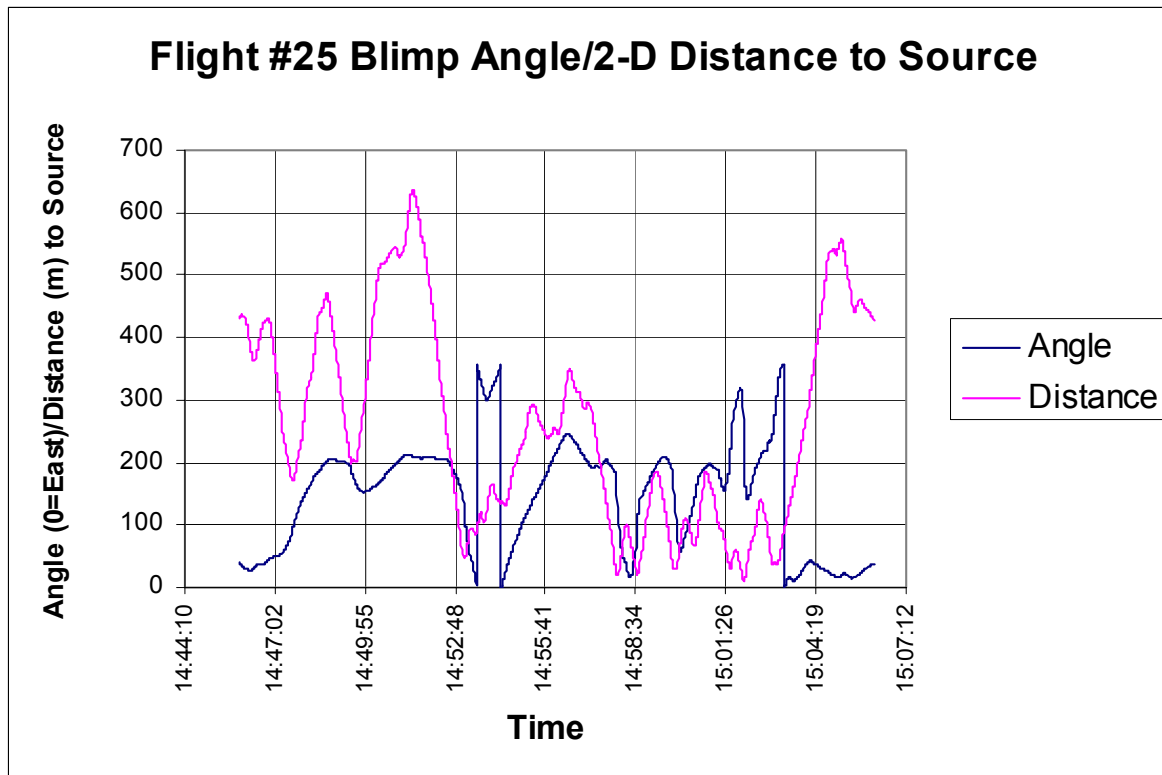


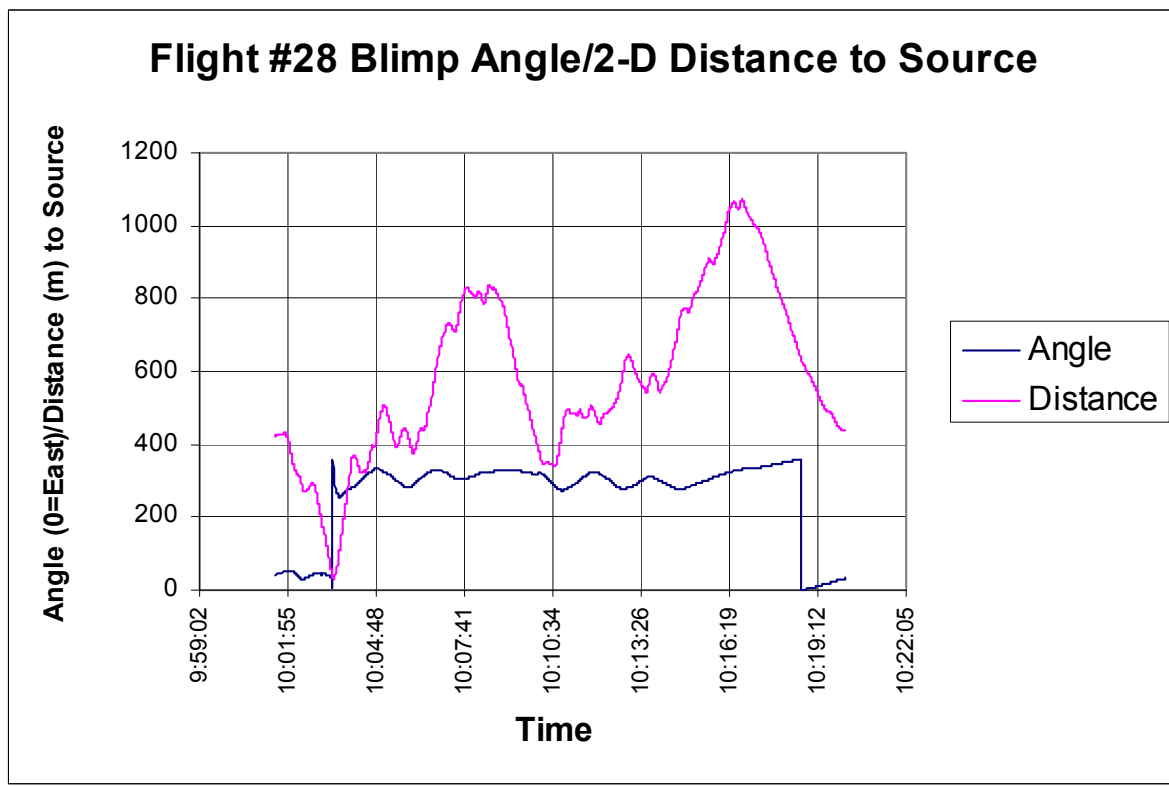
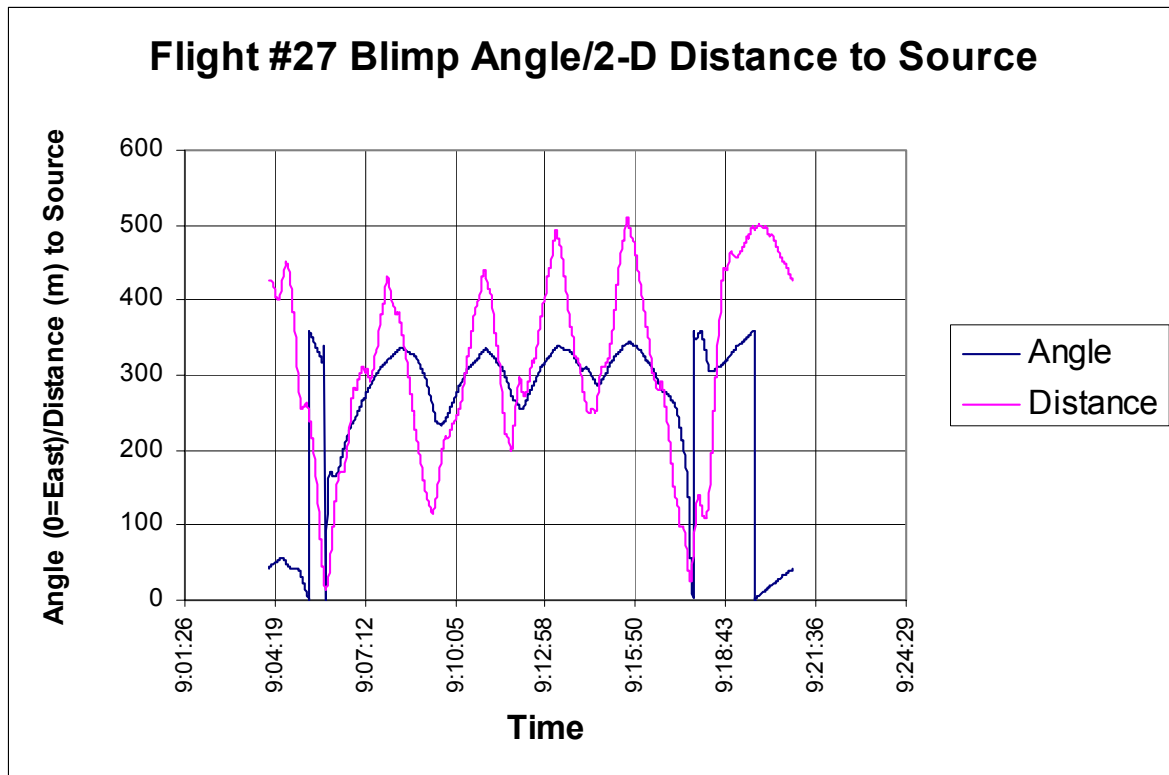
Flight #20 Blimp Angle/2-D Distance to Source



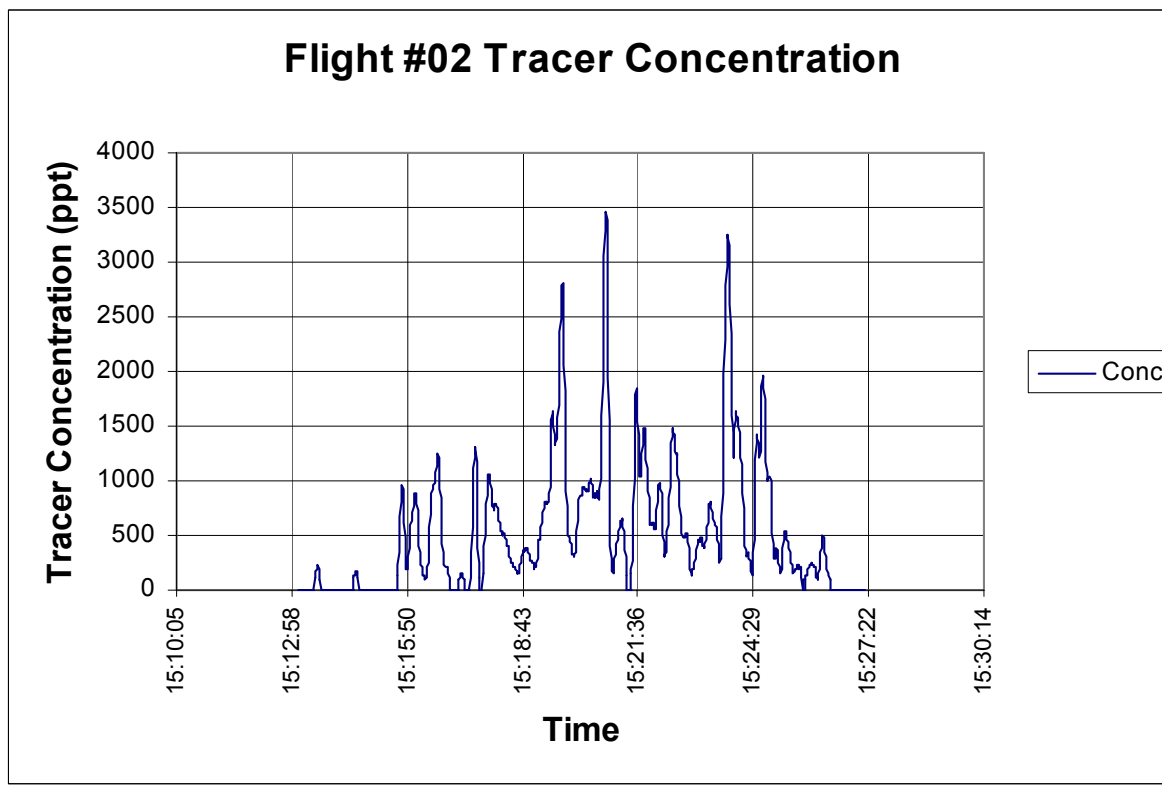
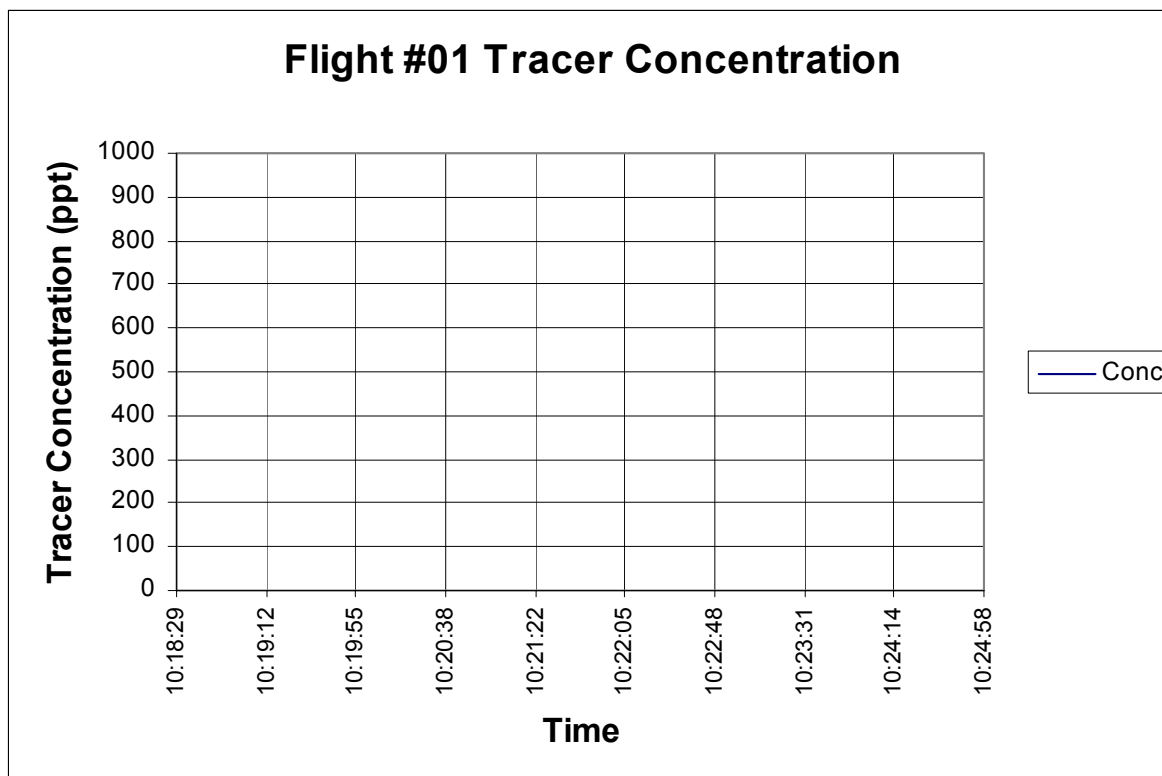


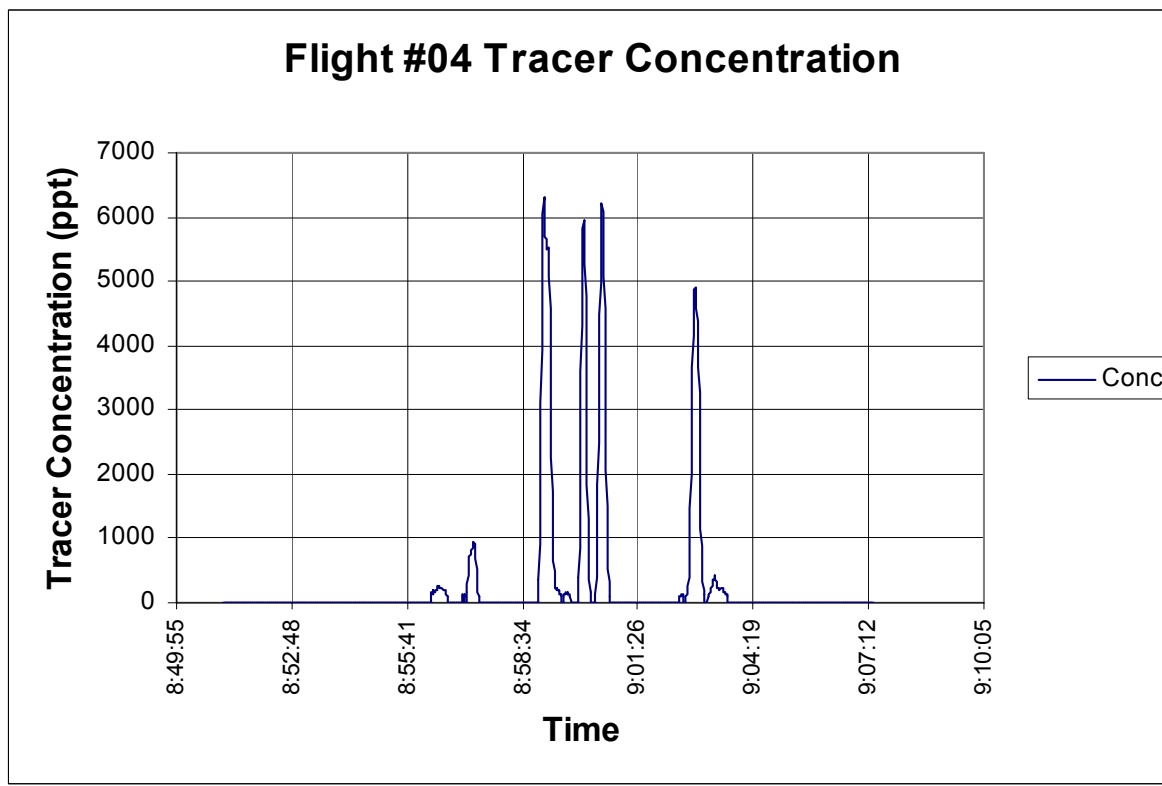
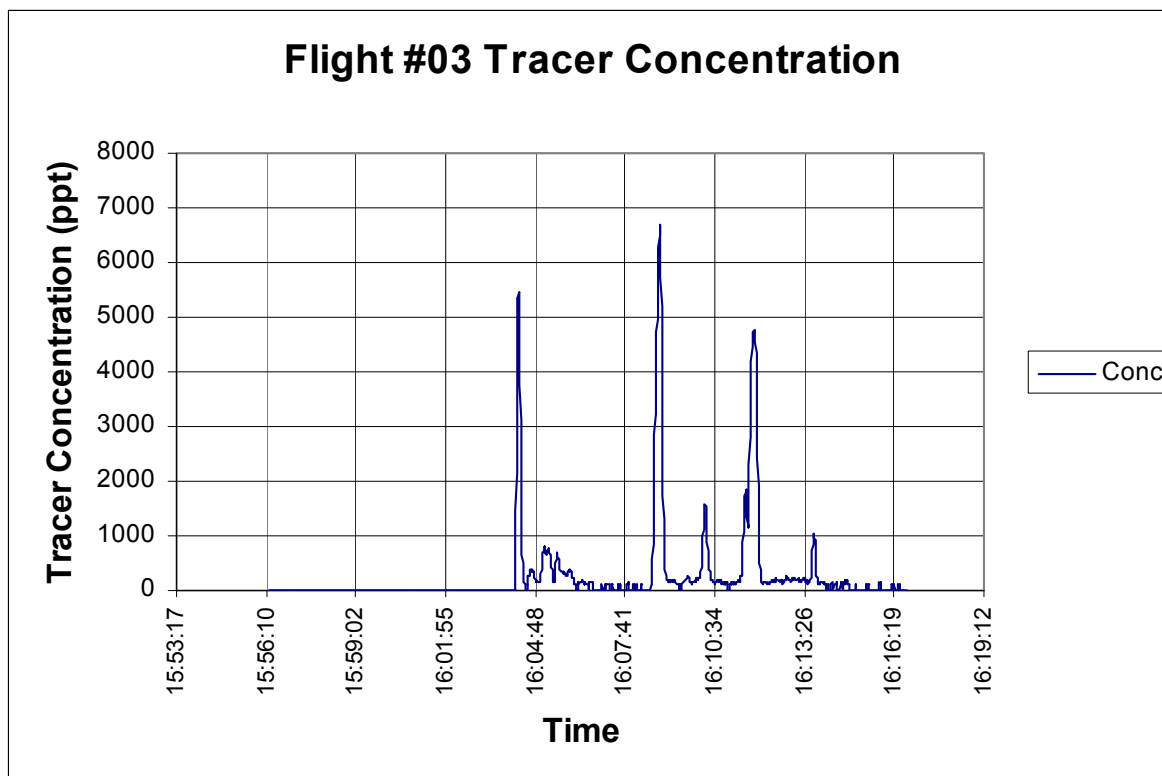


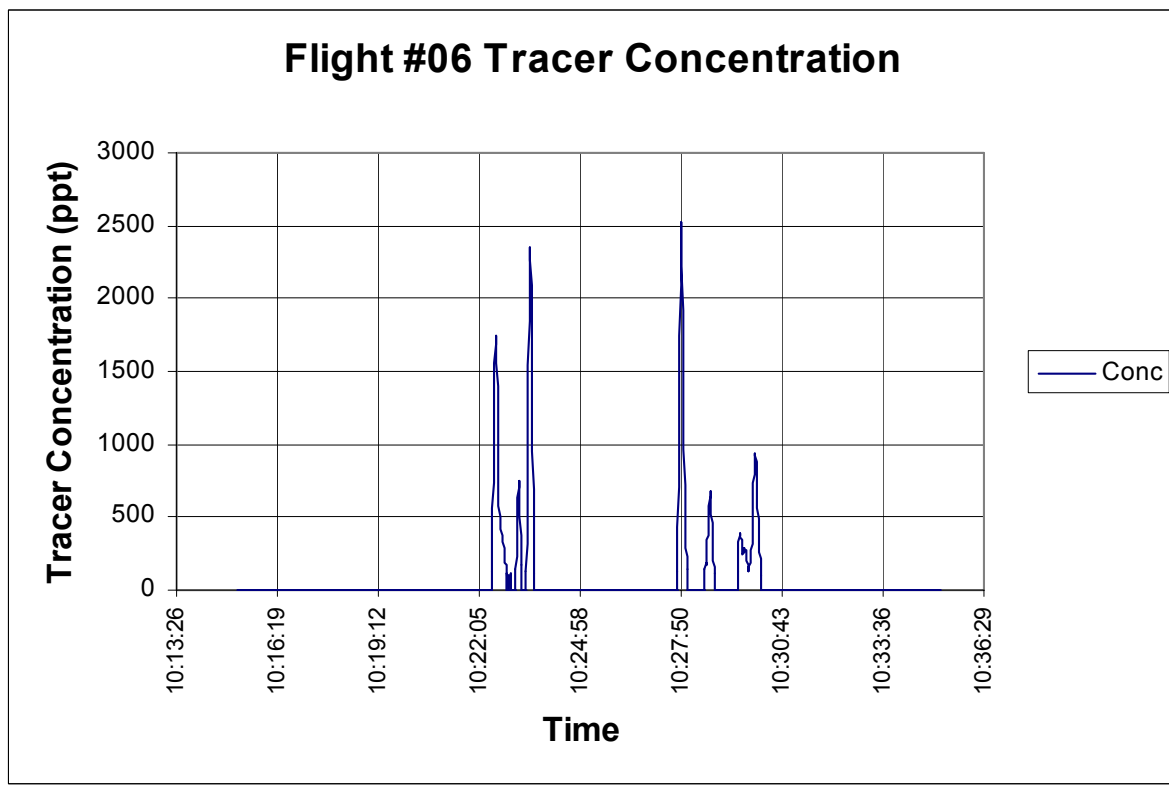
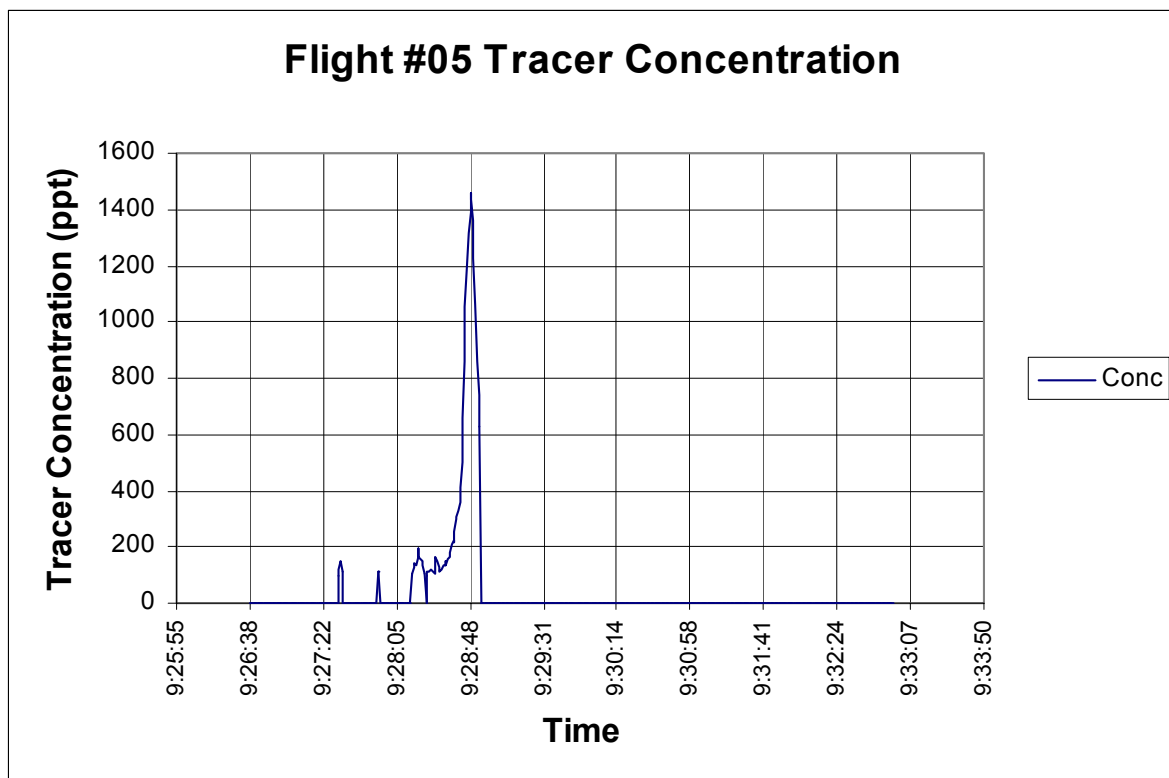


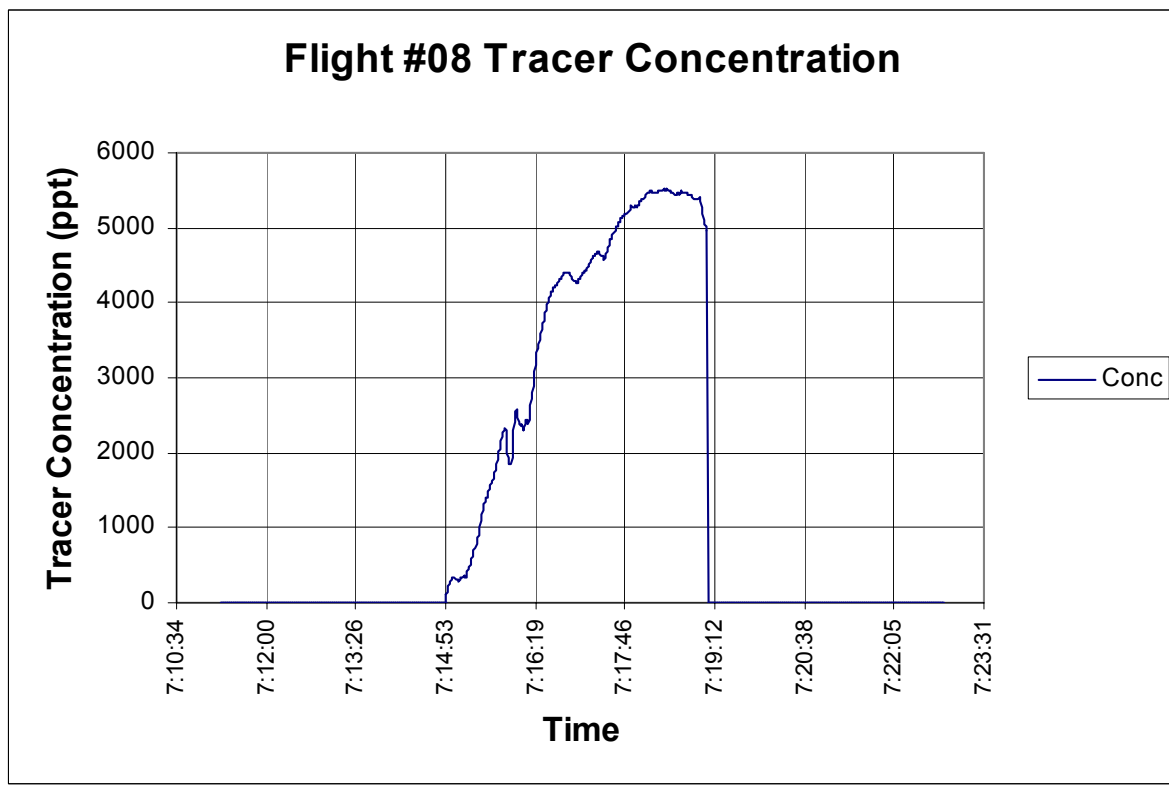
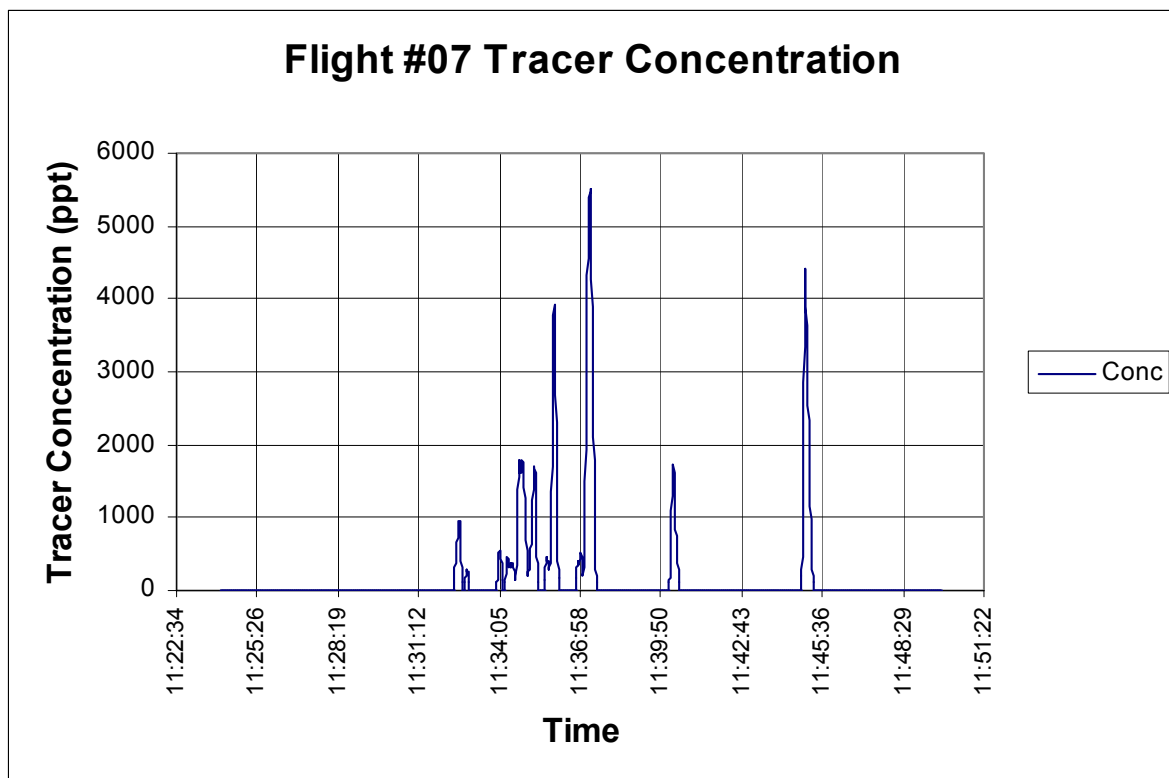


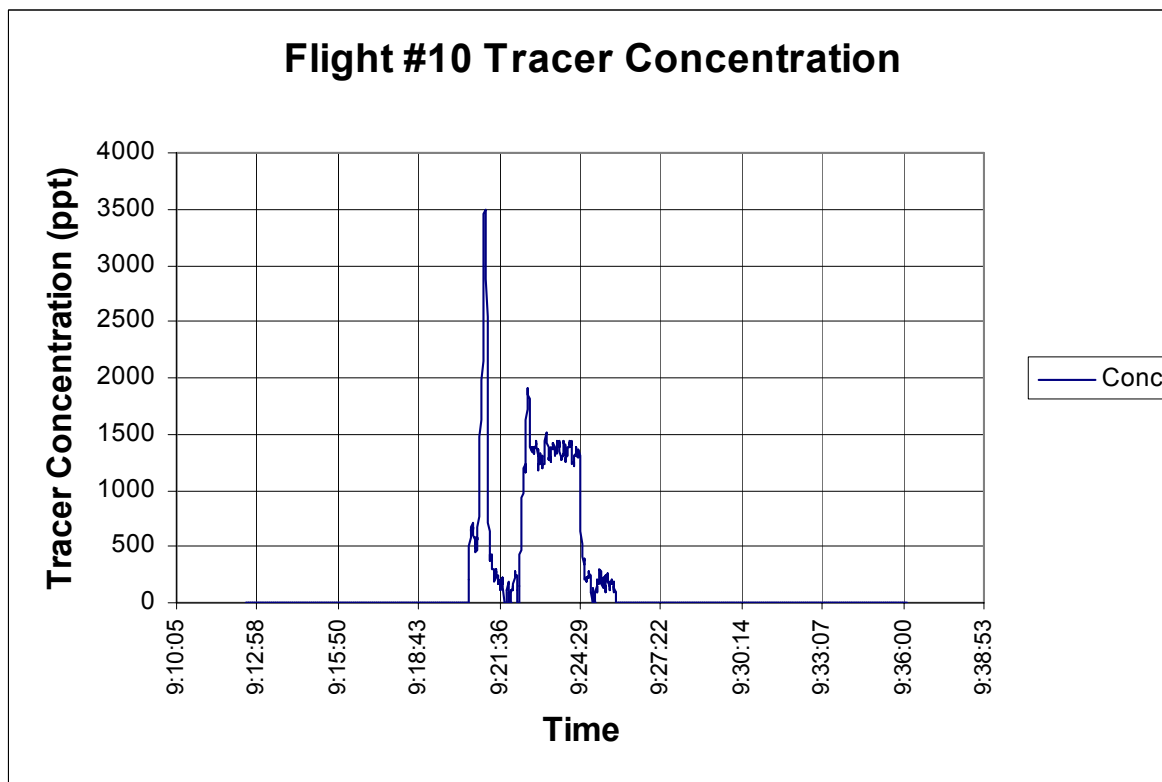
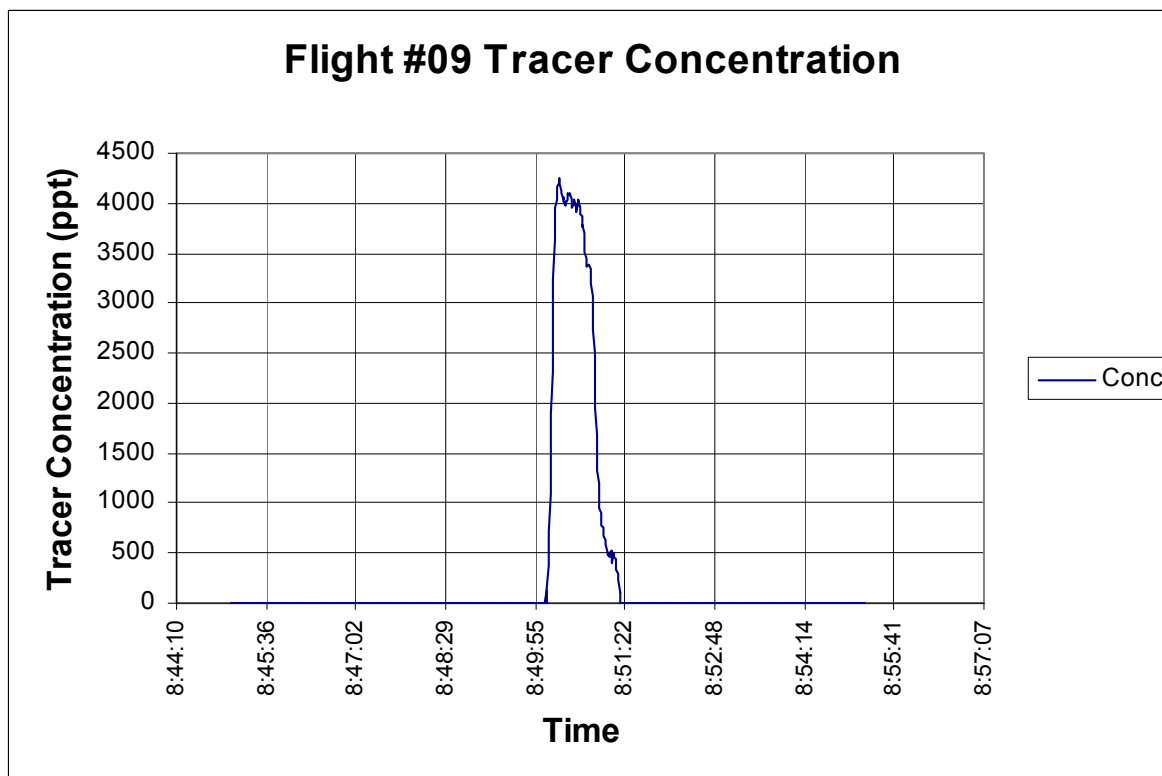
APPENDIX C
SF₆ CONCENTRATION TIME GRAPHS

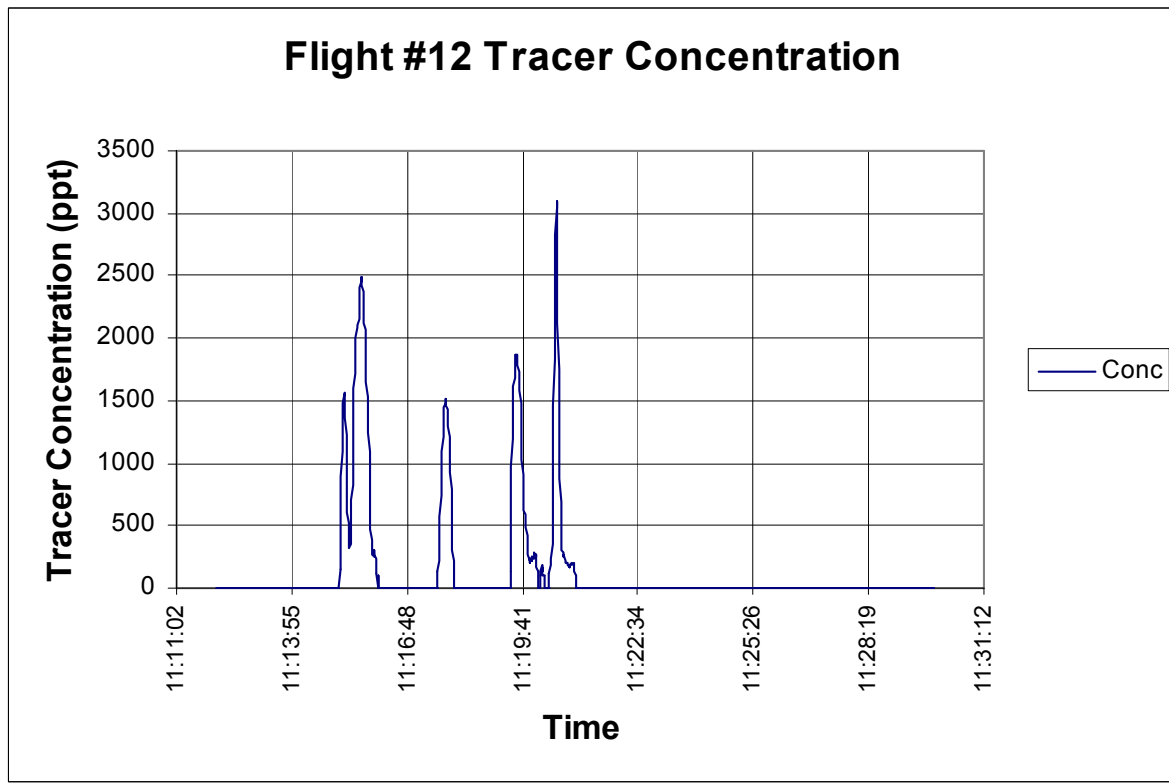
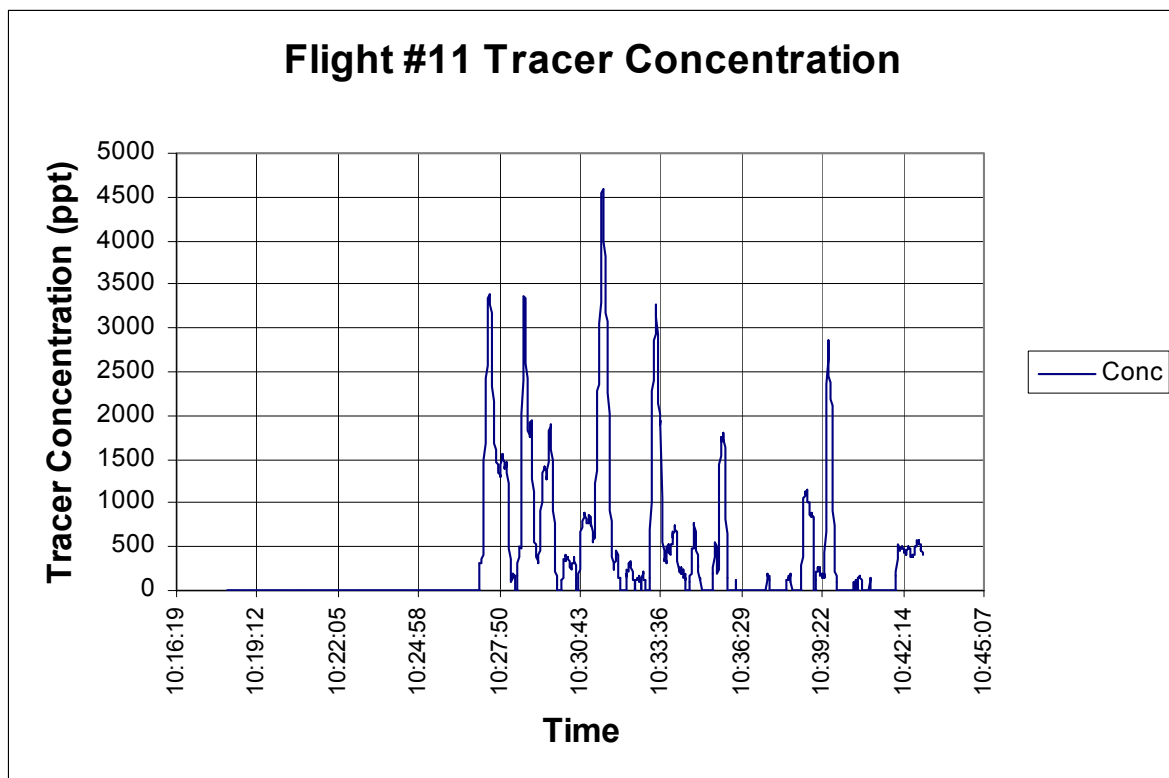


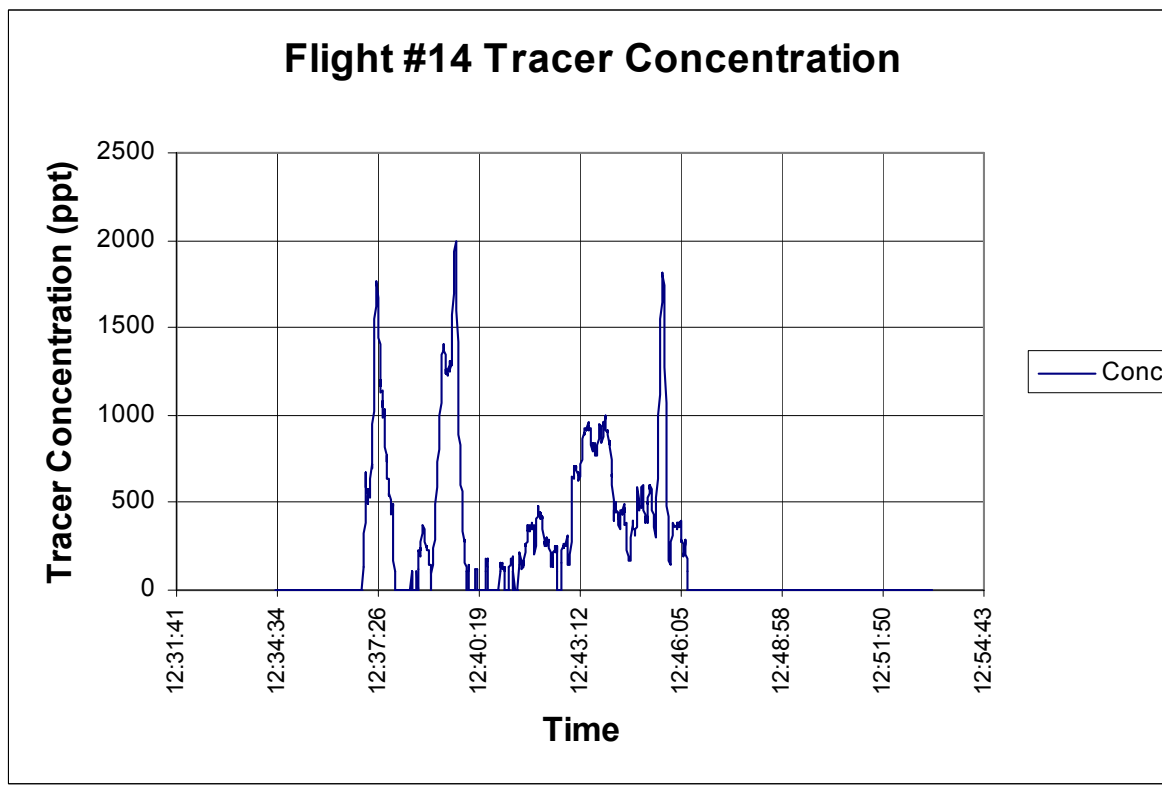
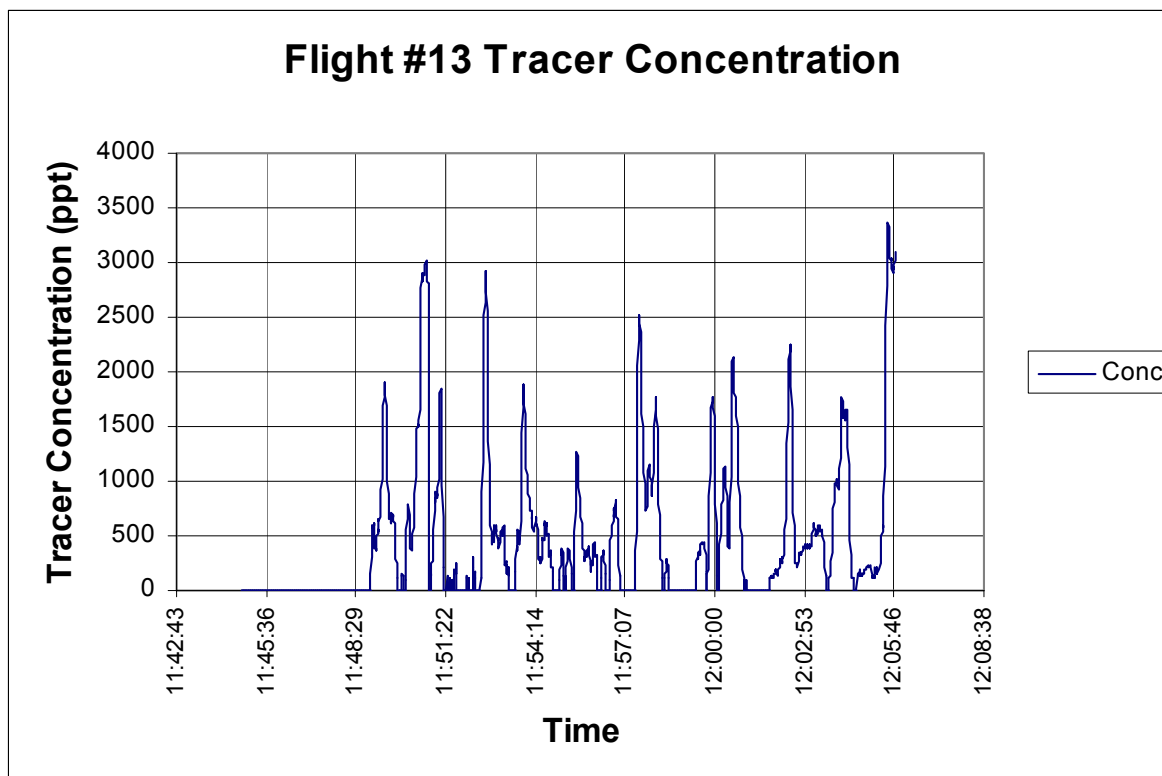


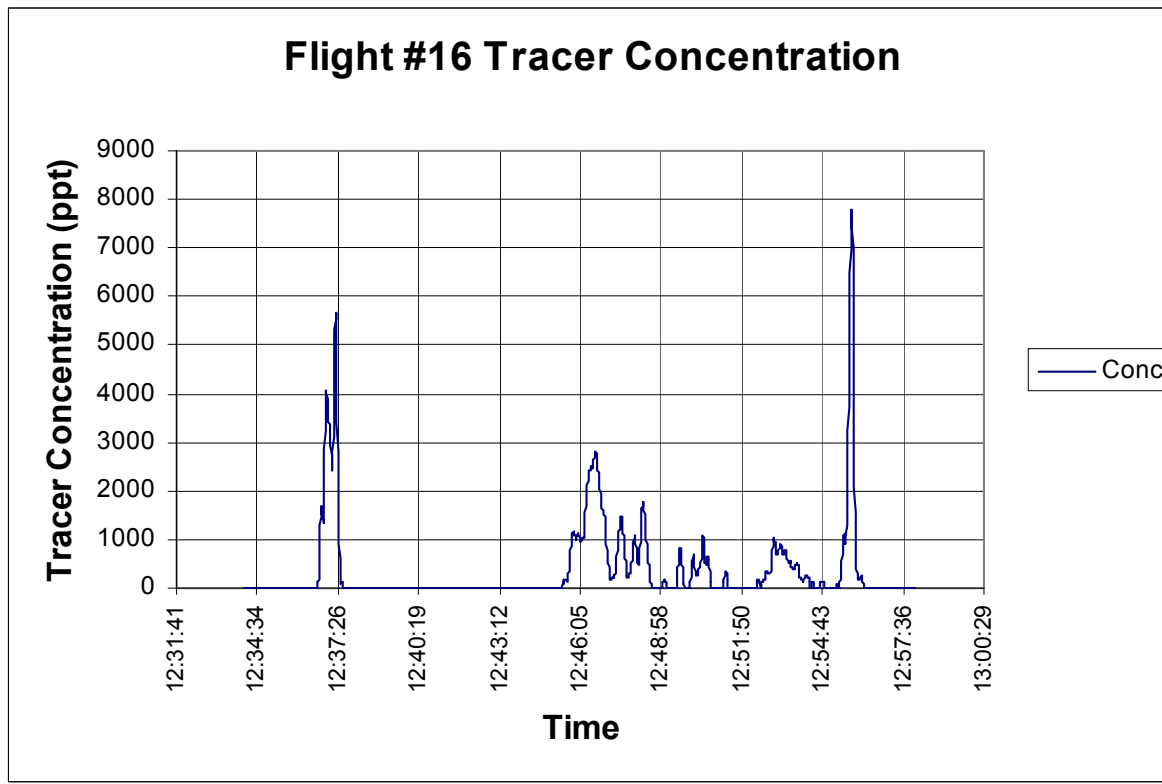
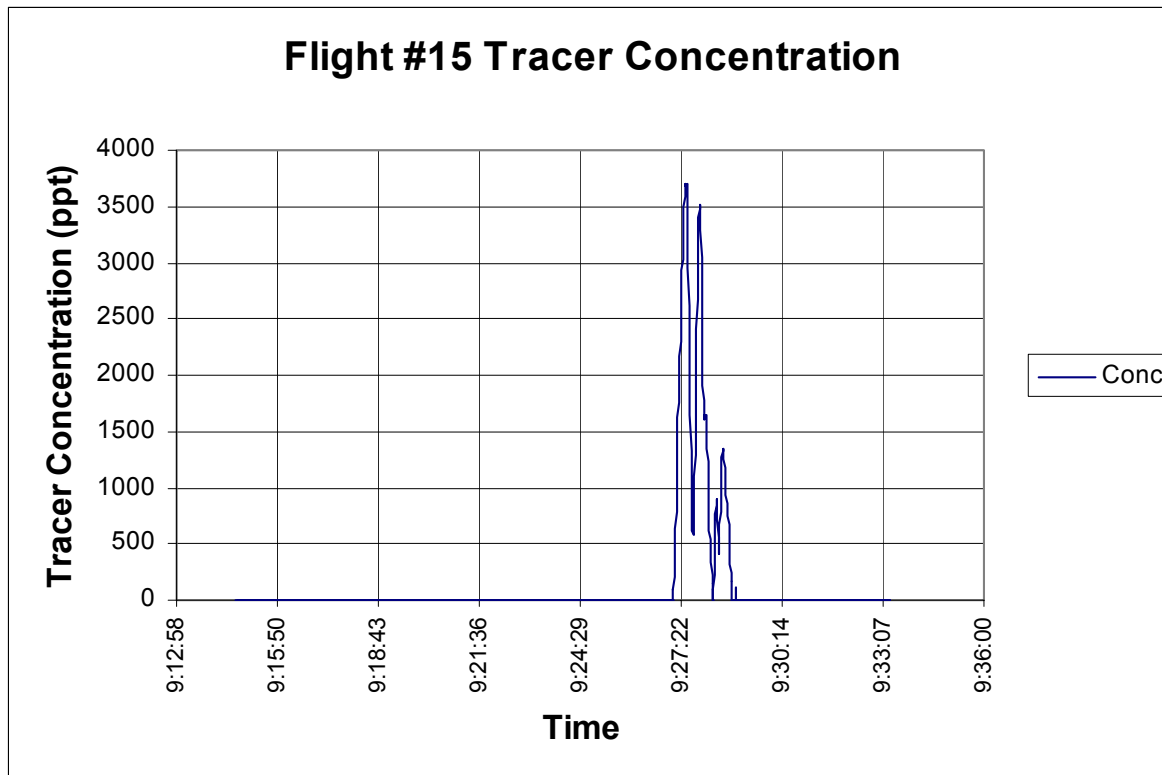


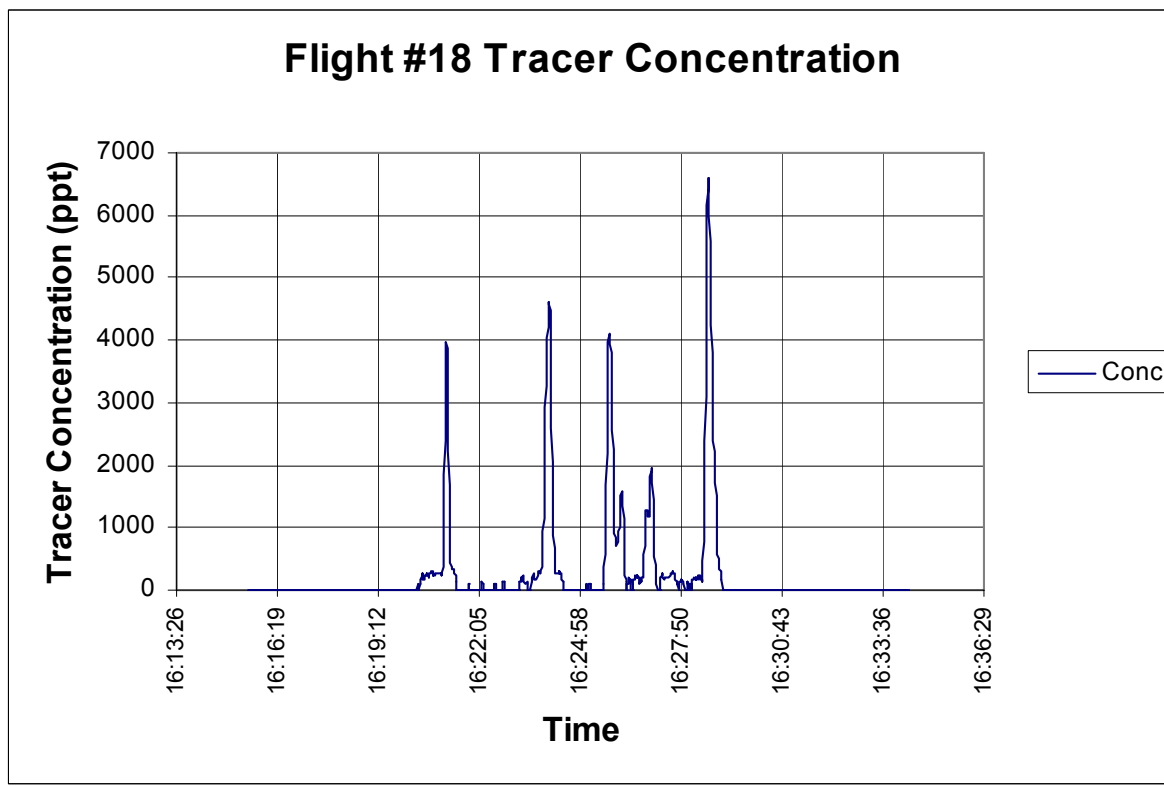
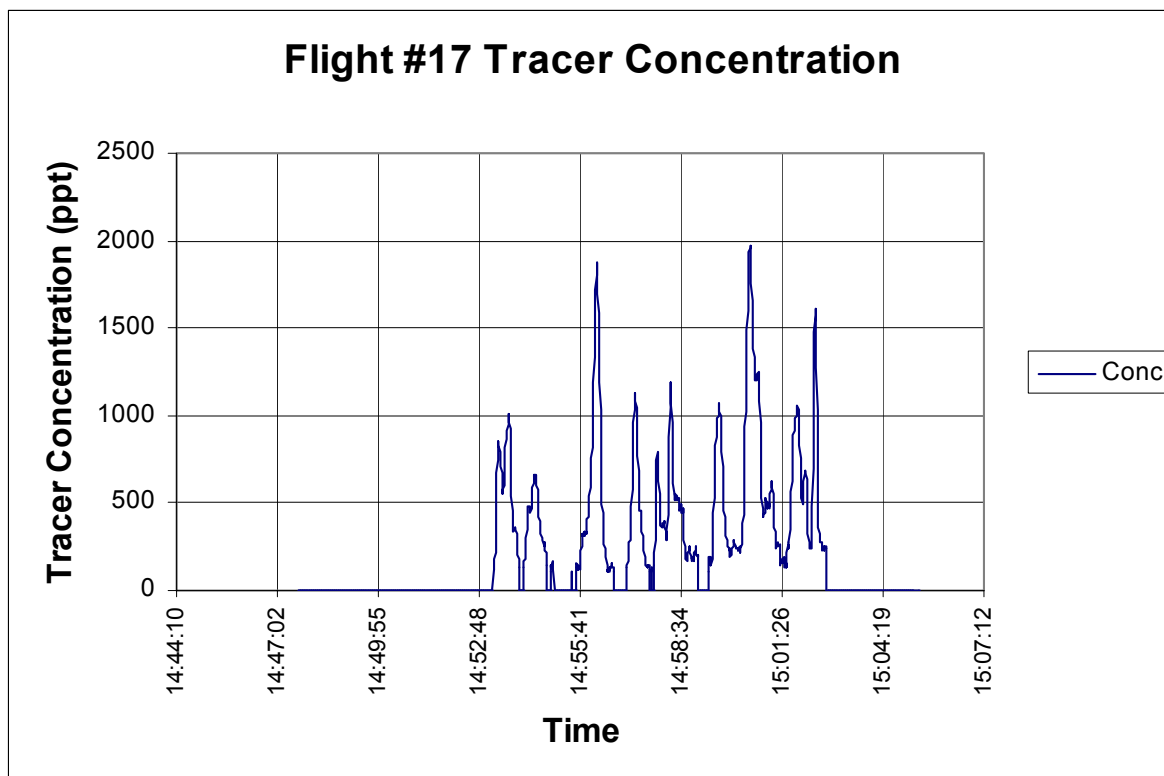


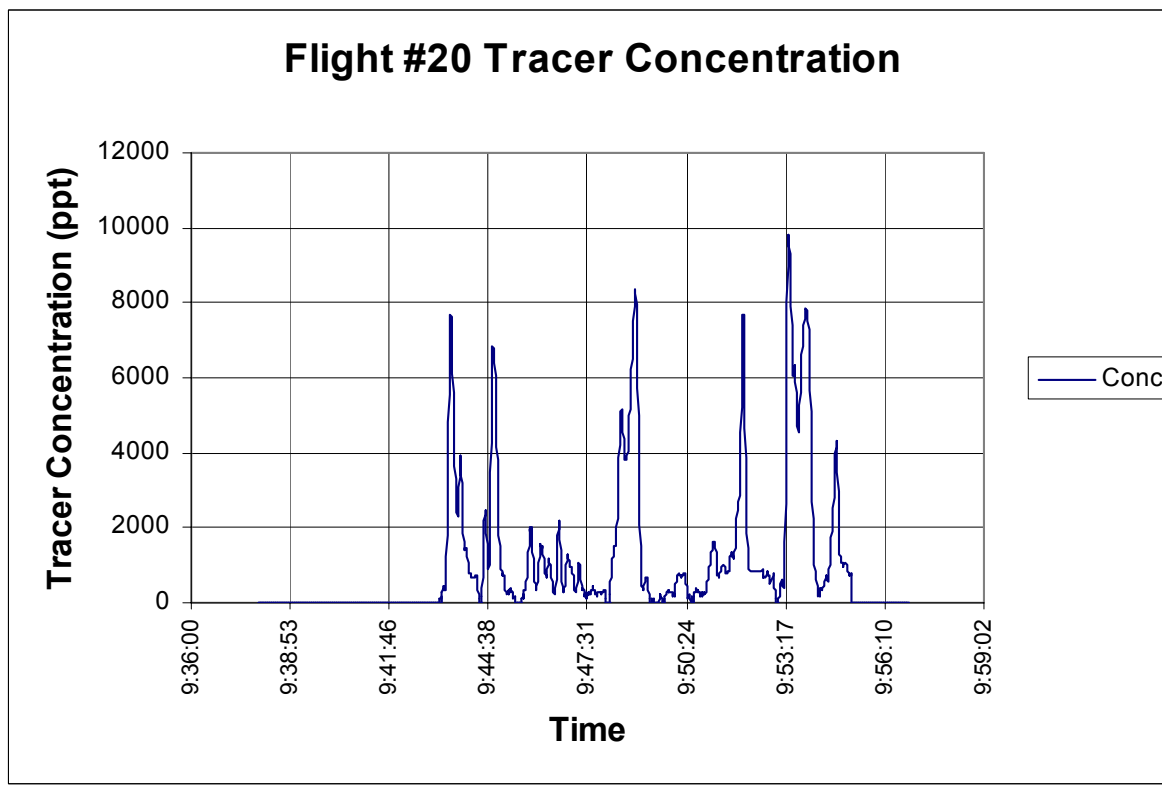
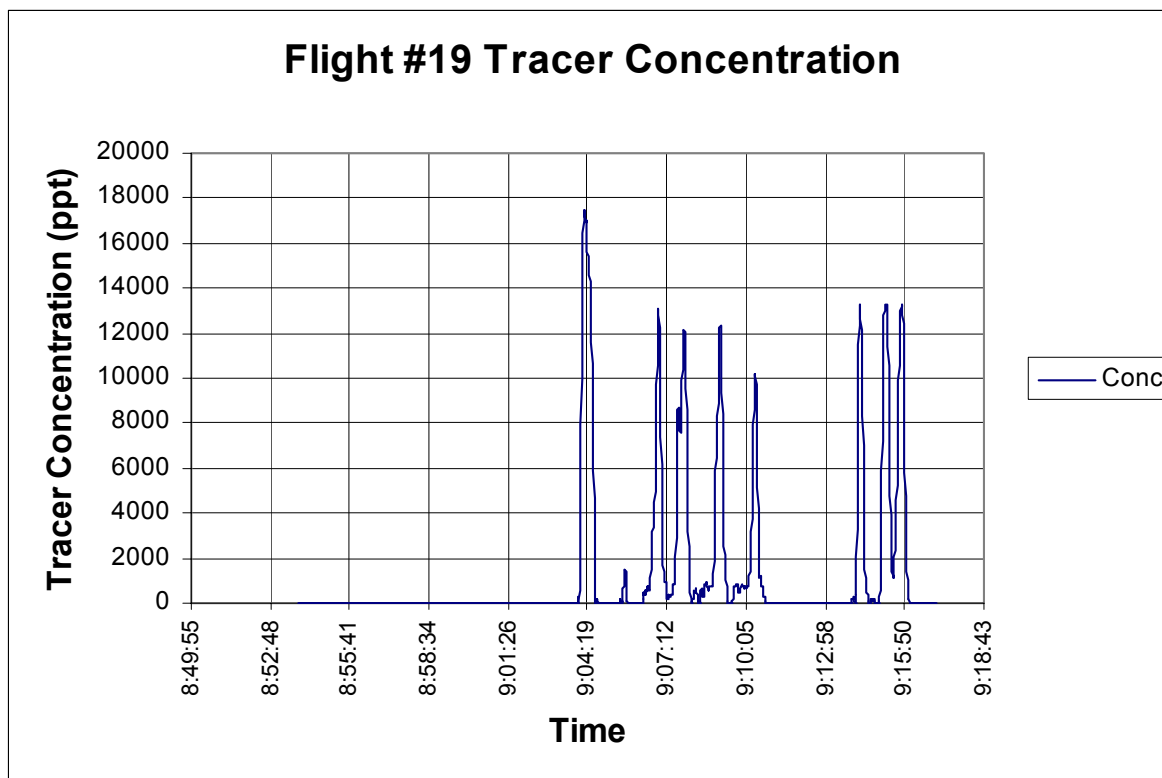


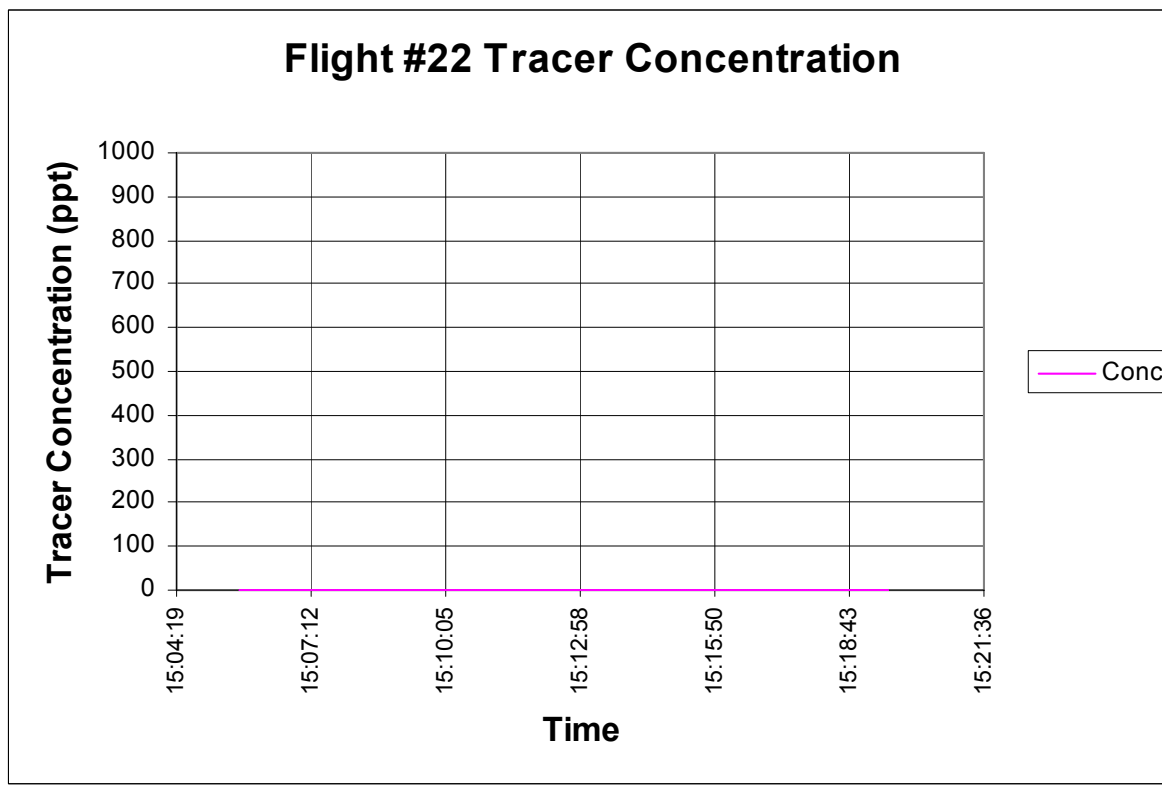
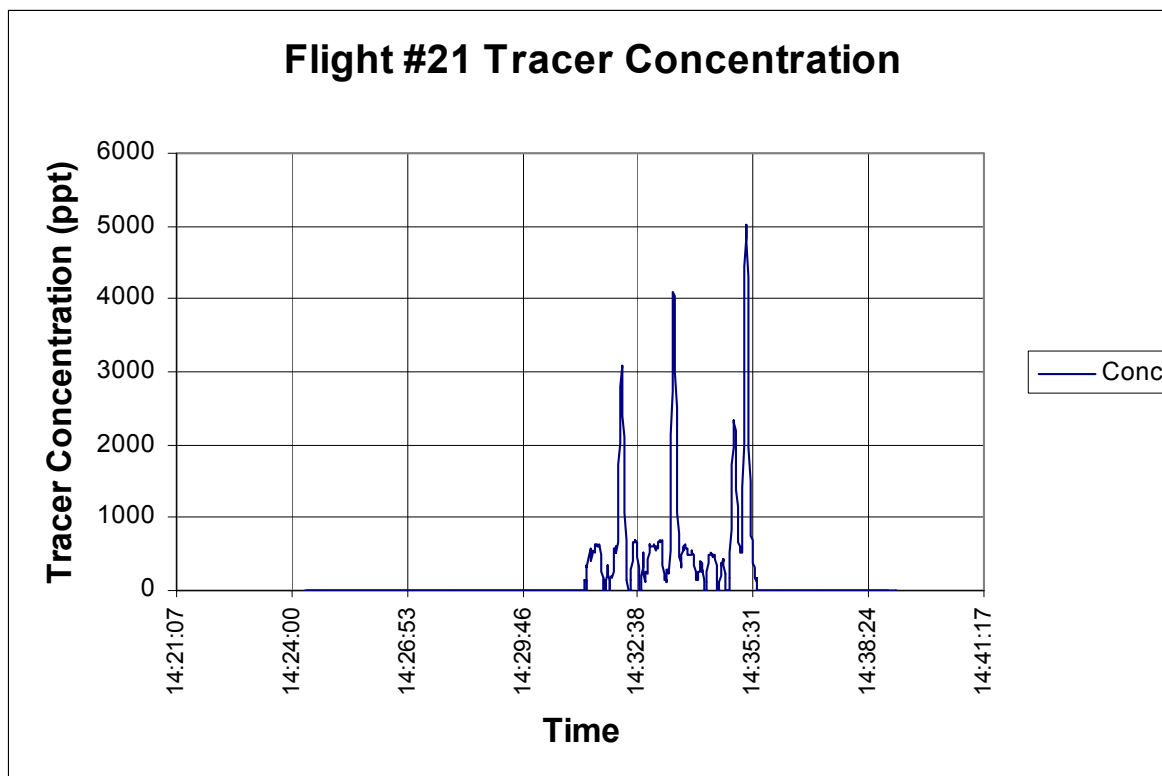


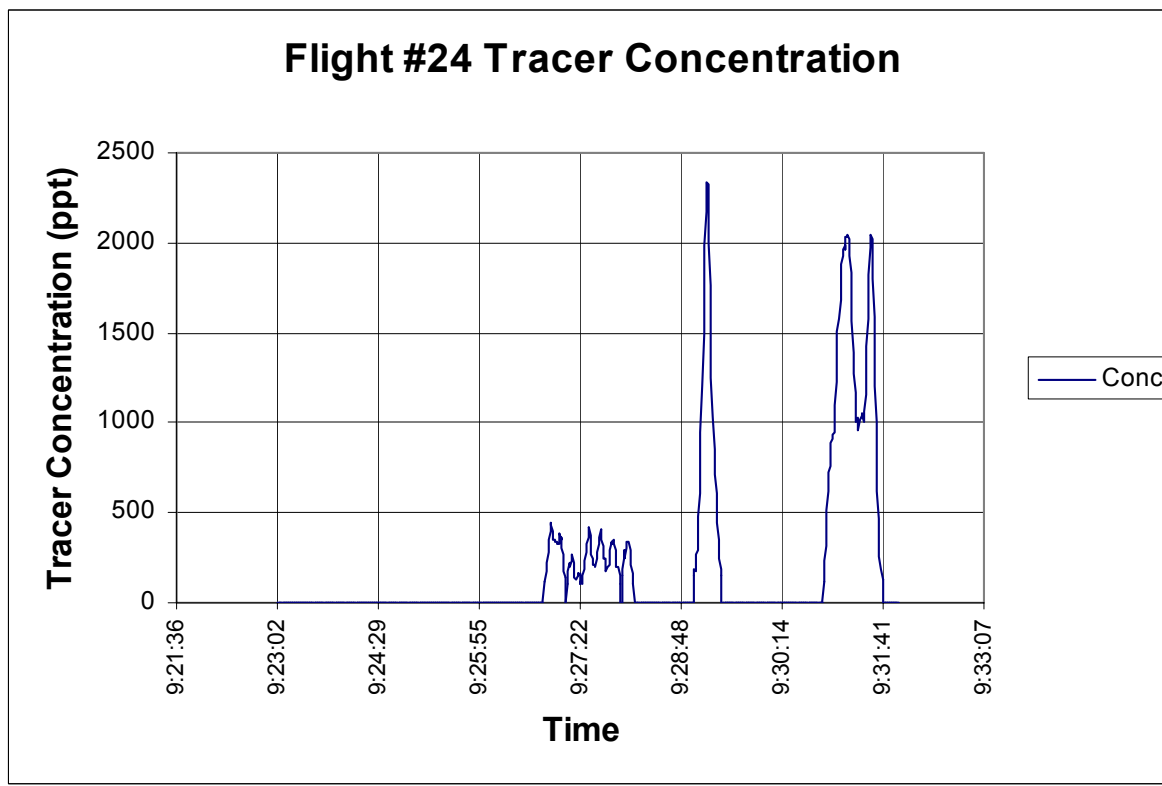
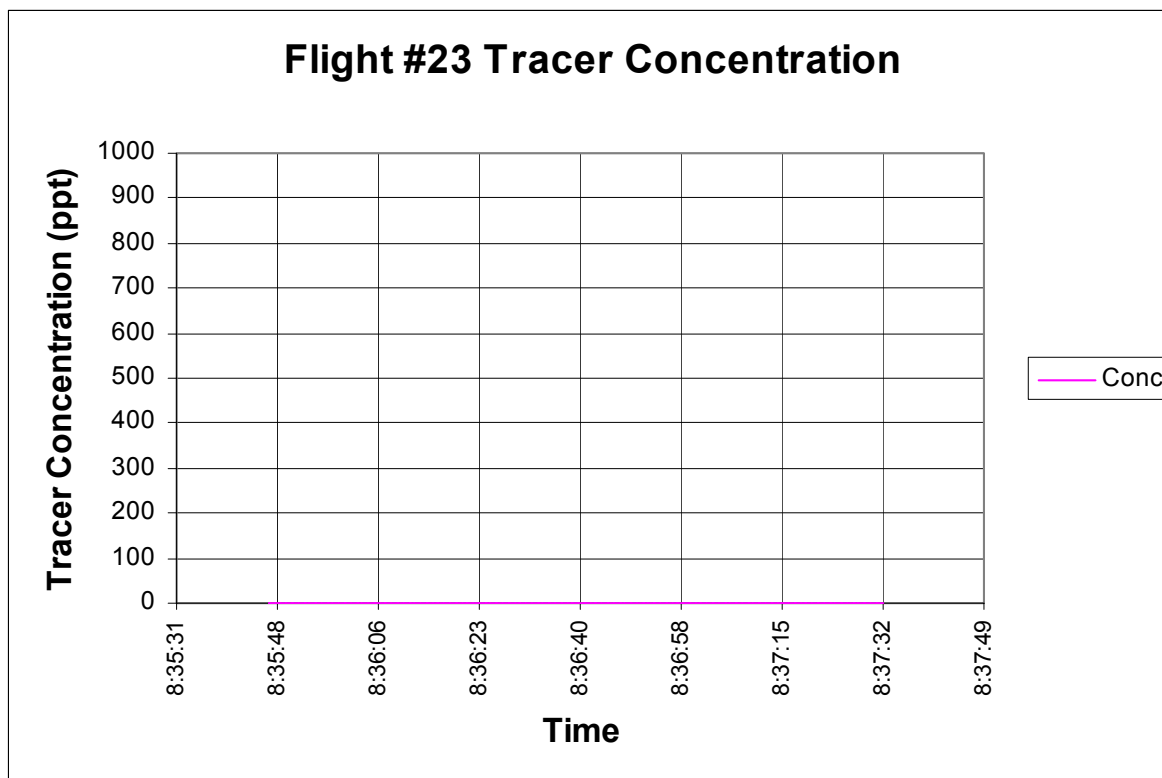


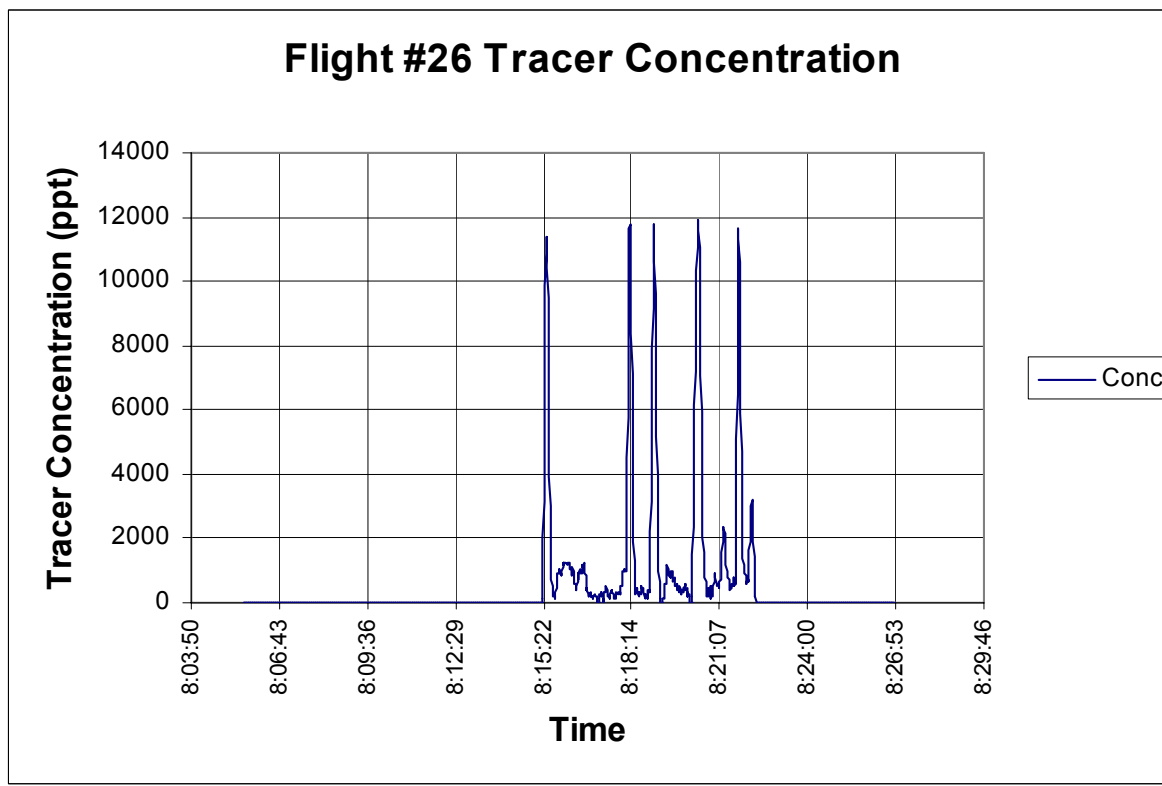
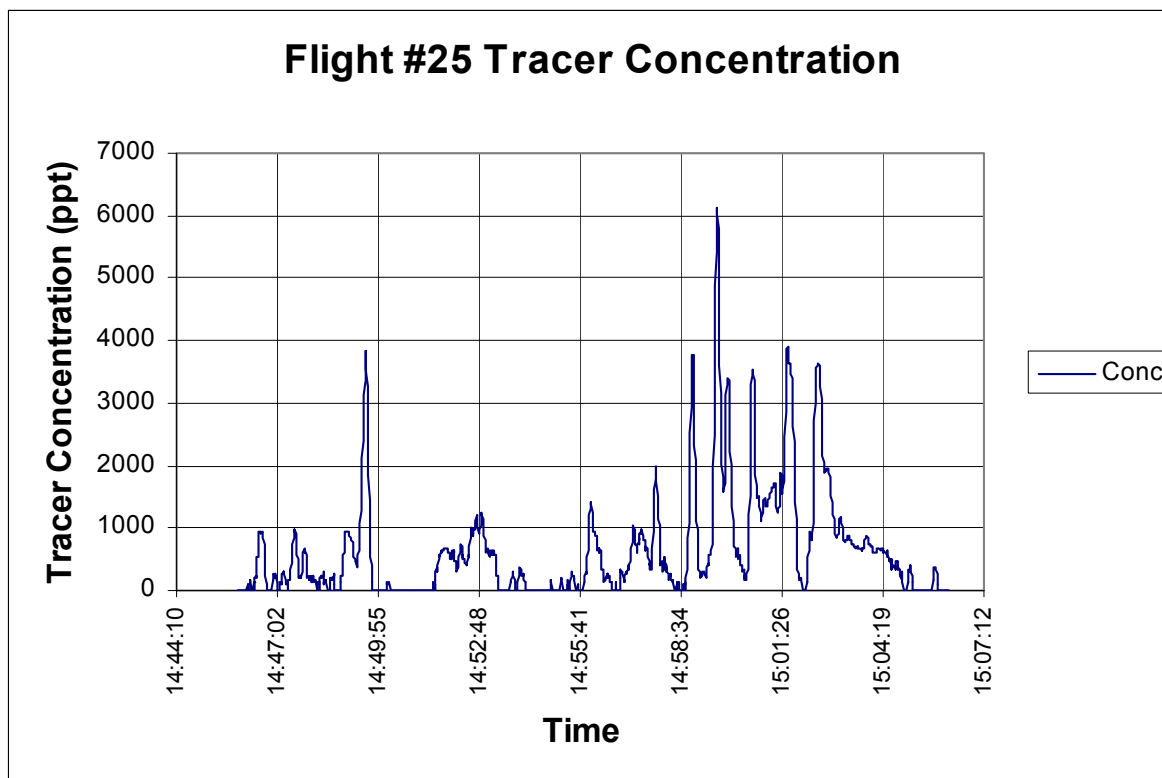


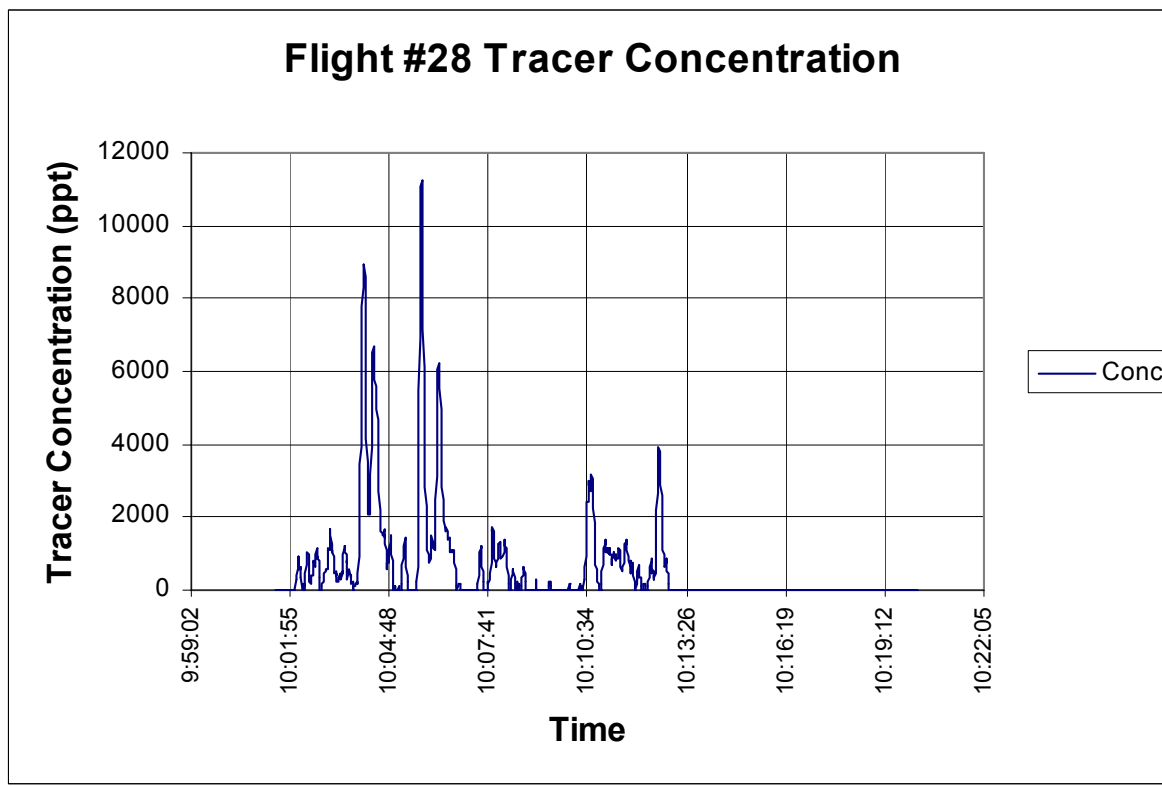
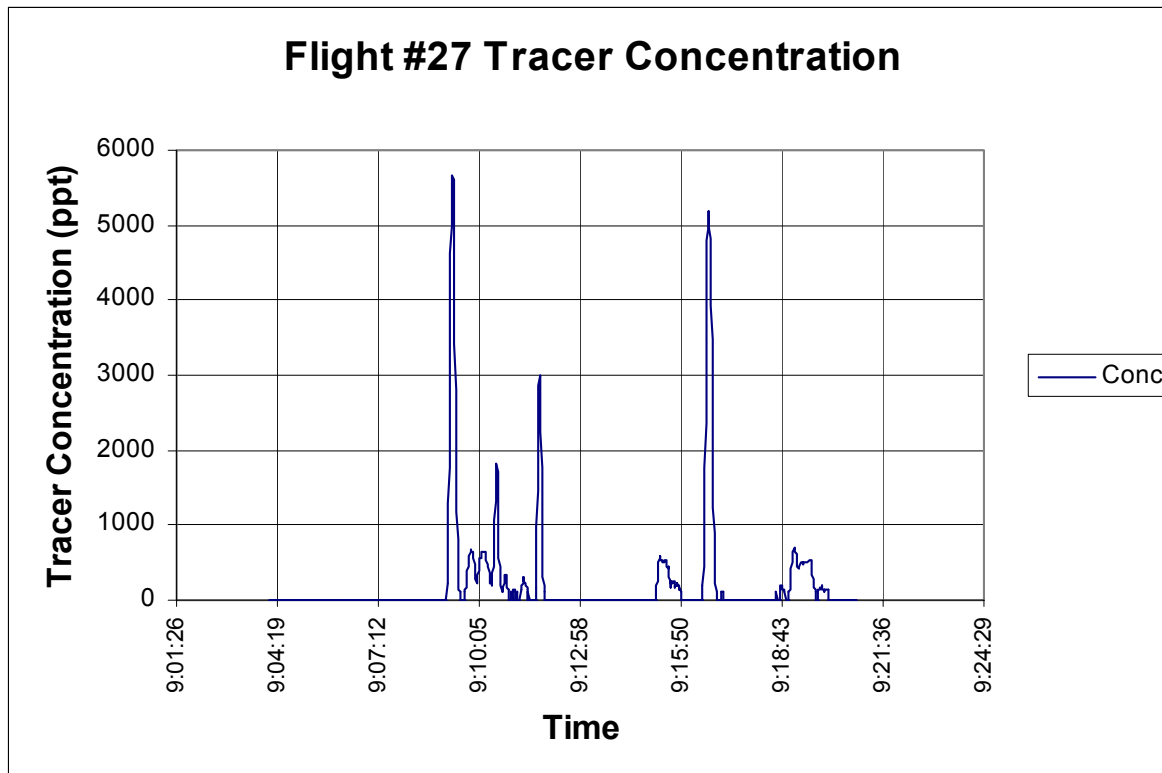






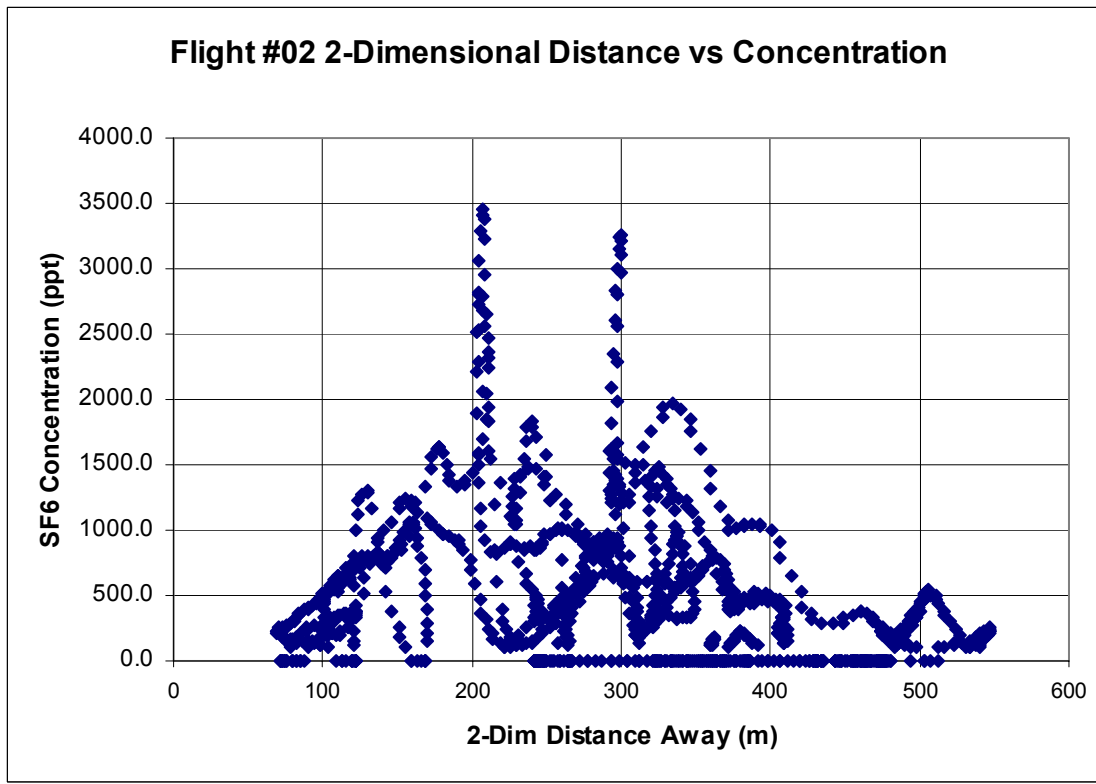
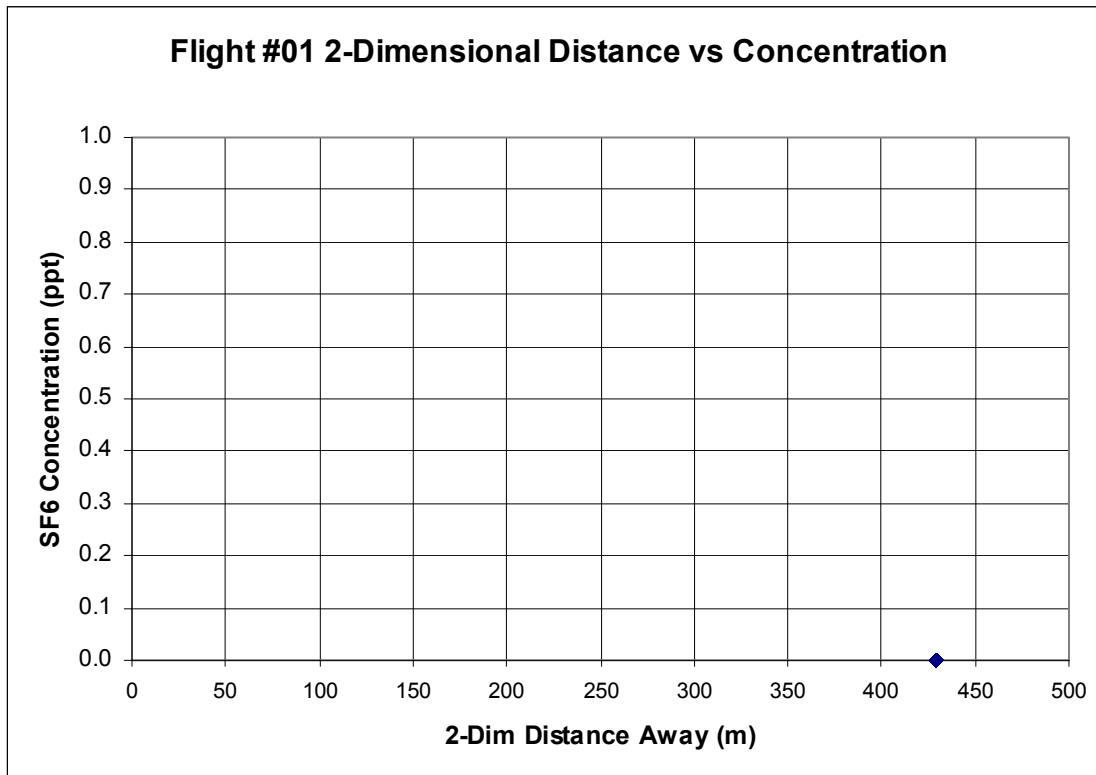


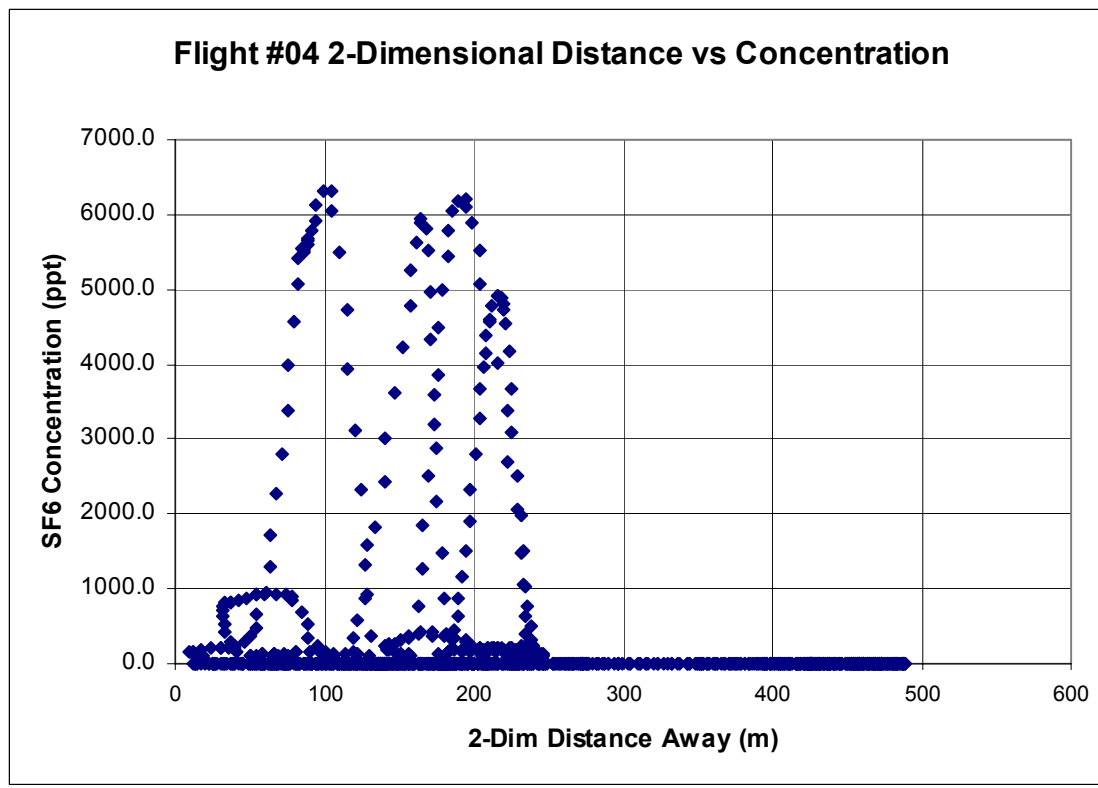
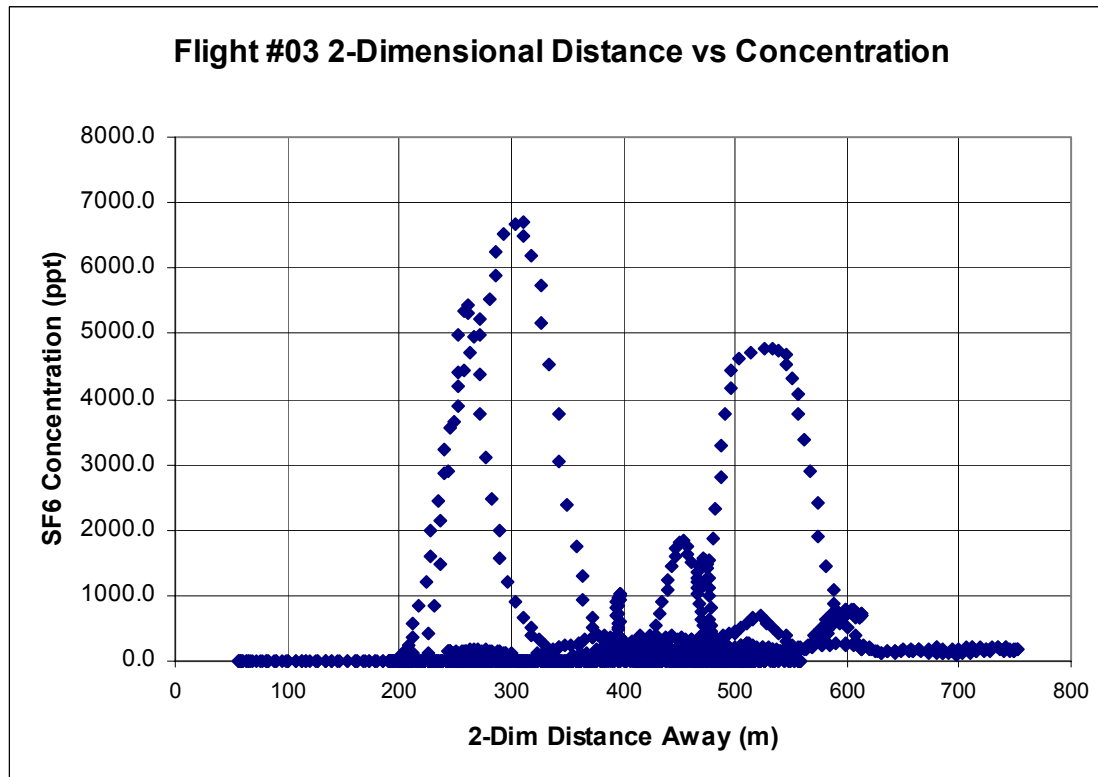


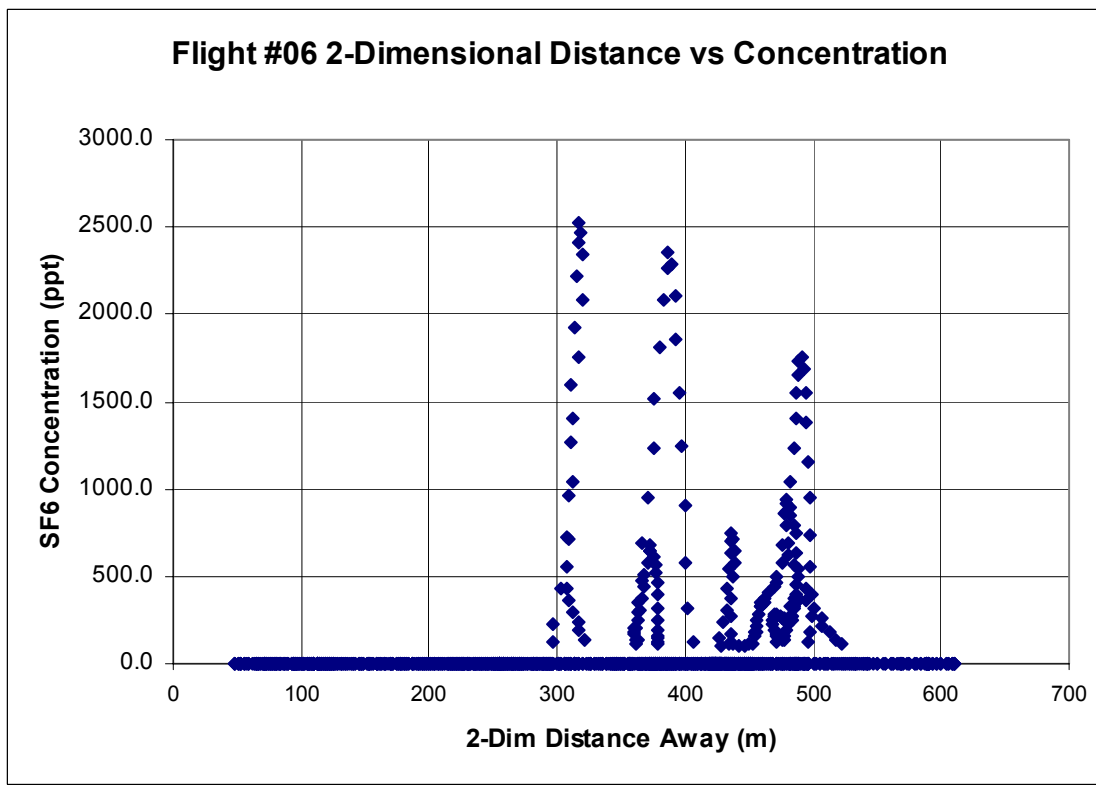
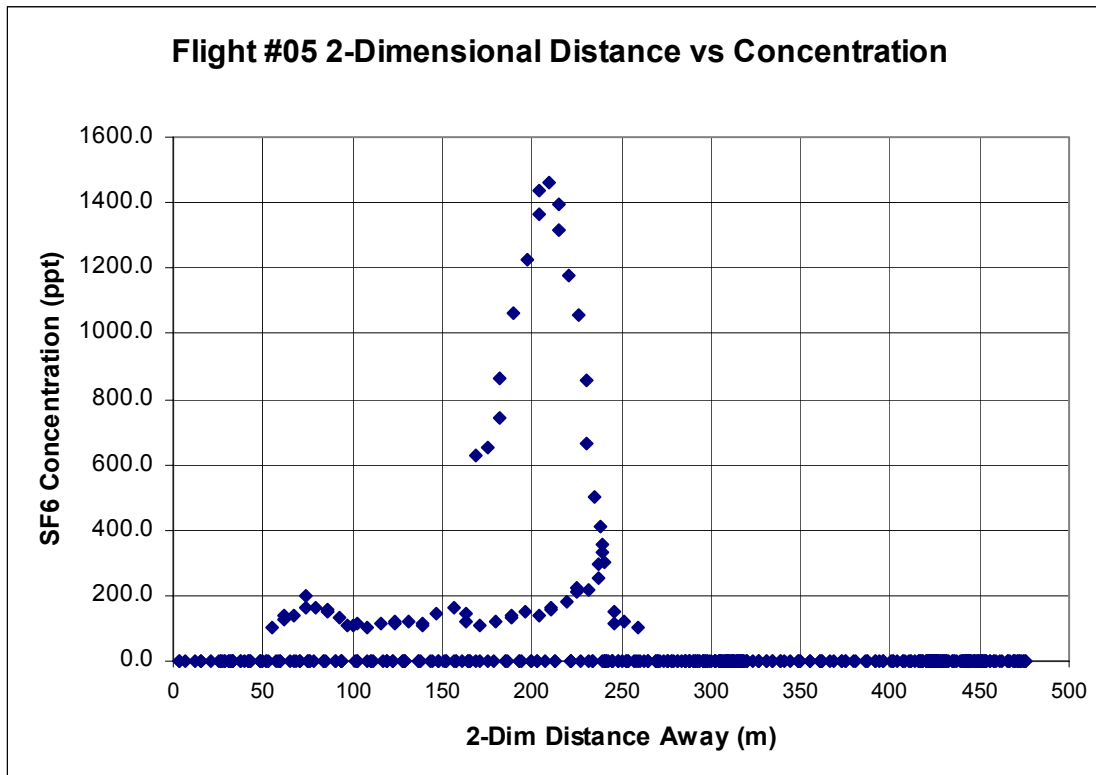


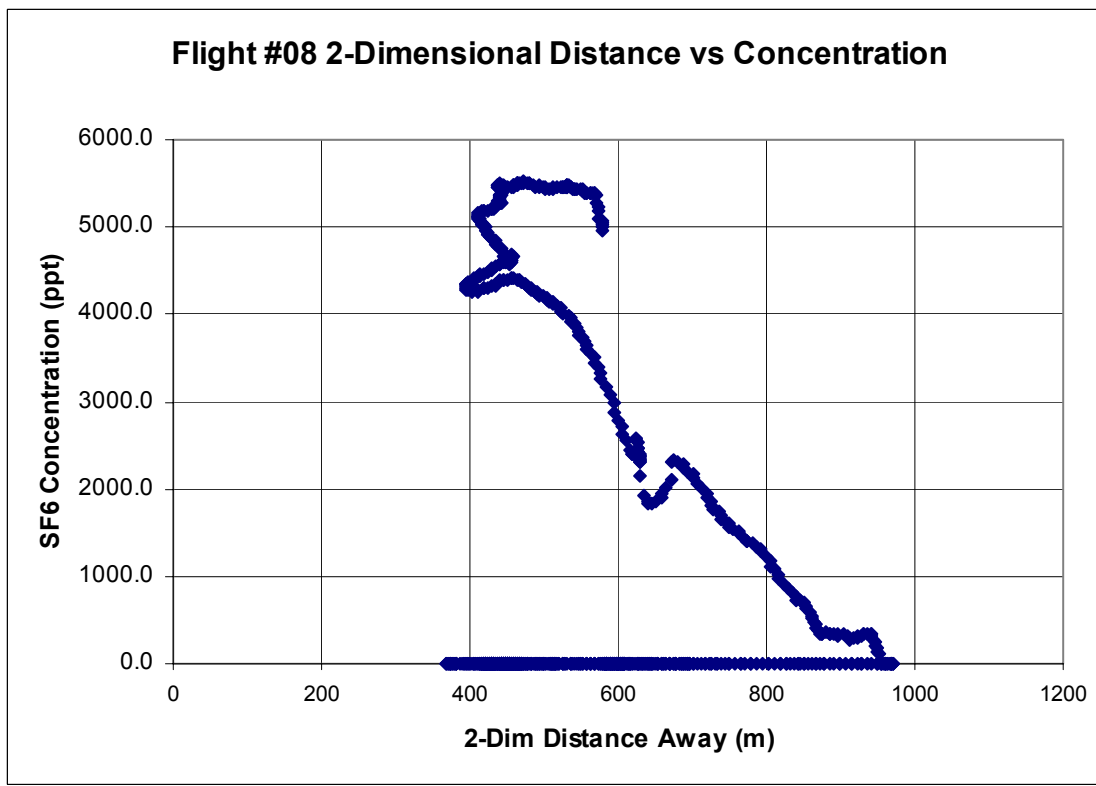
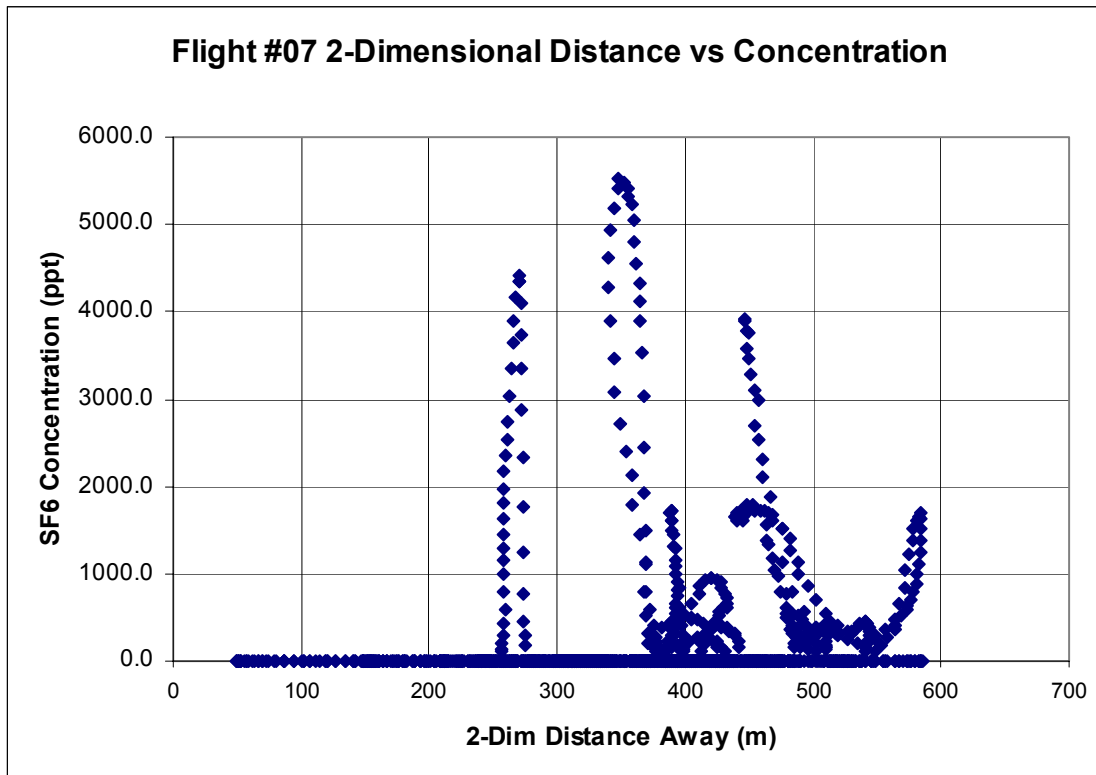
APPENDIX D

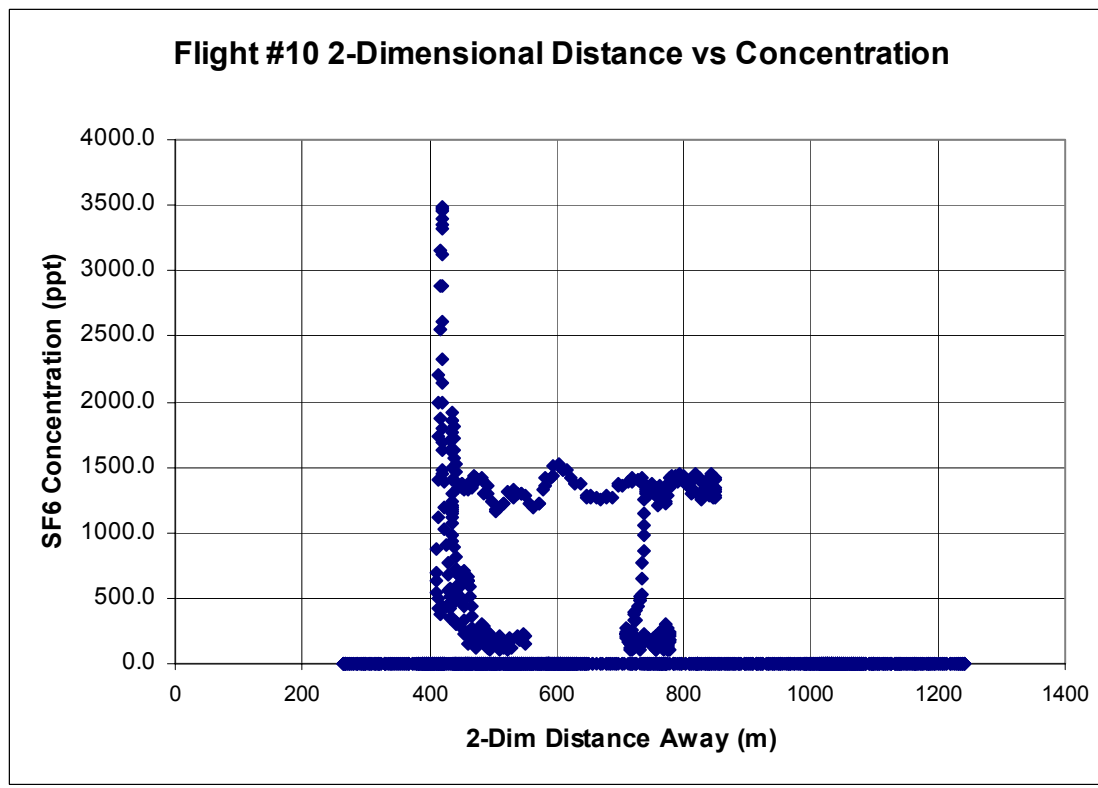
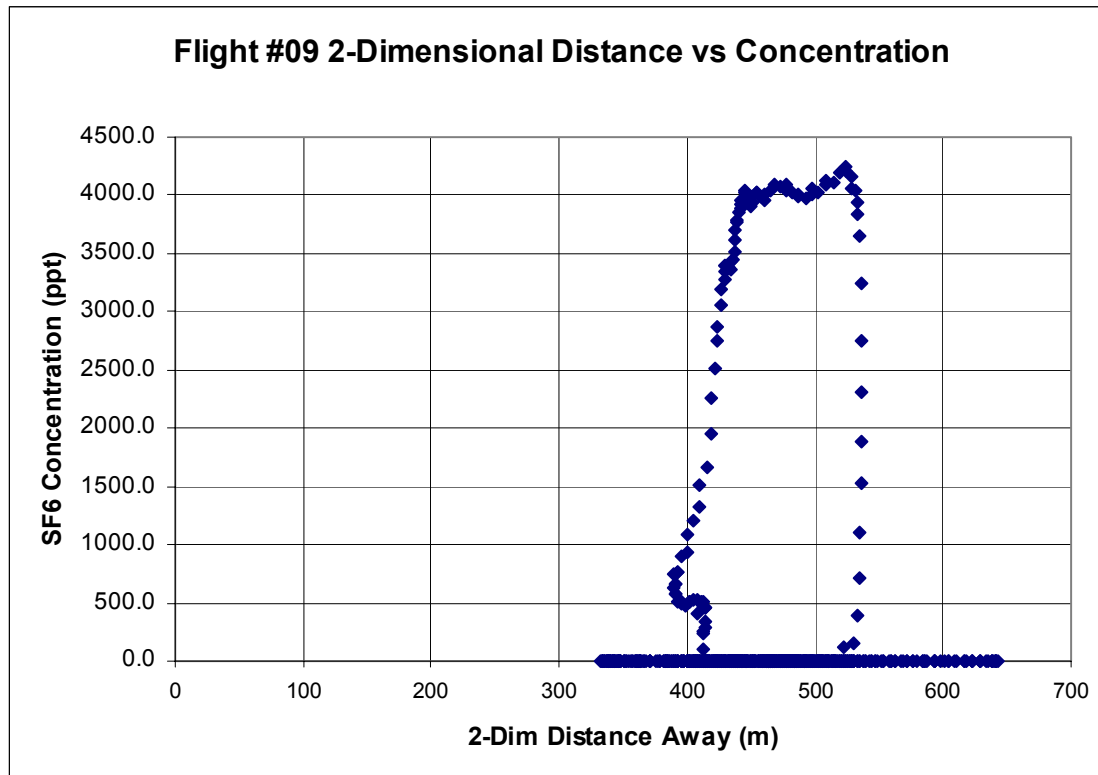
SF₆ CONCENTRATION DISTANCE GRAPHS

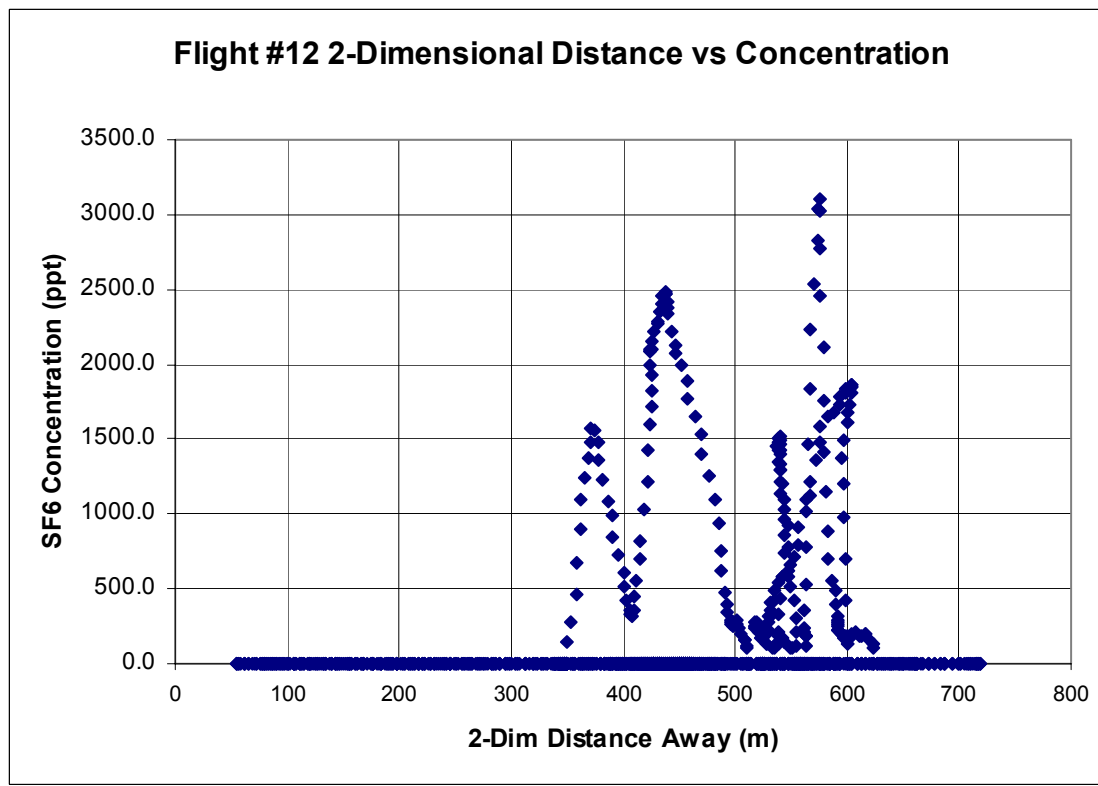
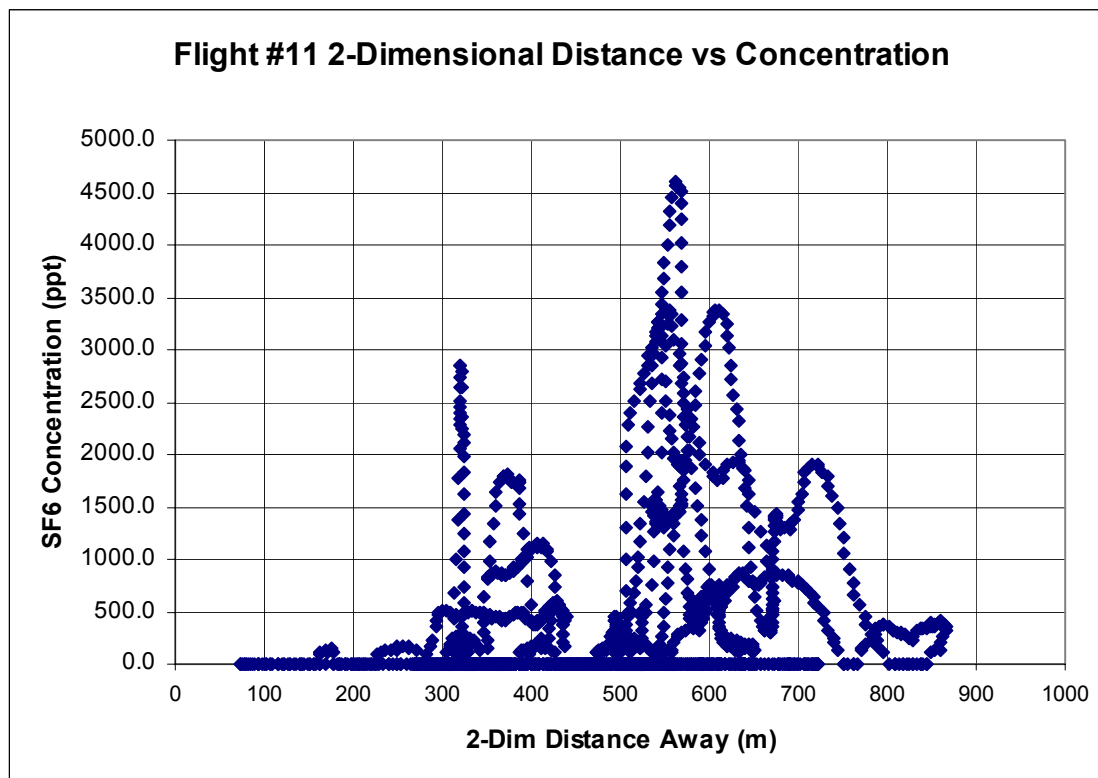


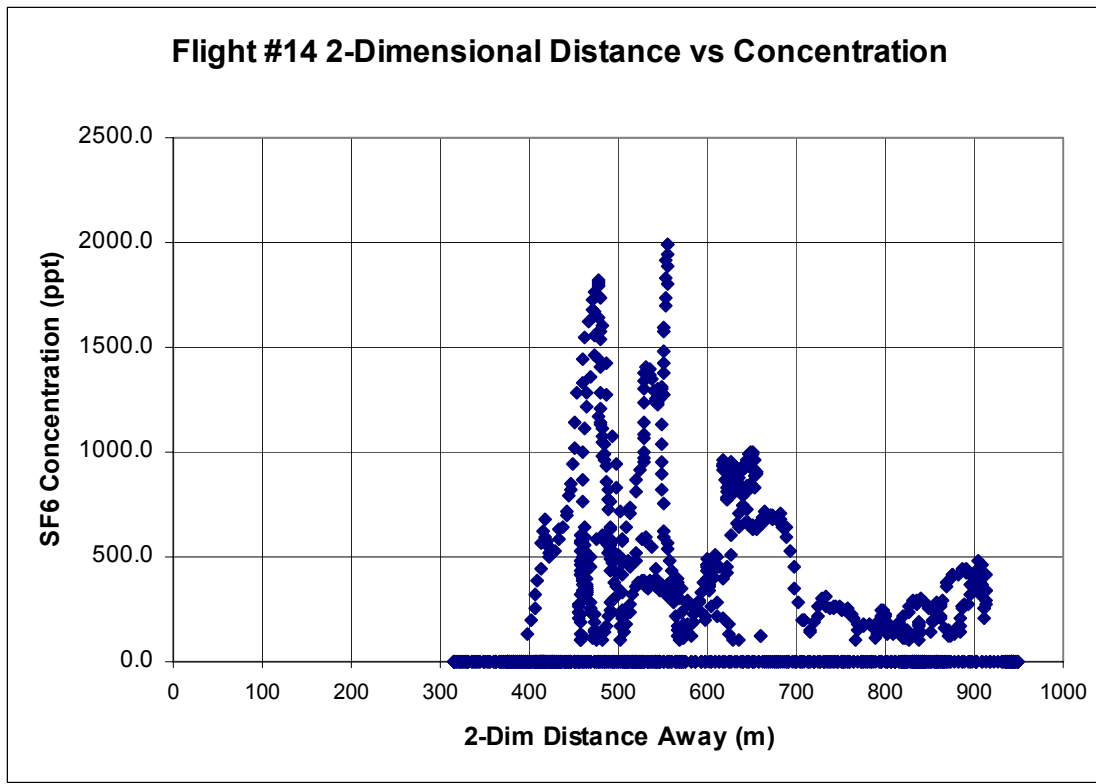
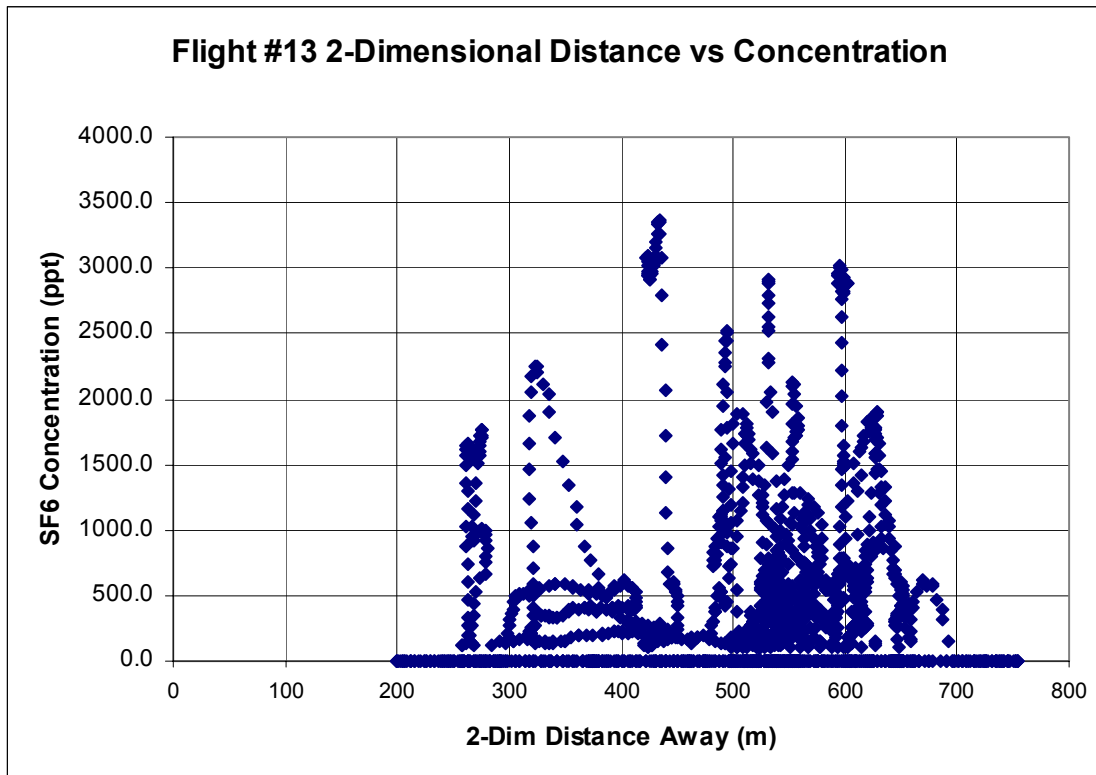


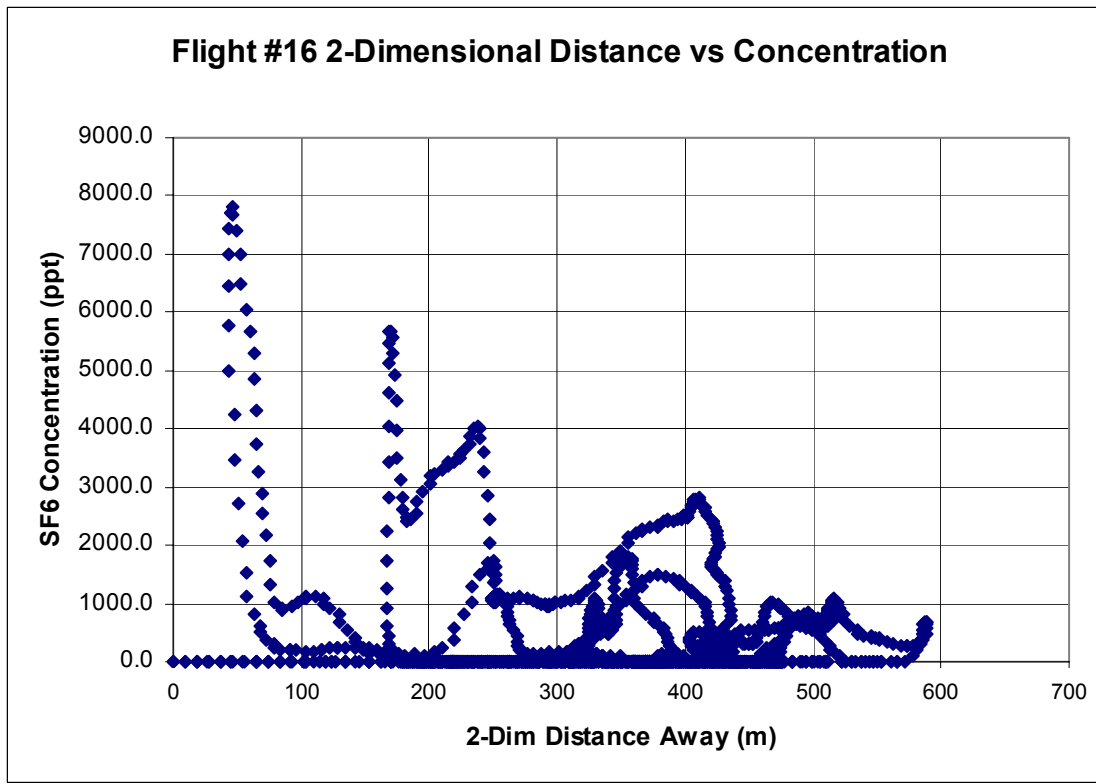
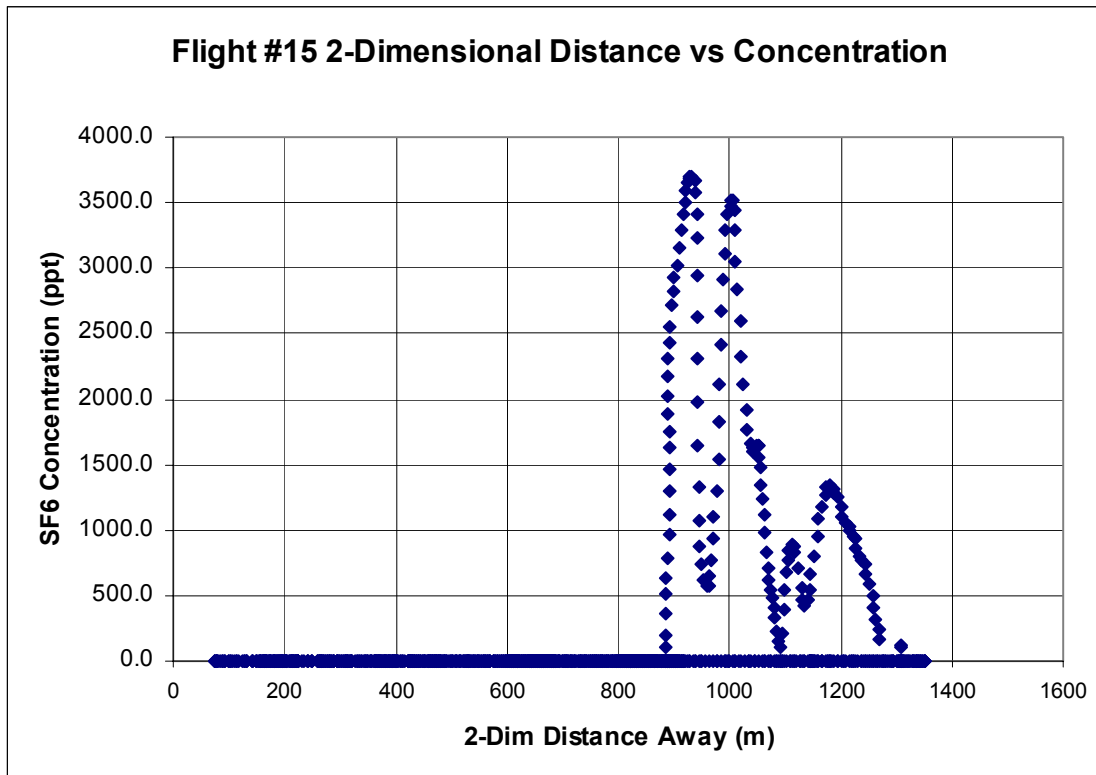


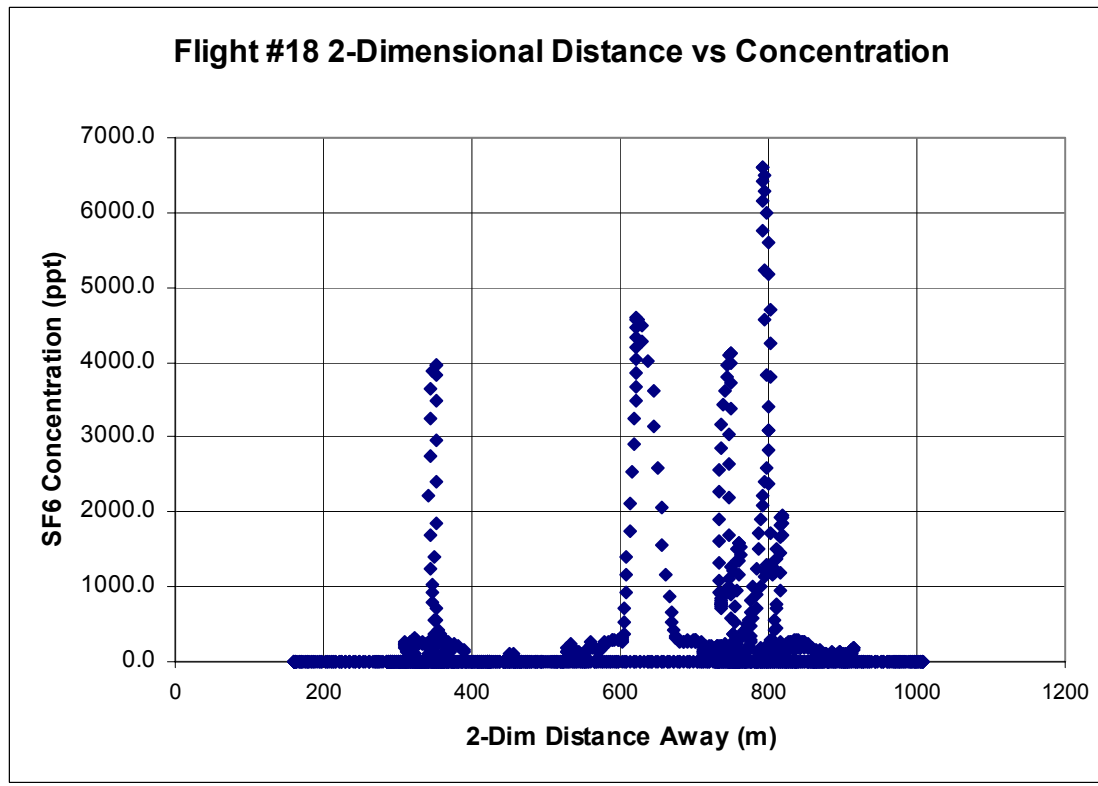
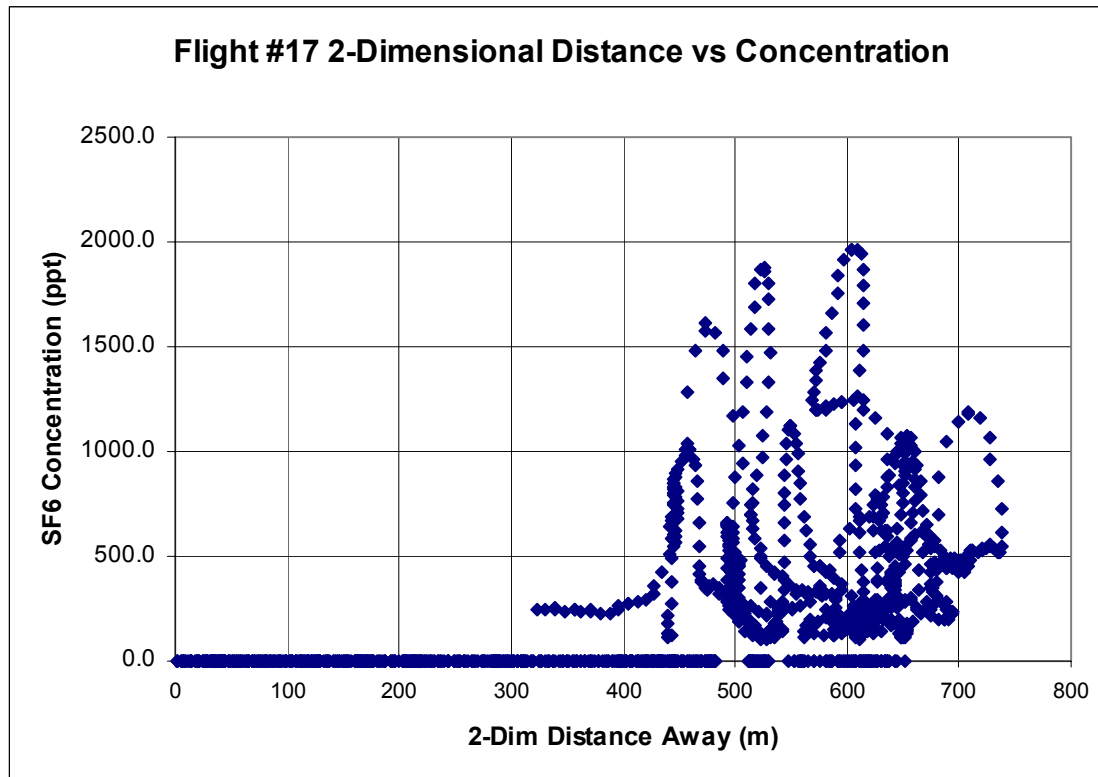


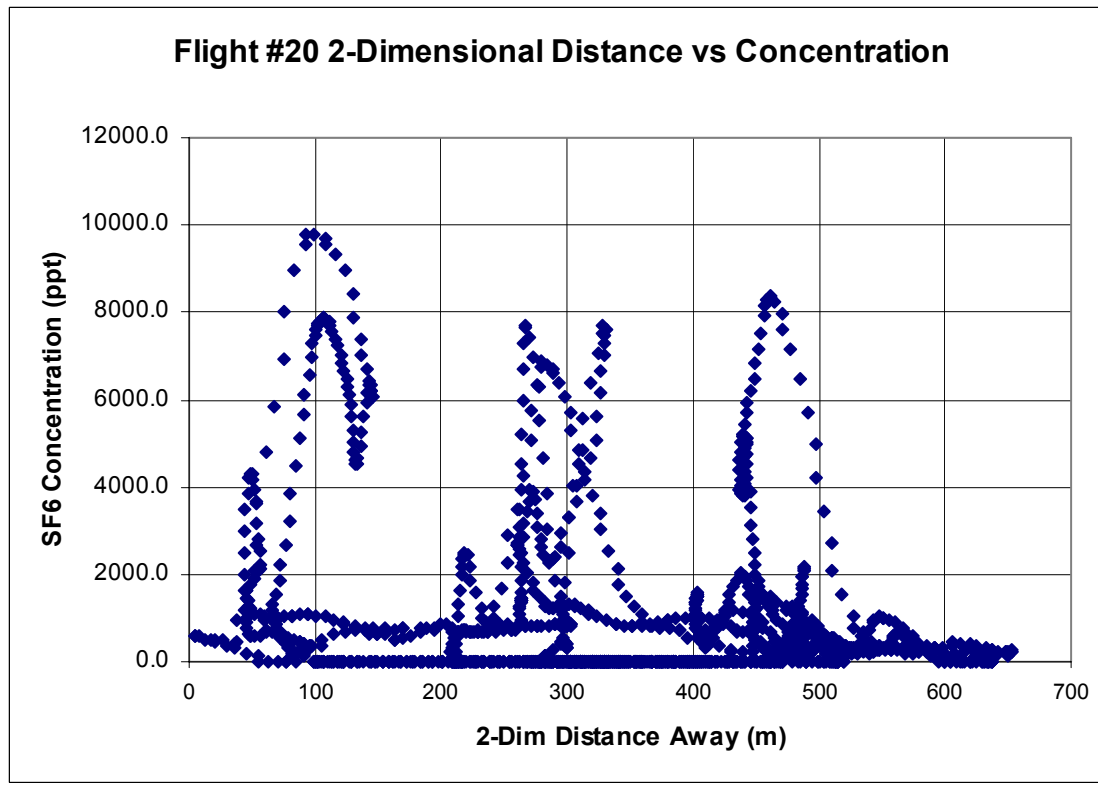
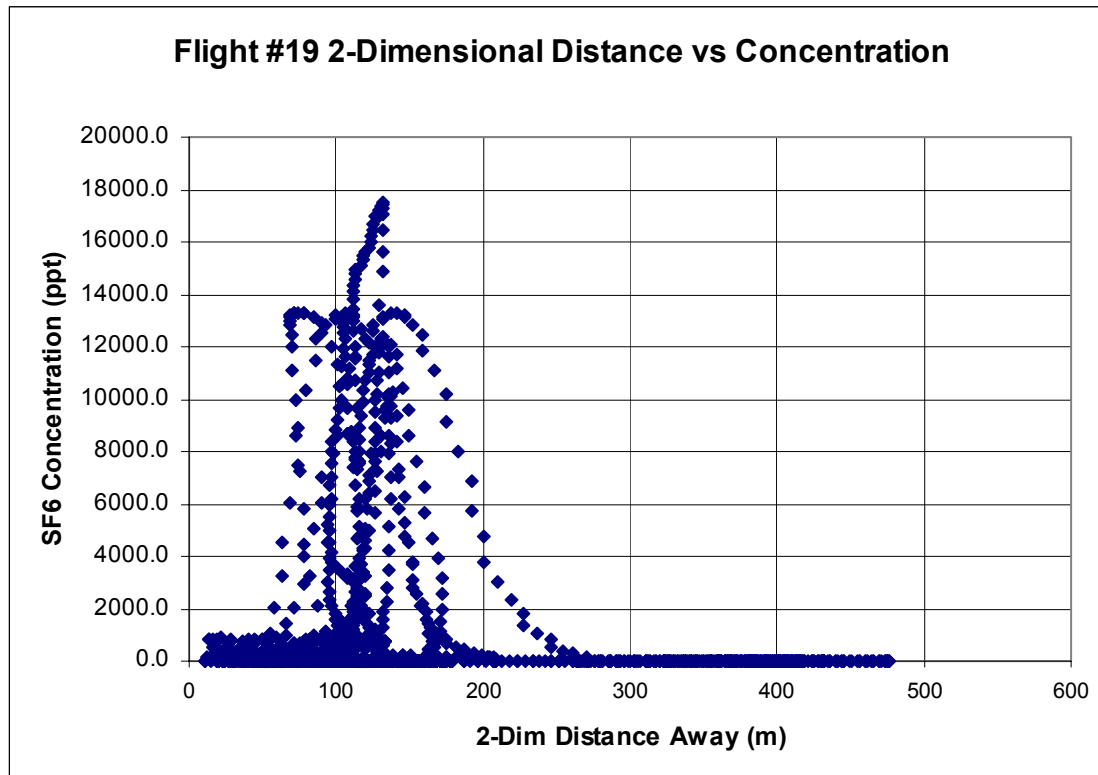


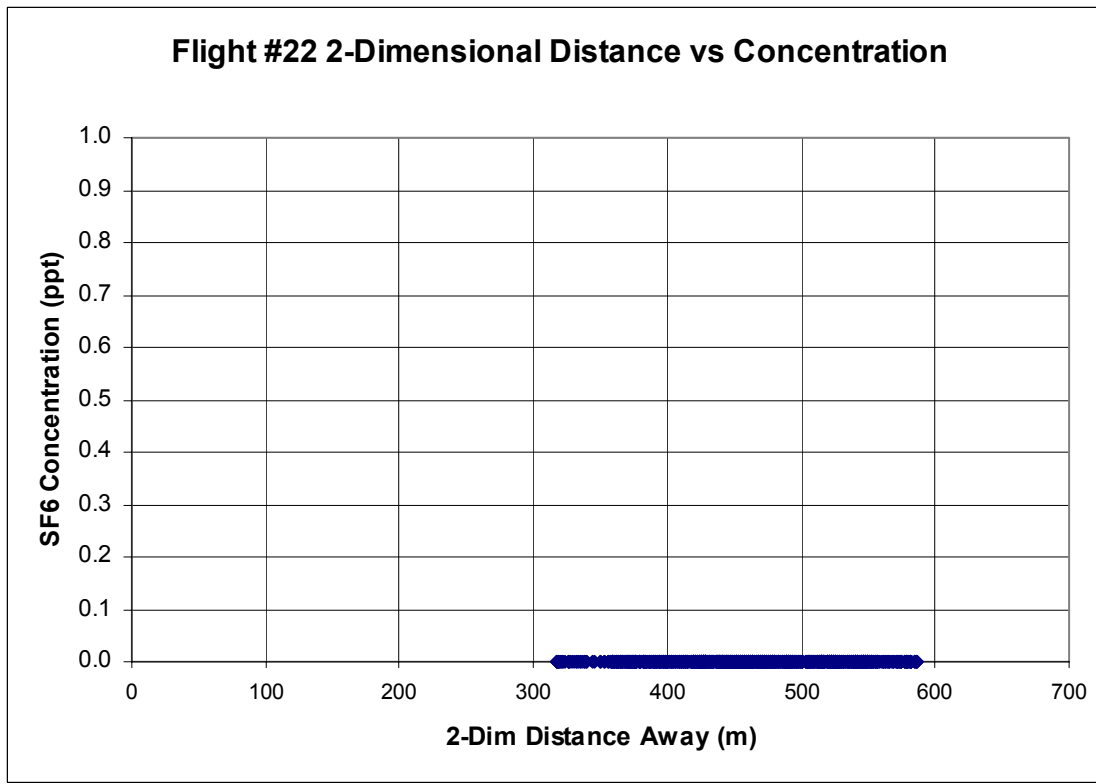
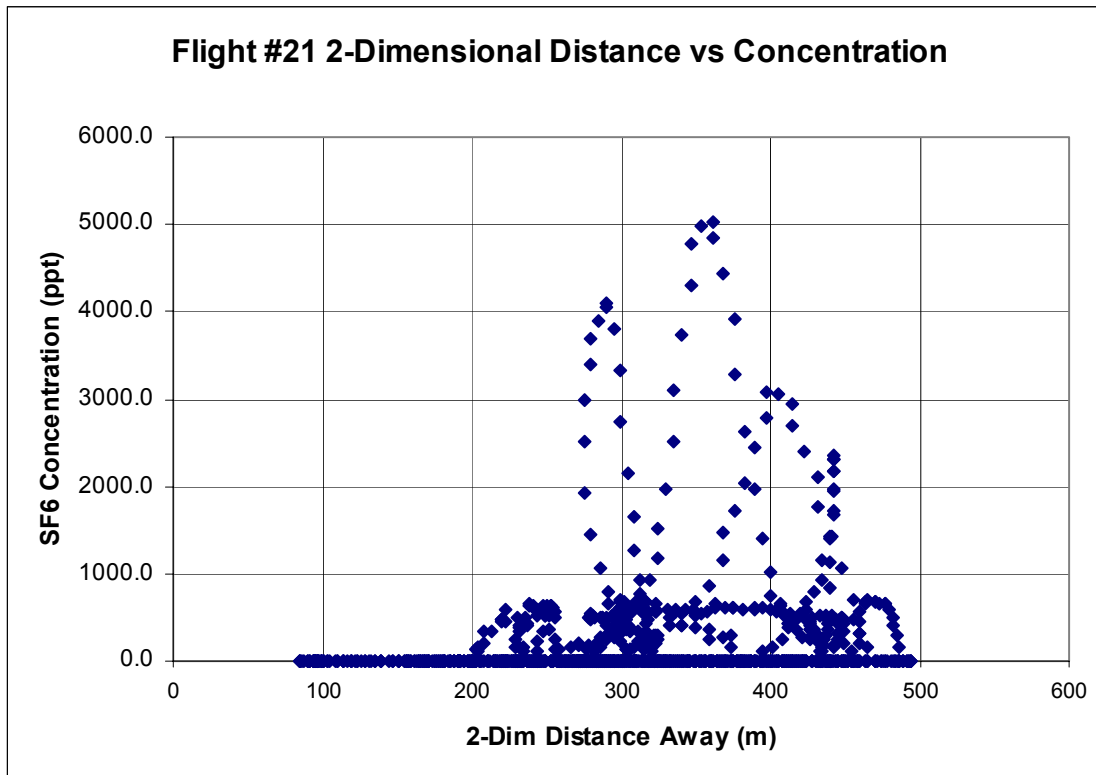


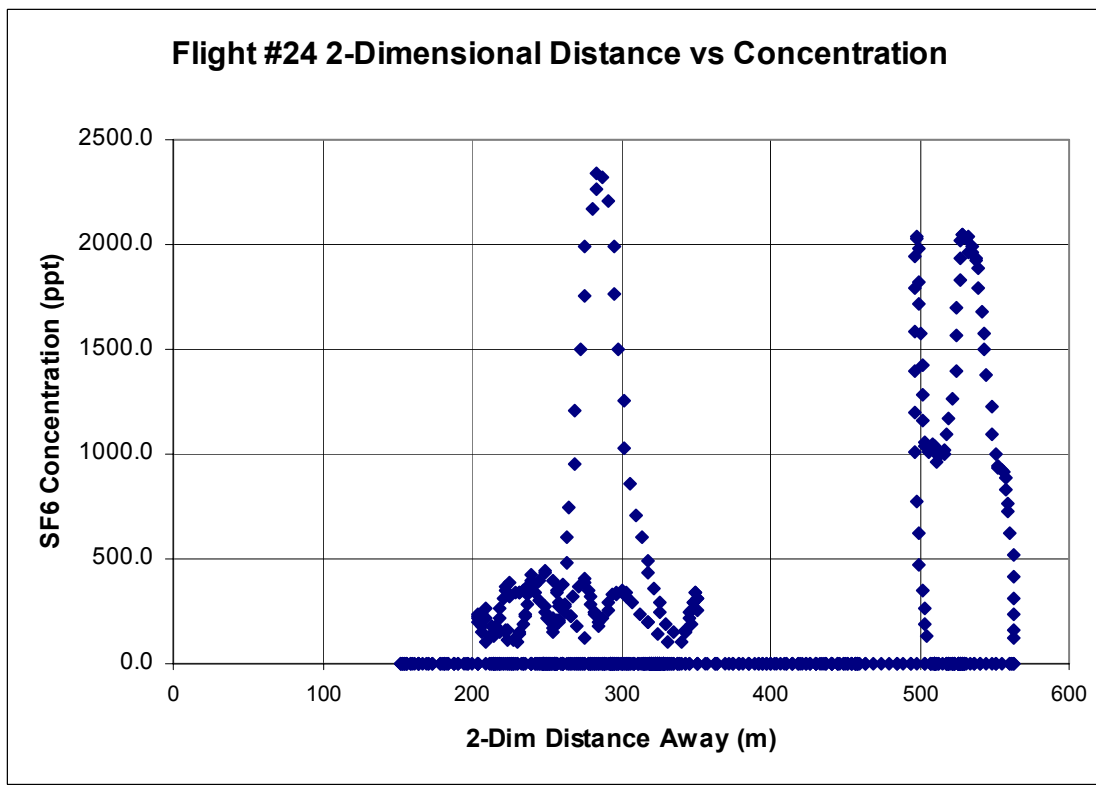
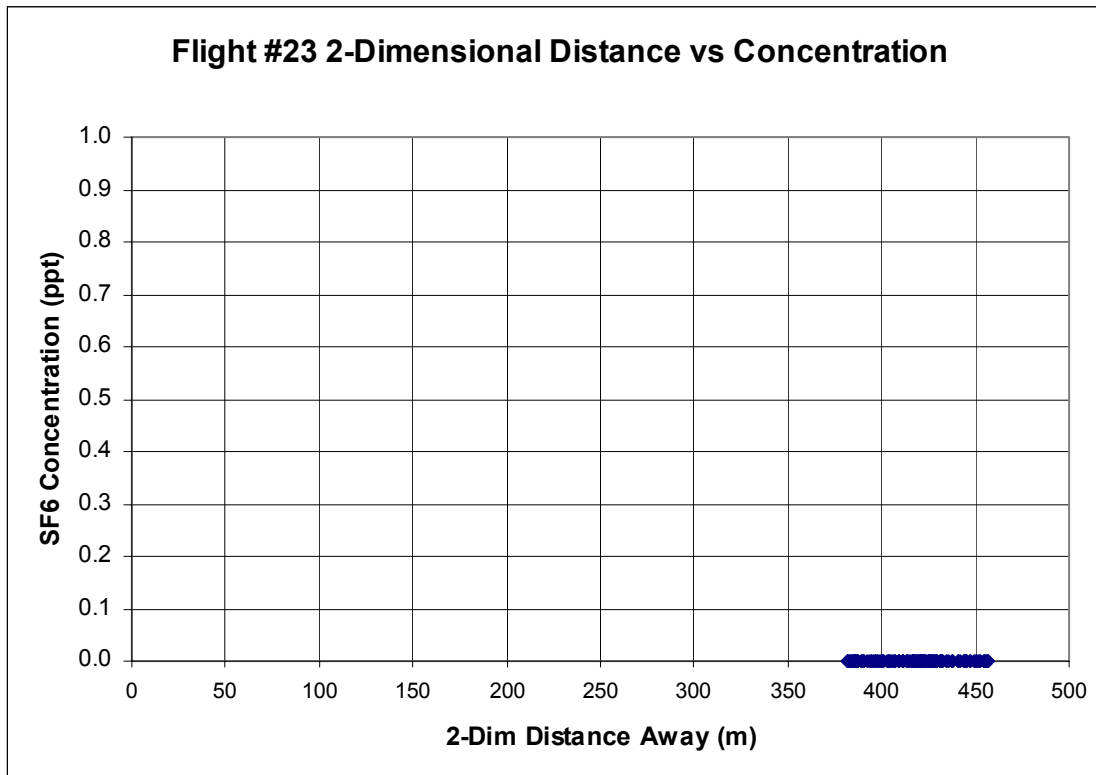


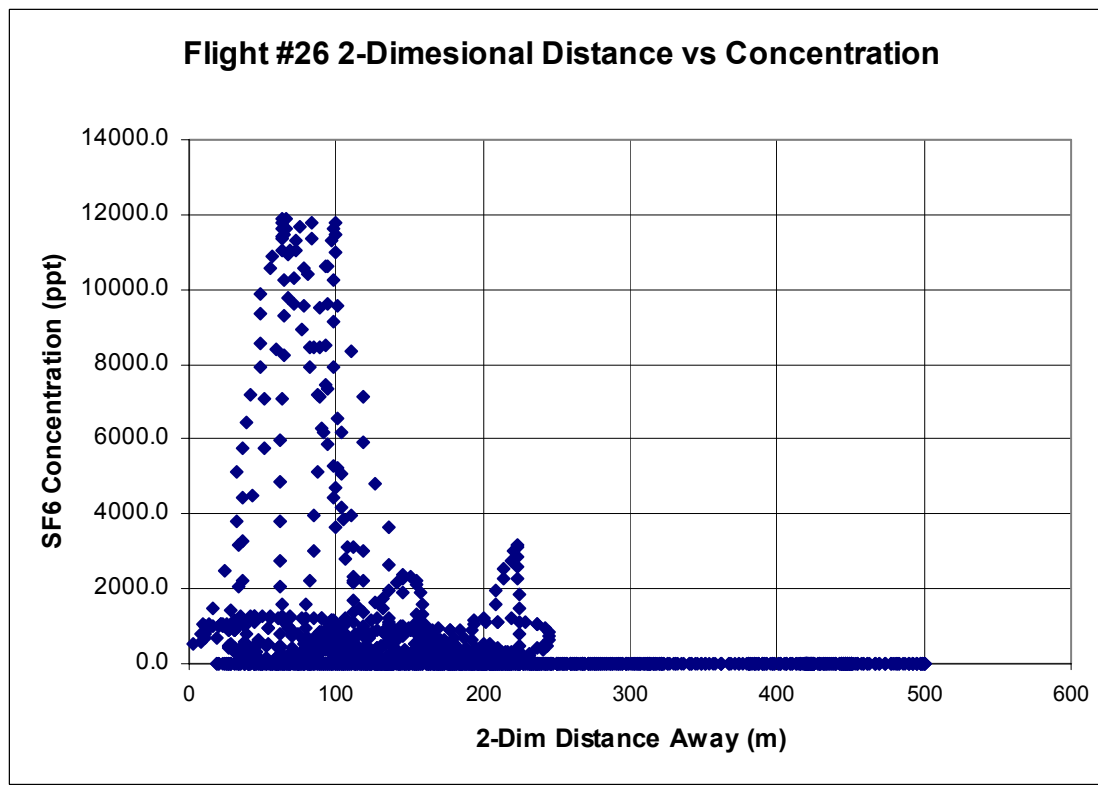
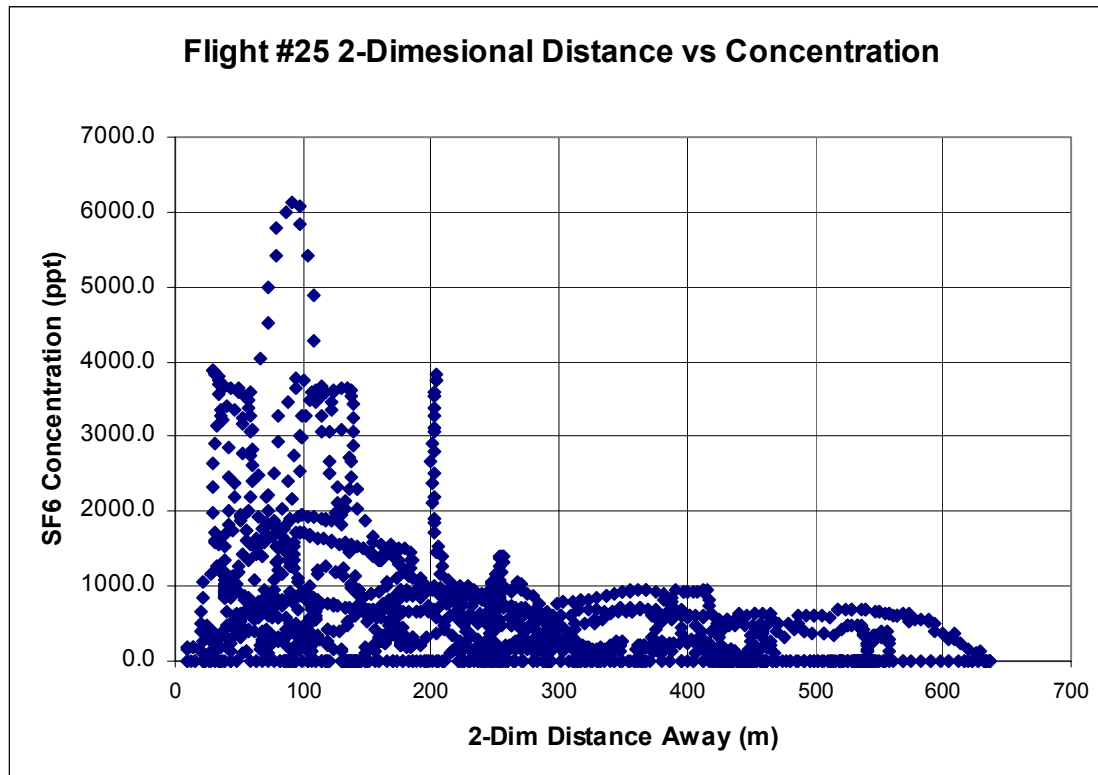


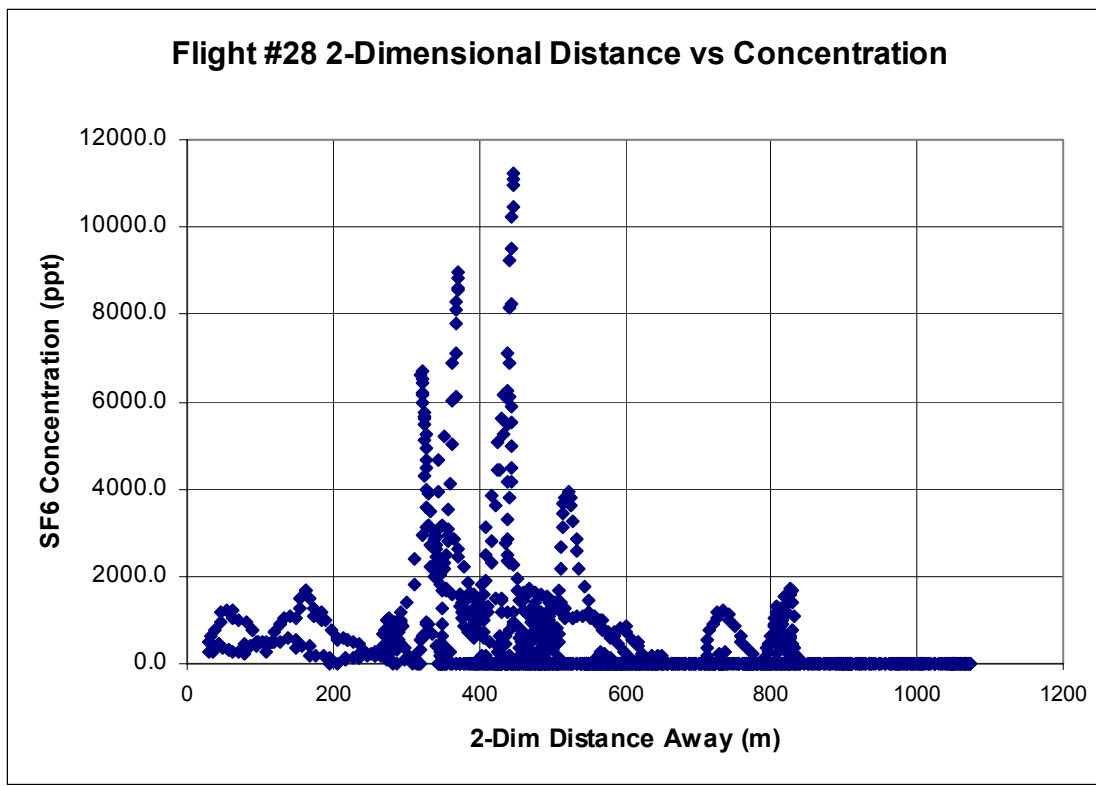
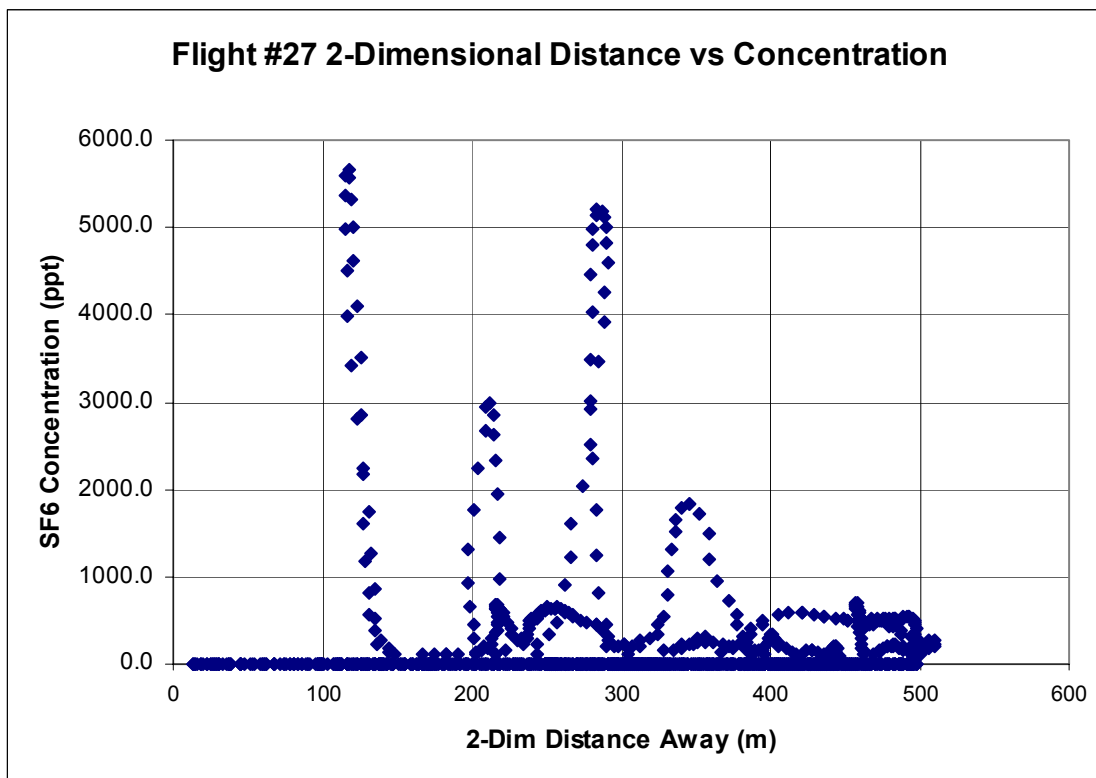






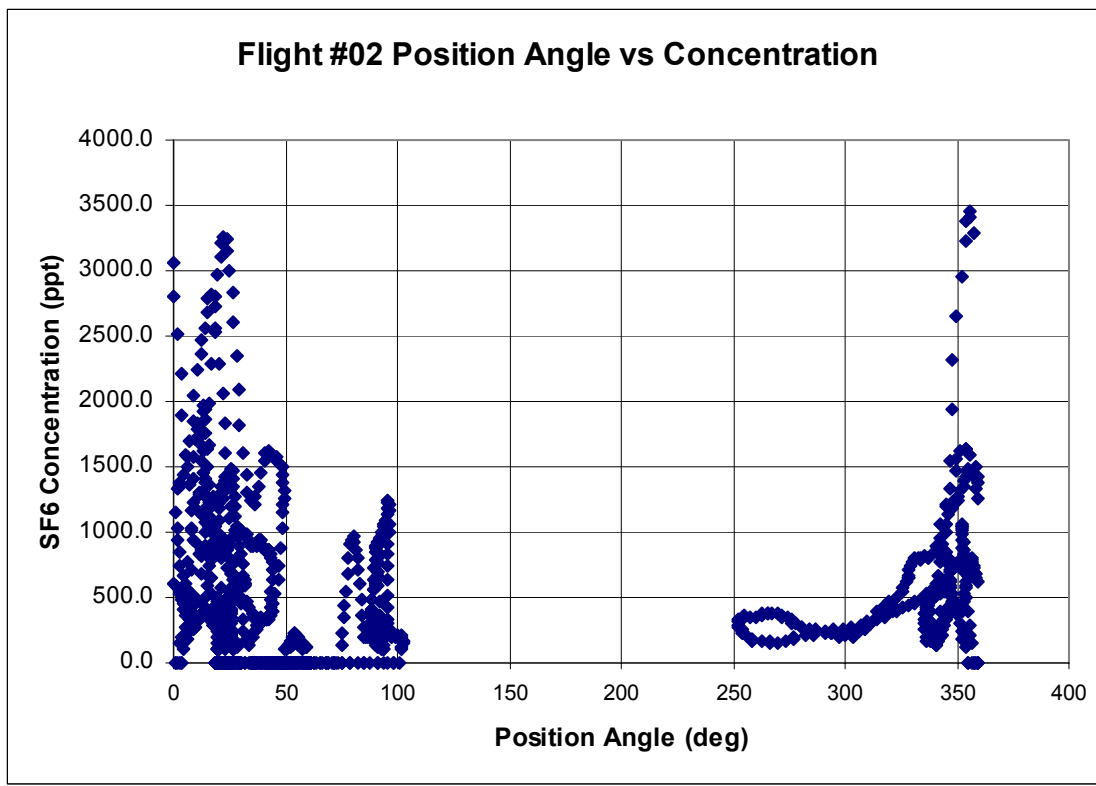
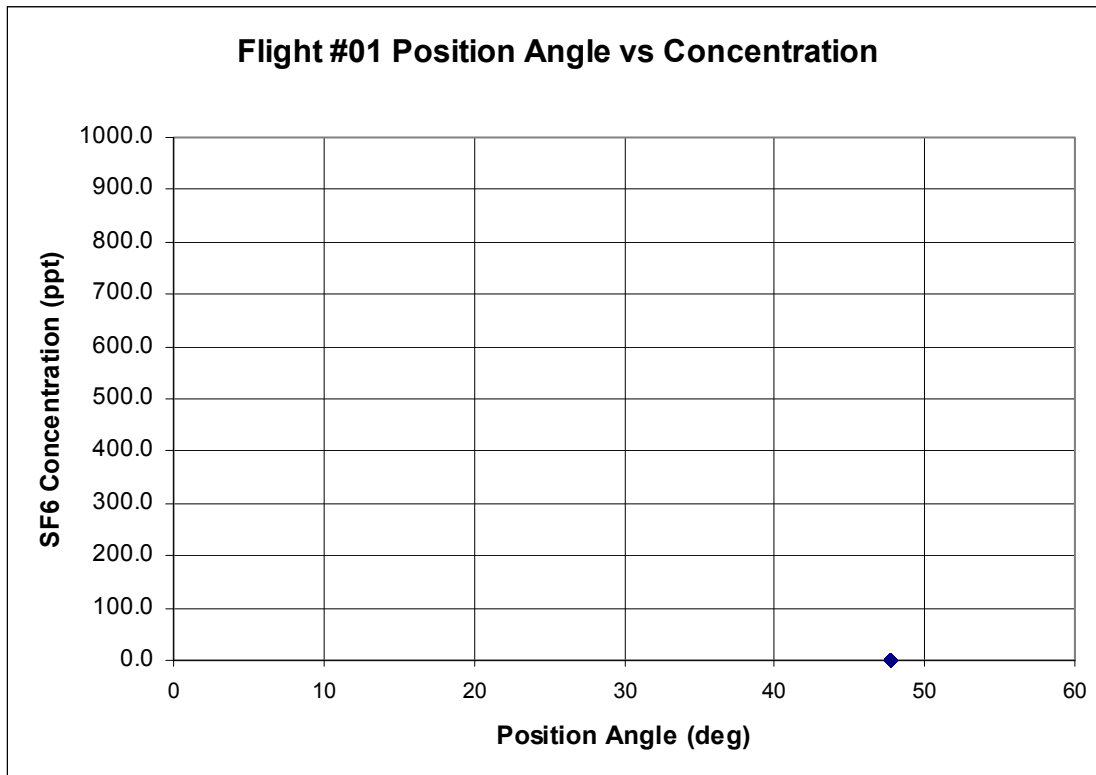


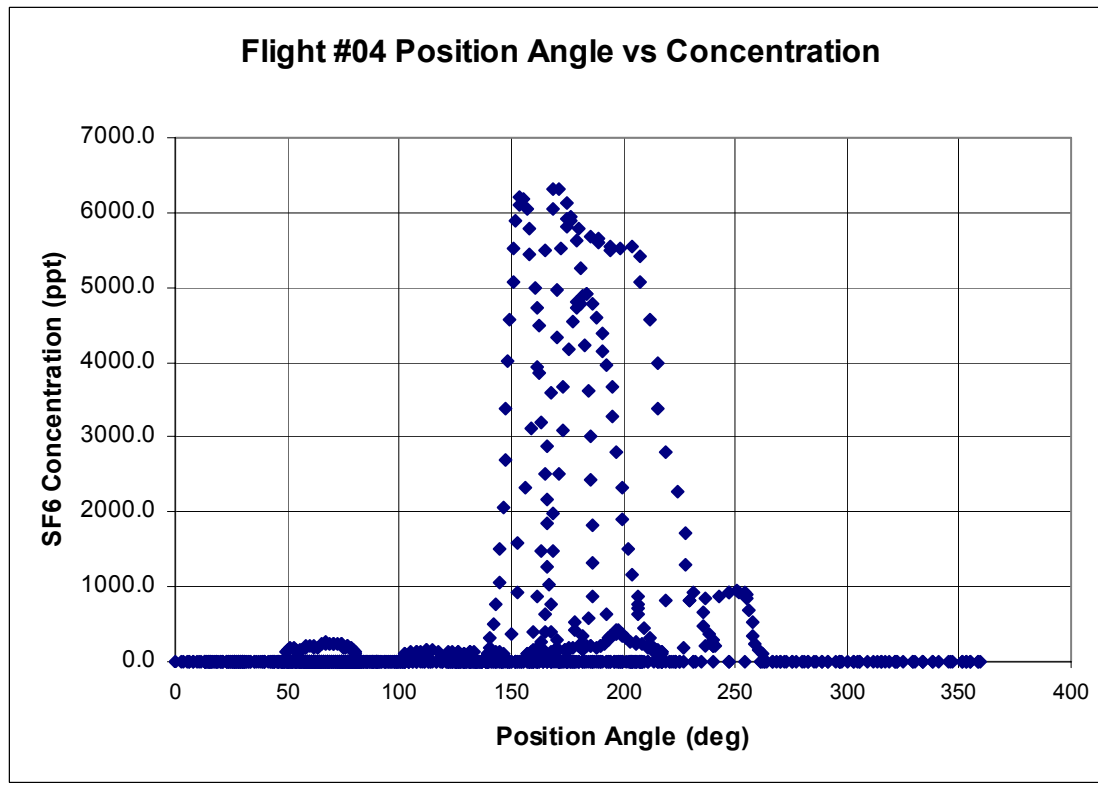
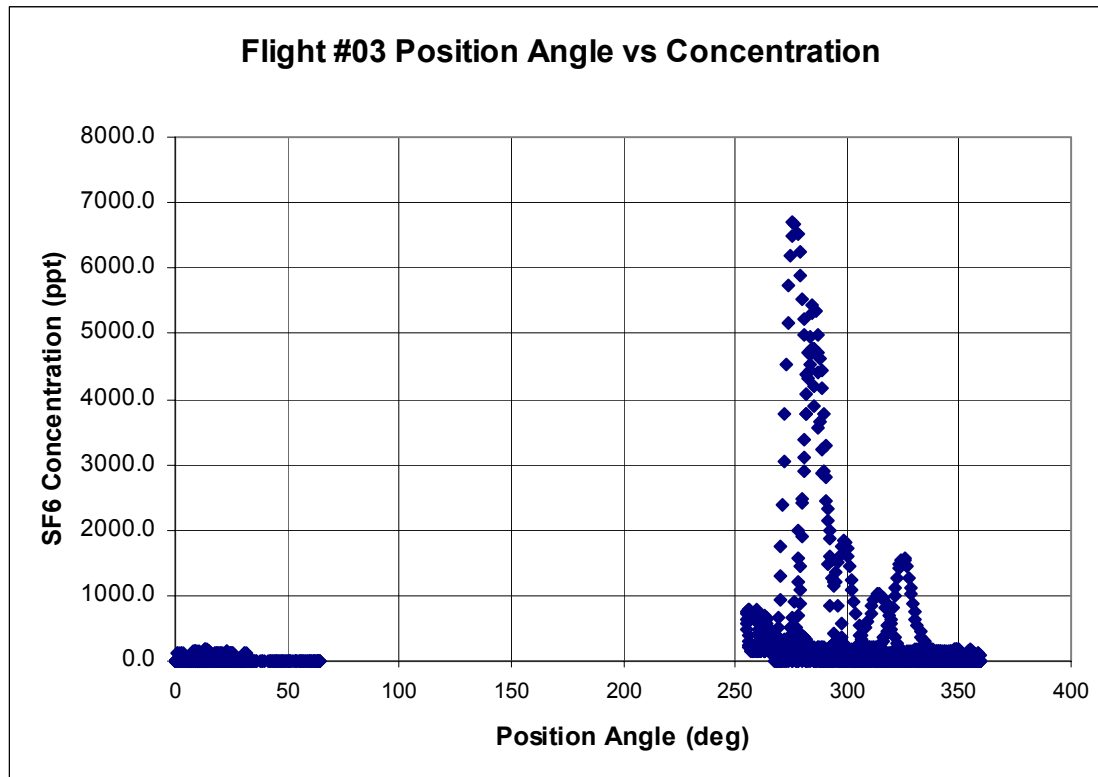


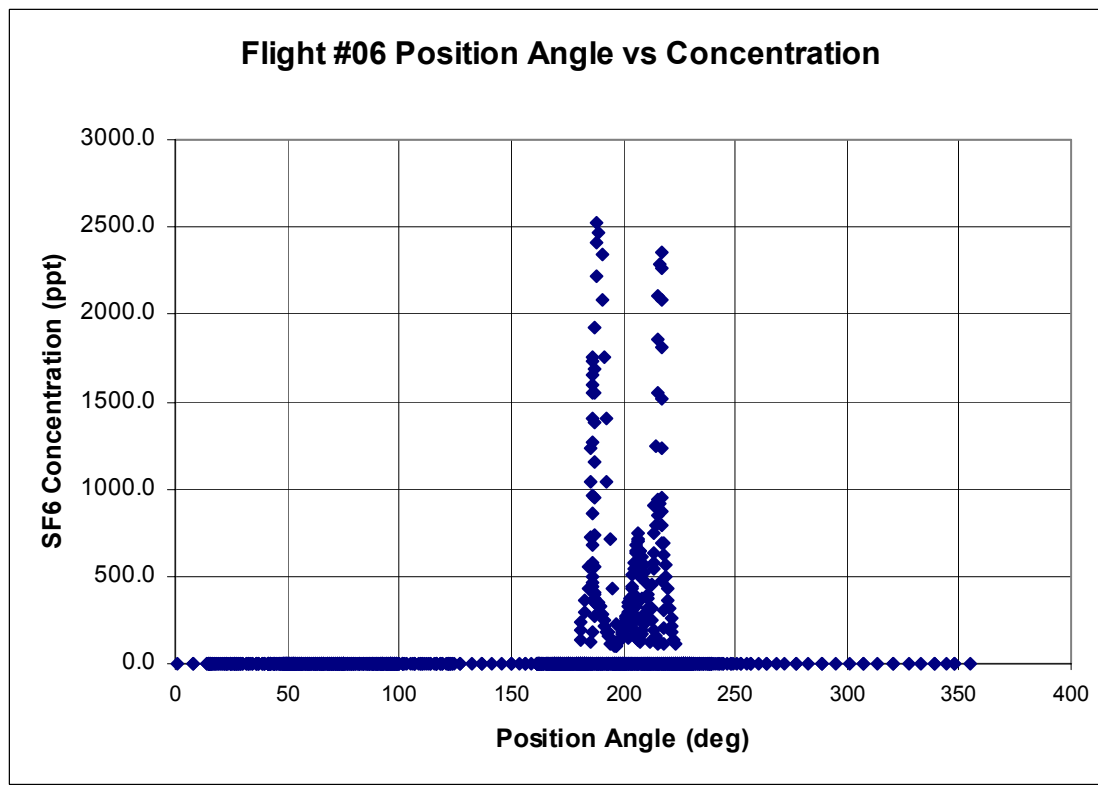
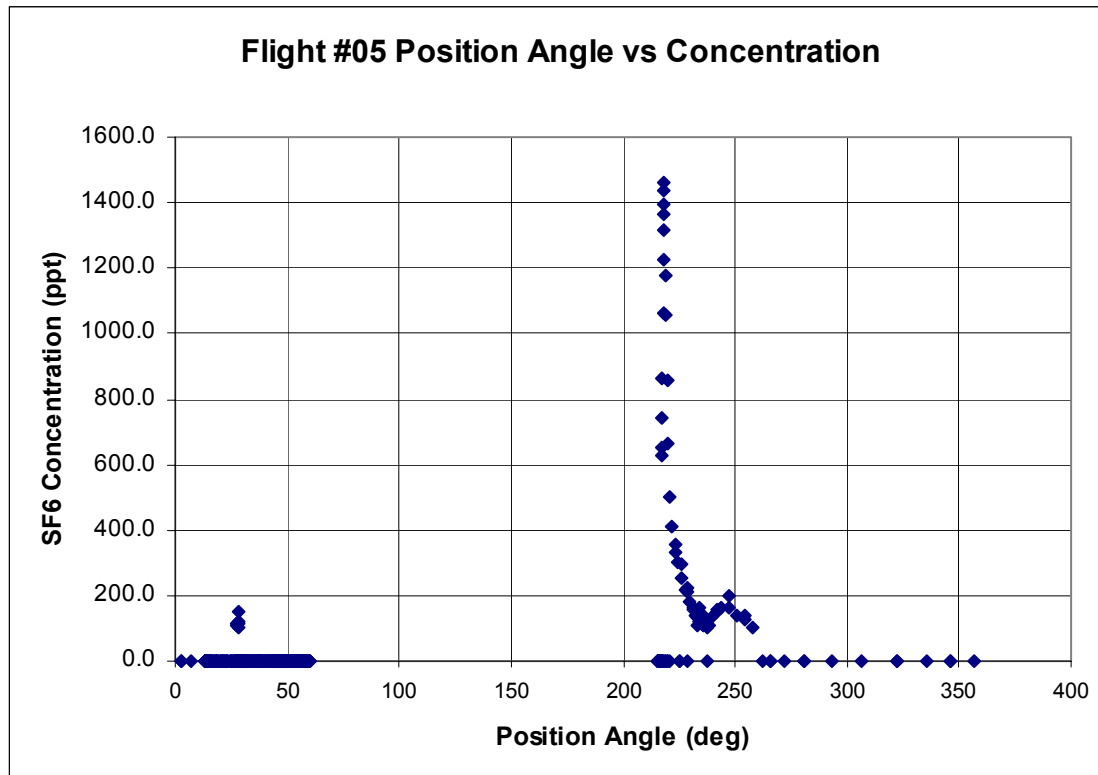


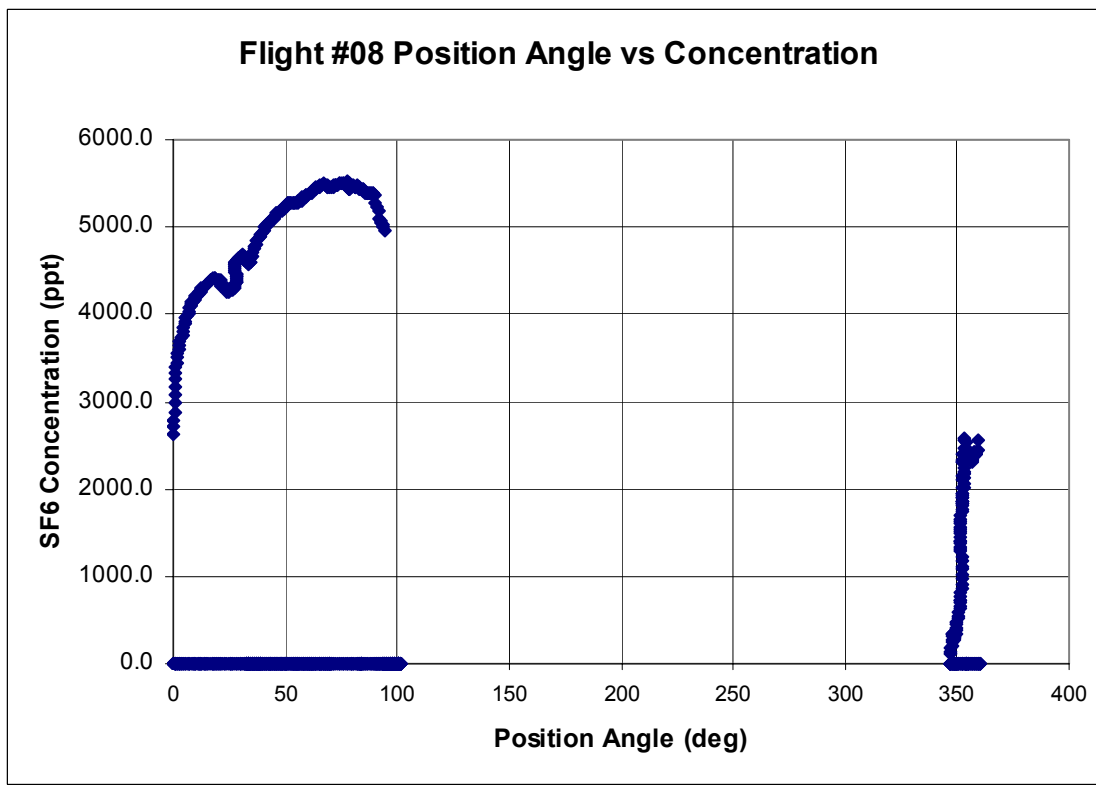
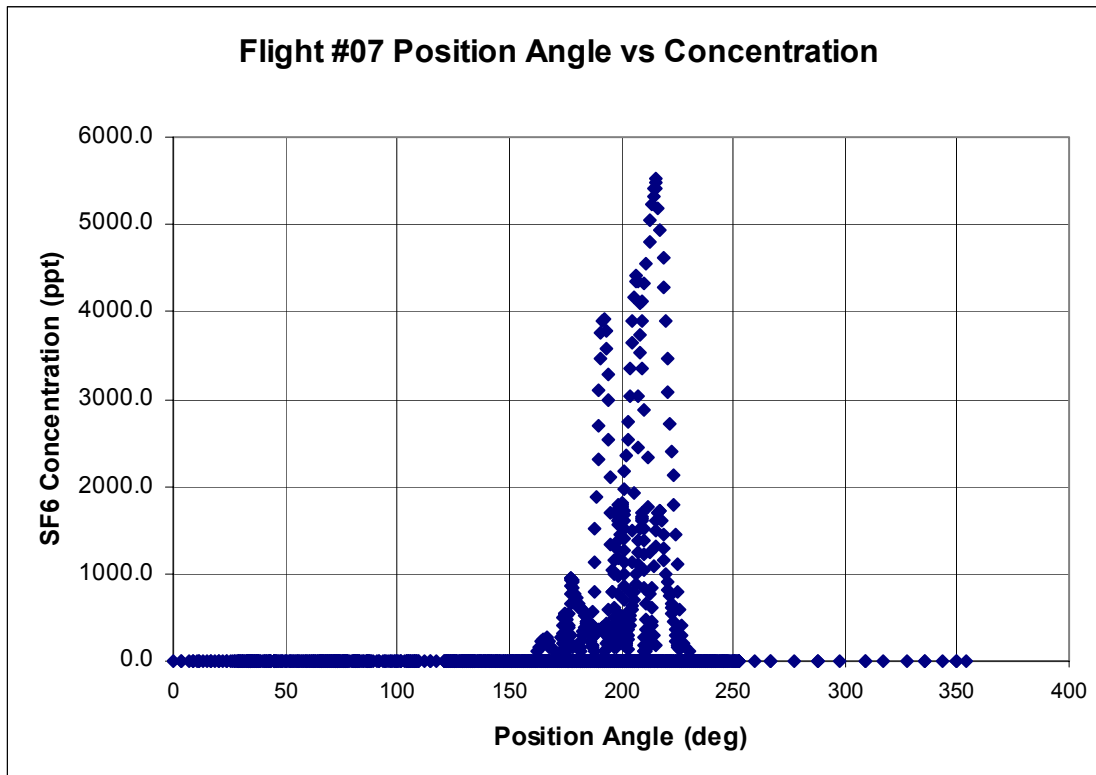
APPENDIX E

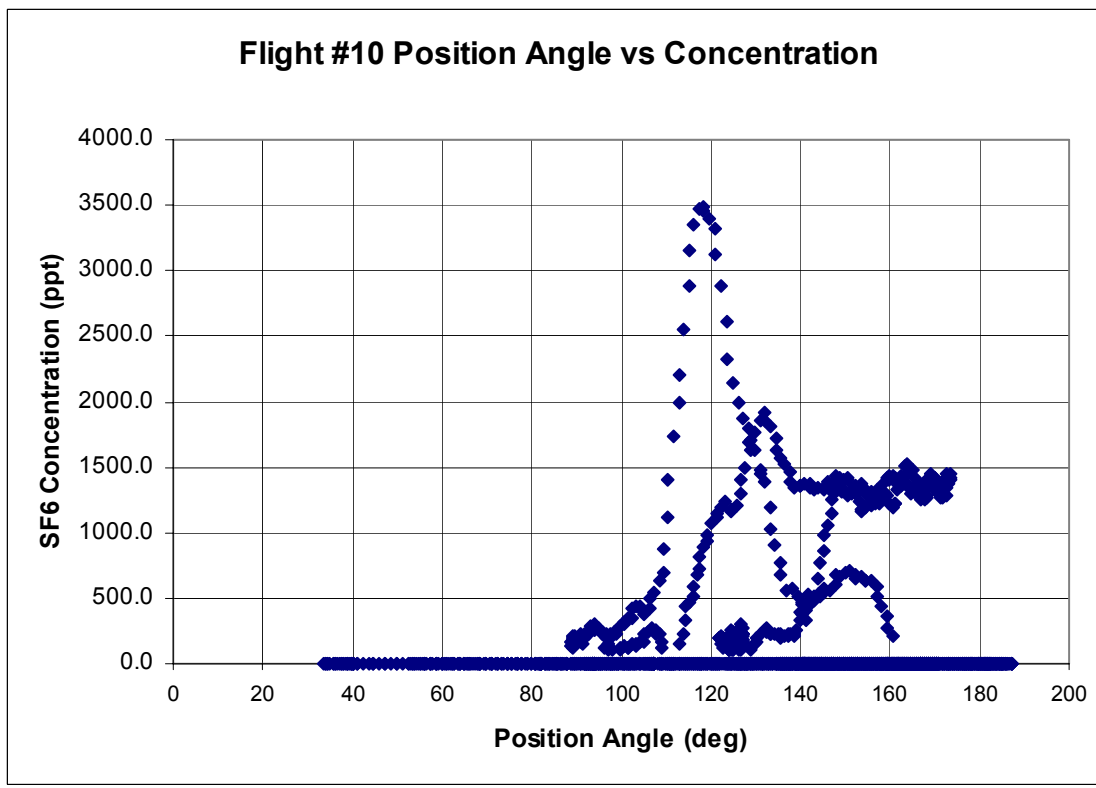
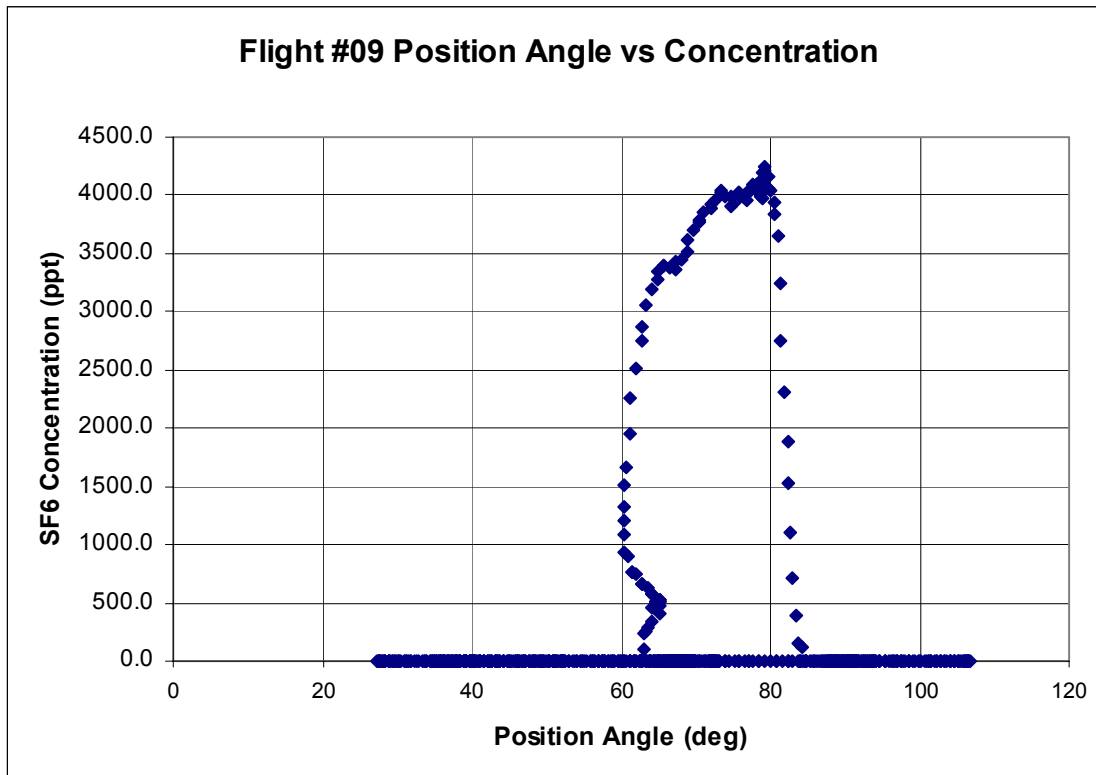
SF₆ CONCENTRATION ANGLE GRAPHS

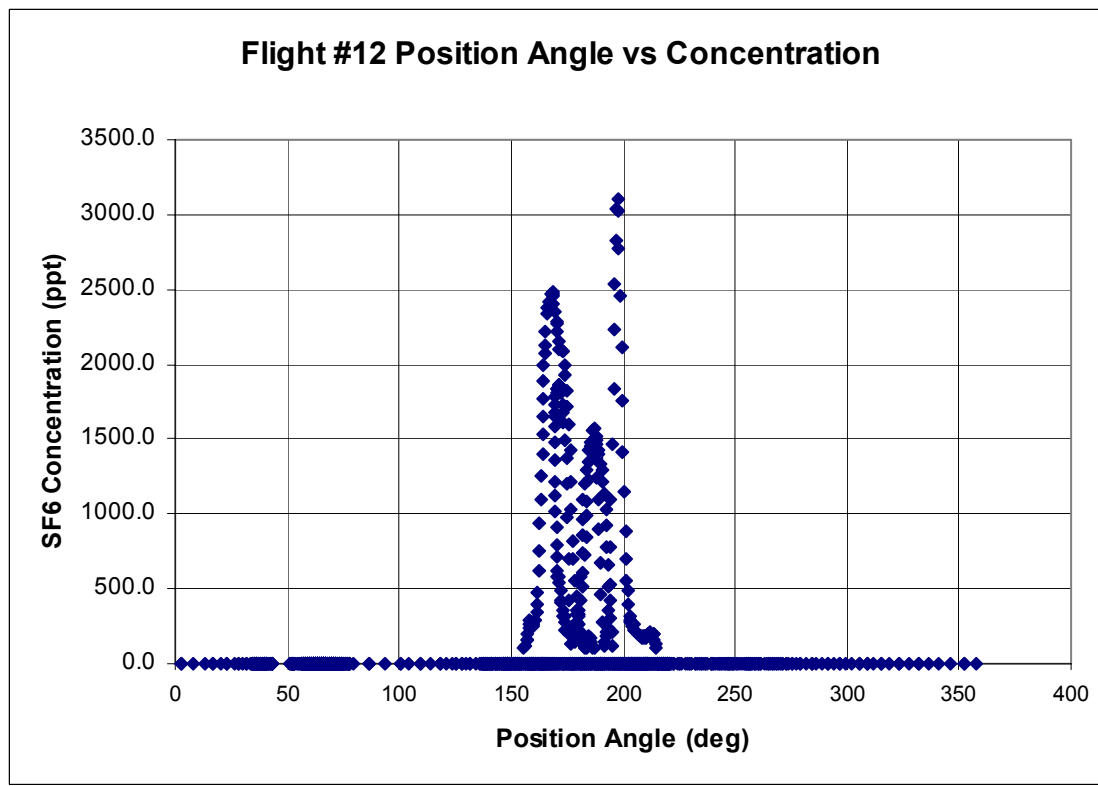
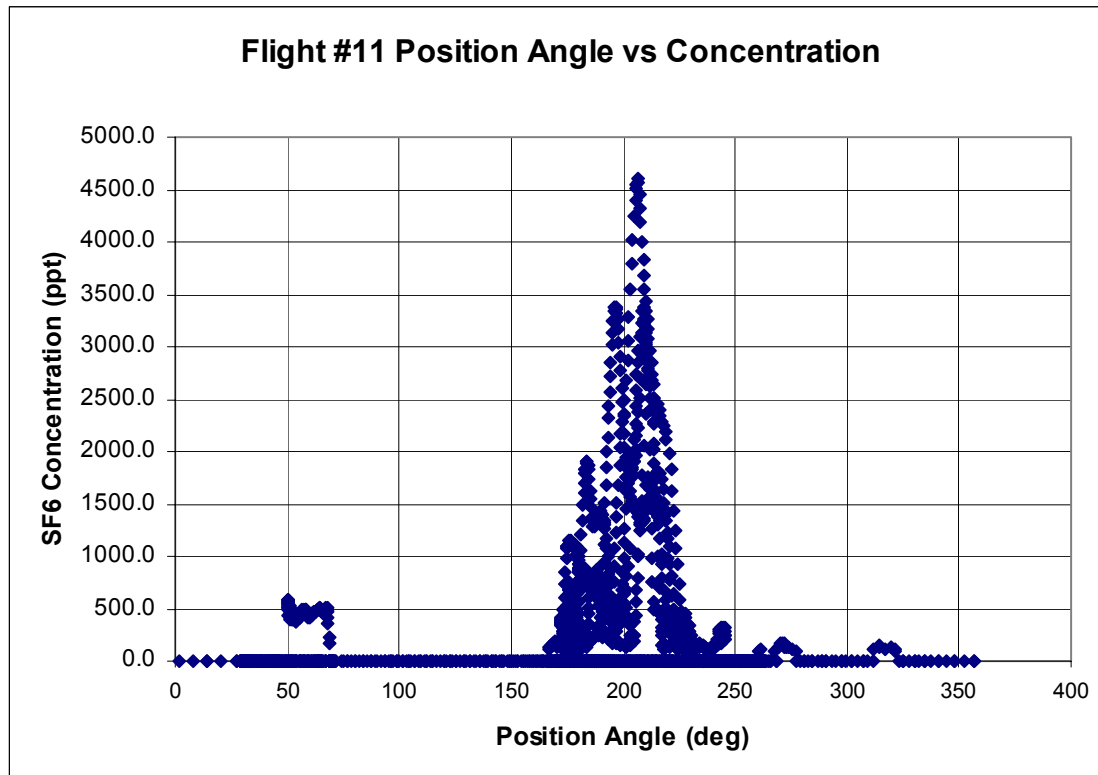


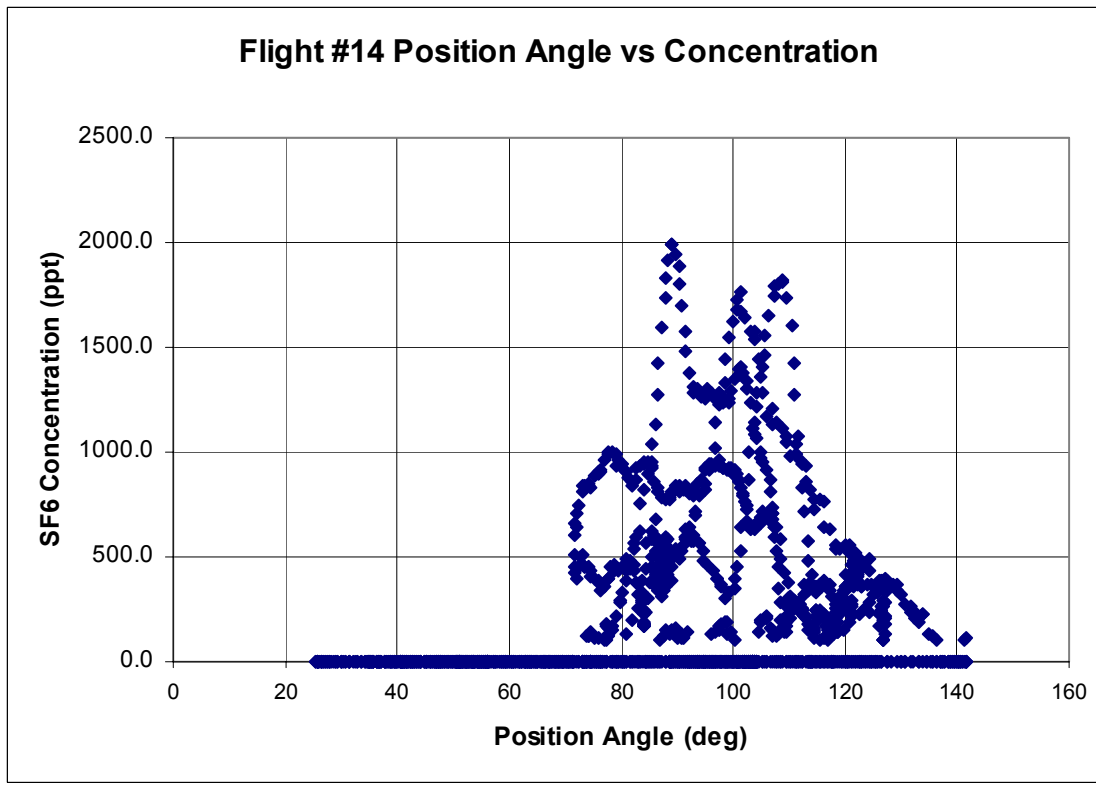
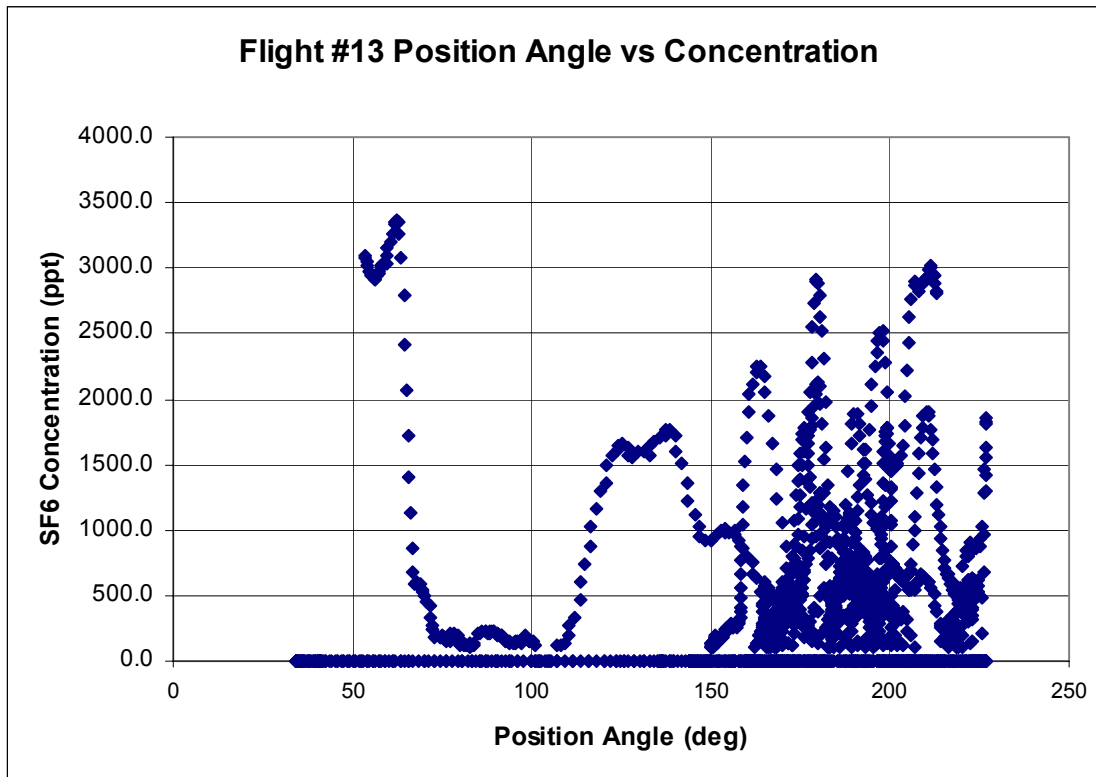


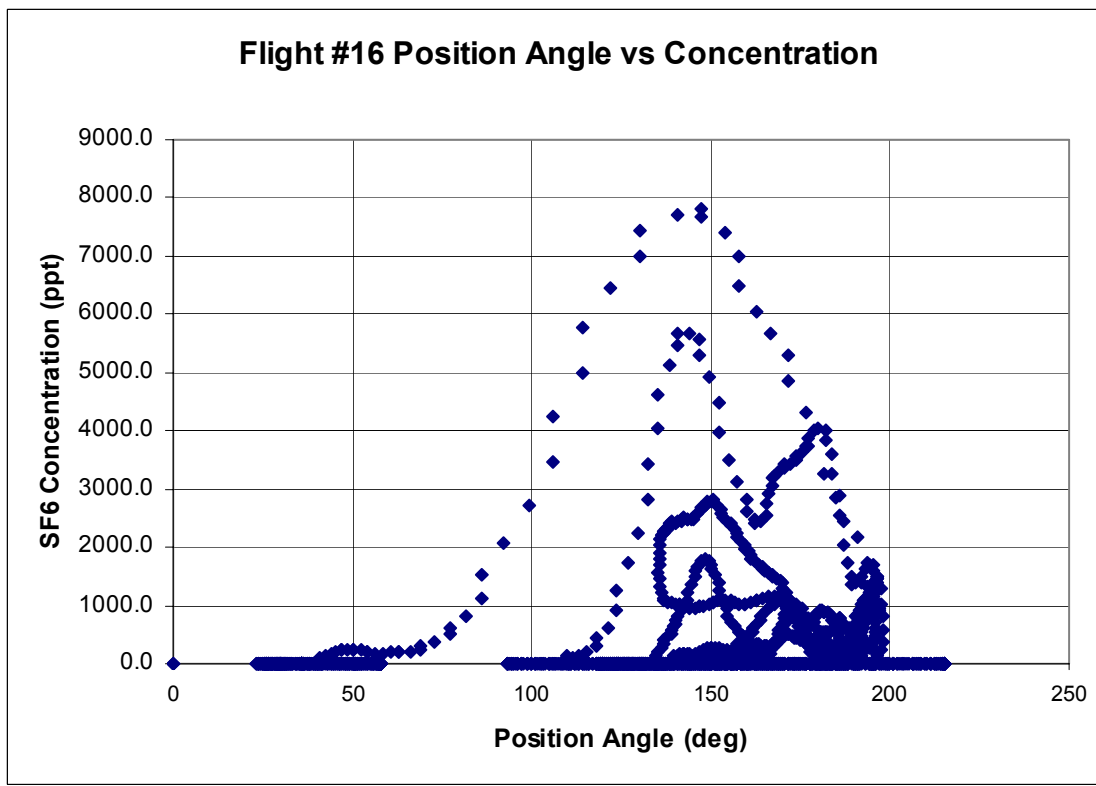
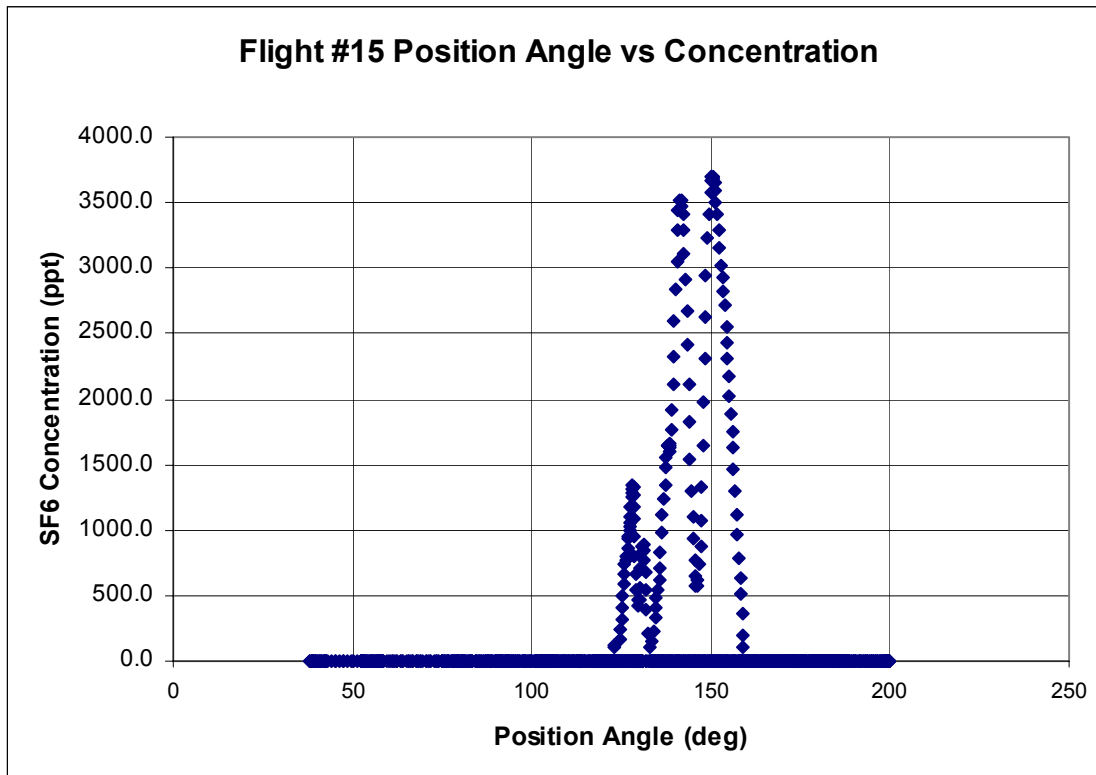


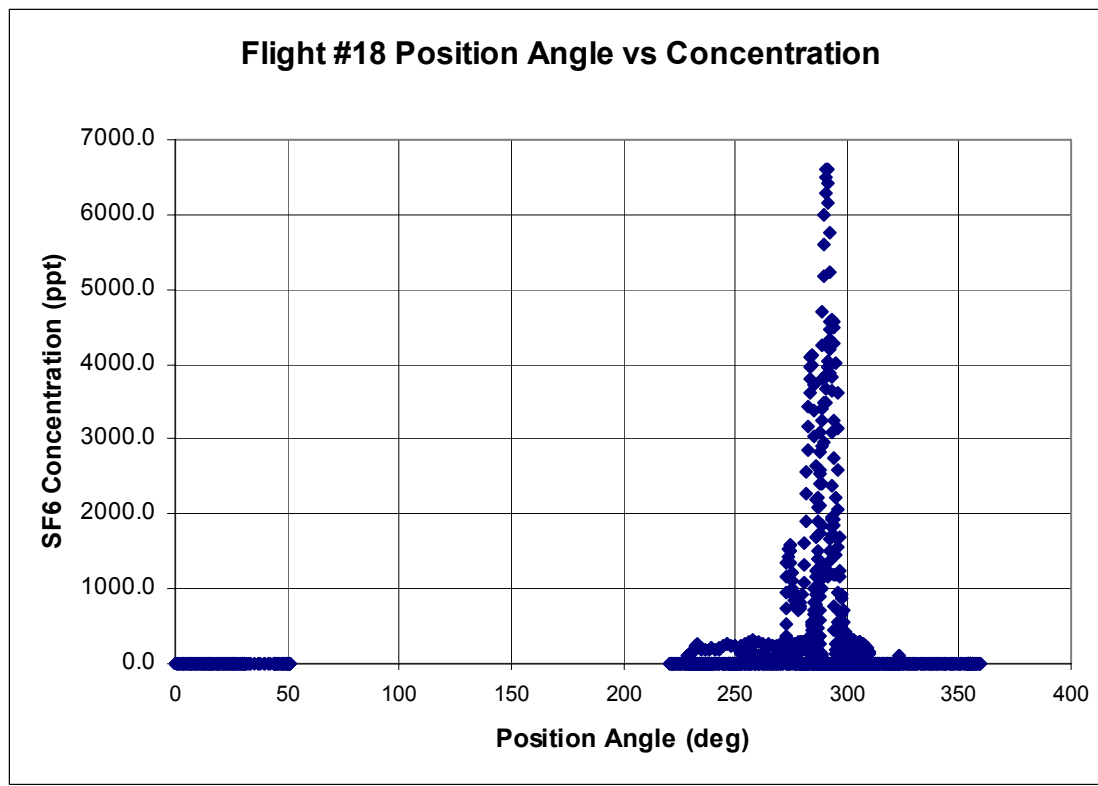
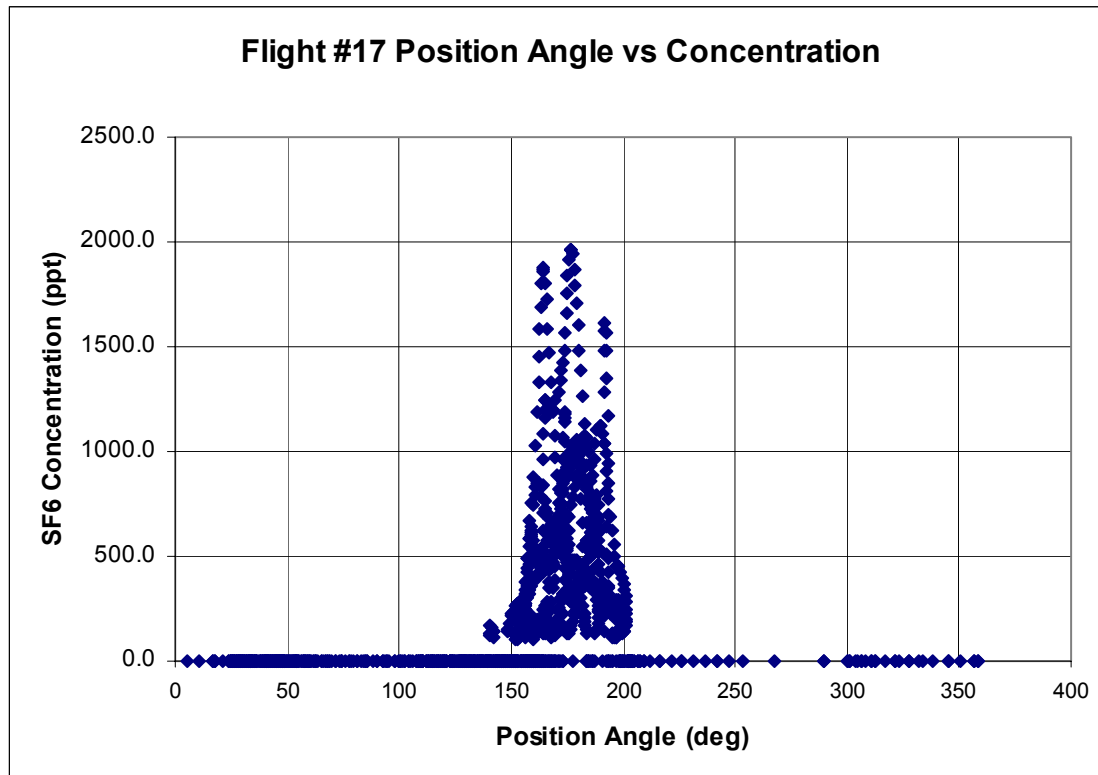


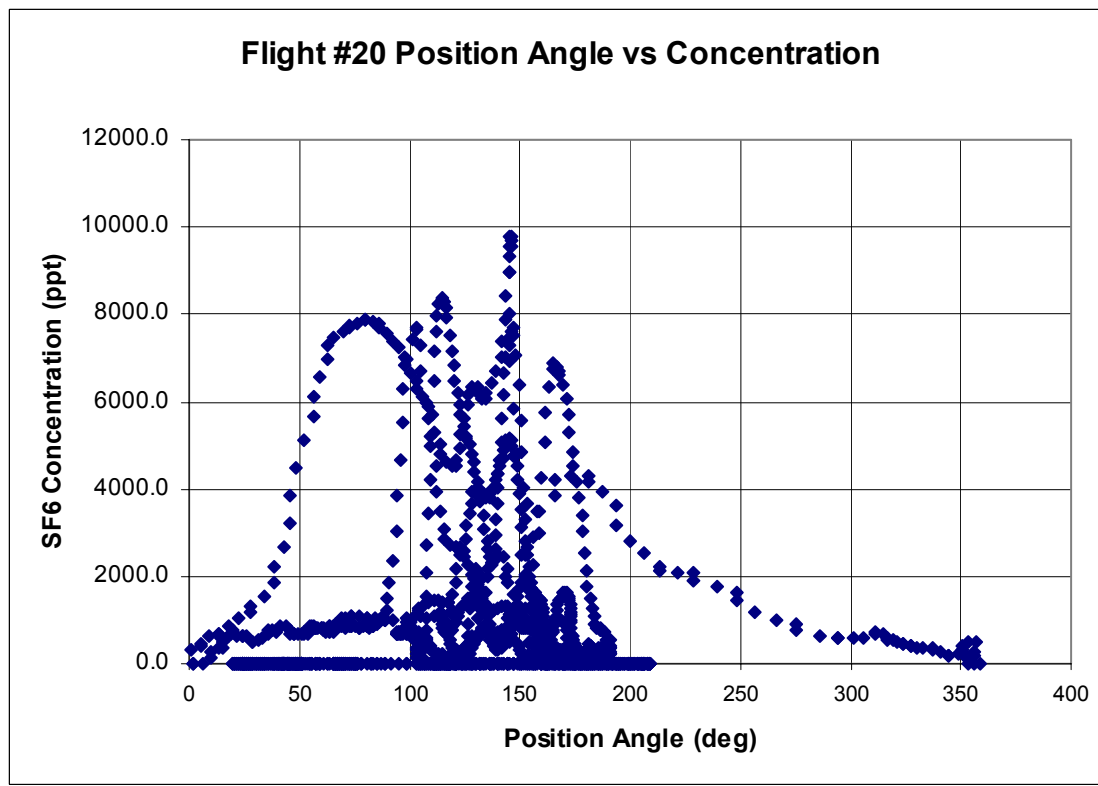
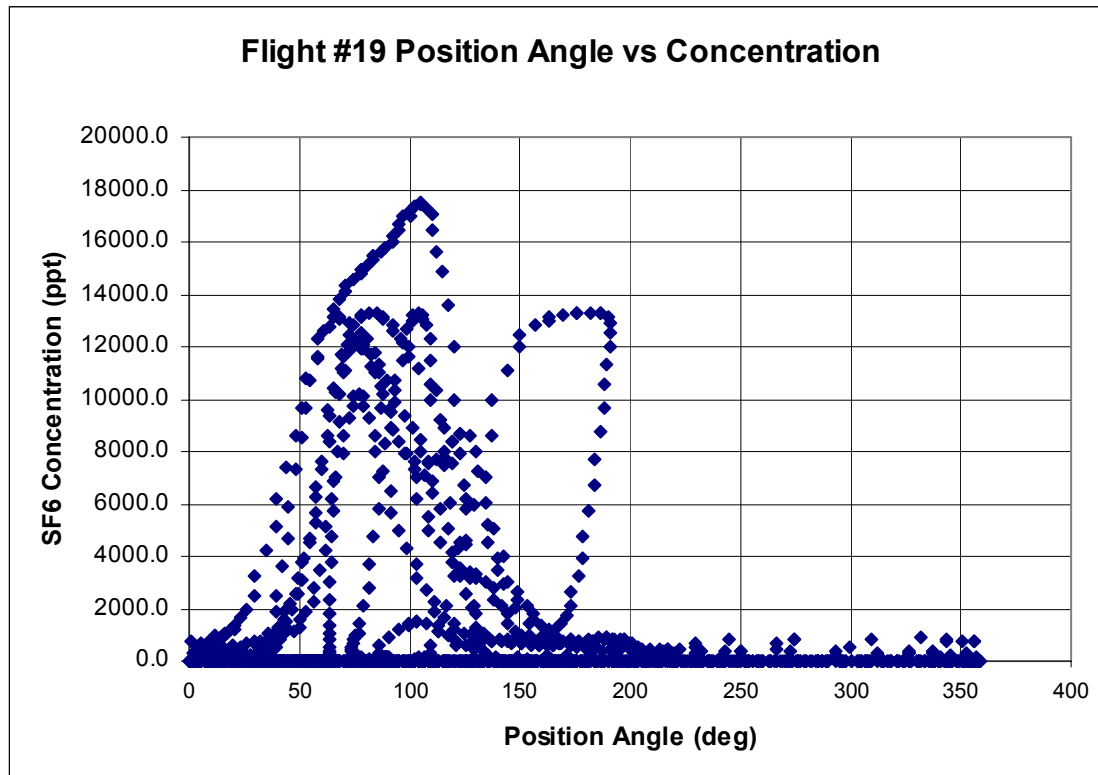


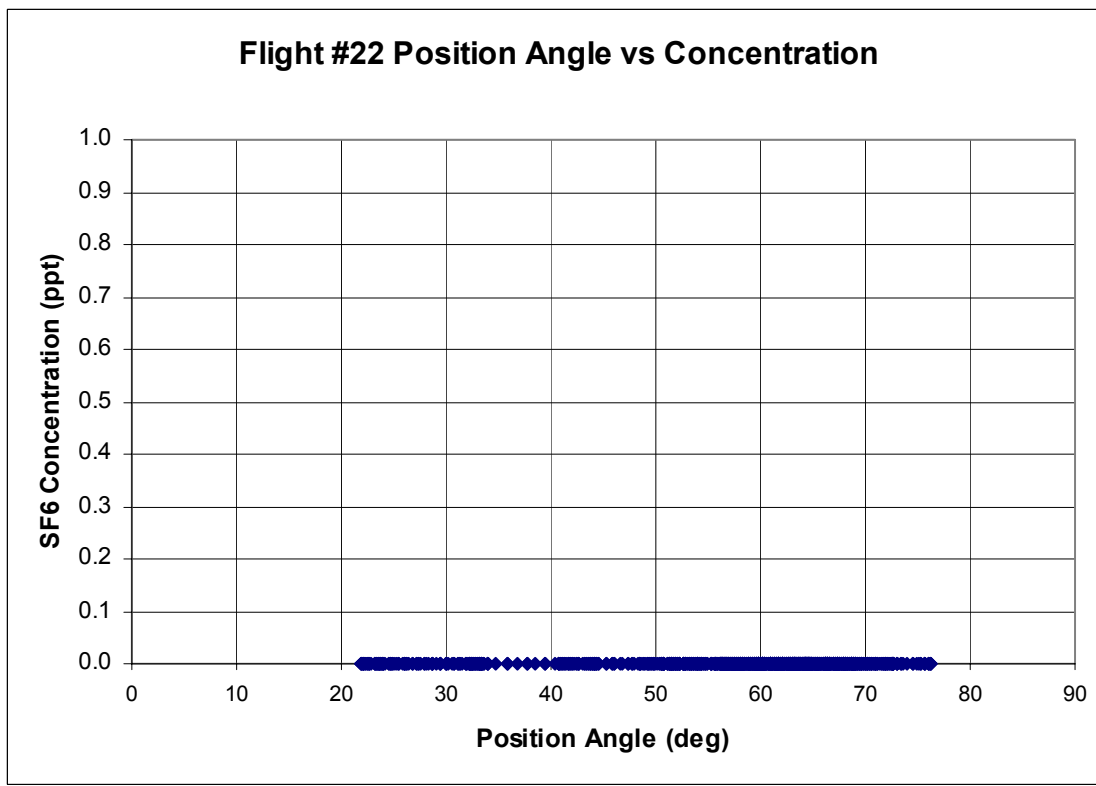
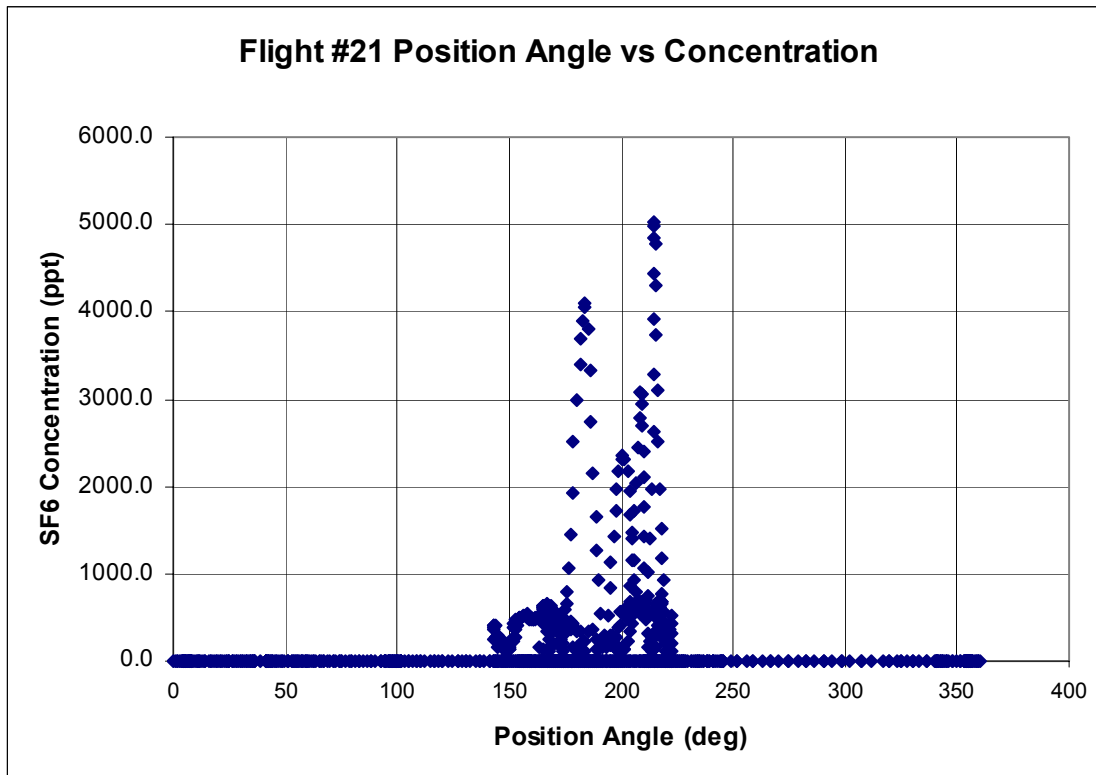


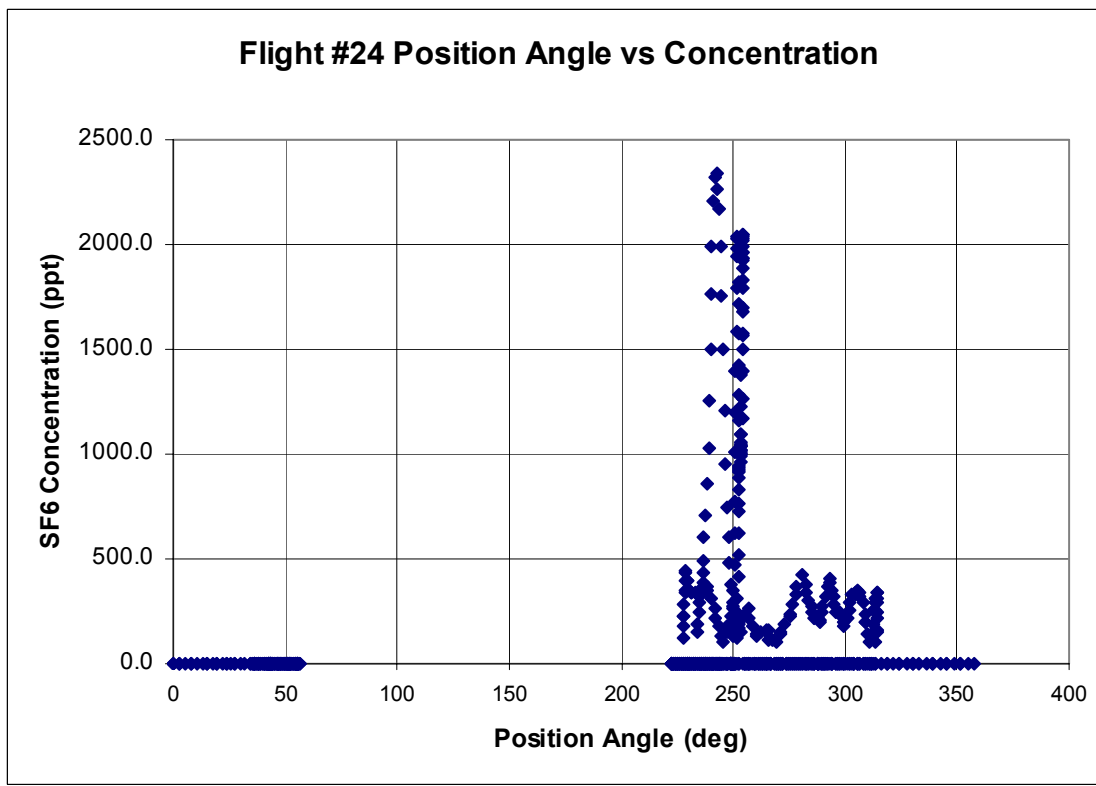
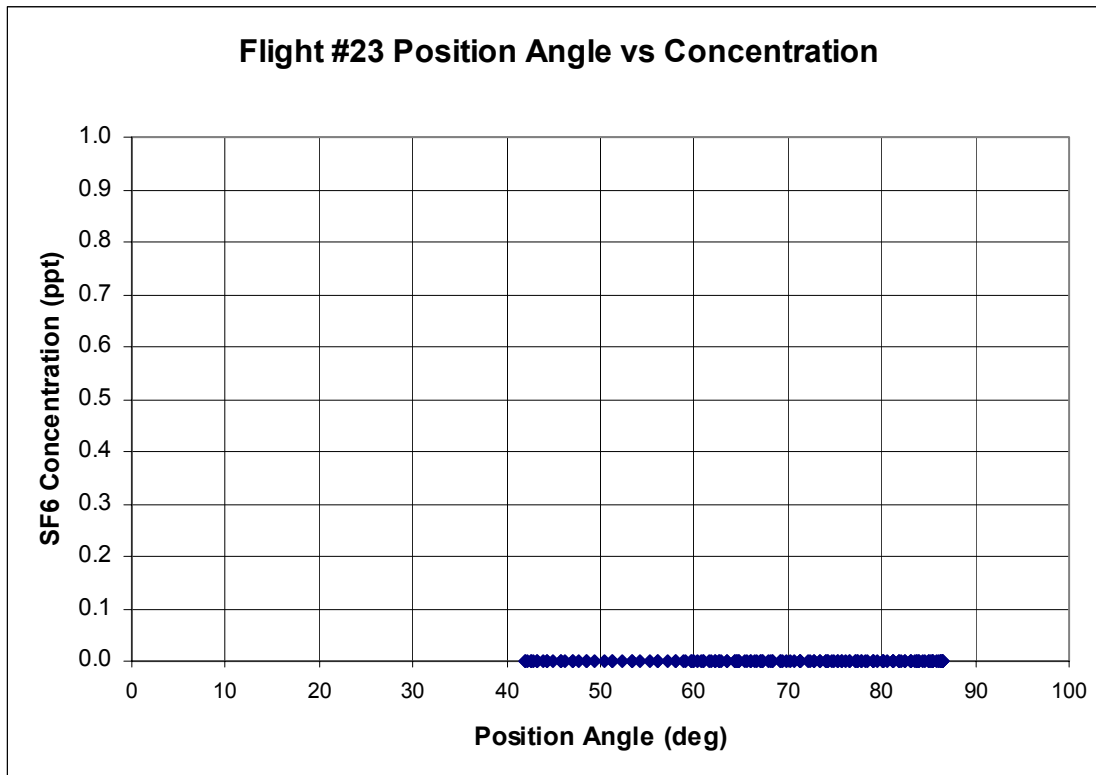


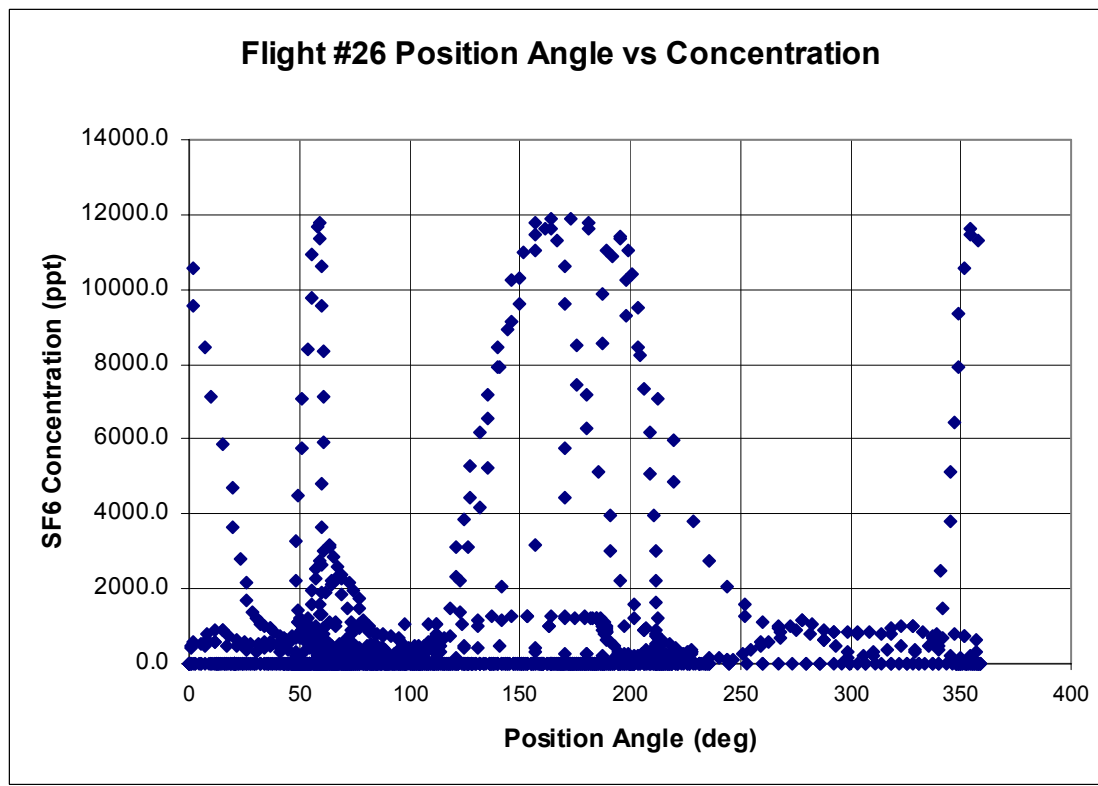
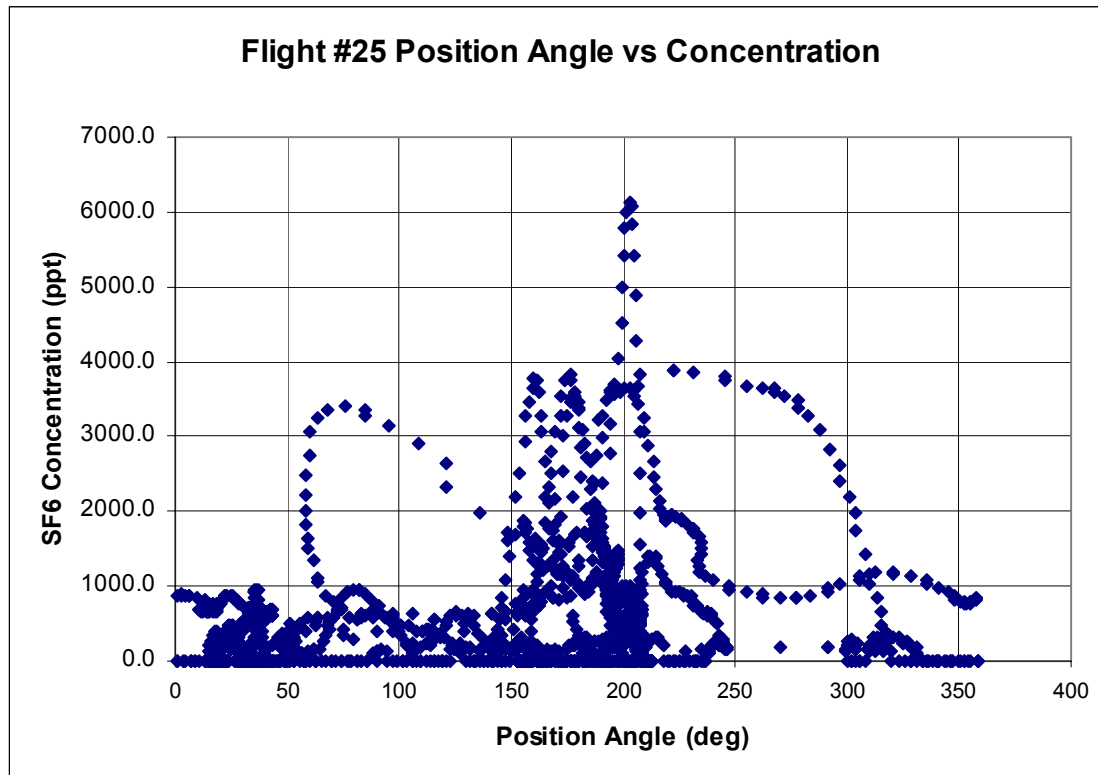


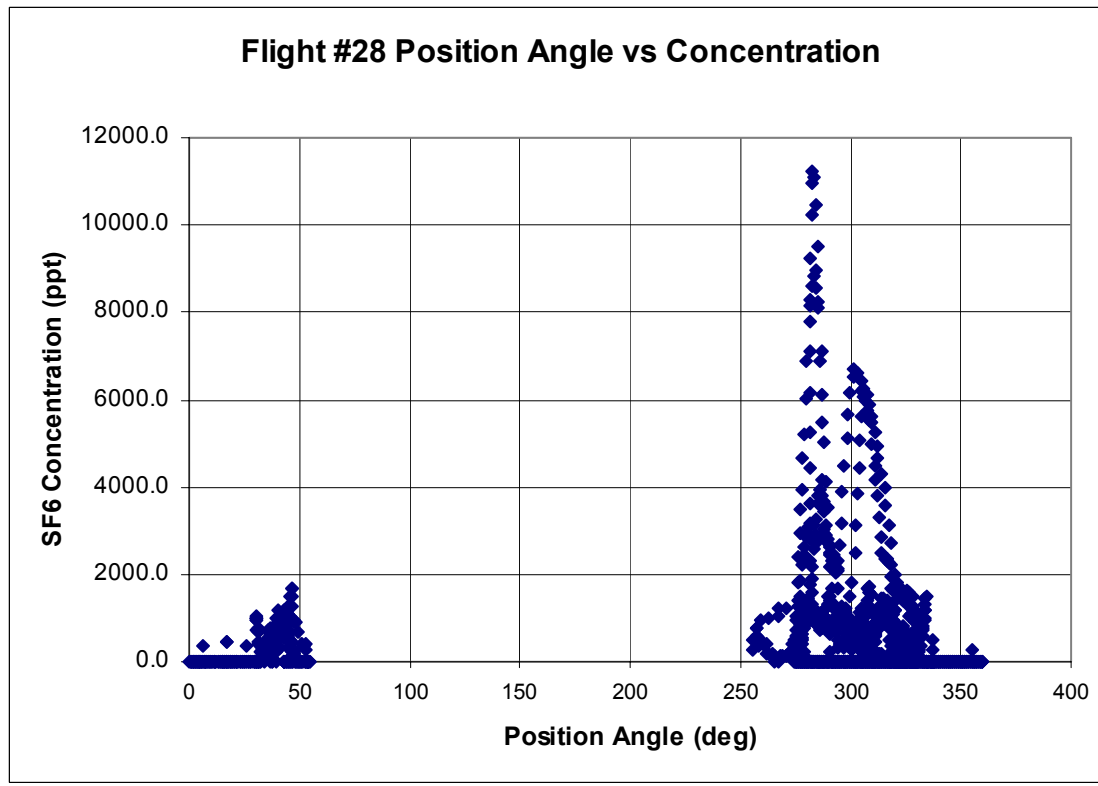
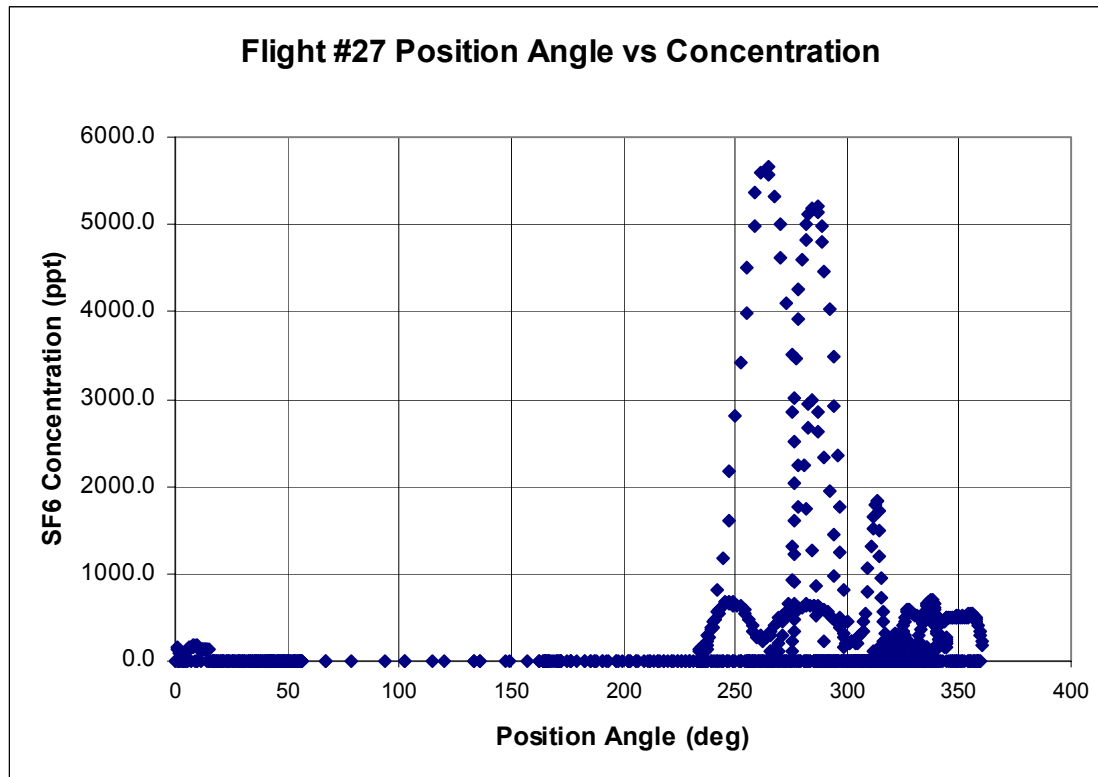






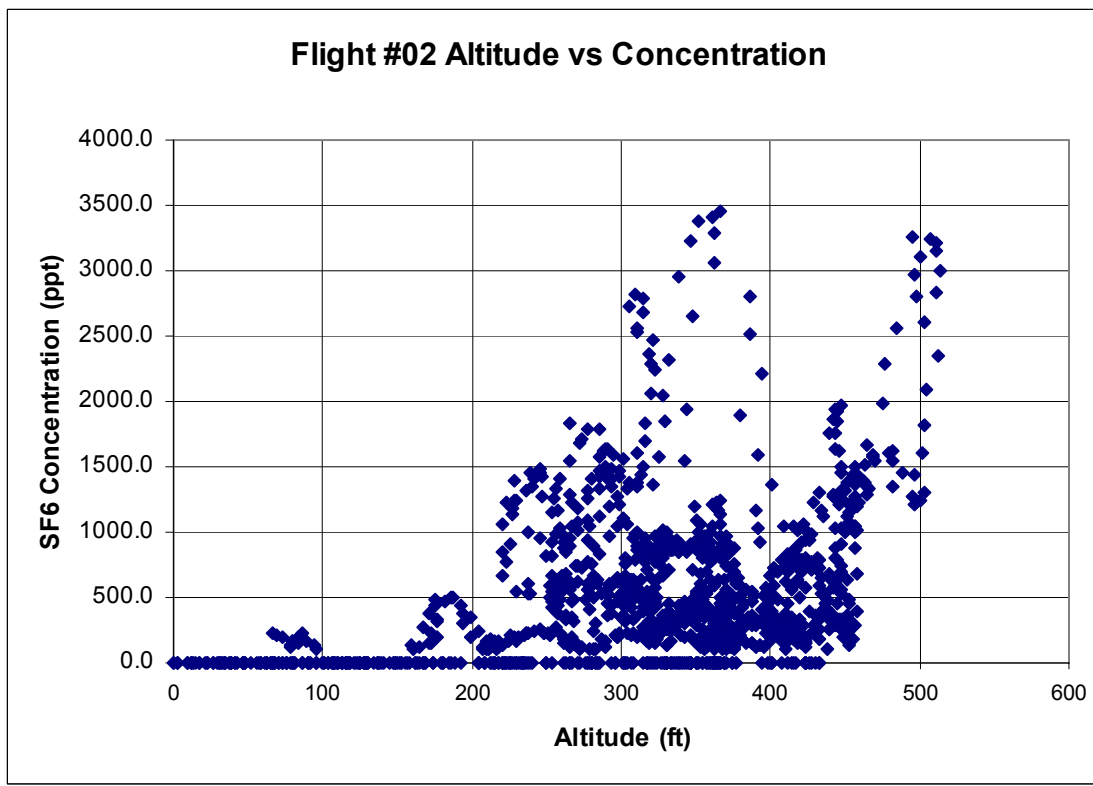
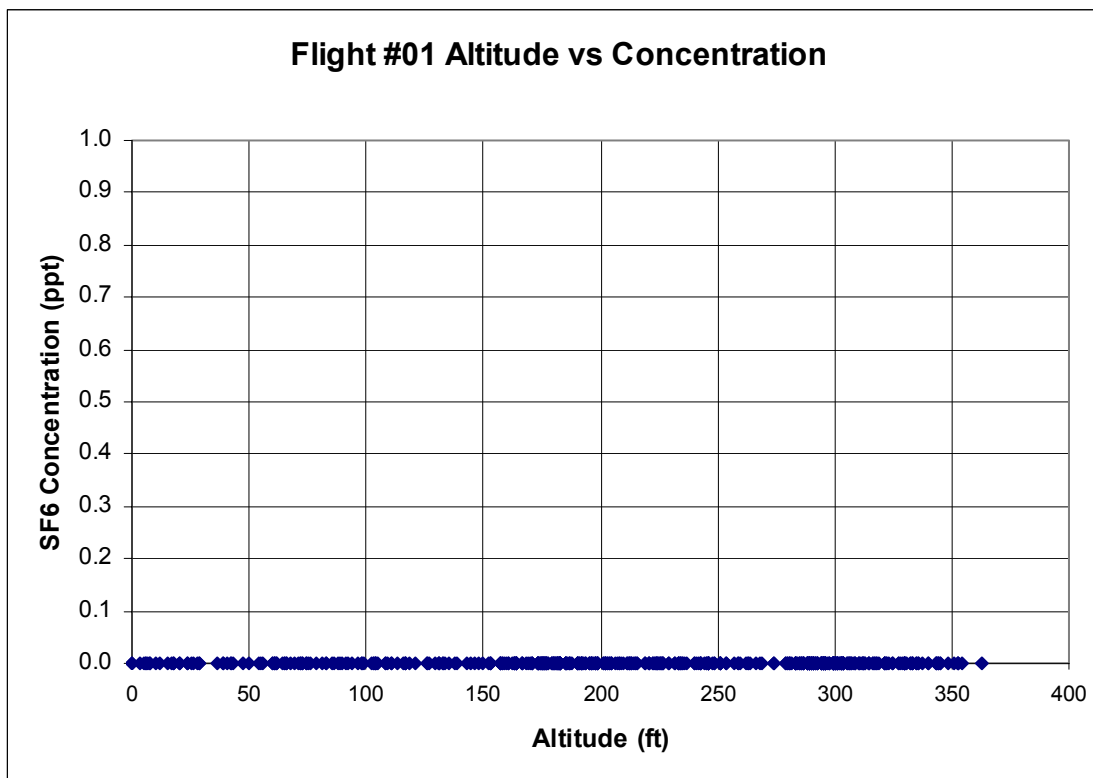


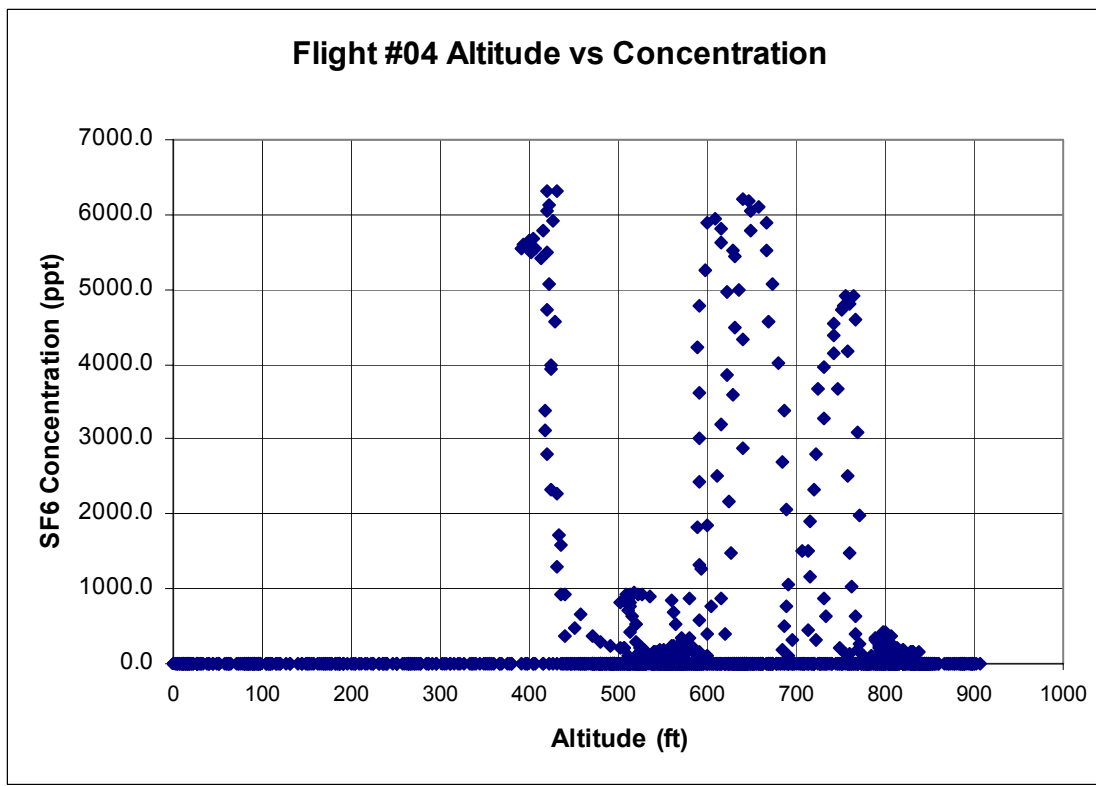
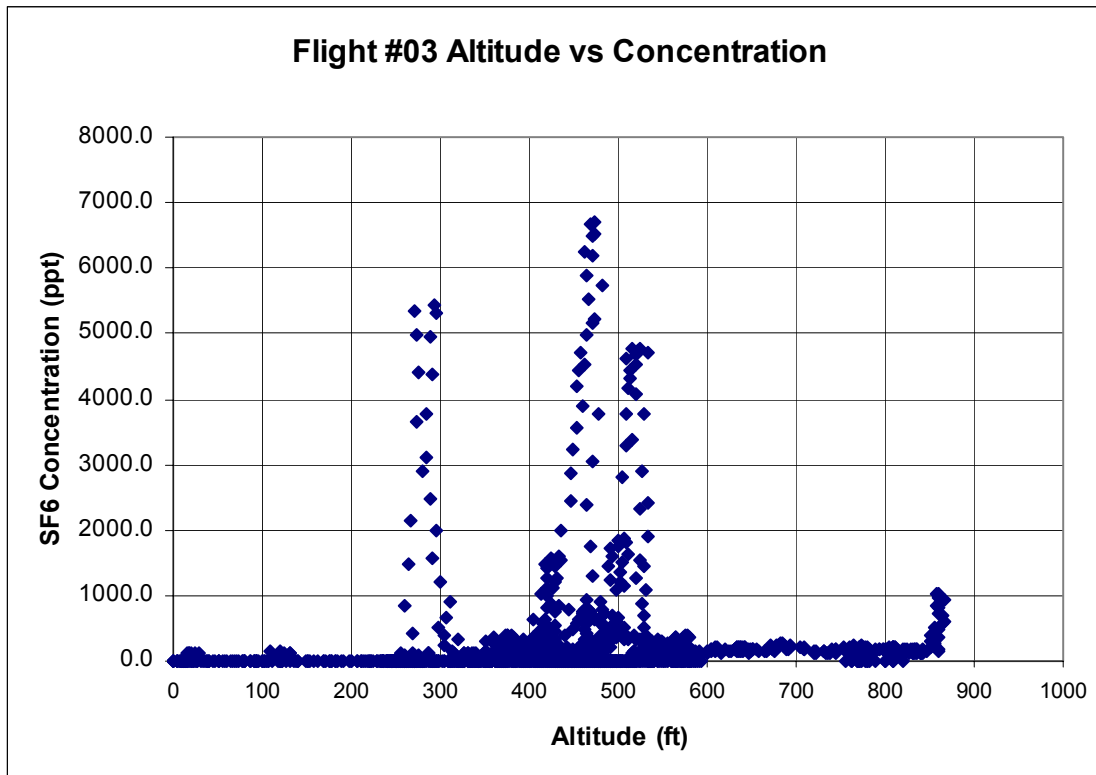


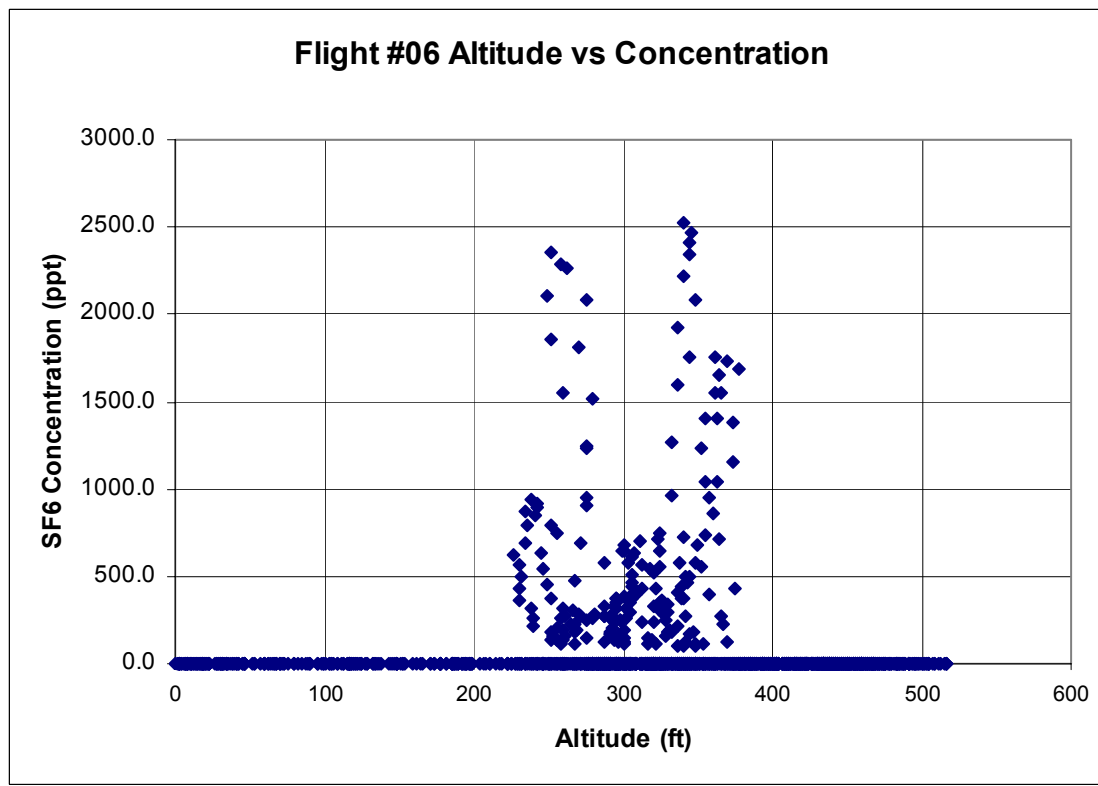
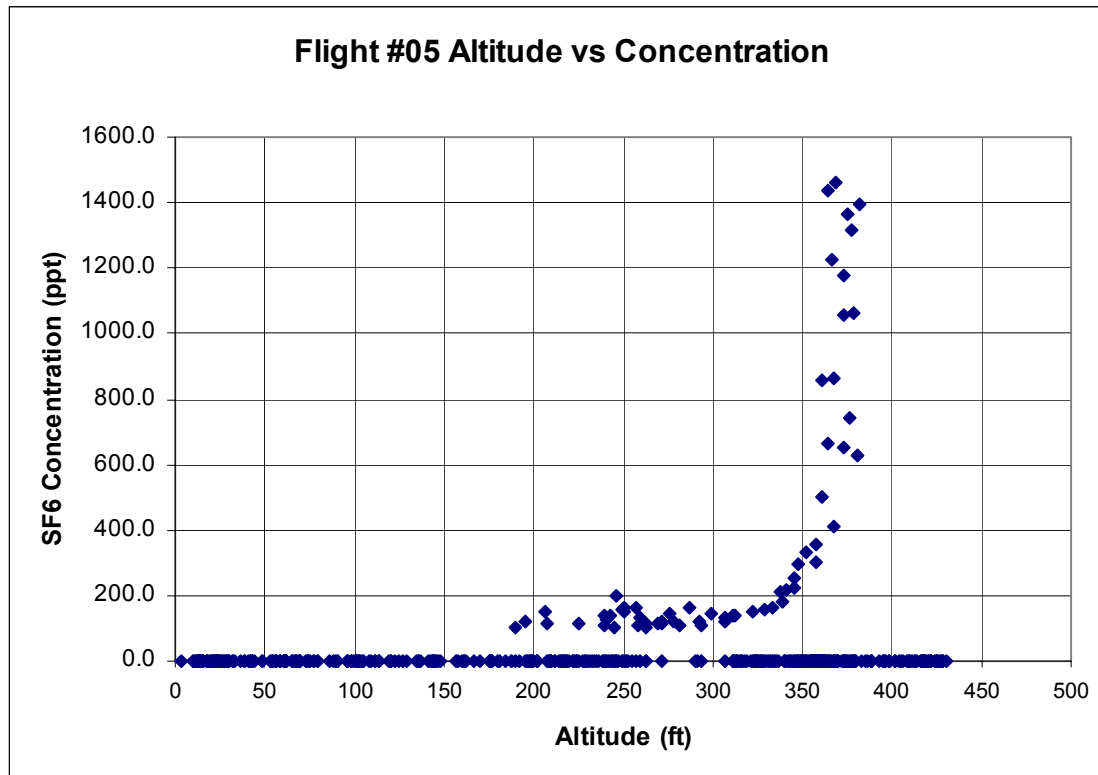


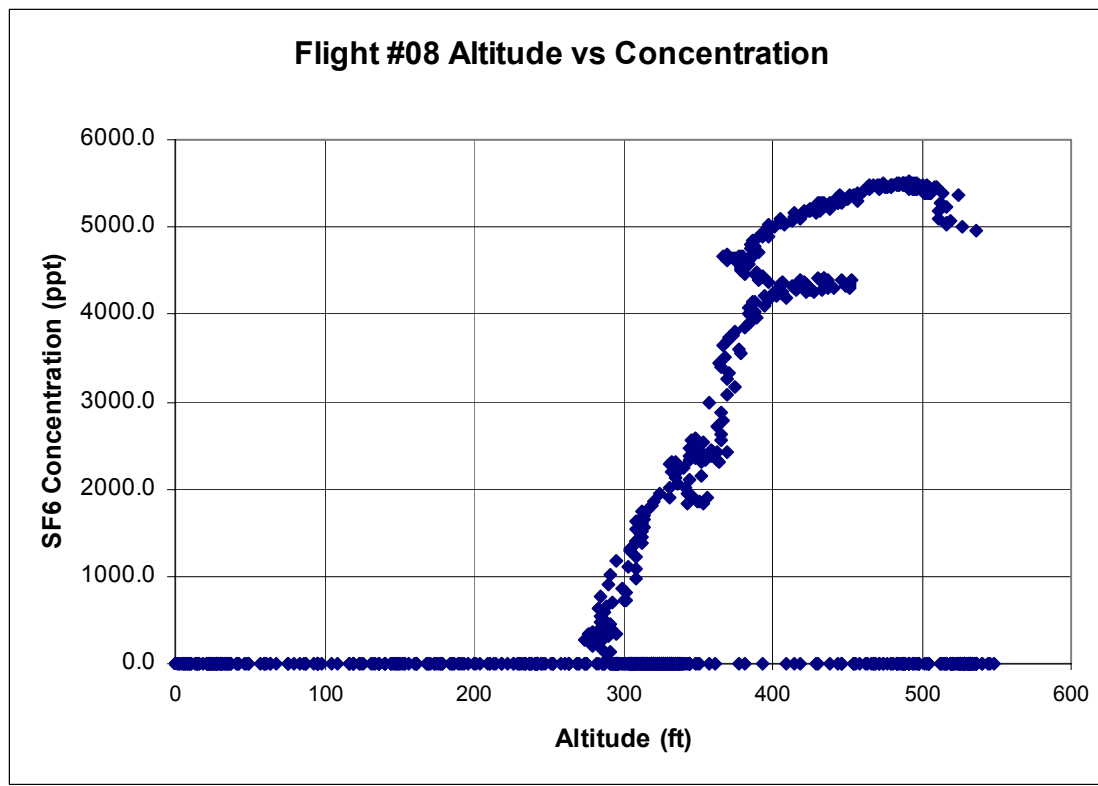
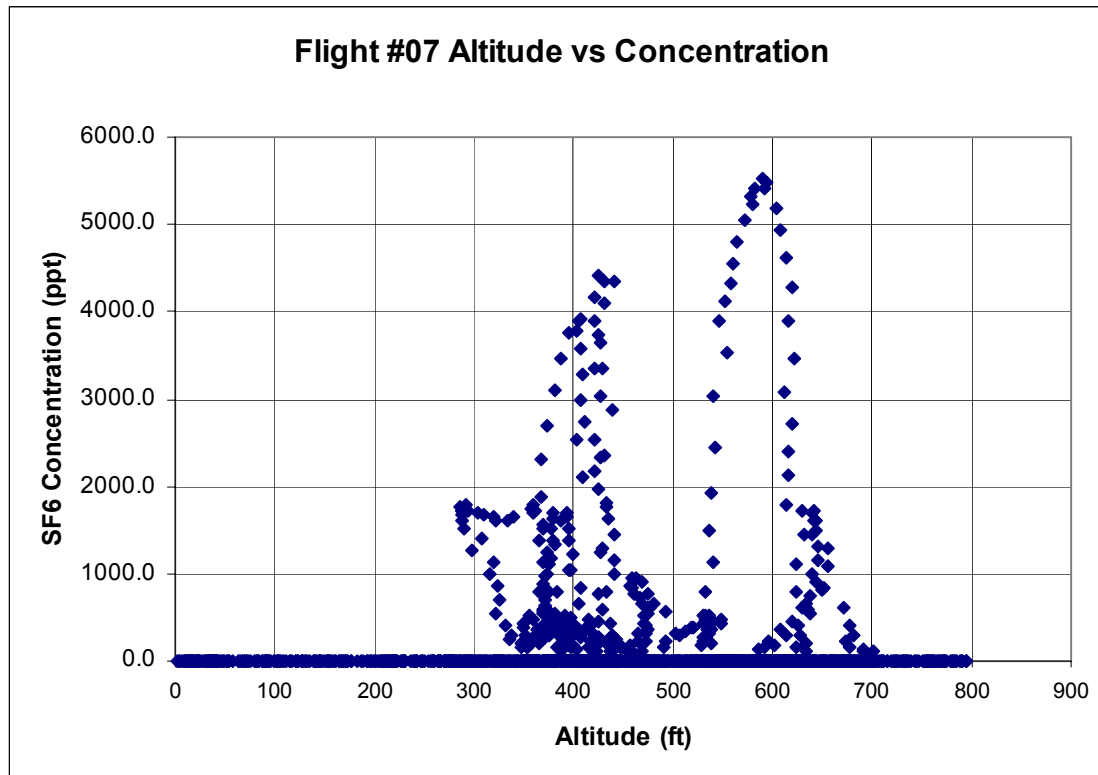
APPENDIX F

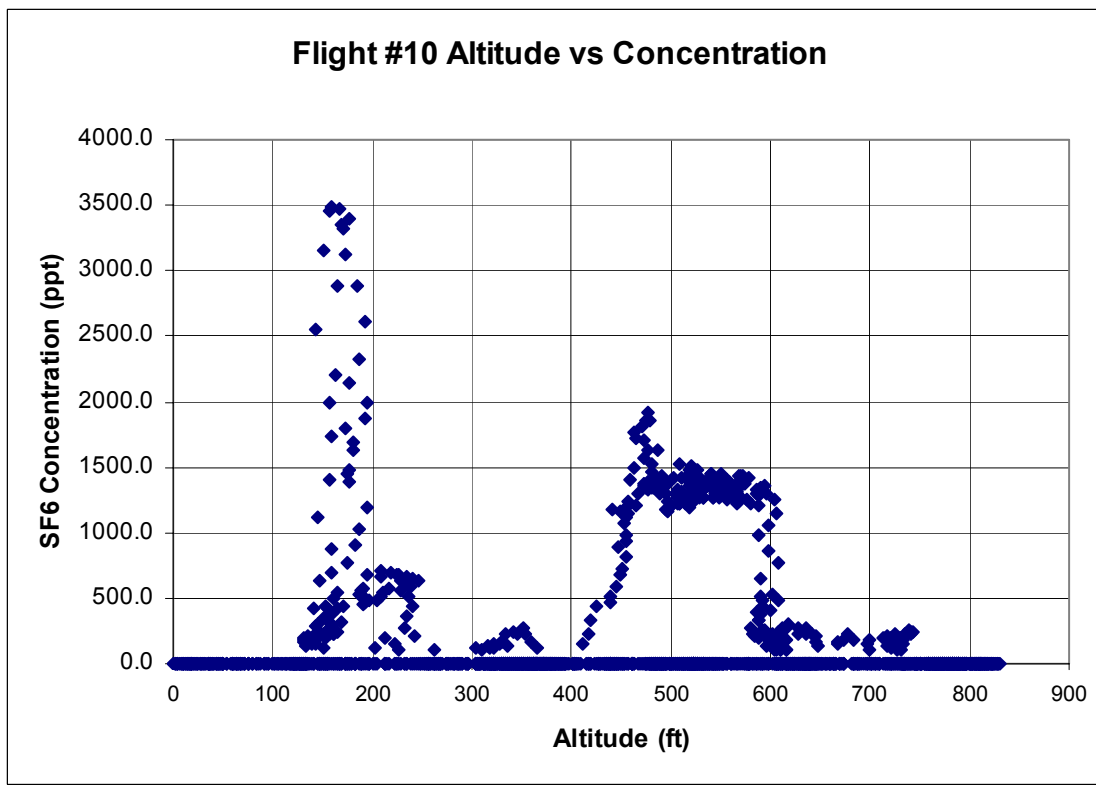
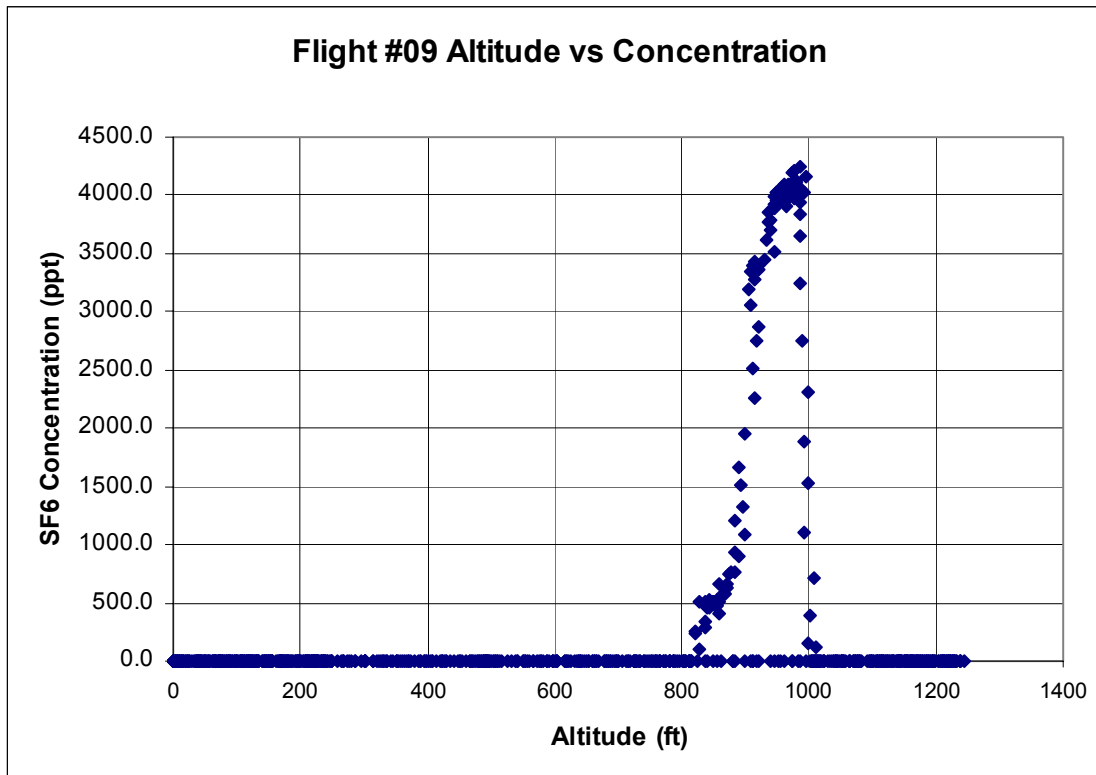
SF₆ CONCENTRATION ALTITUDE GRAPHS

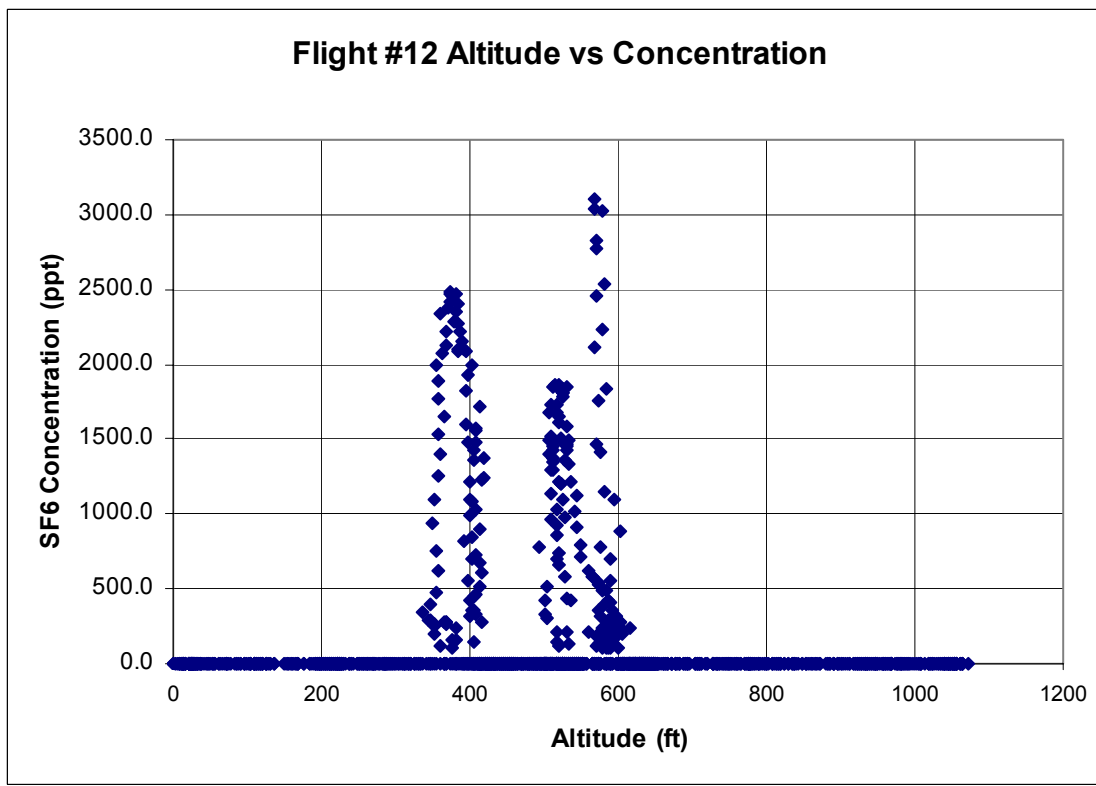
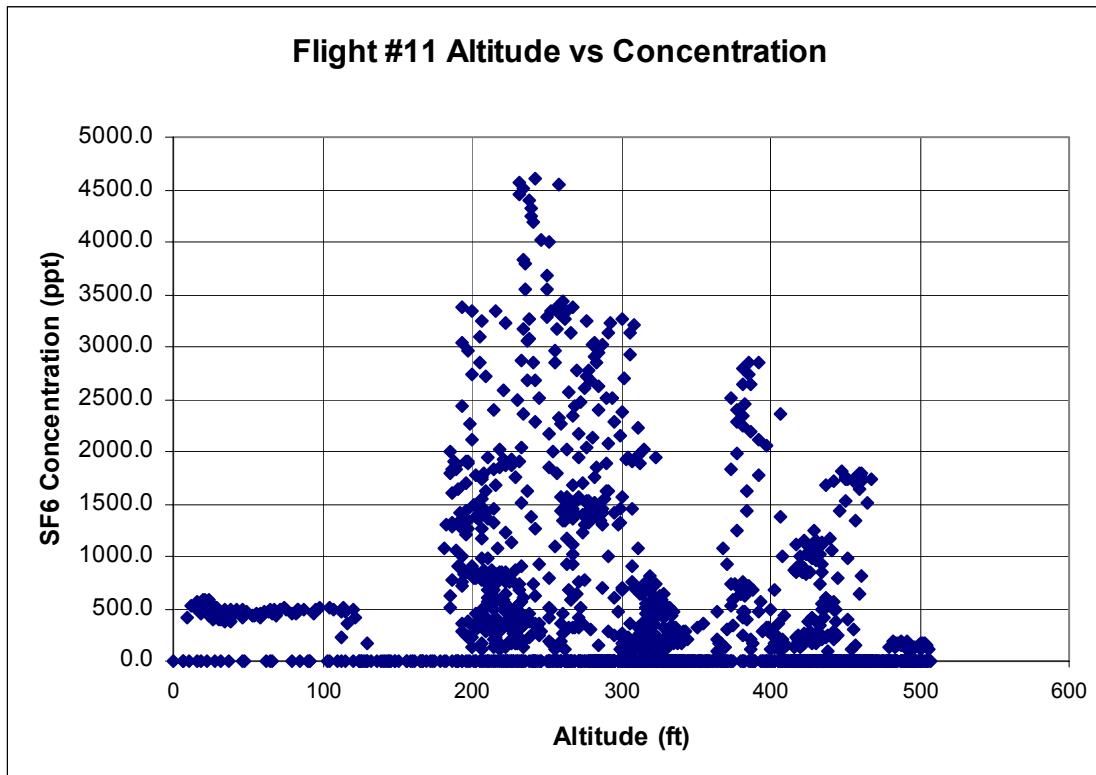


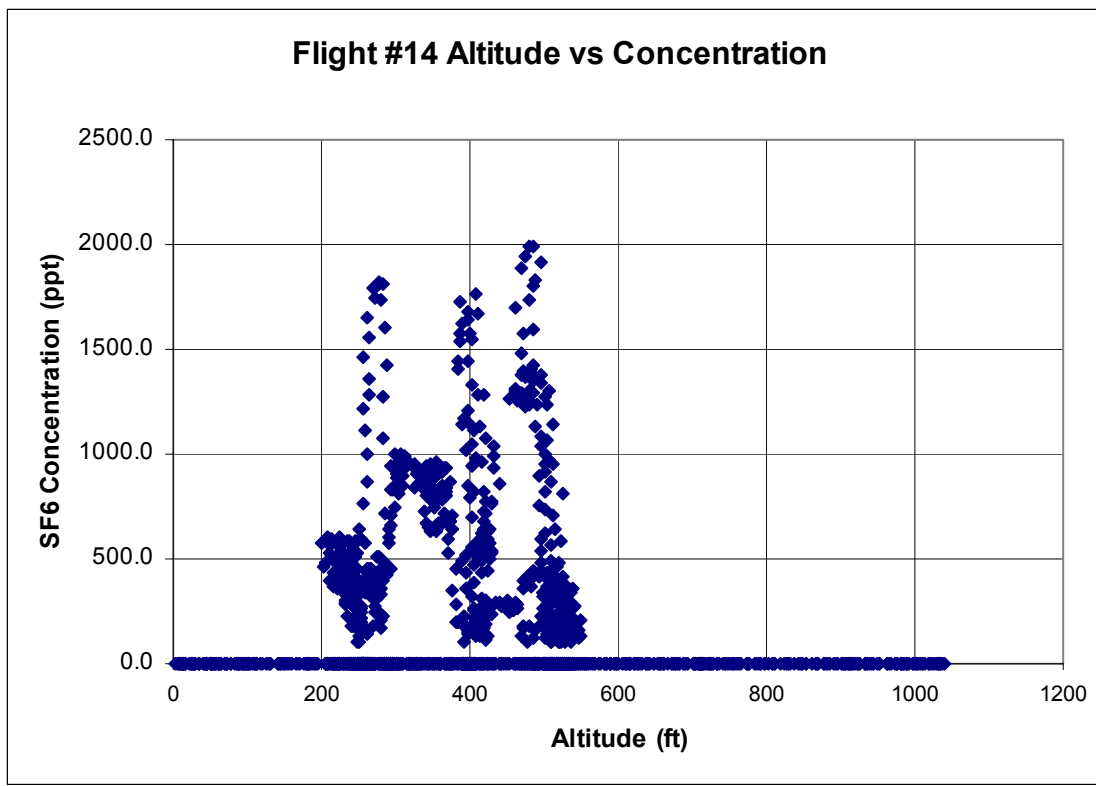
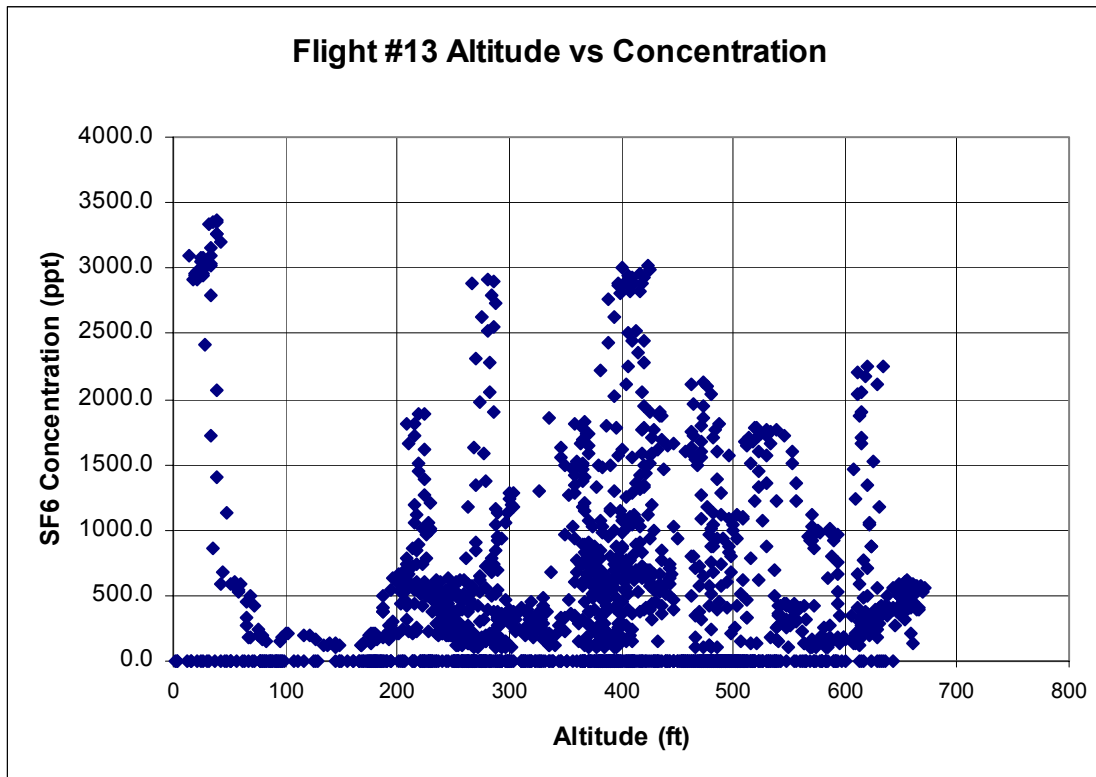


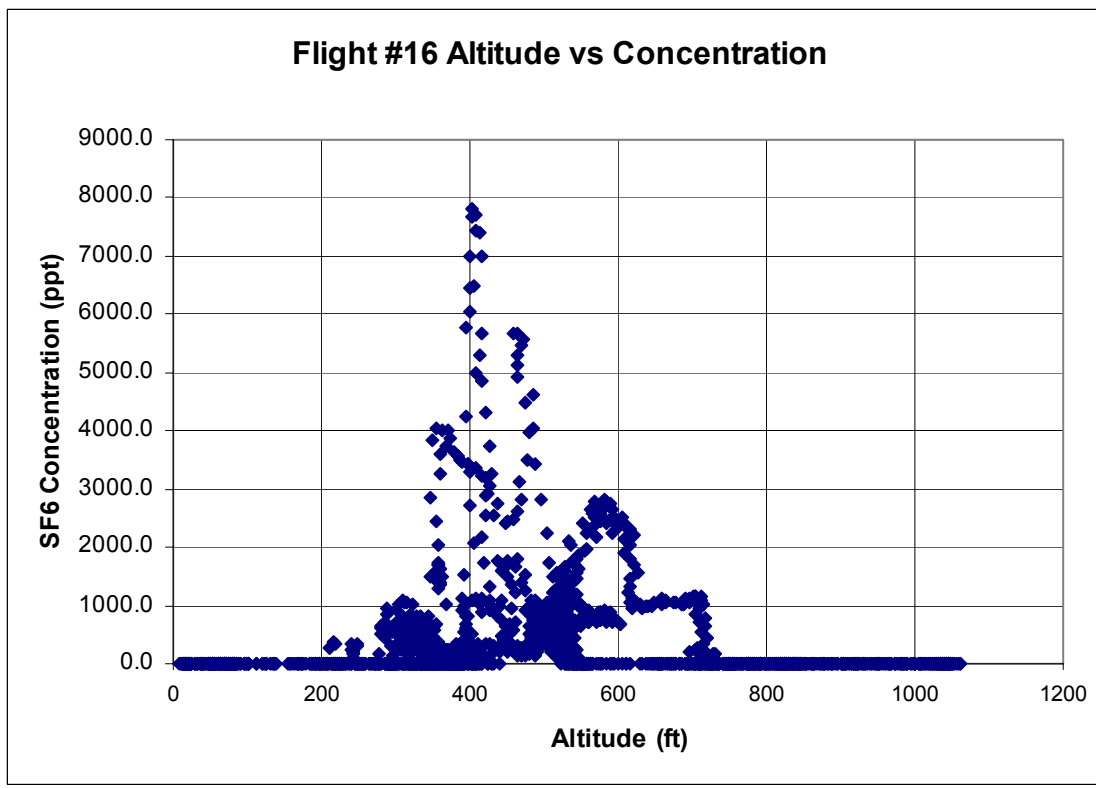
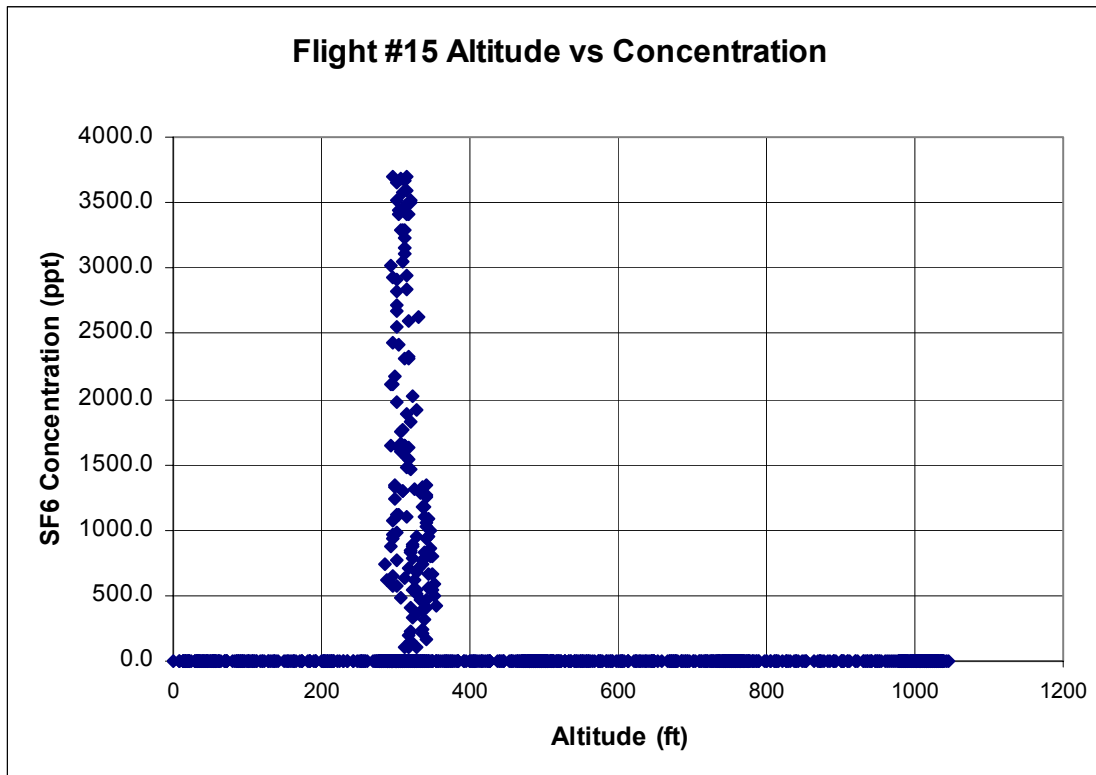


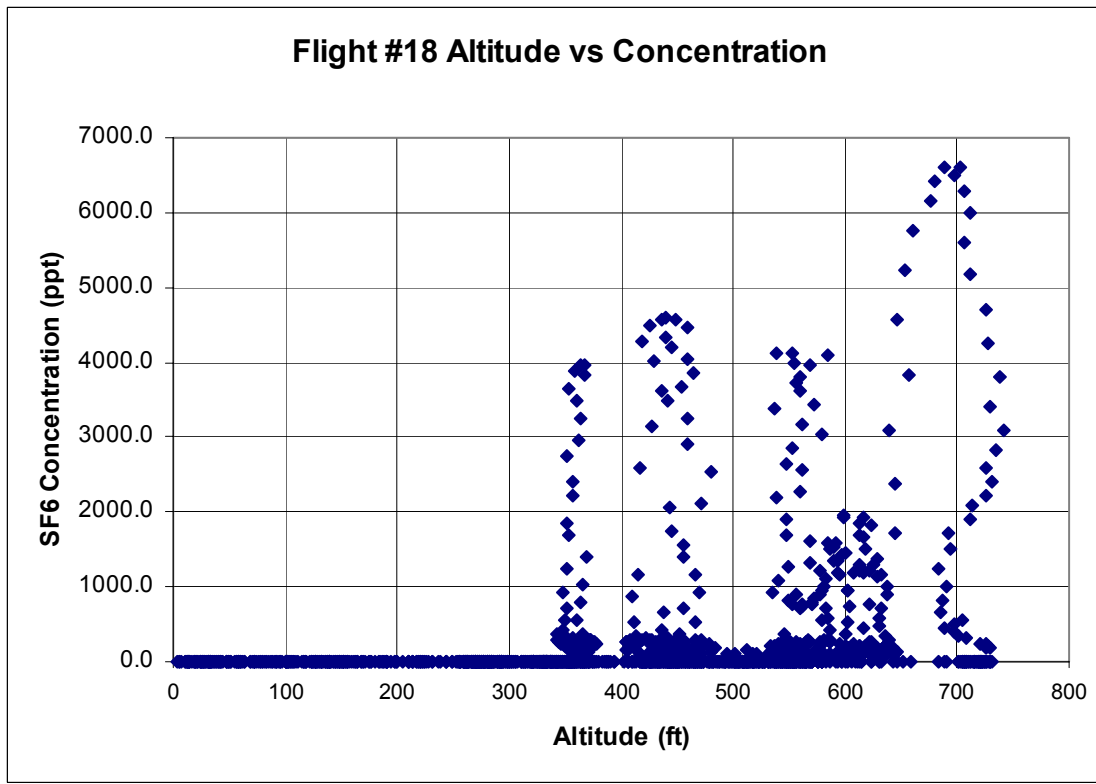
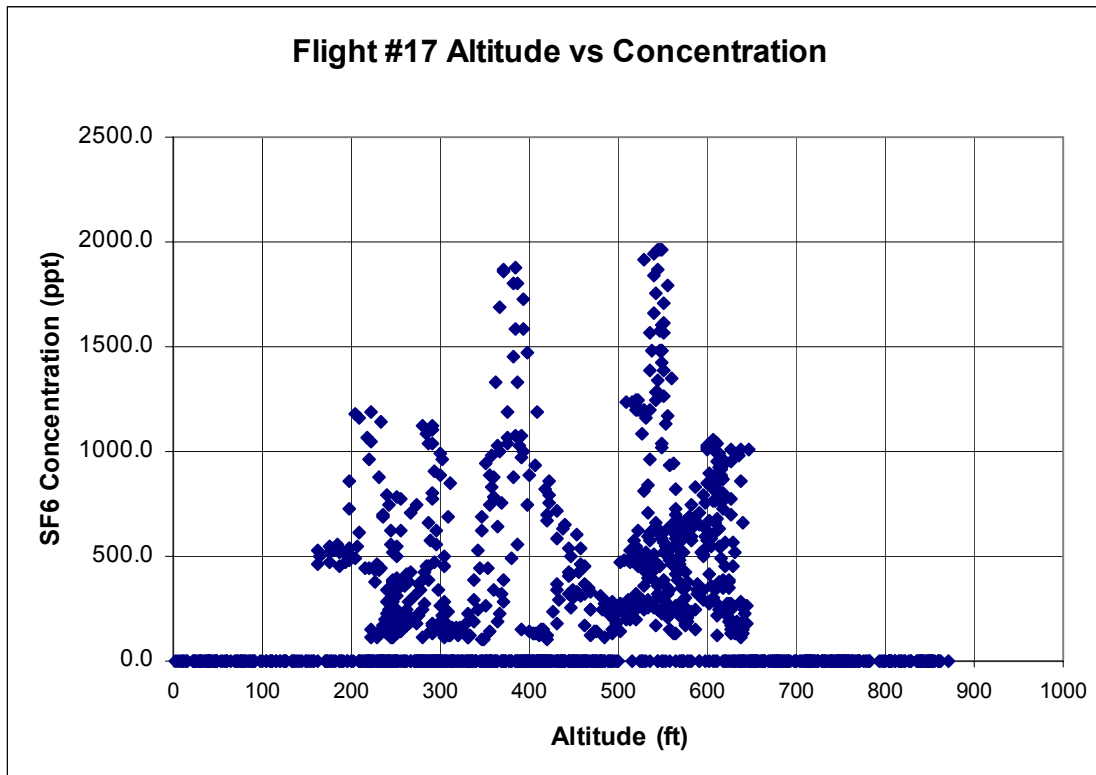


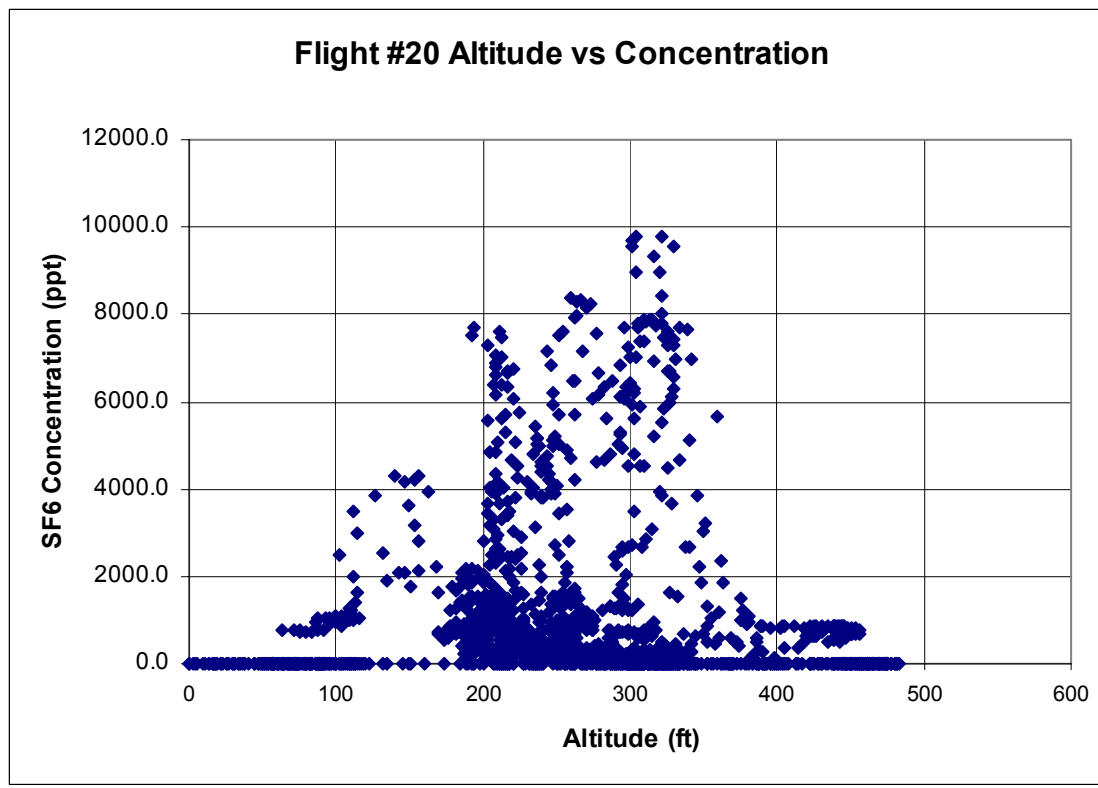
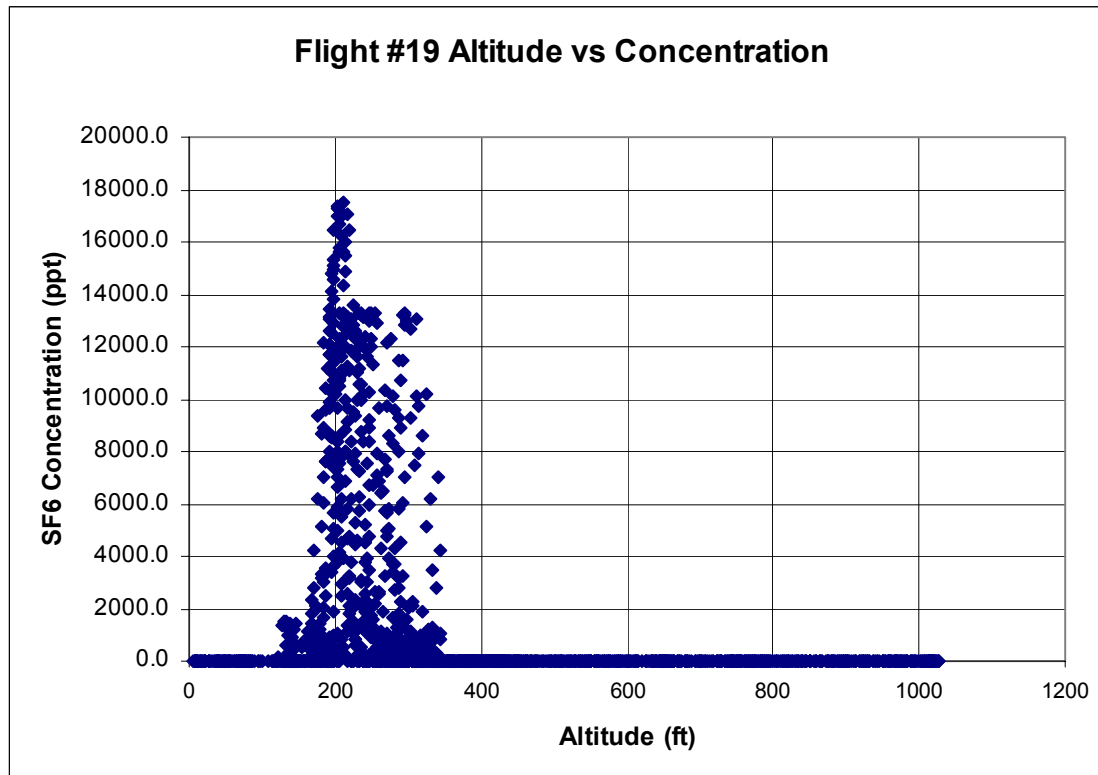


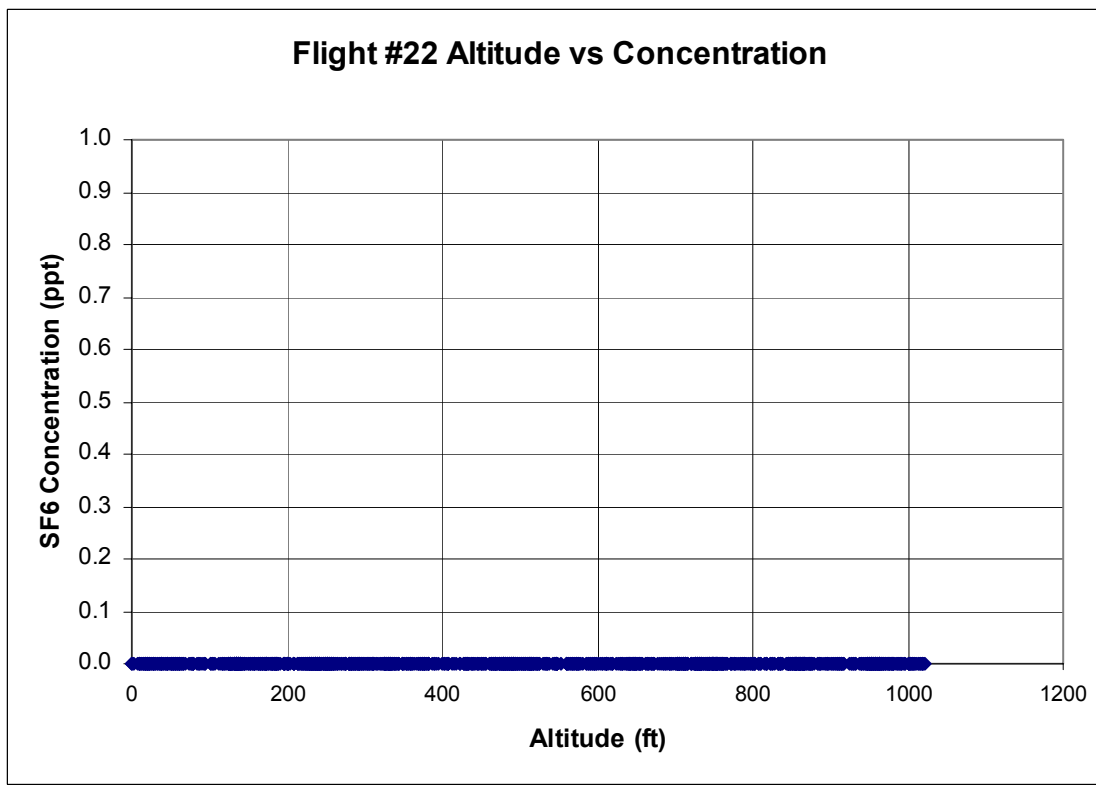
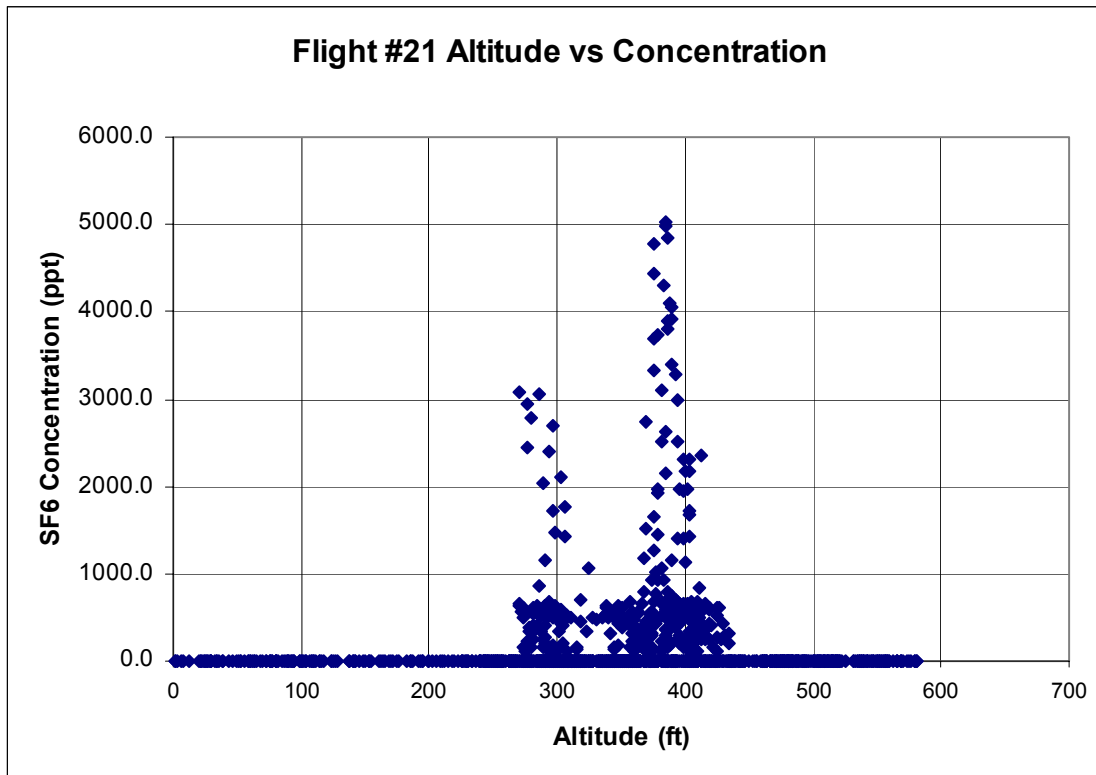


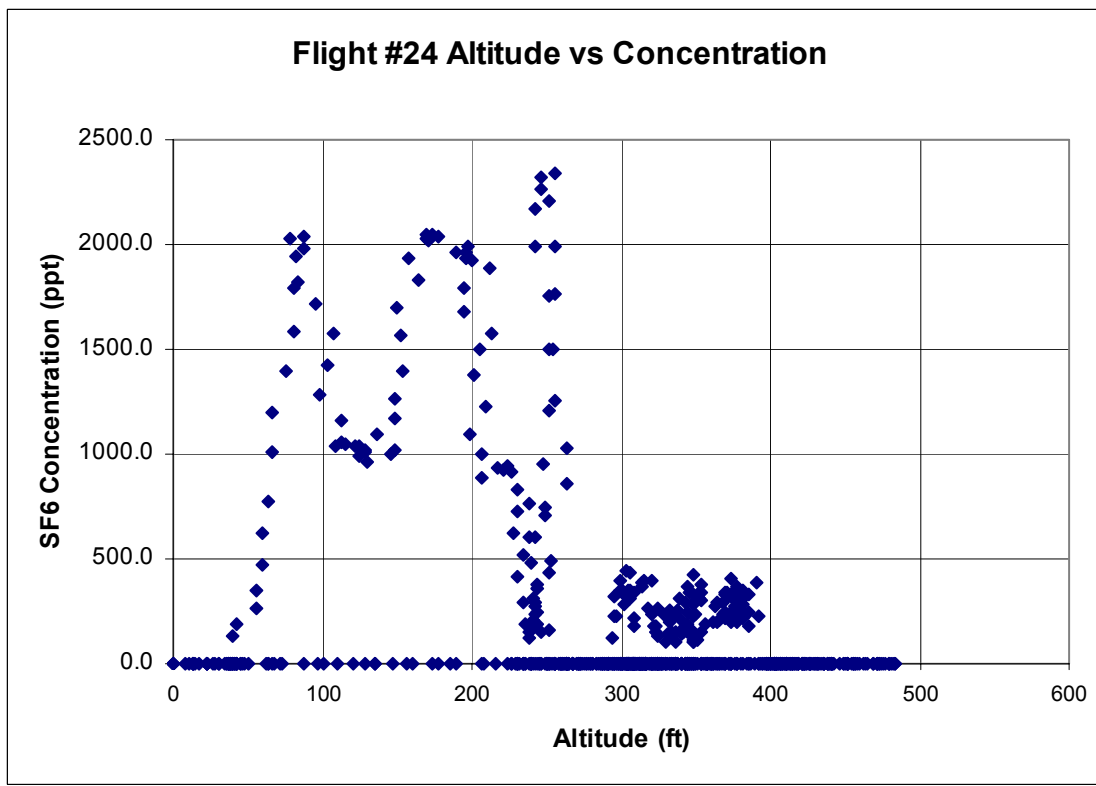
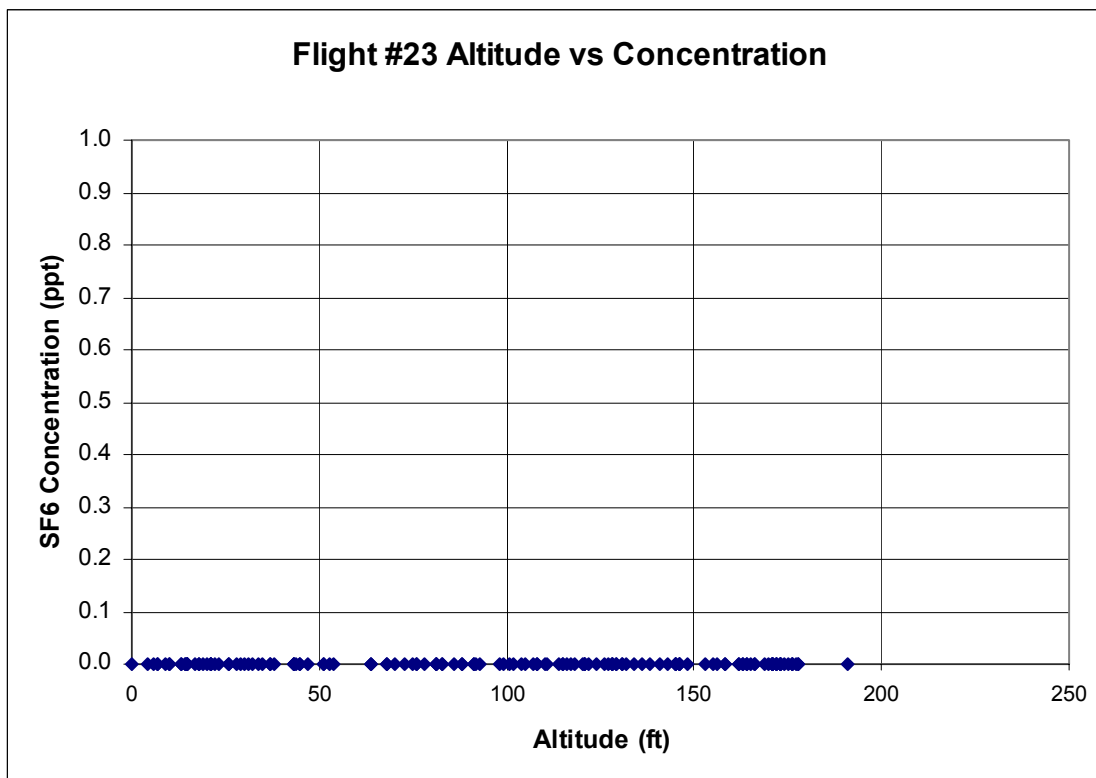


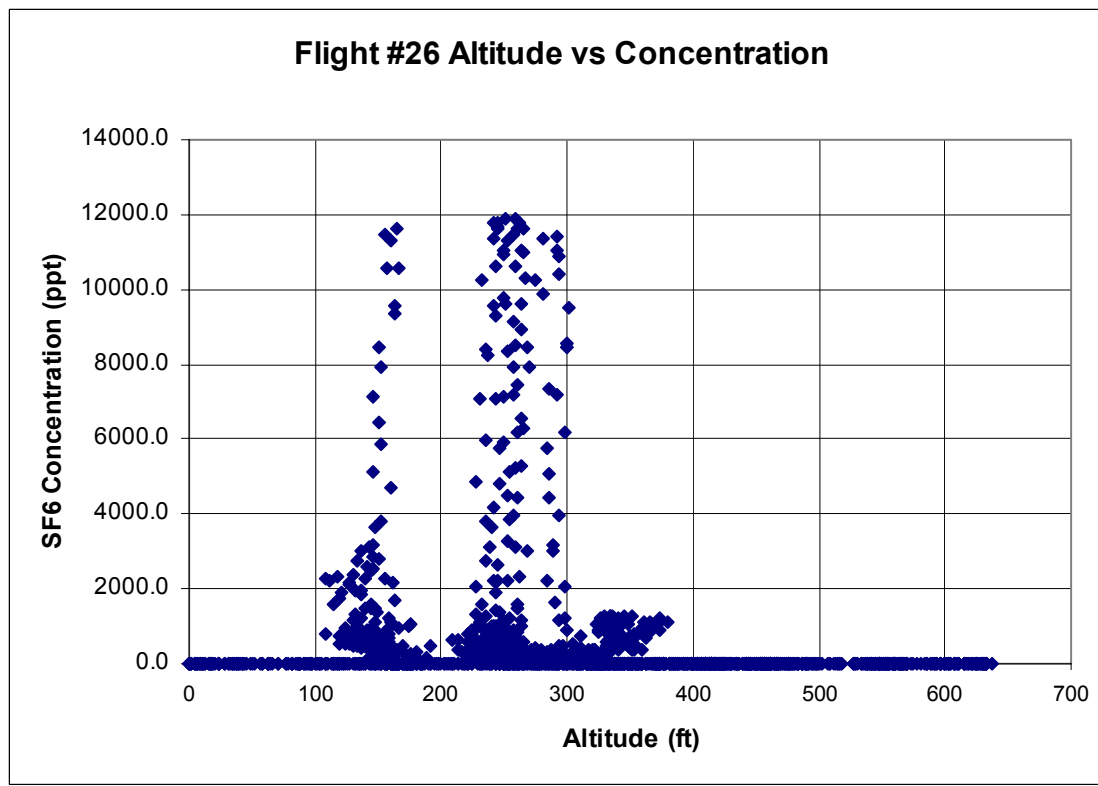
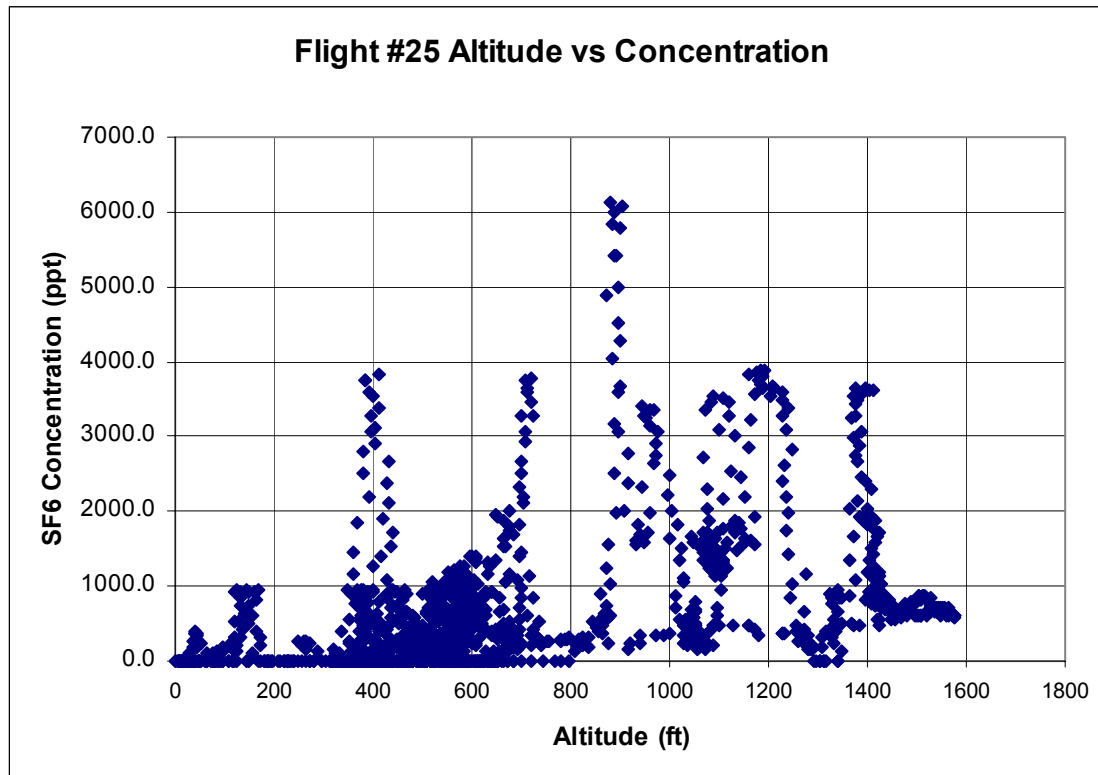


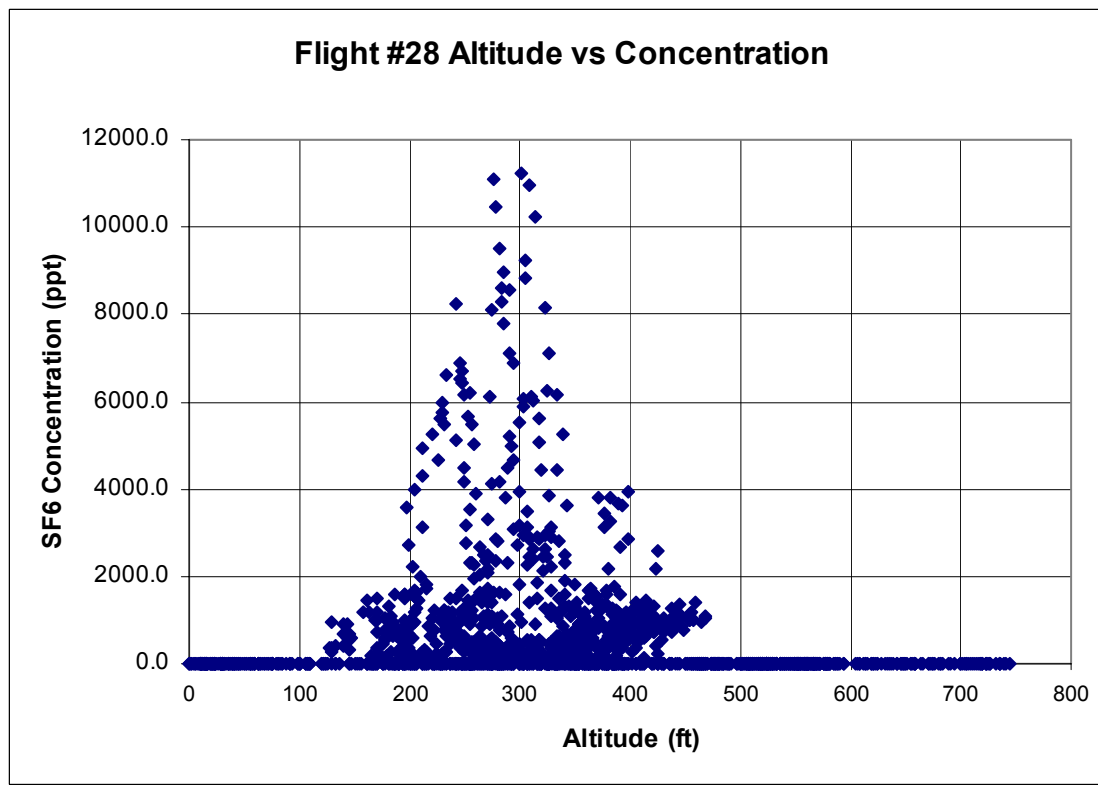
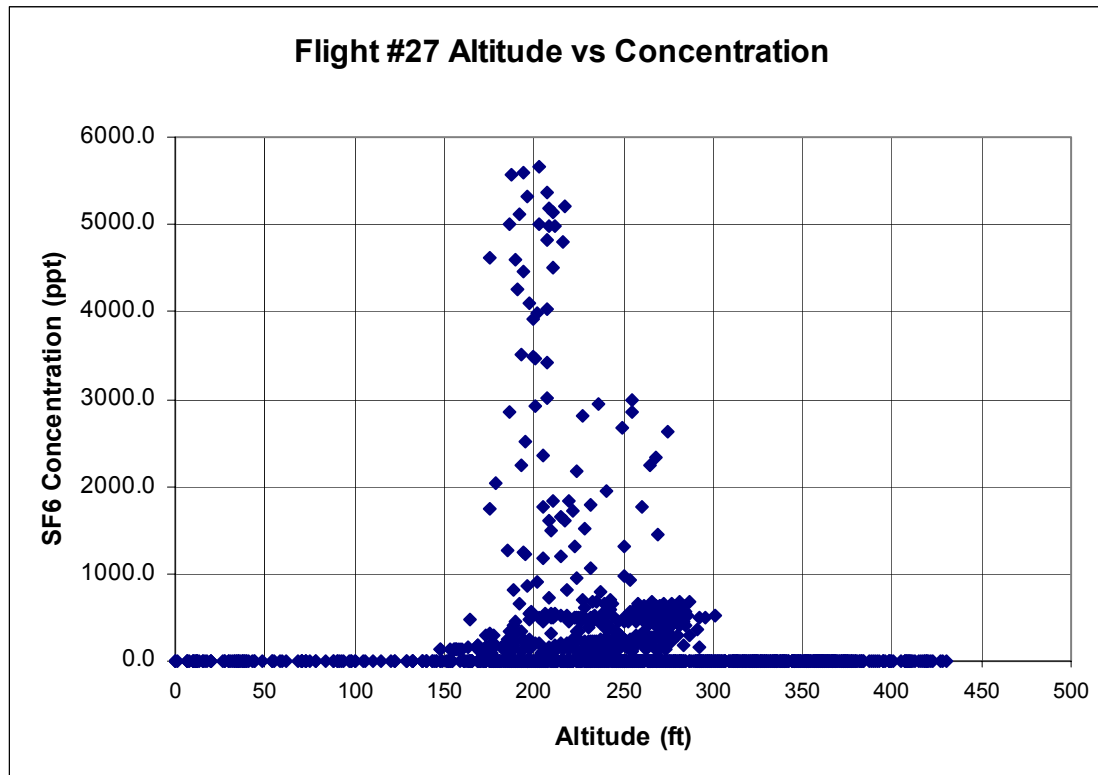




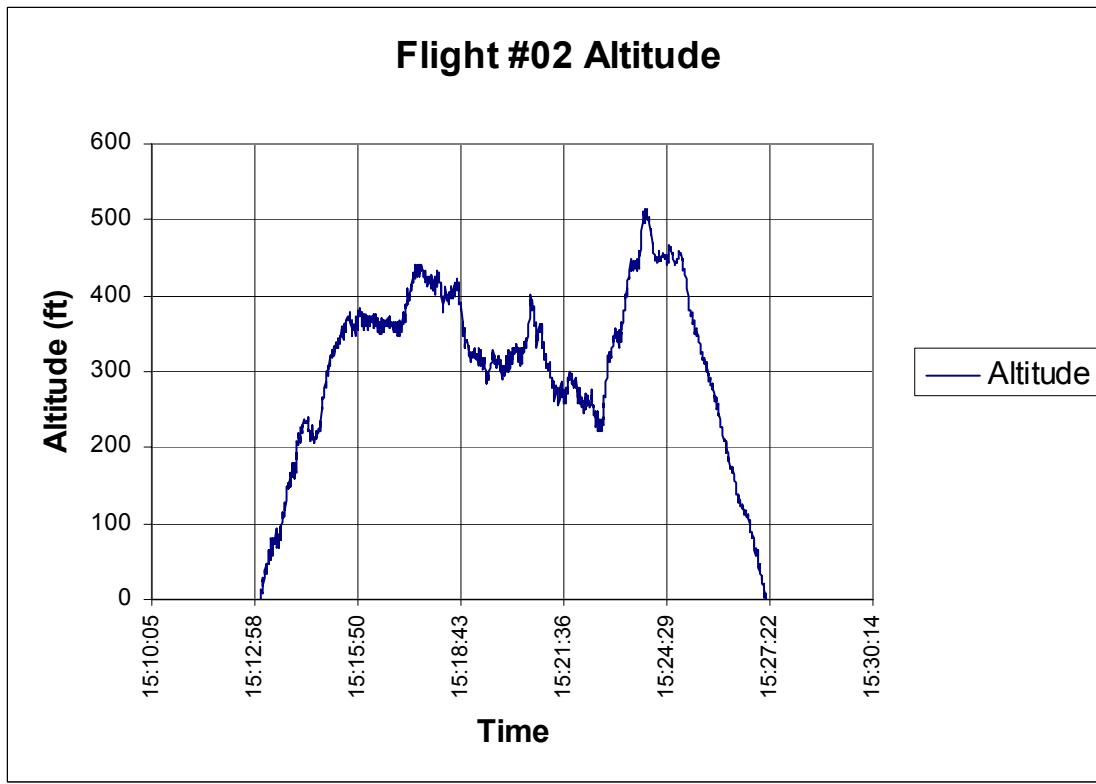
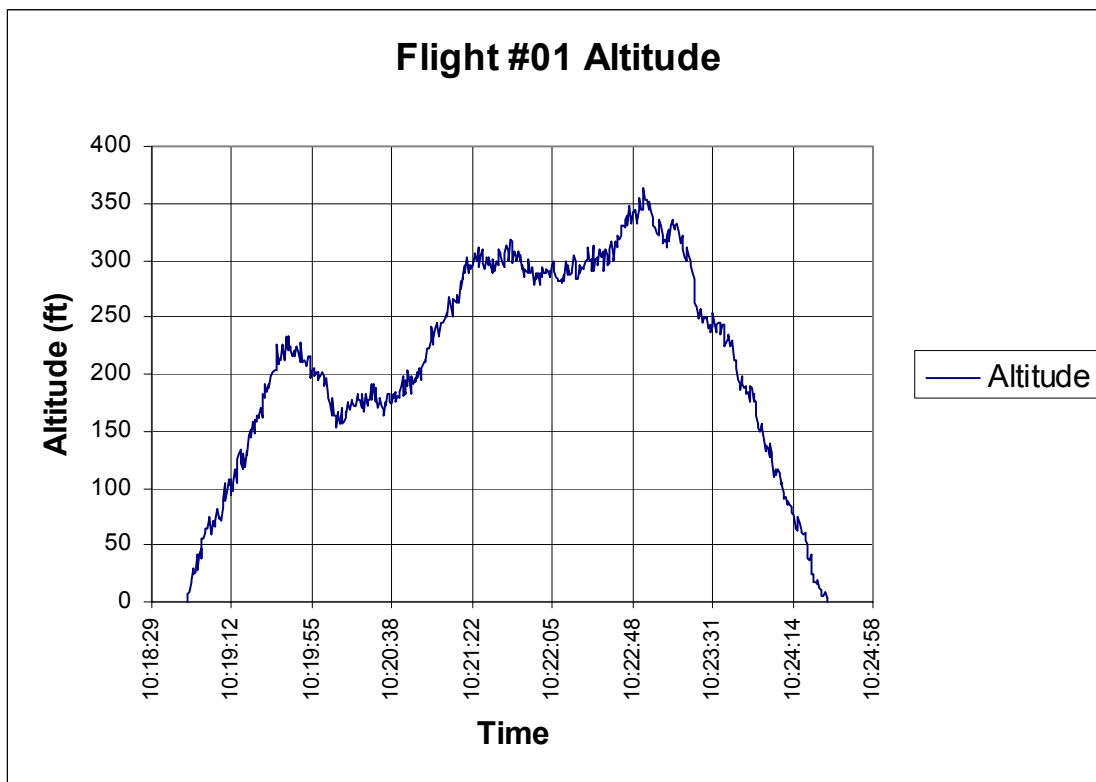


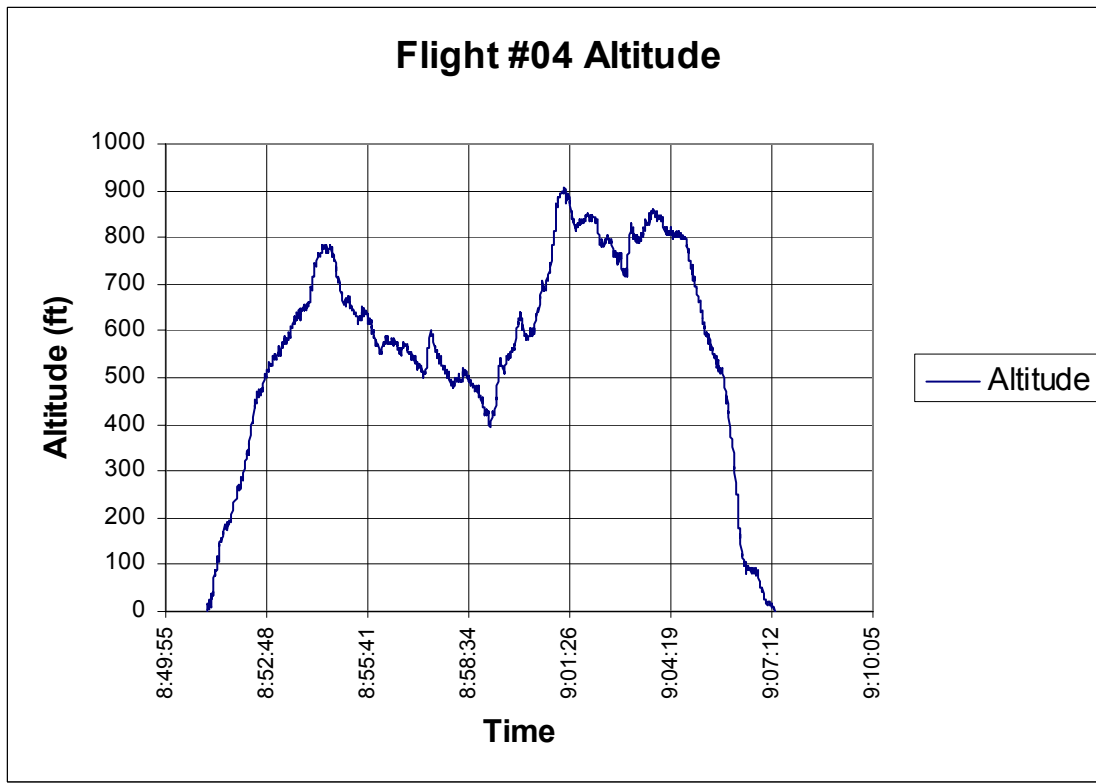
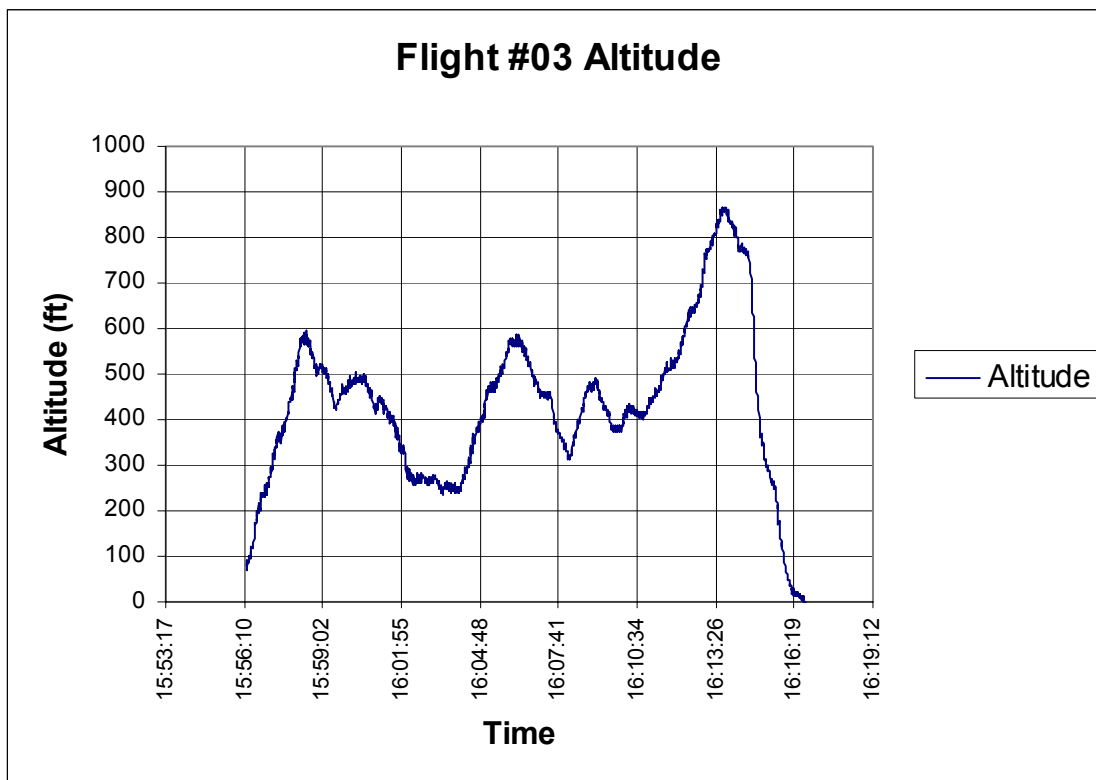


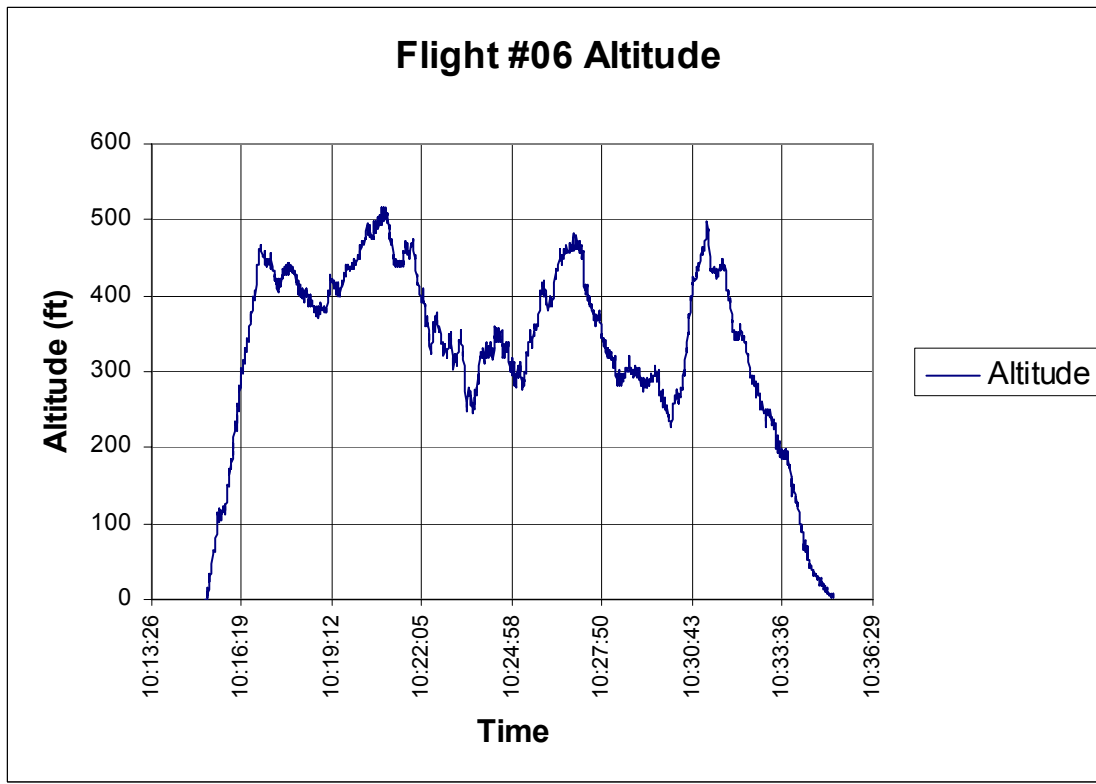
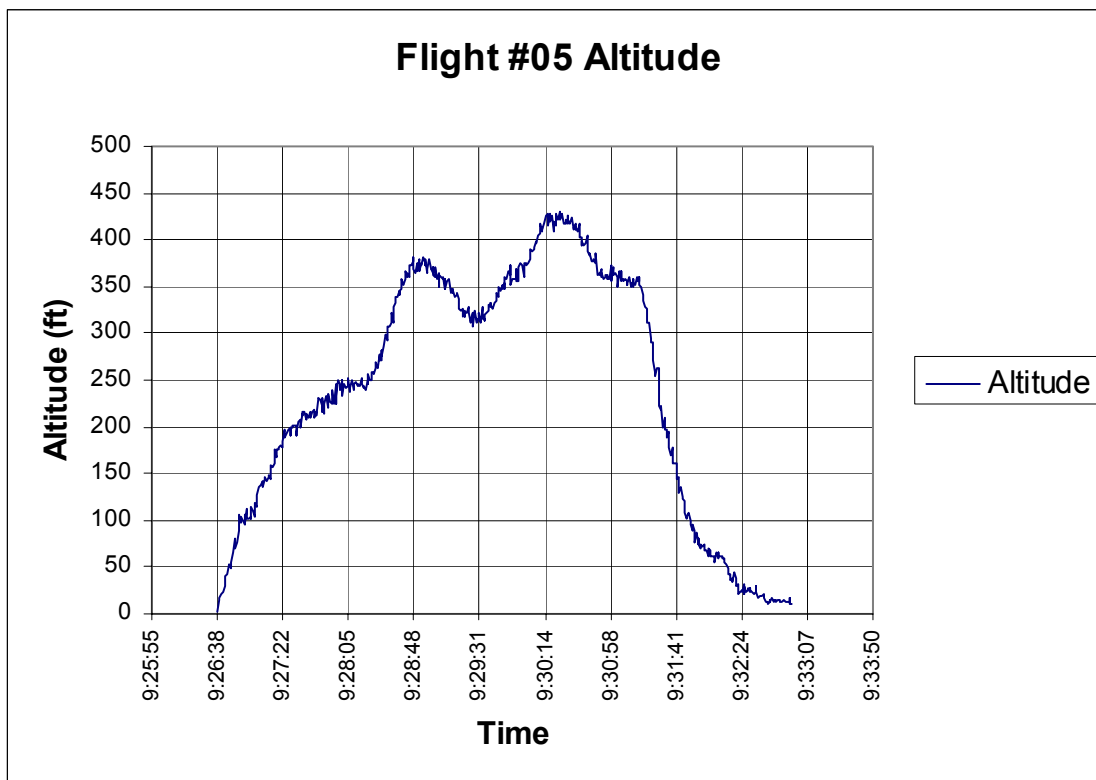


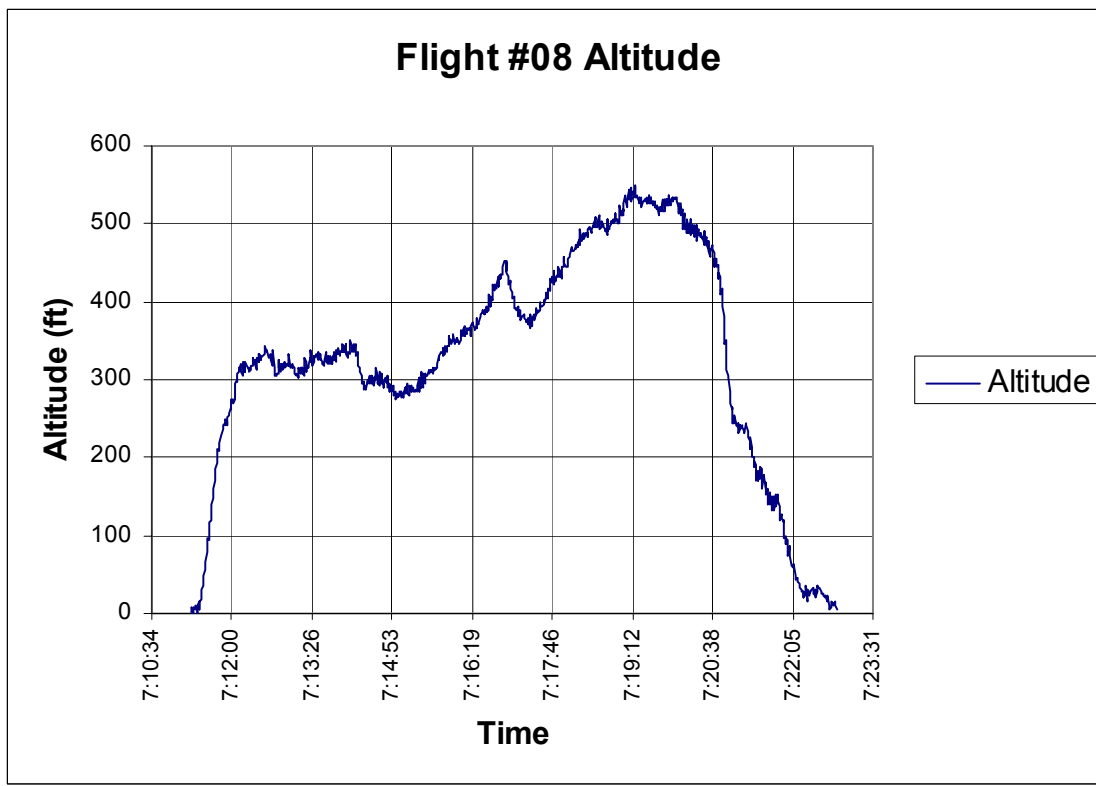
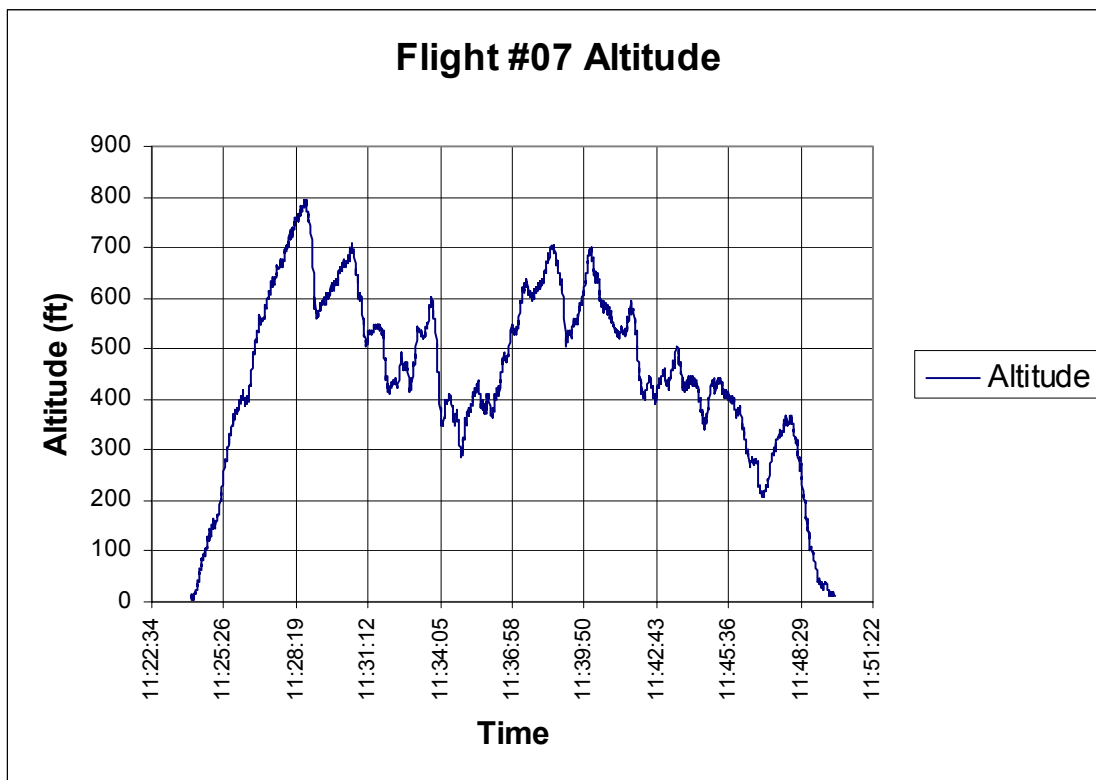


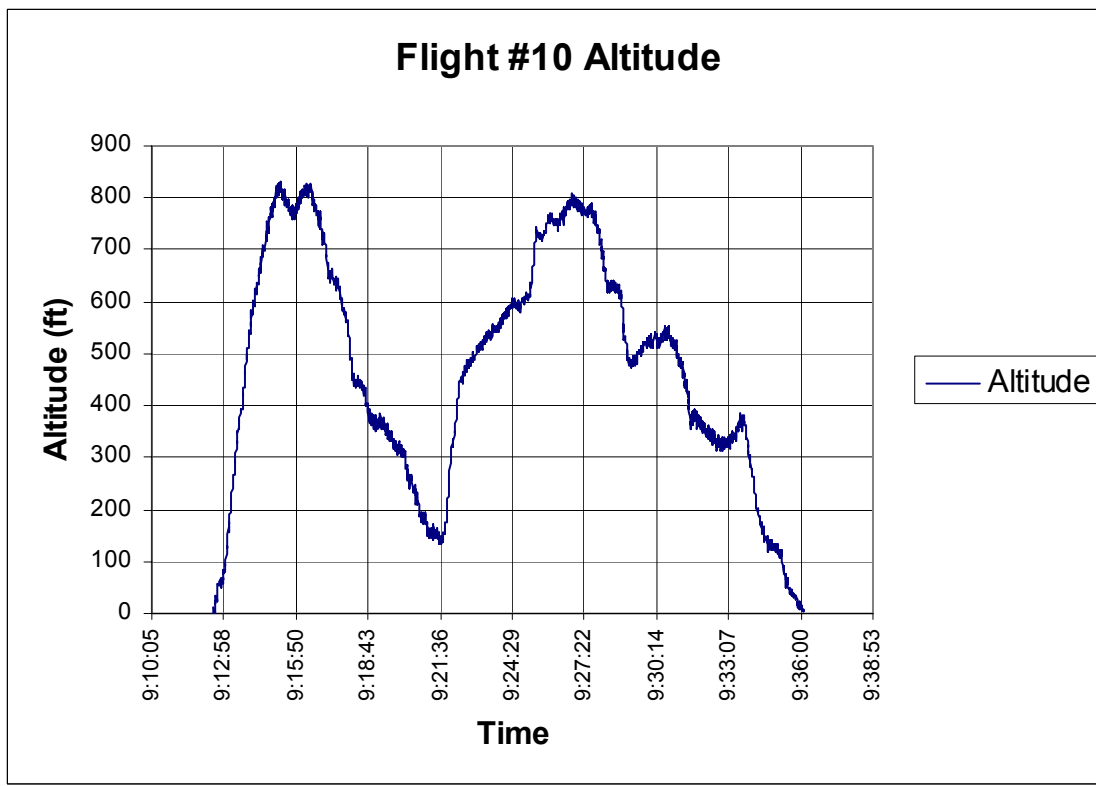
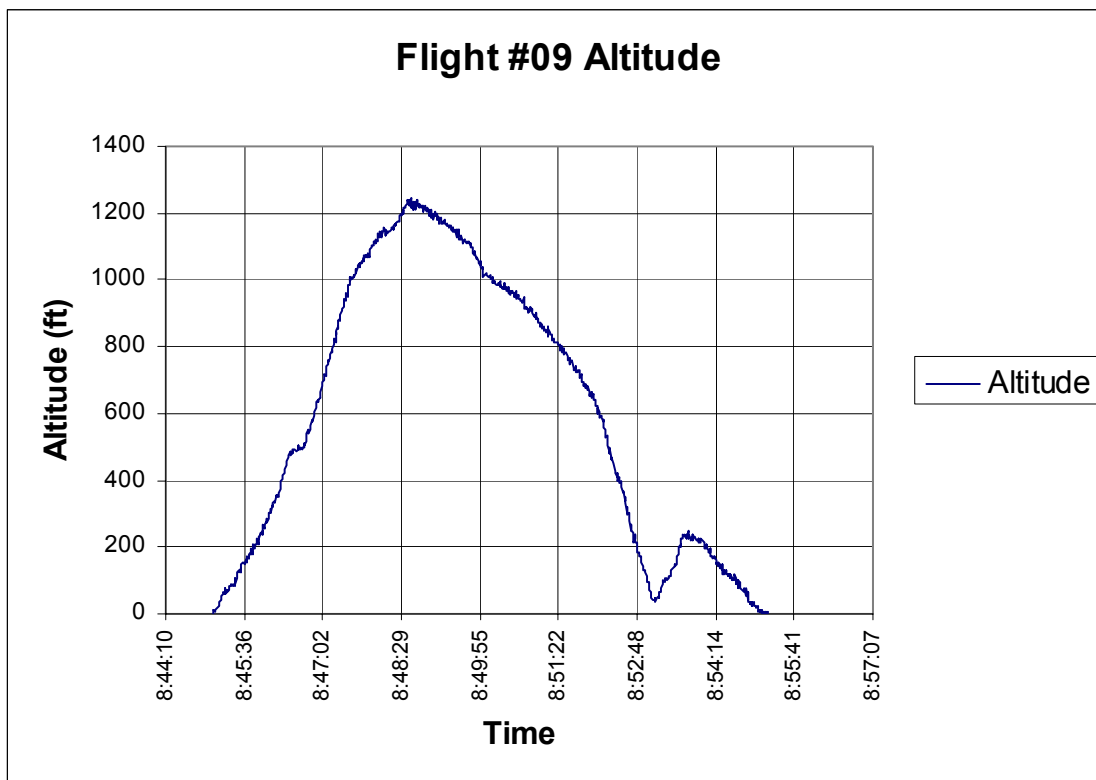
APPENDIX G
ALTITUDE TIME GRAPHS

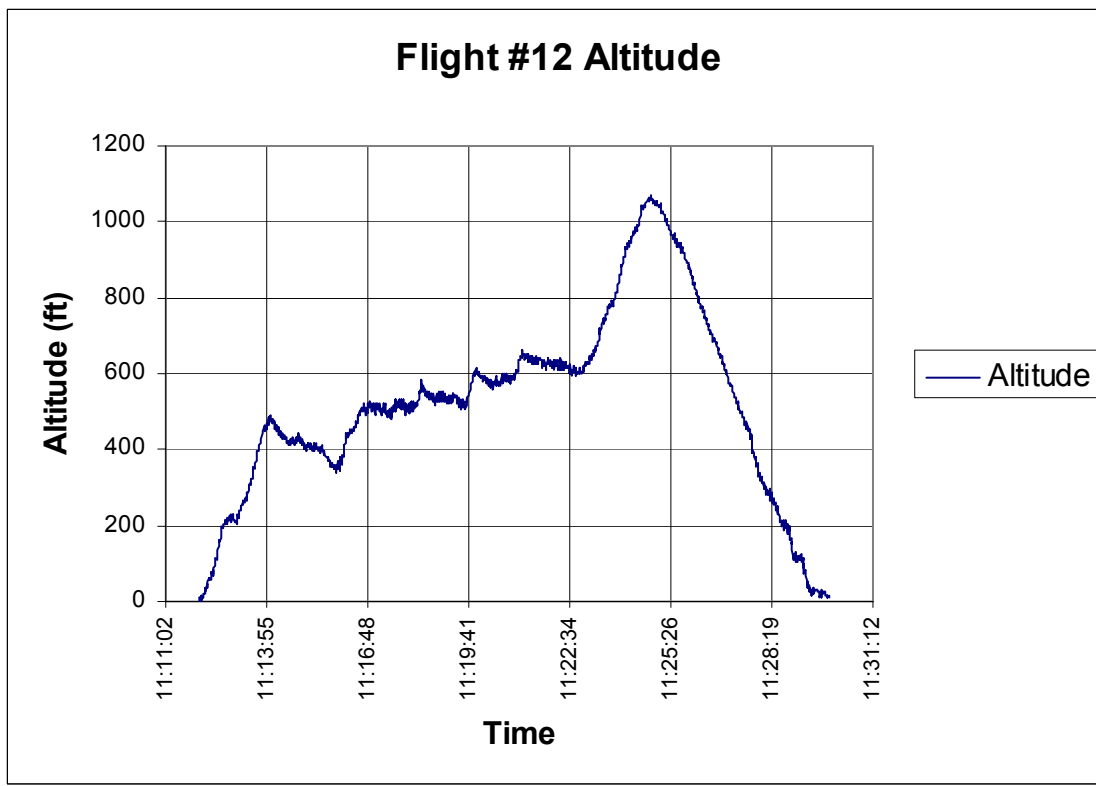
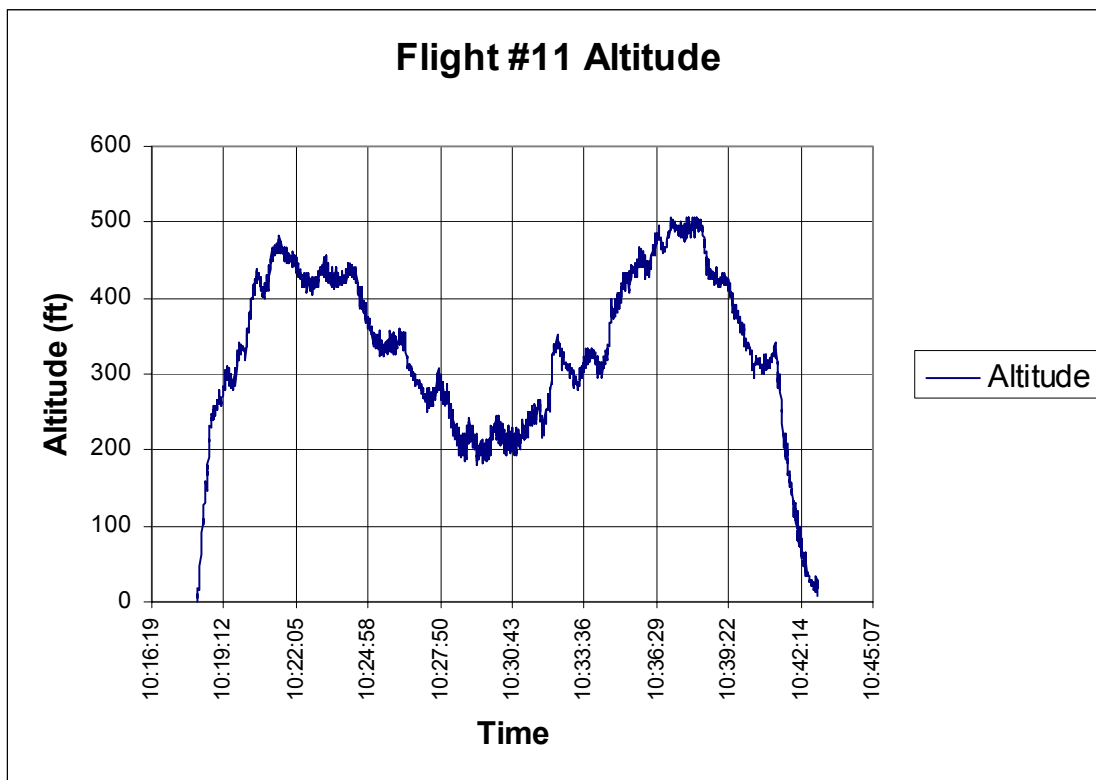


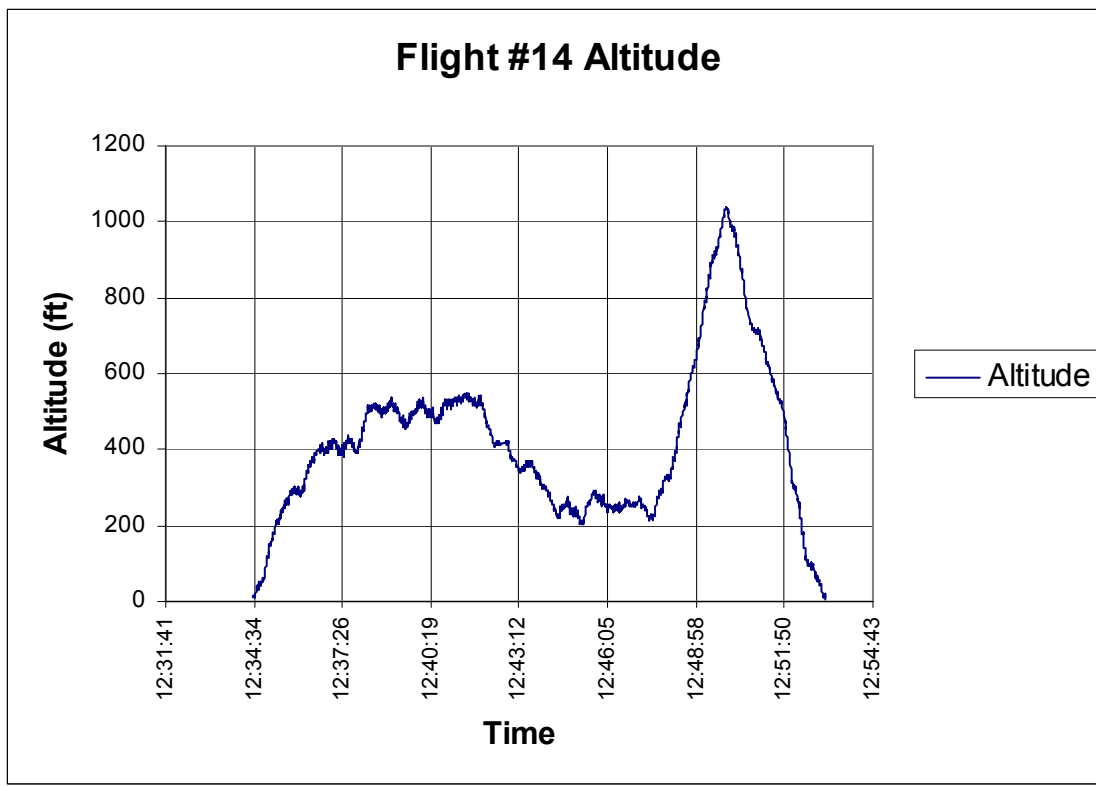
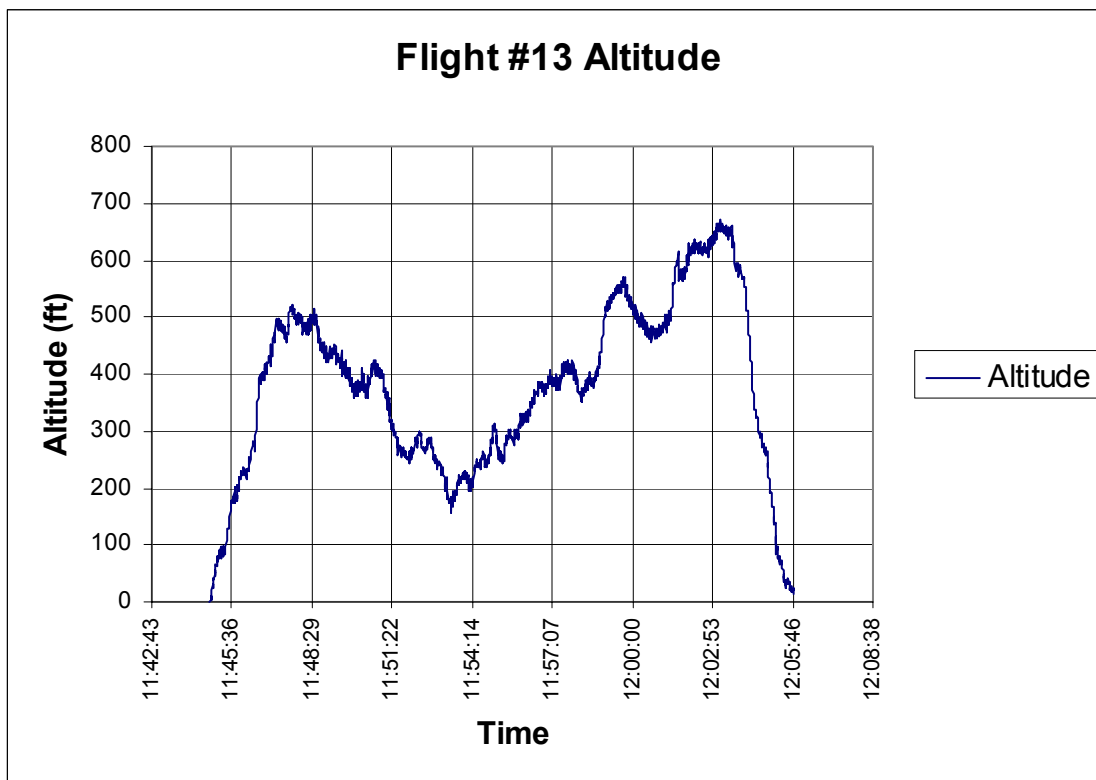


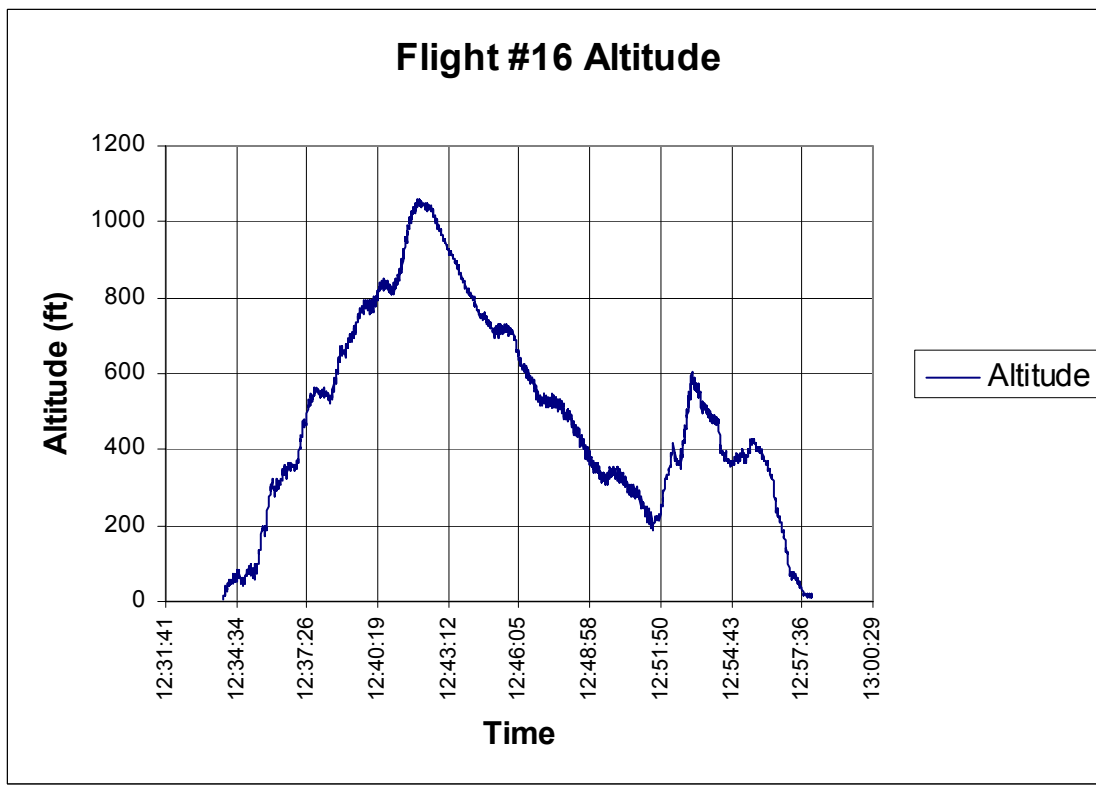
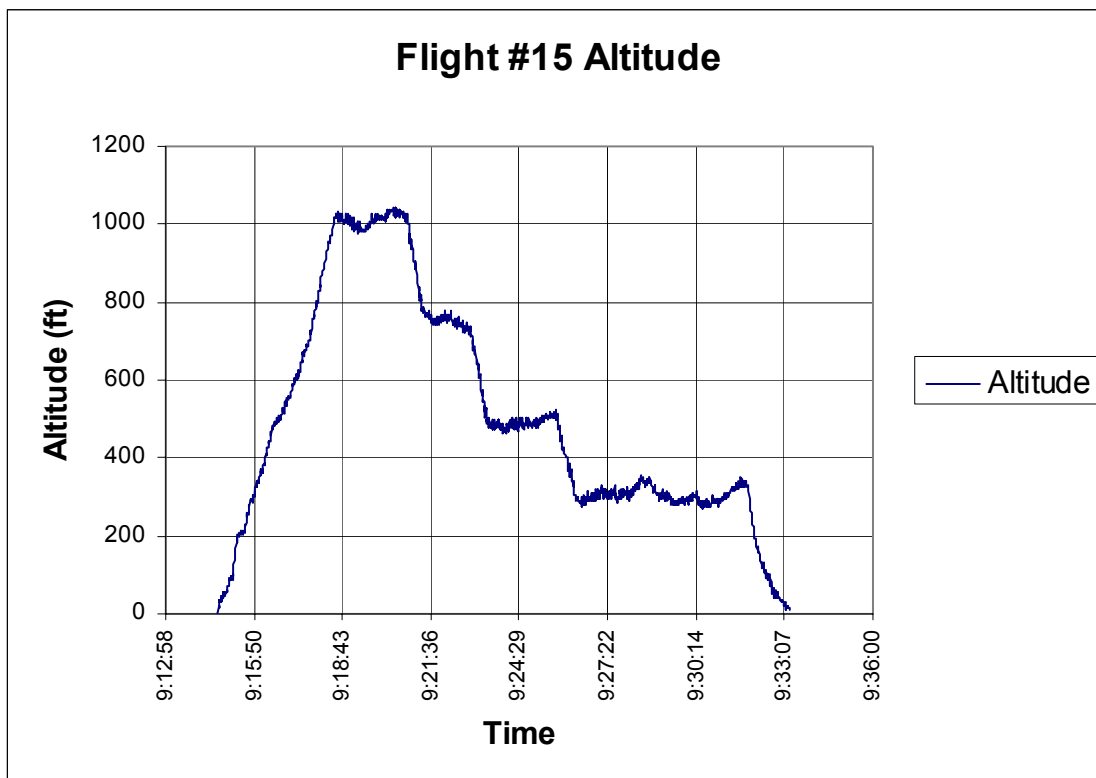


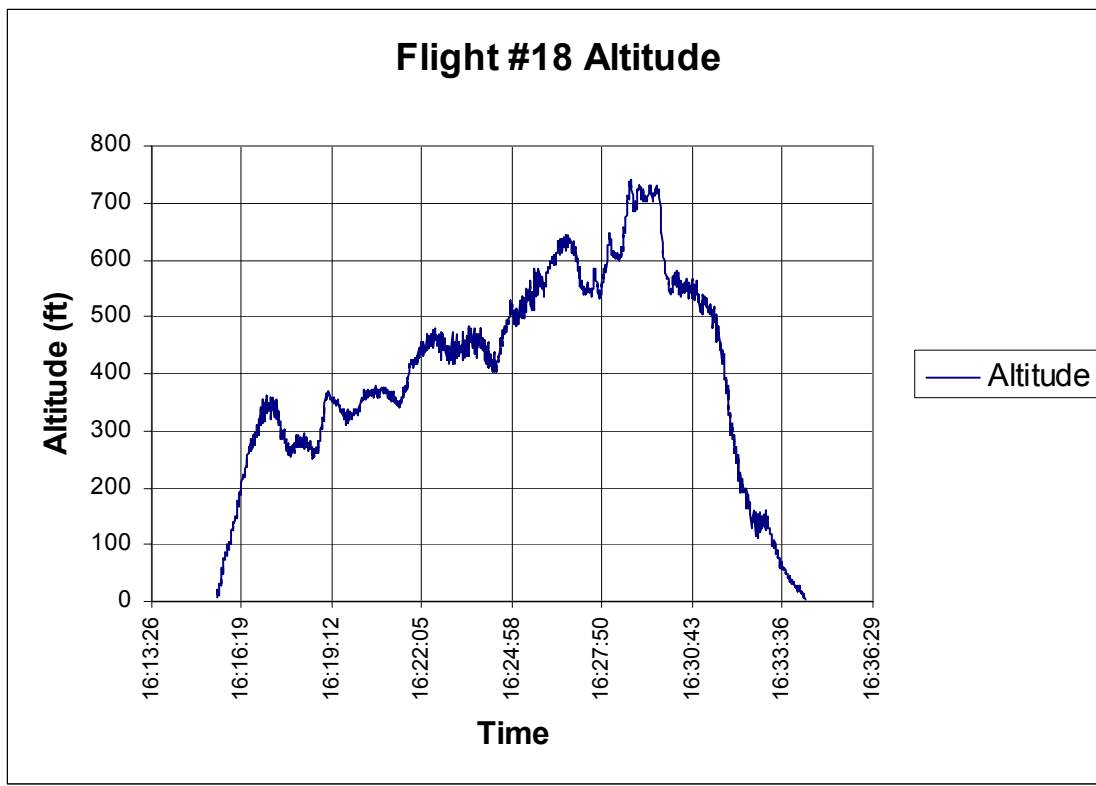
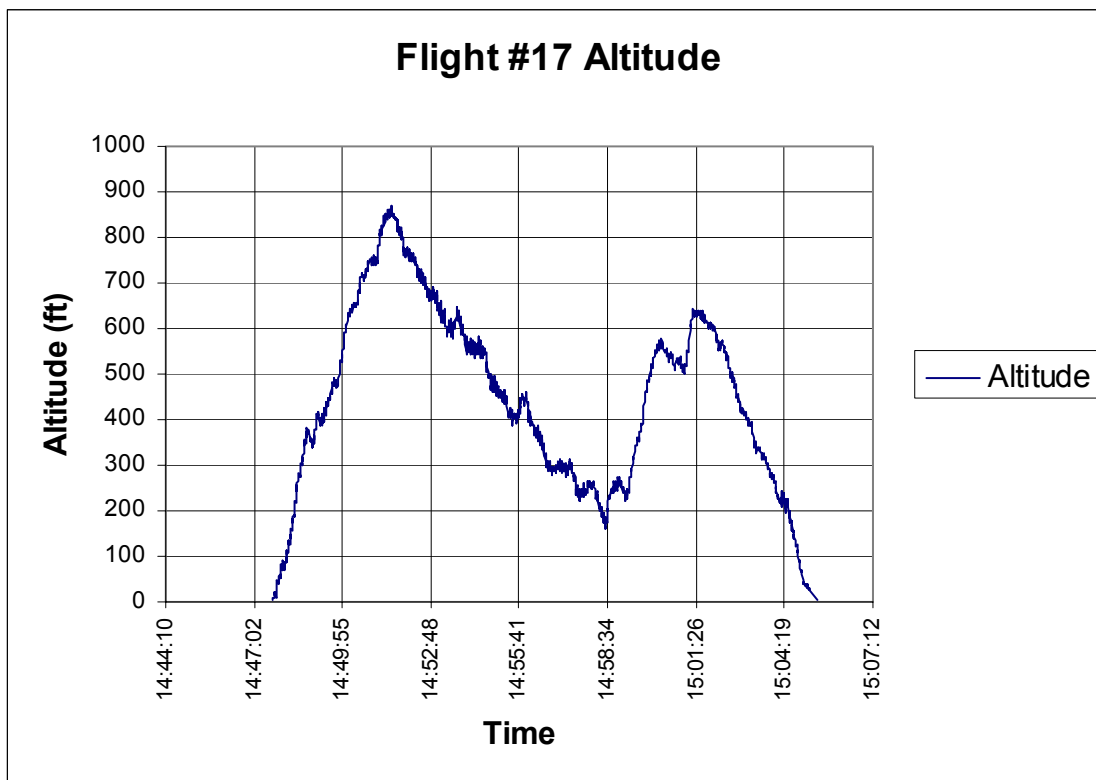


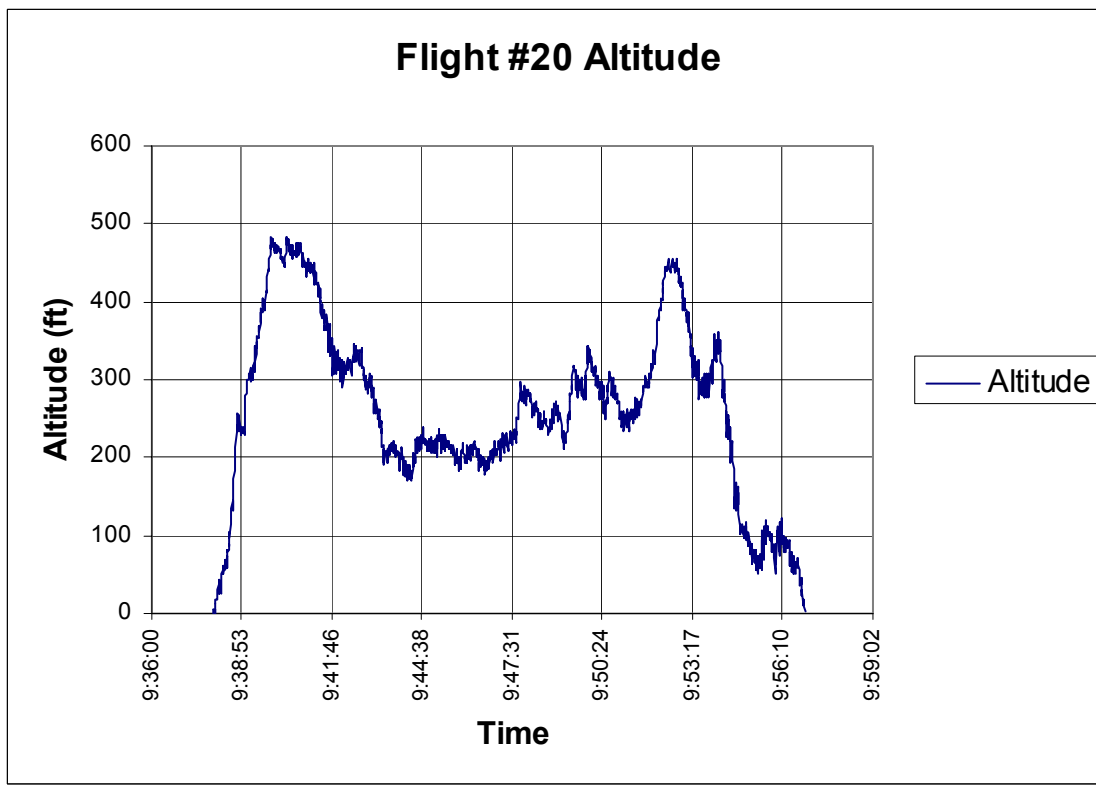
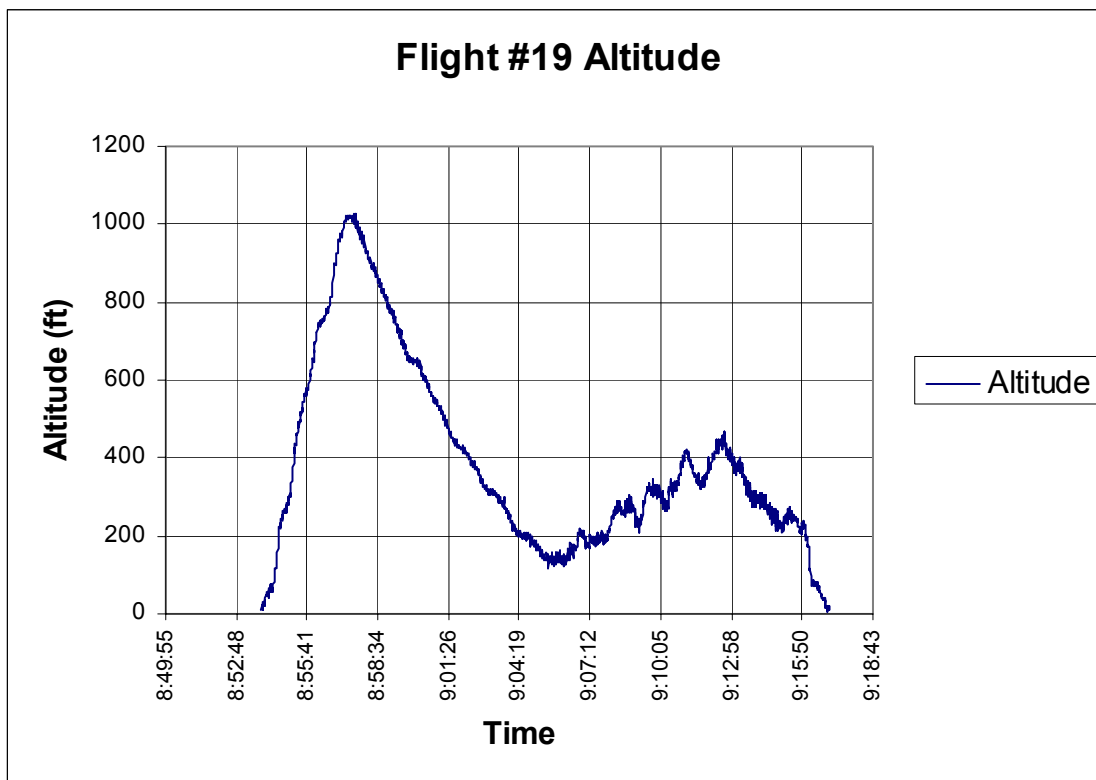


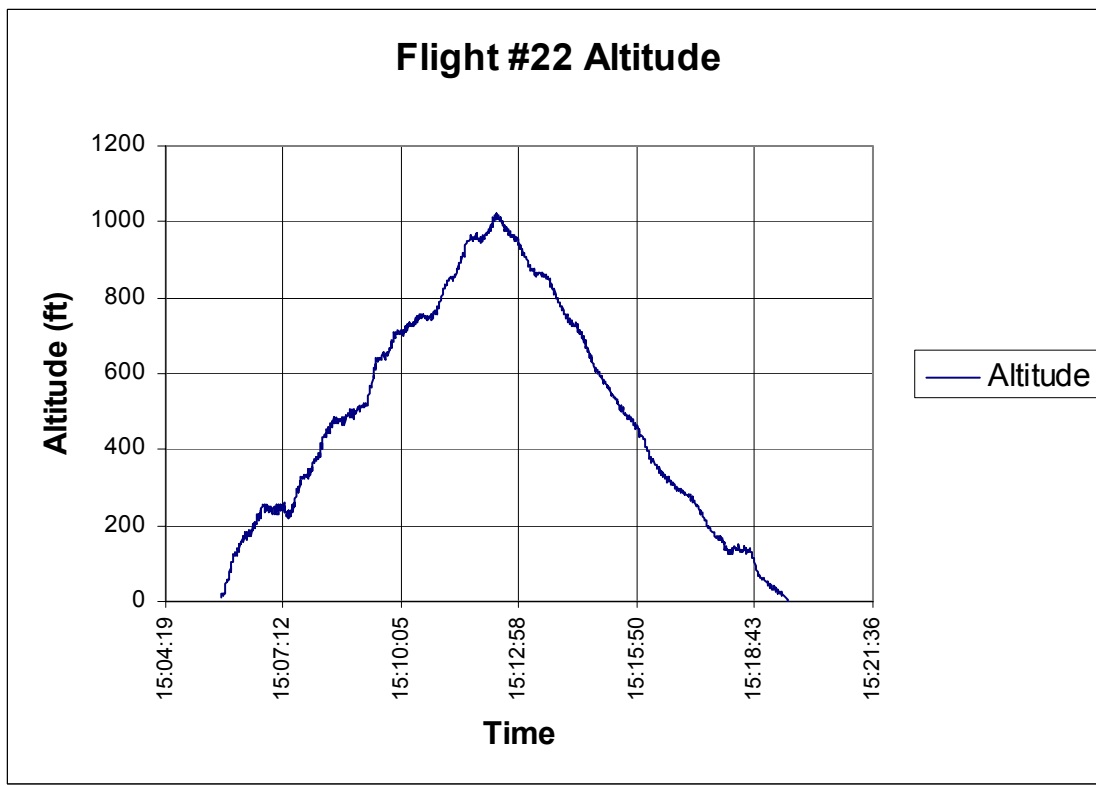
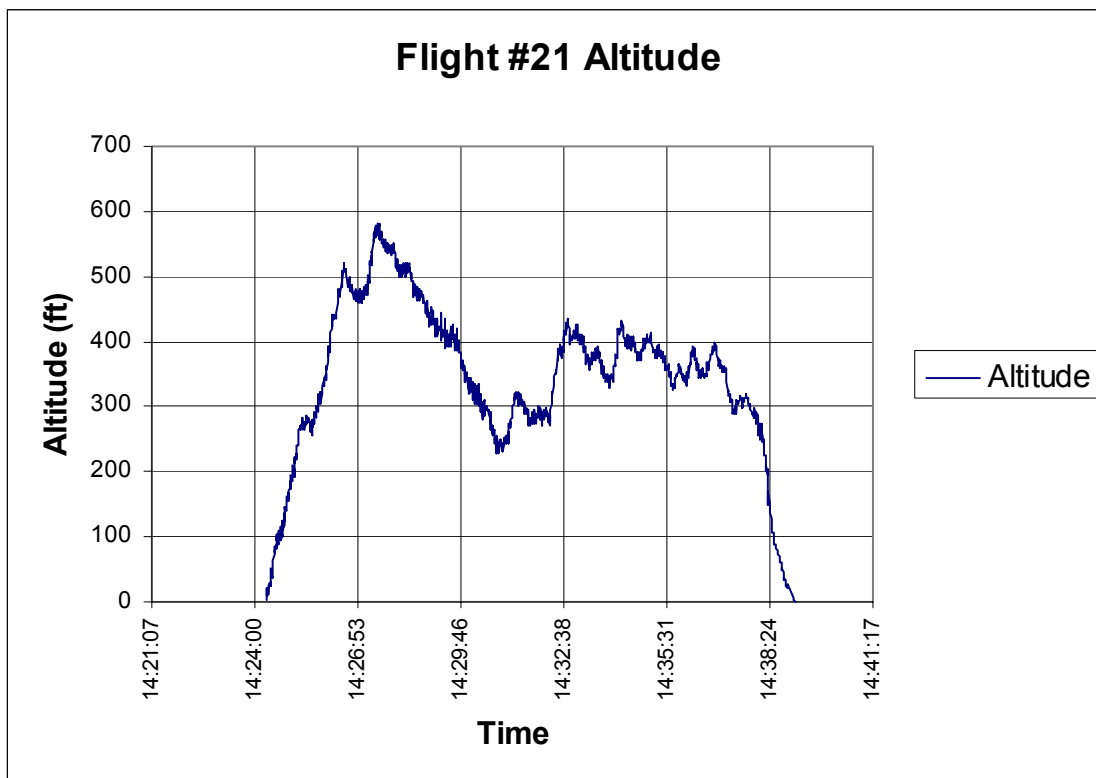


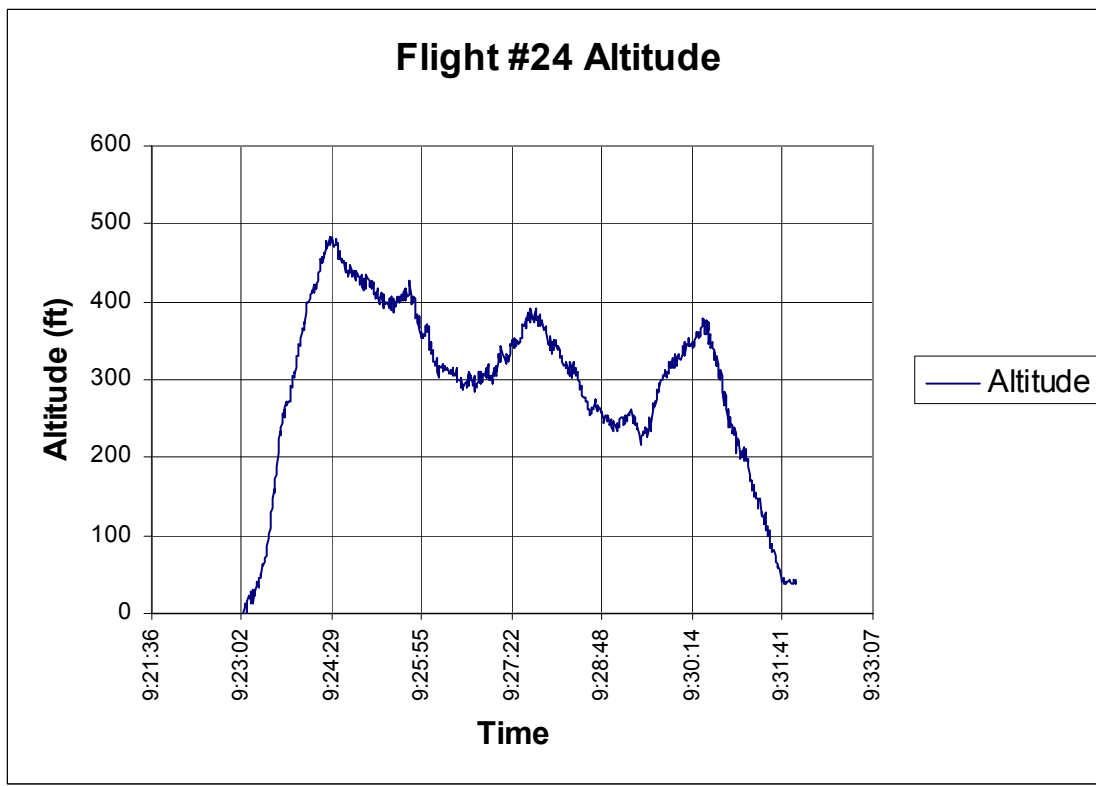
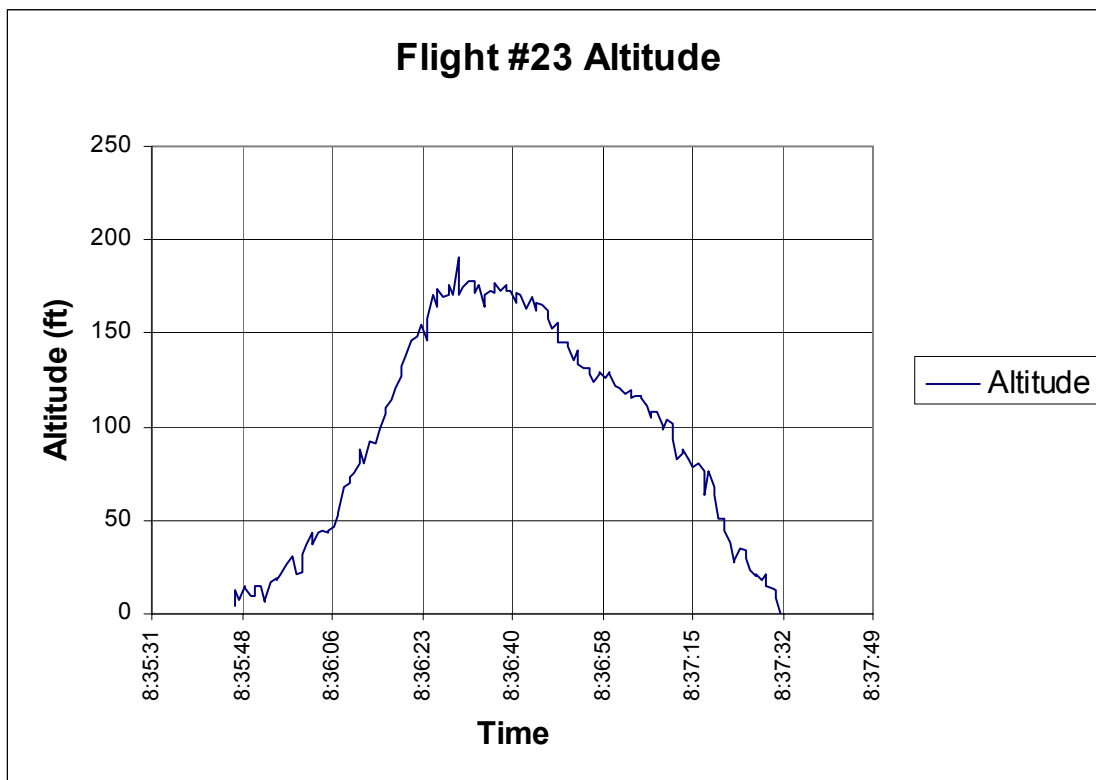


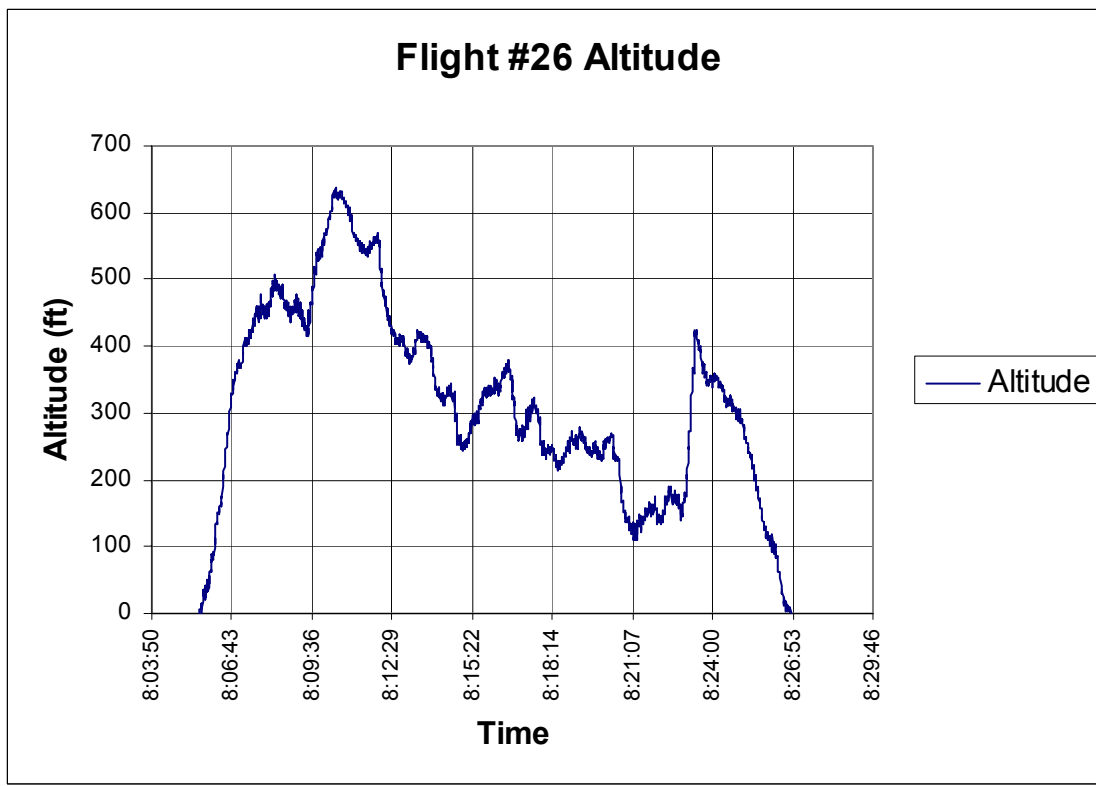
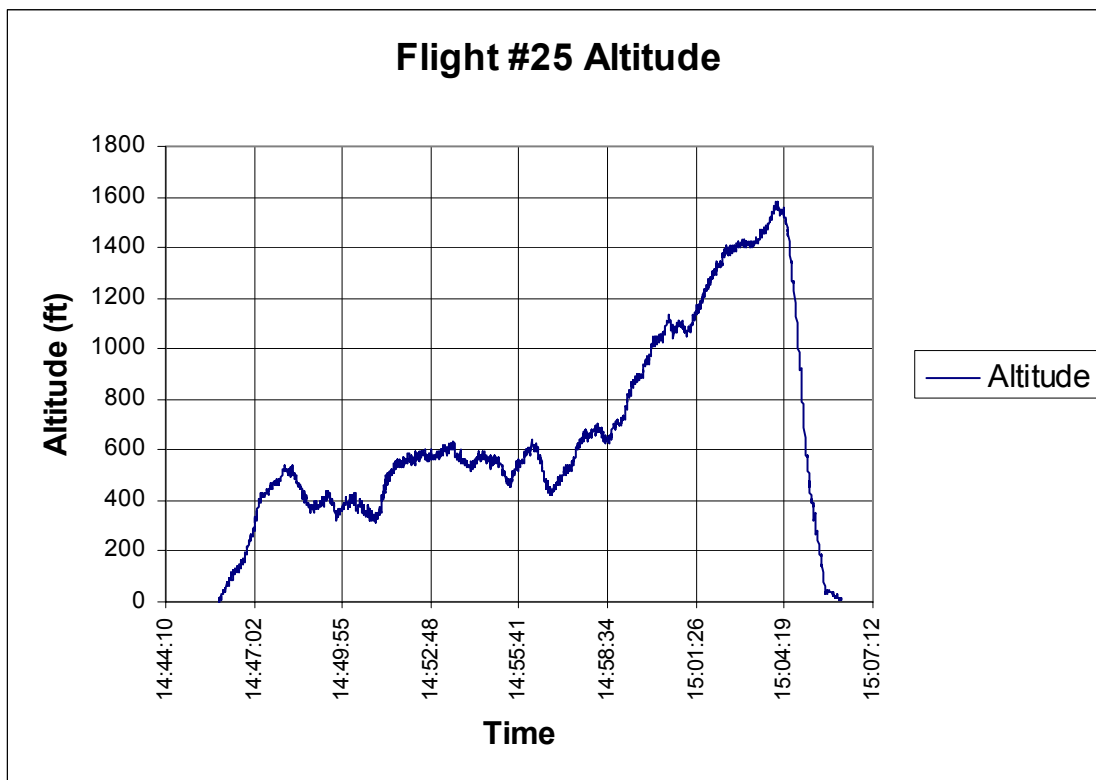


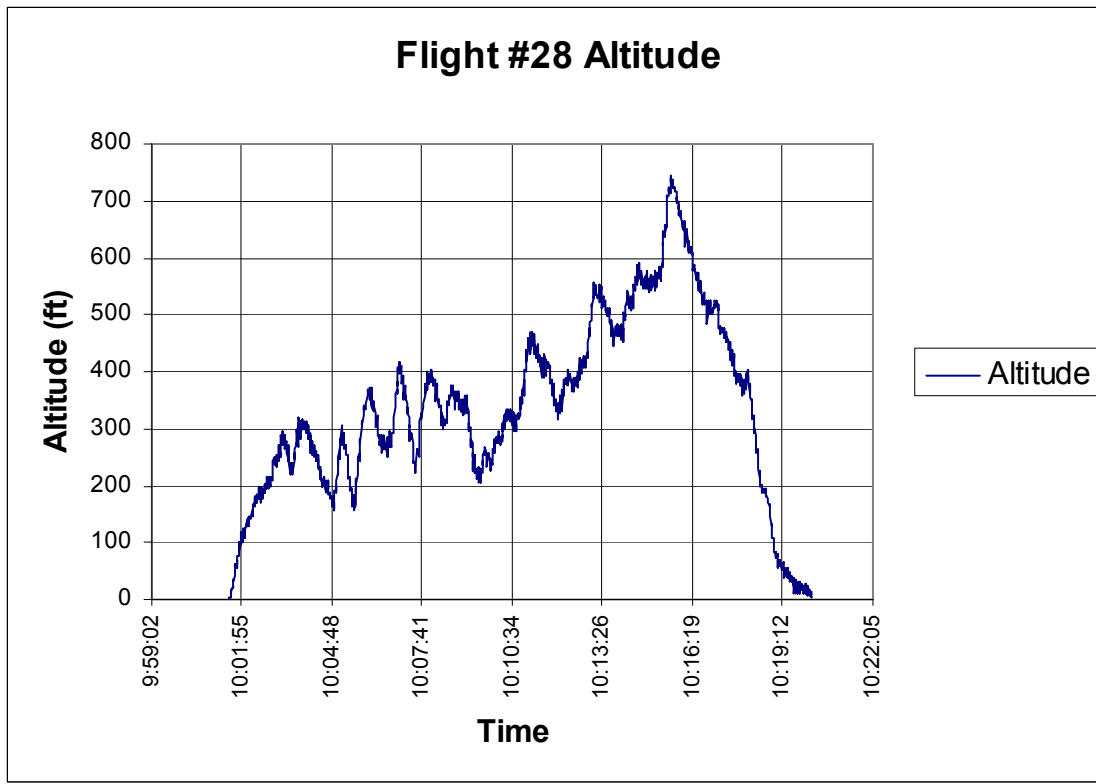
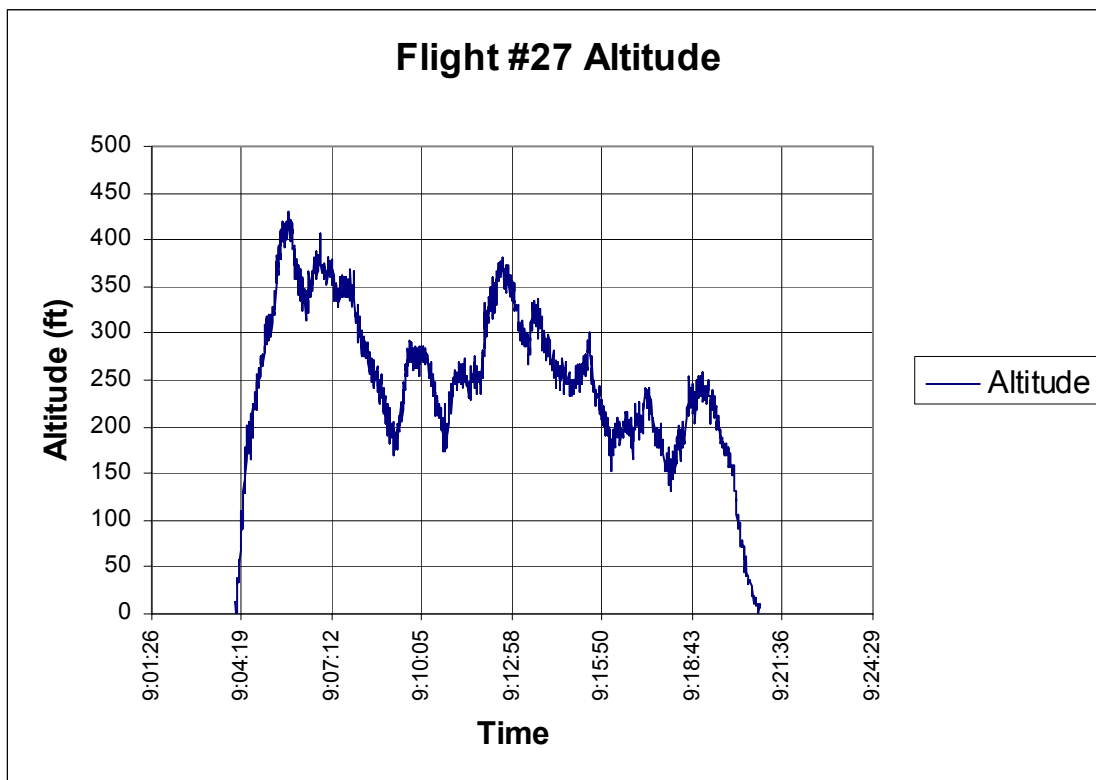




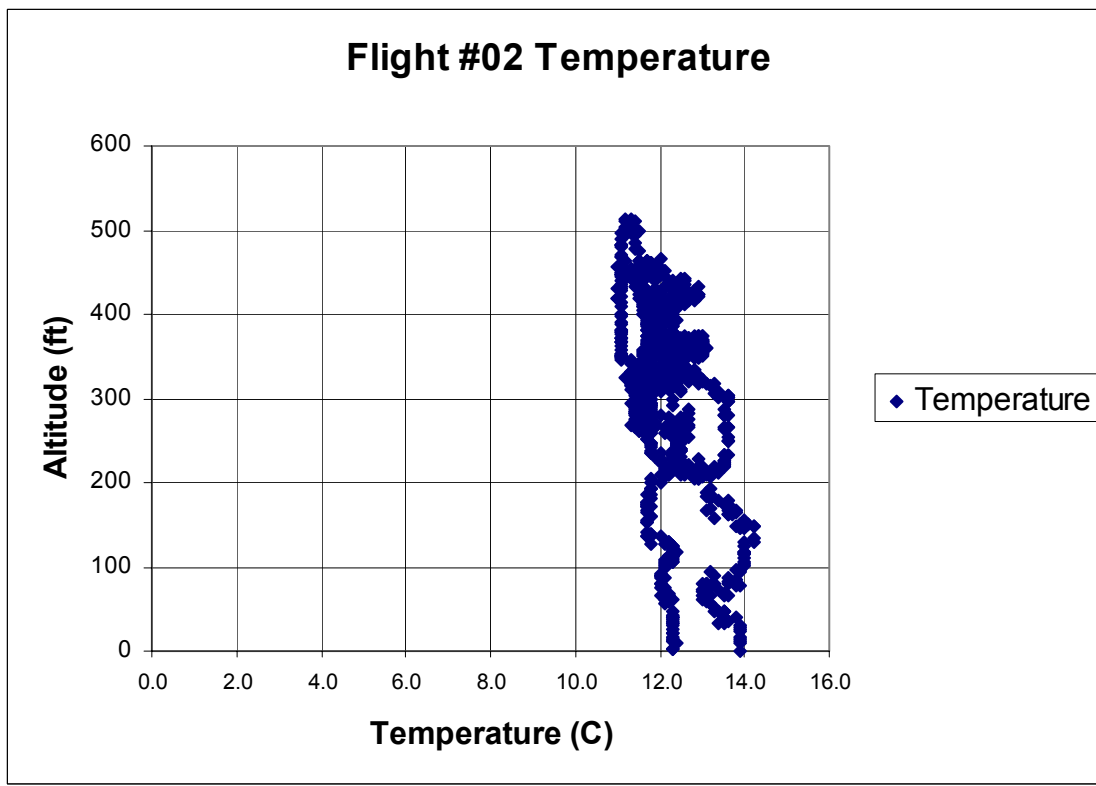
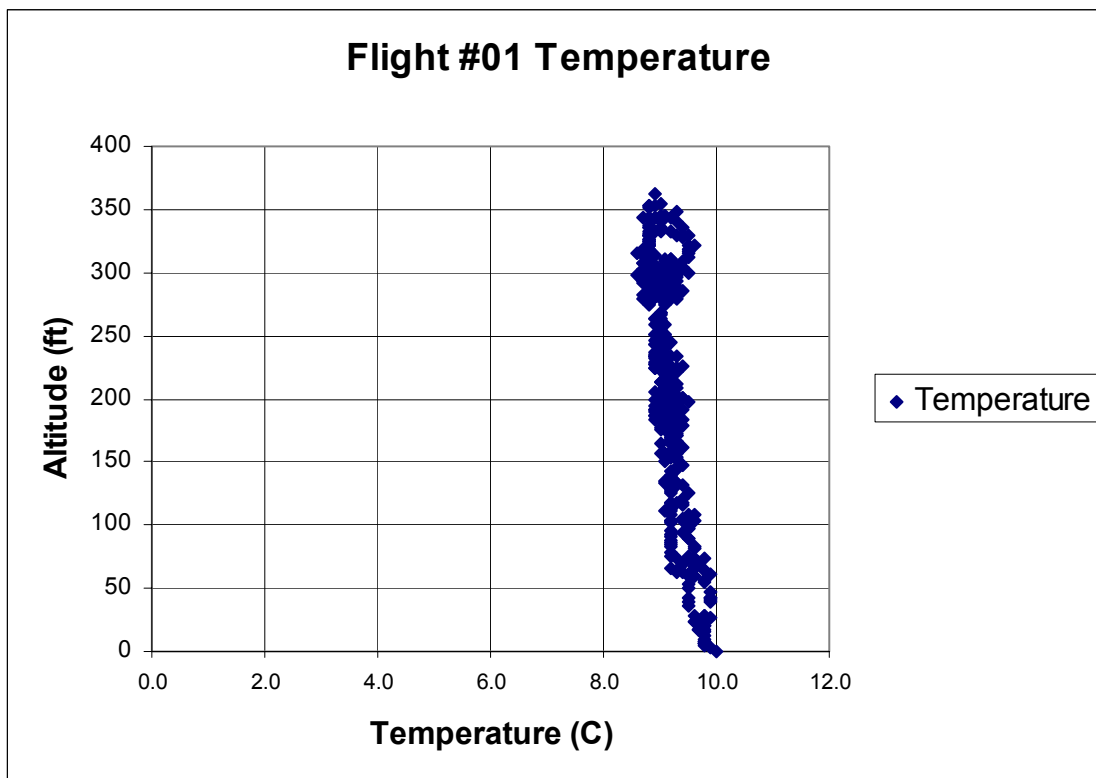


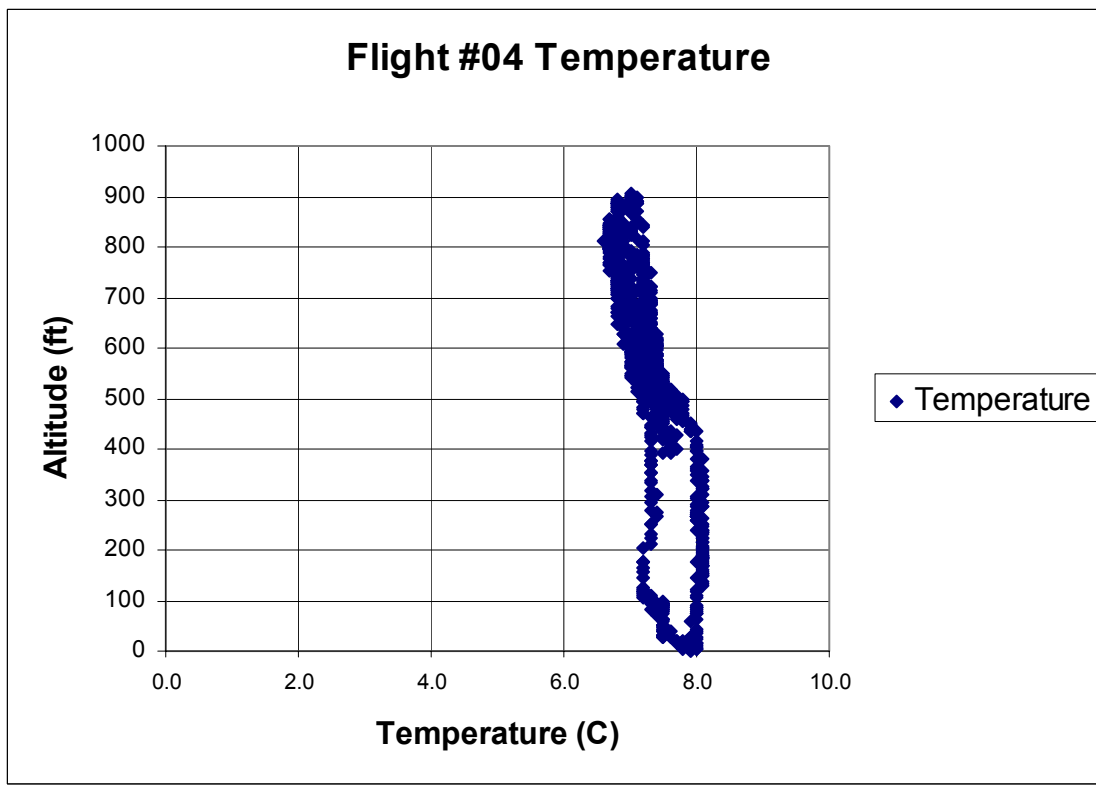
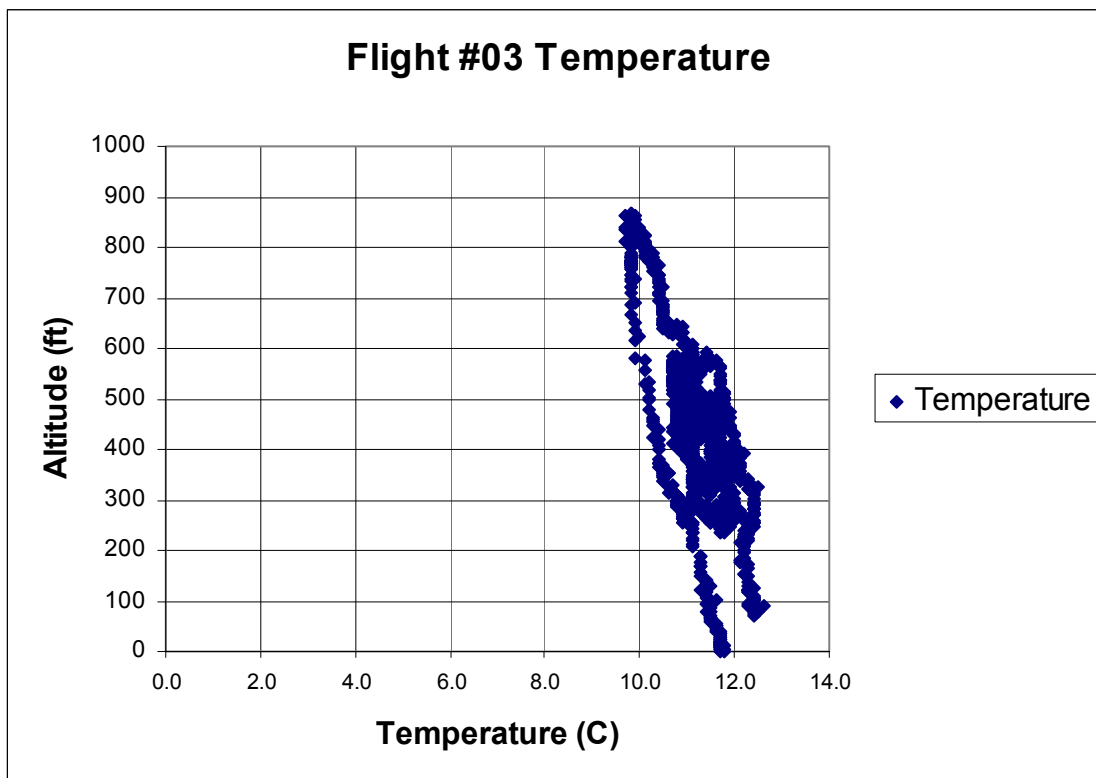


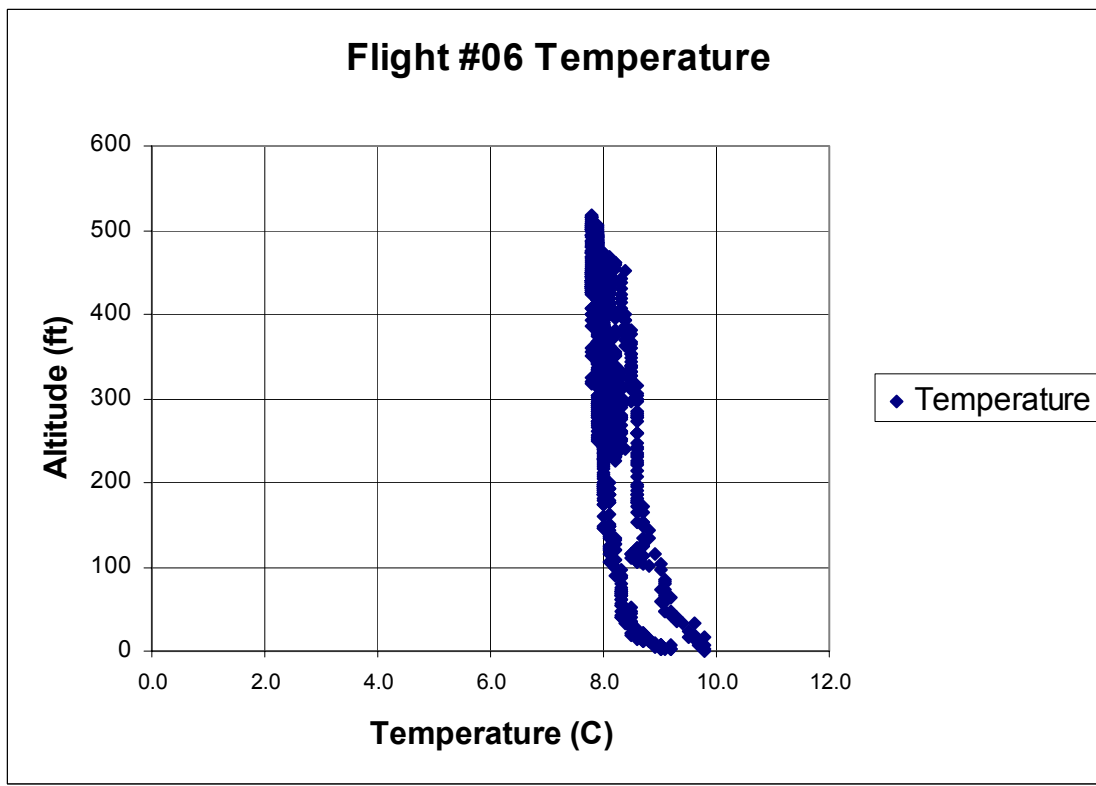
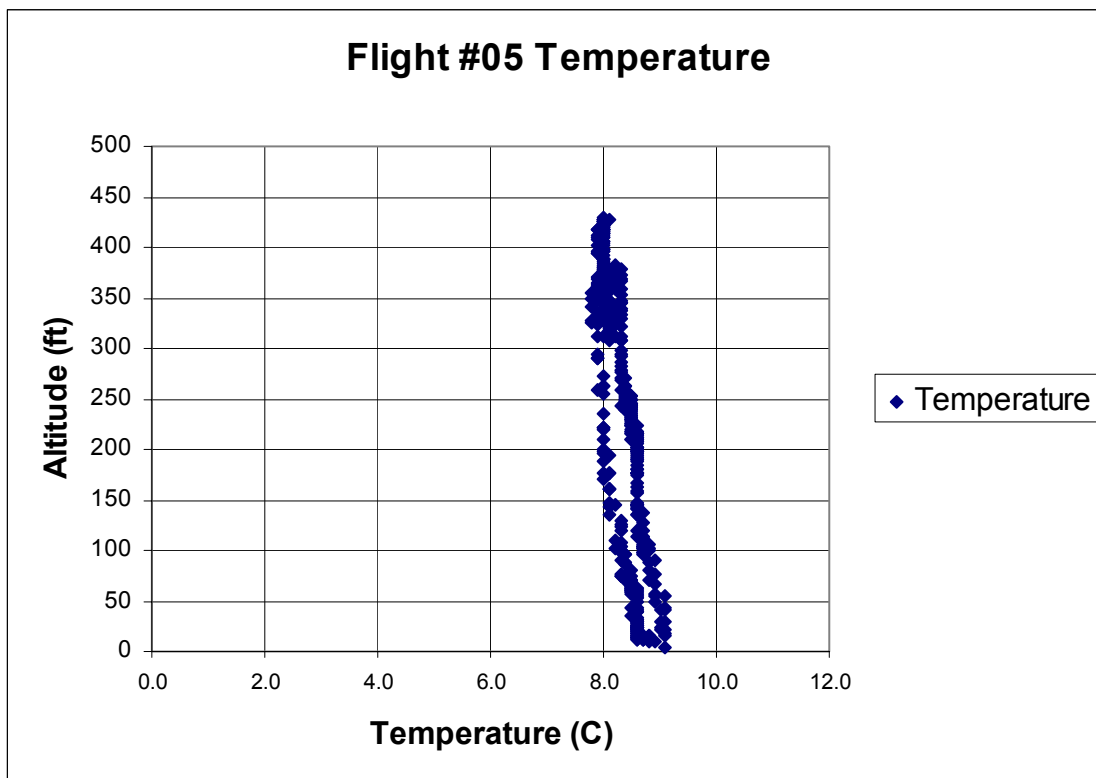


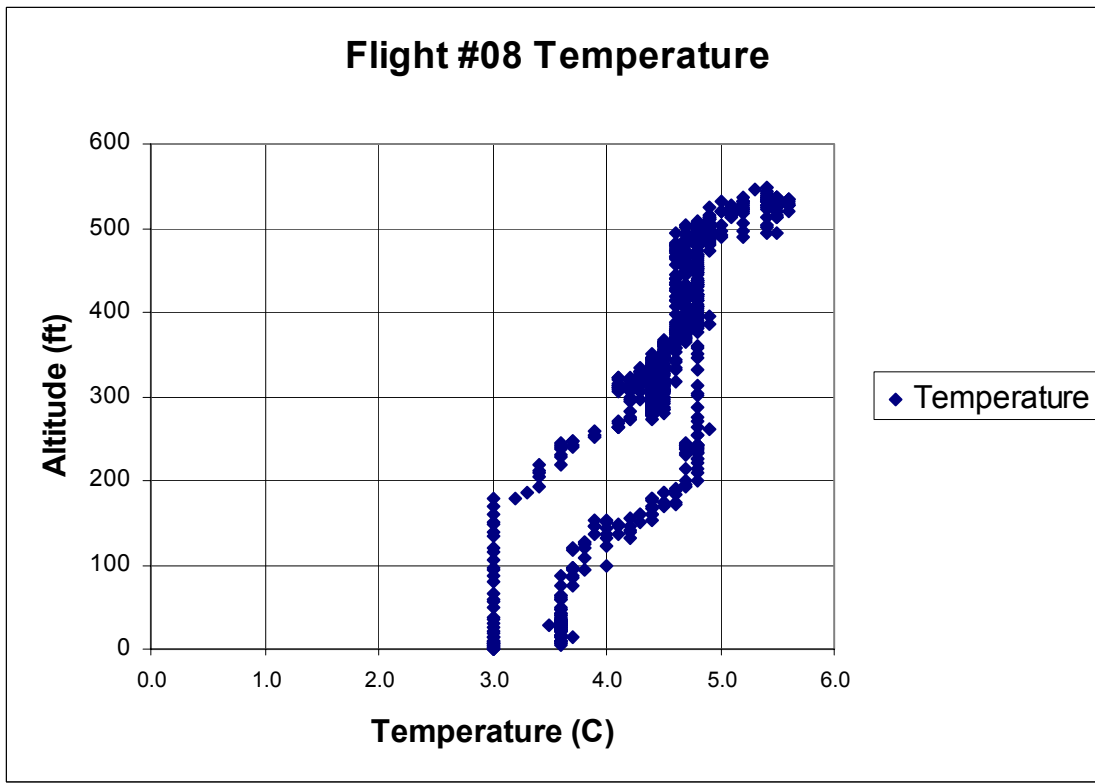
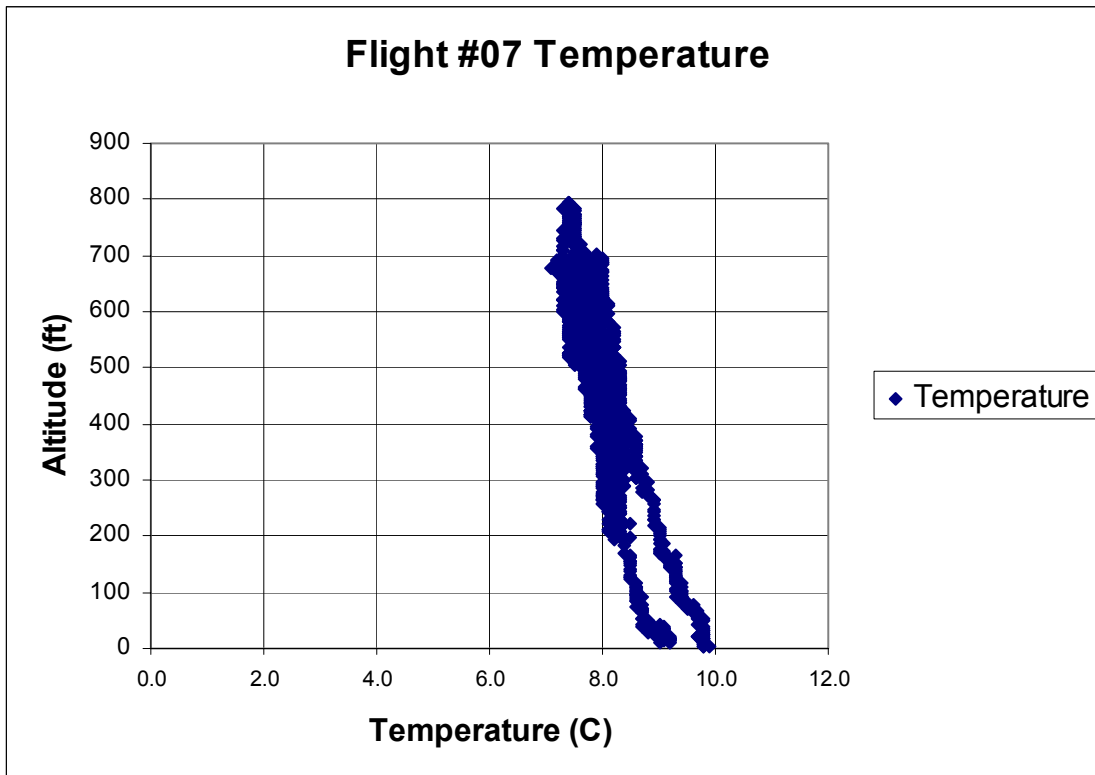


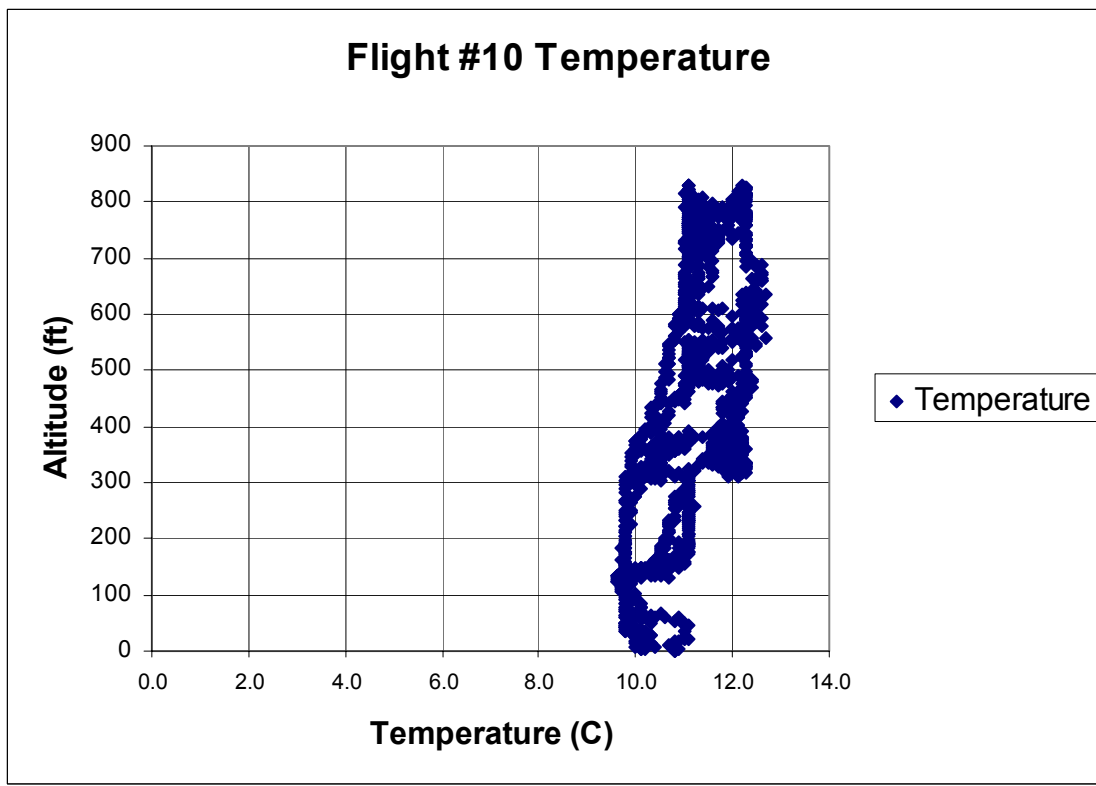
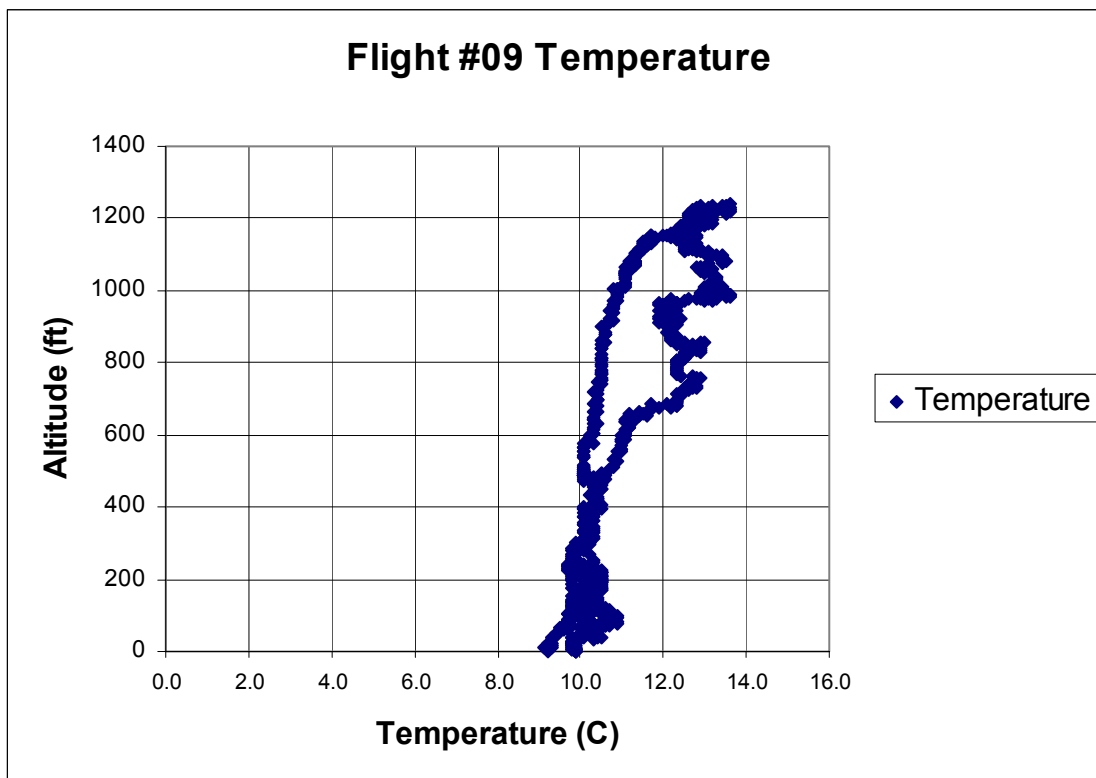
APPENDIX H
ALTITUDE TEMPERATURE GRAPHS

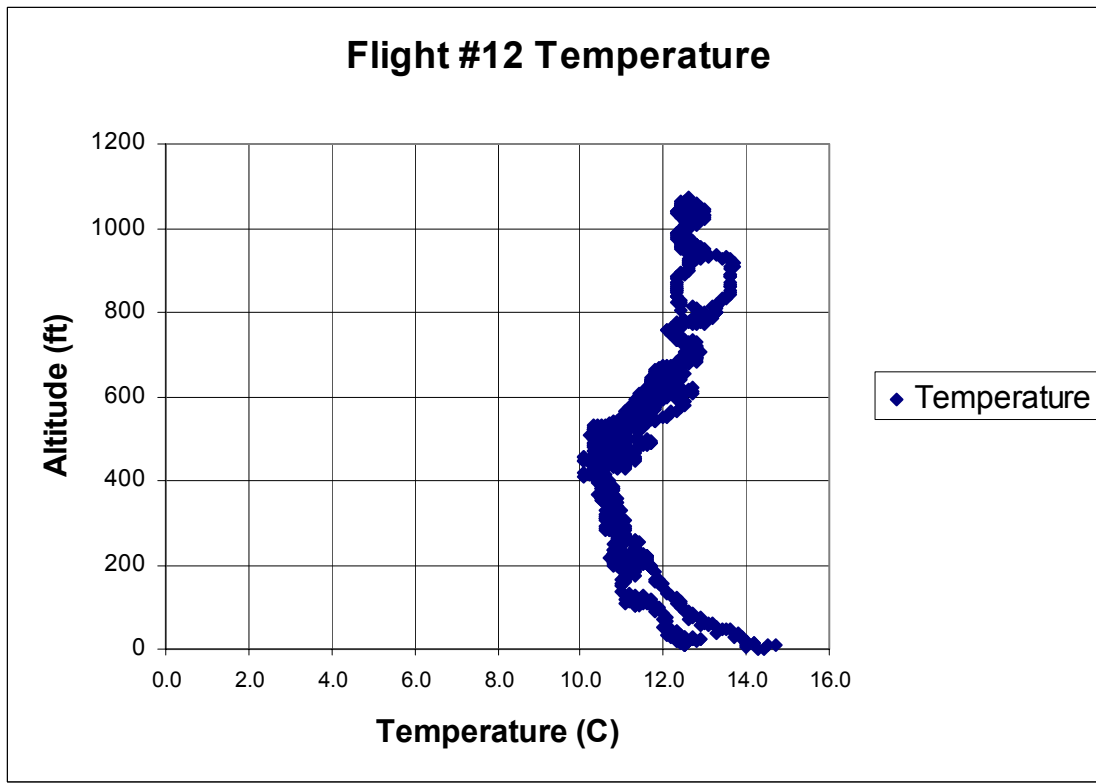
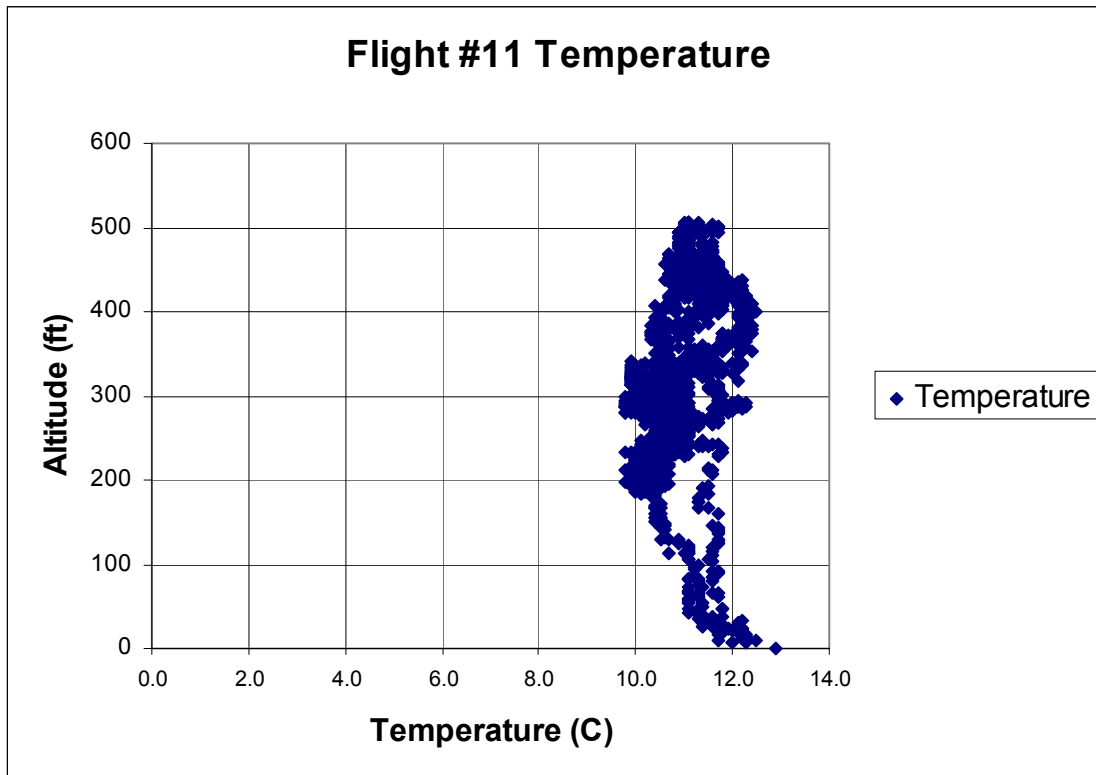


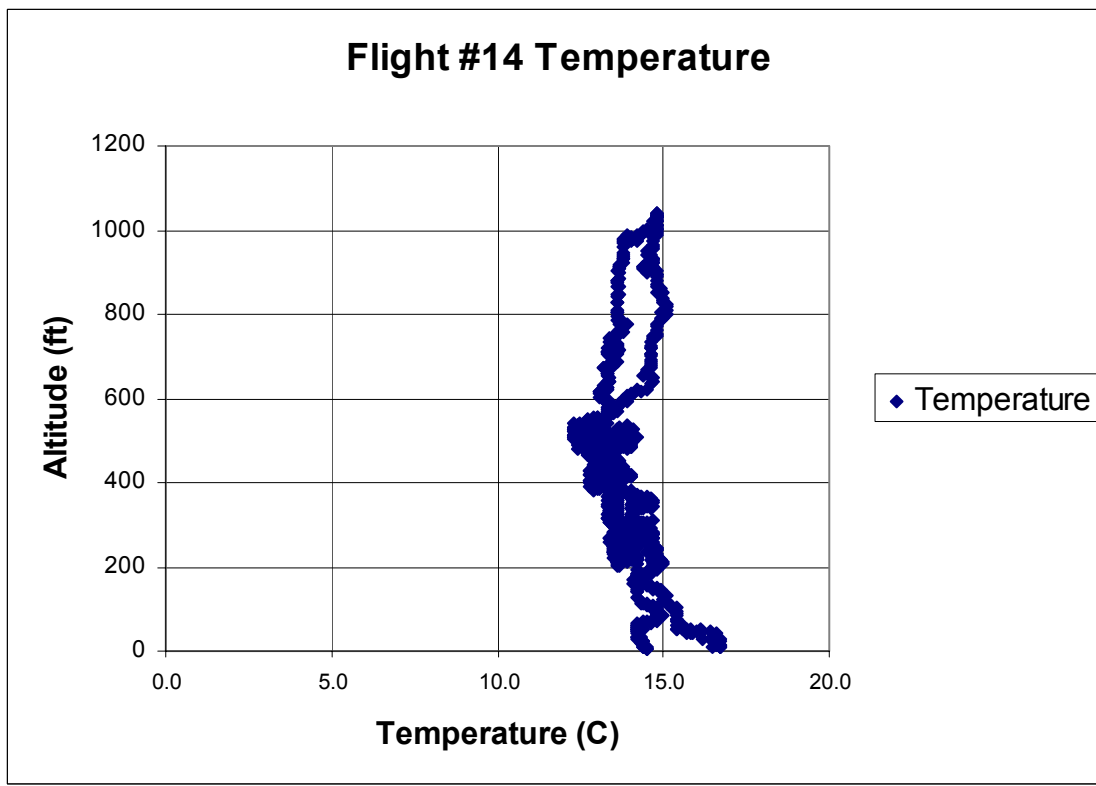
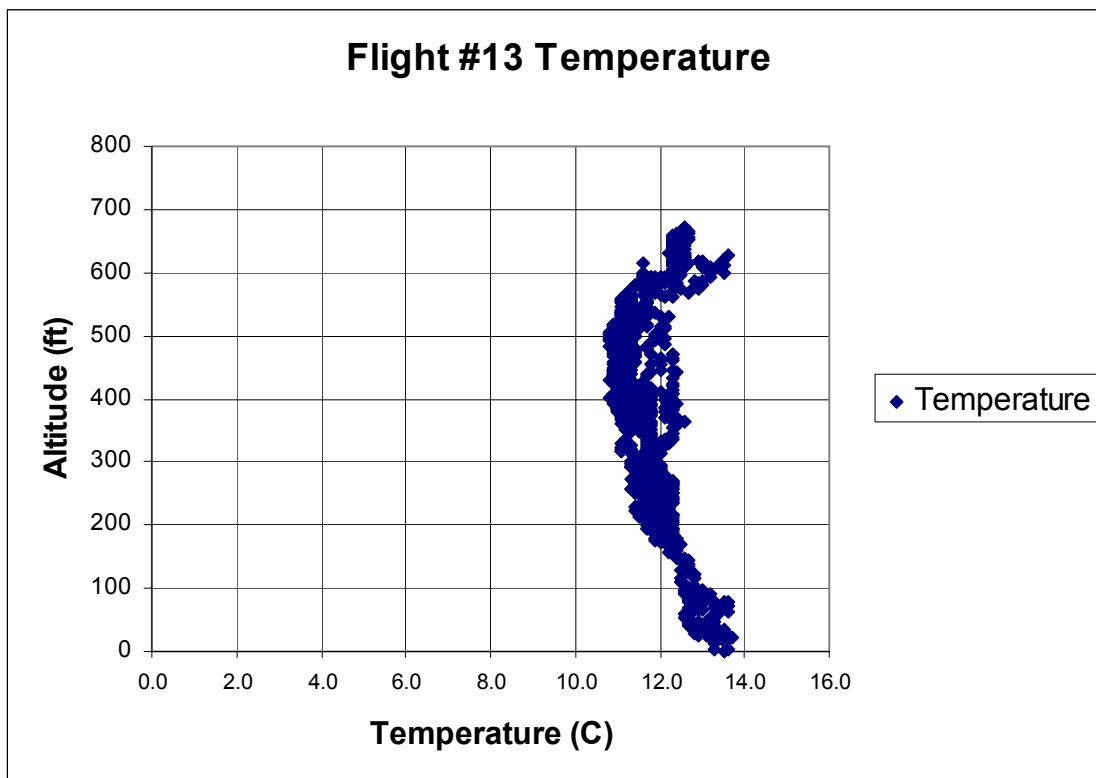


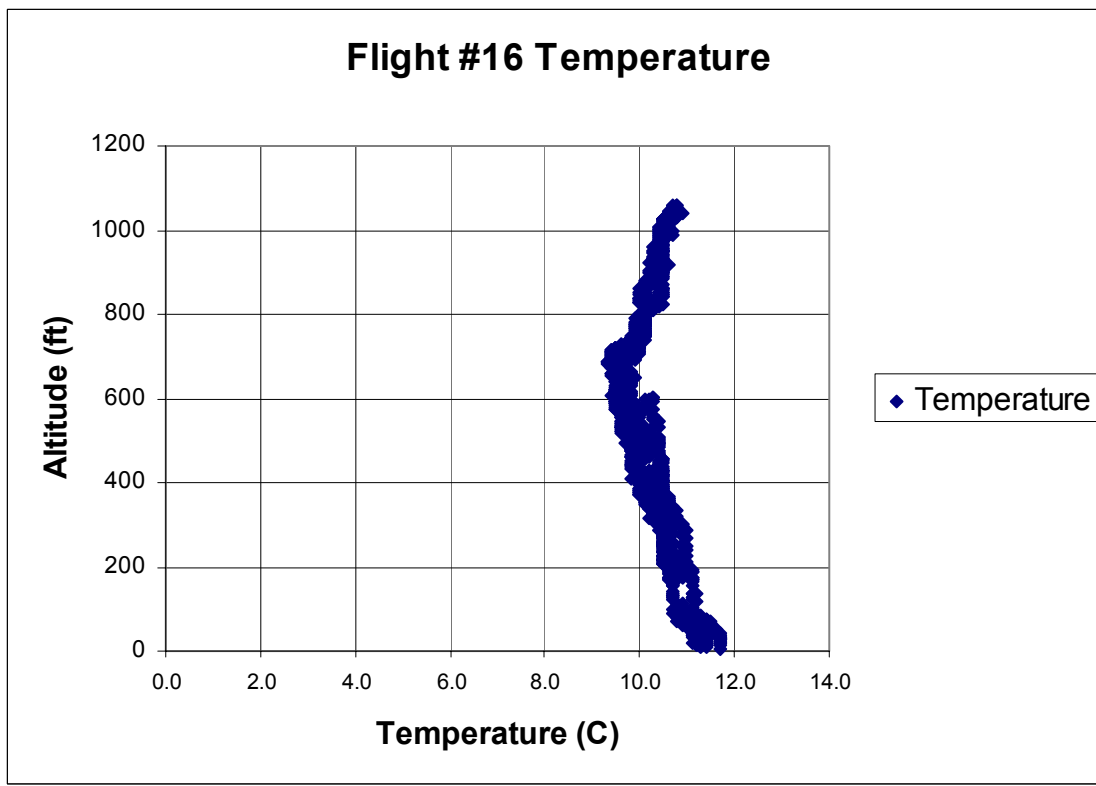
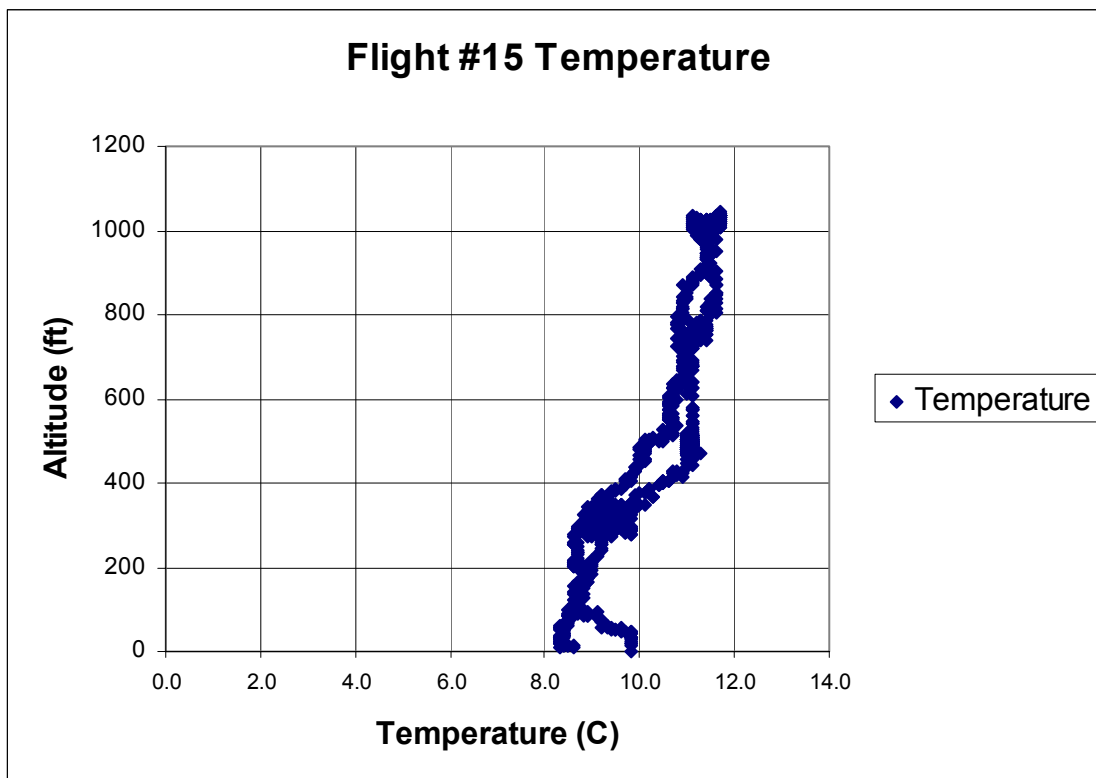


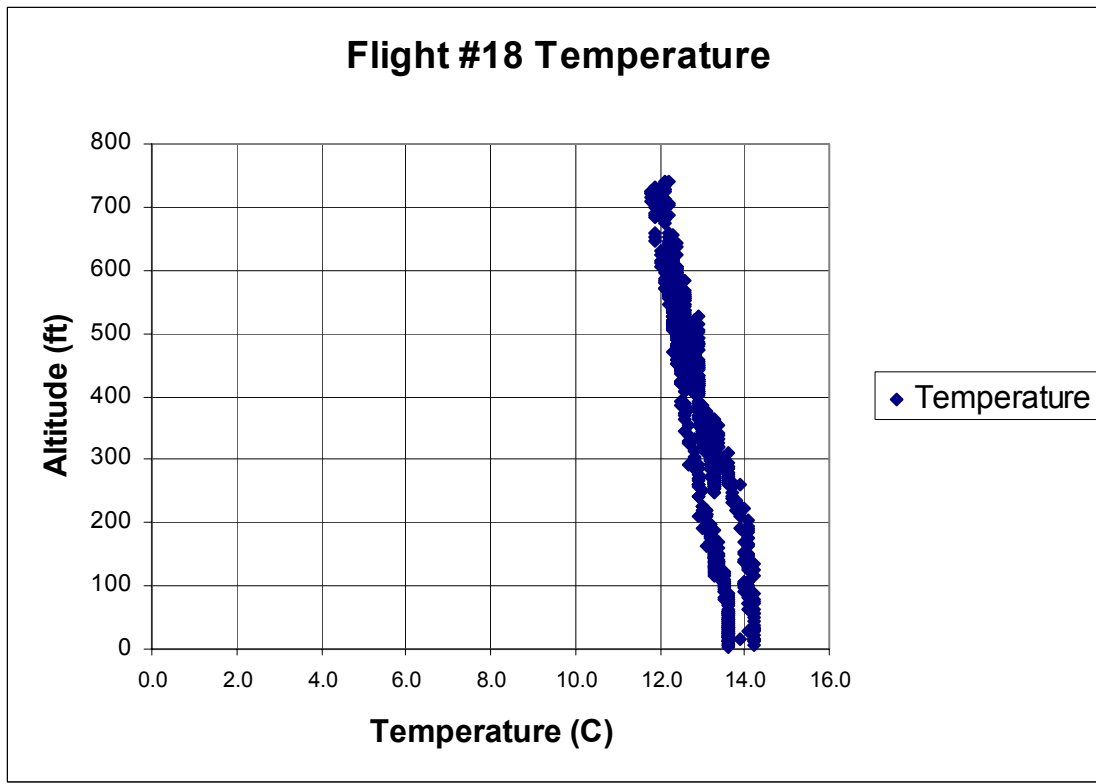
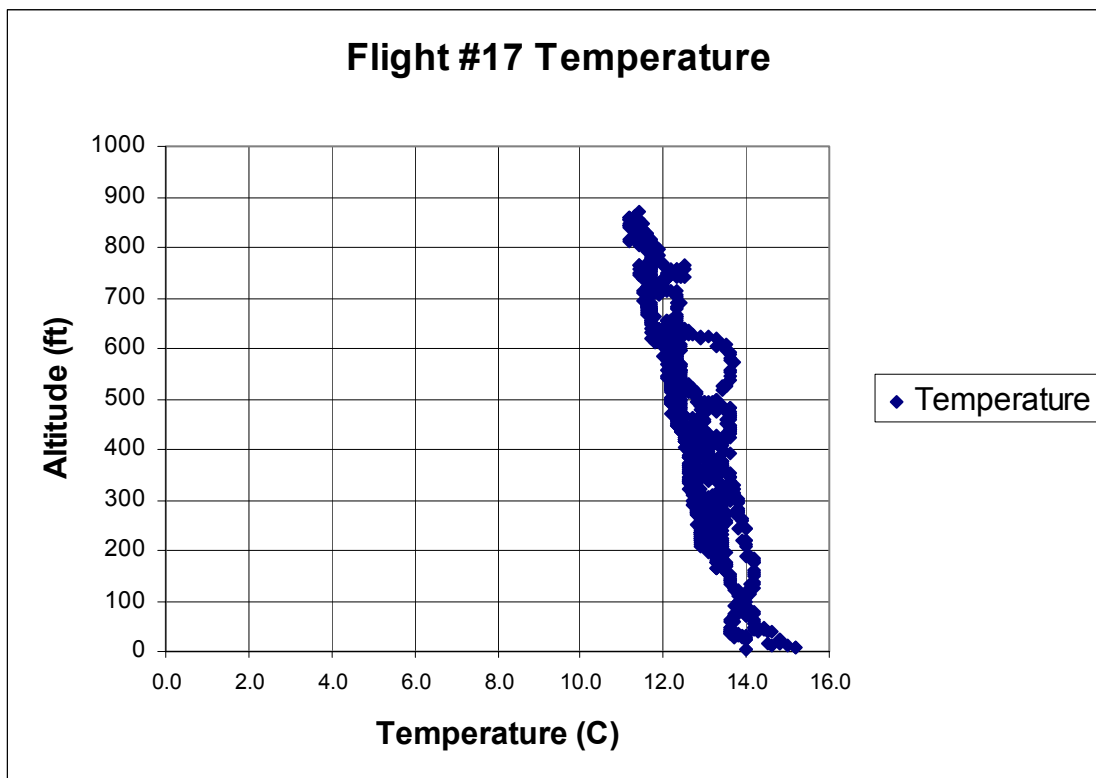


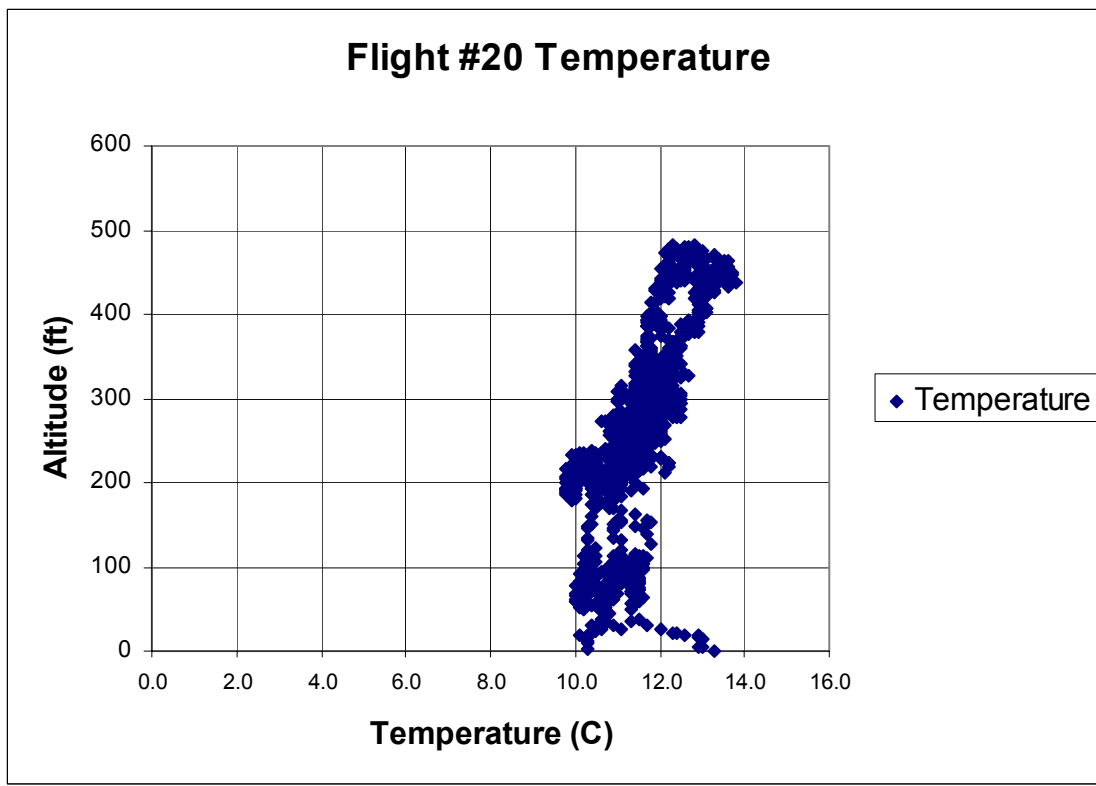
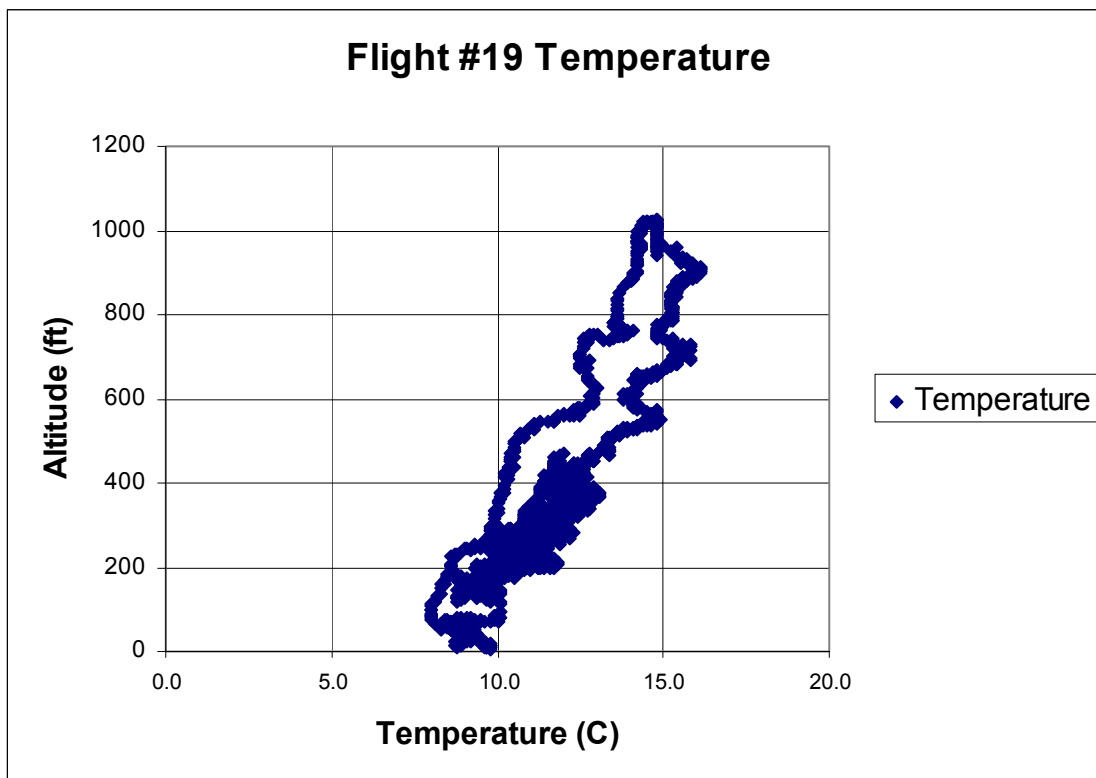


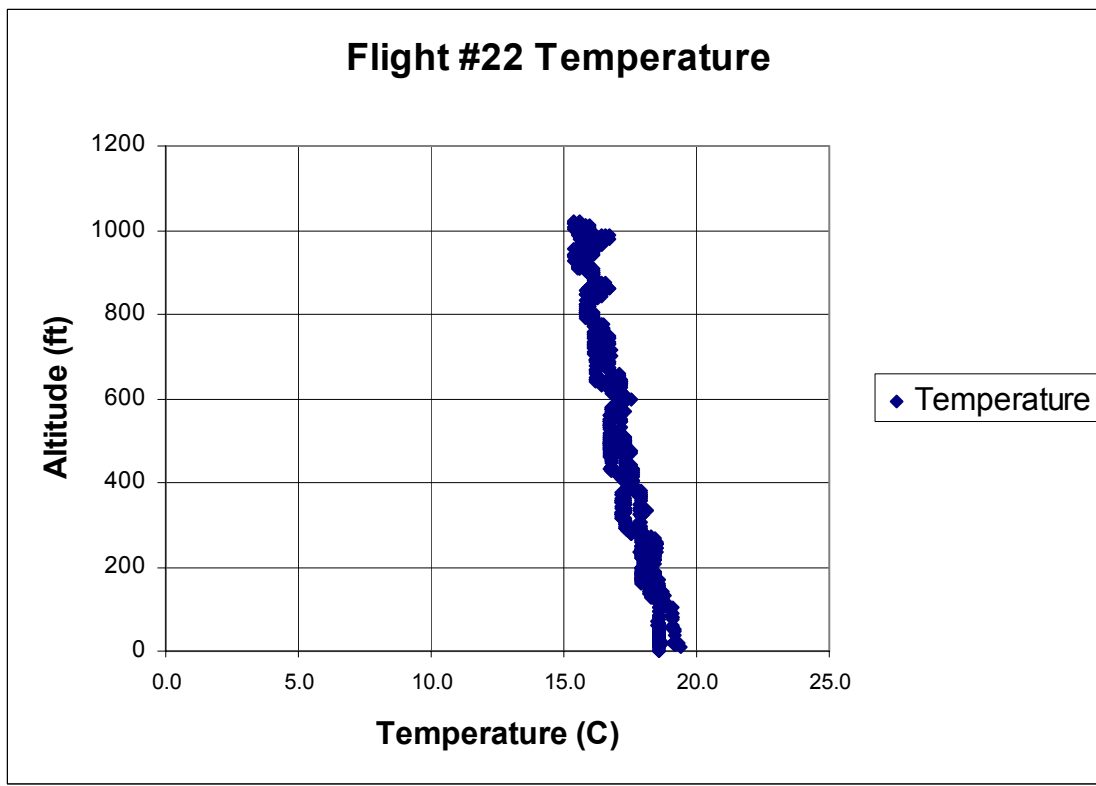
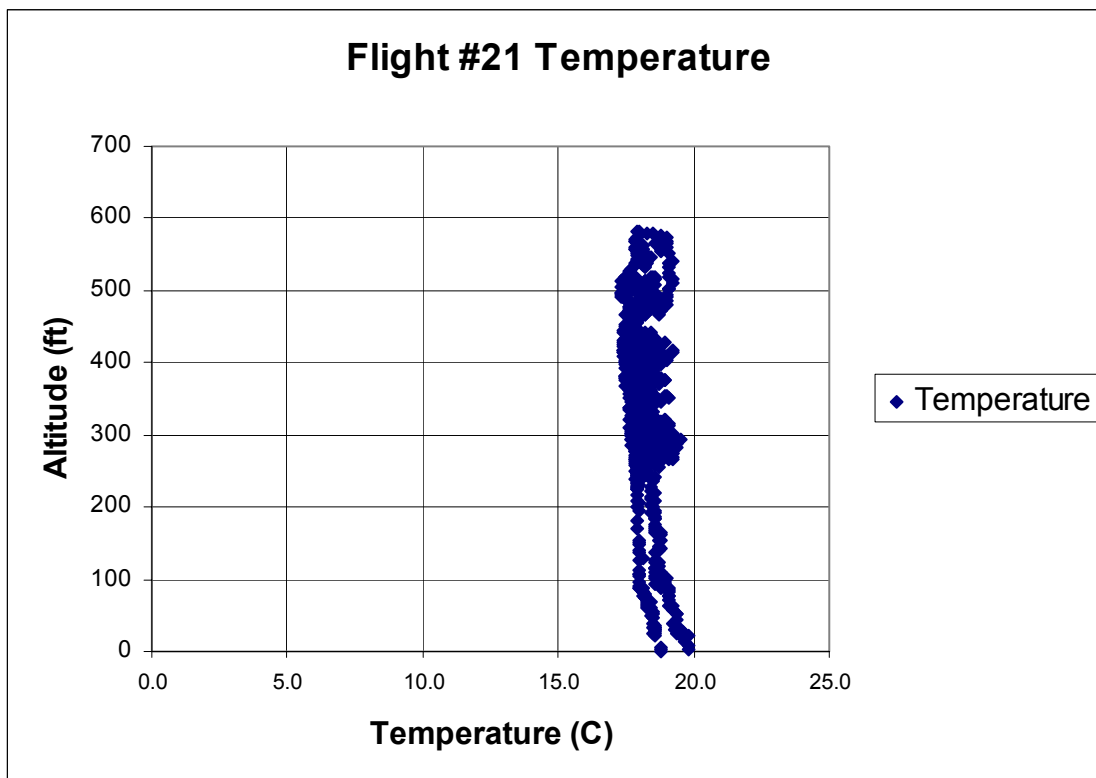


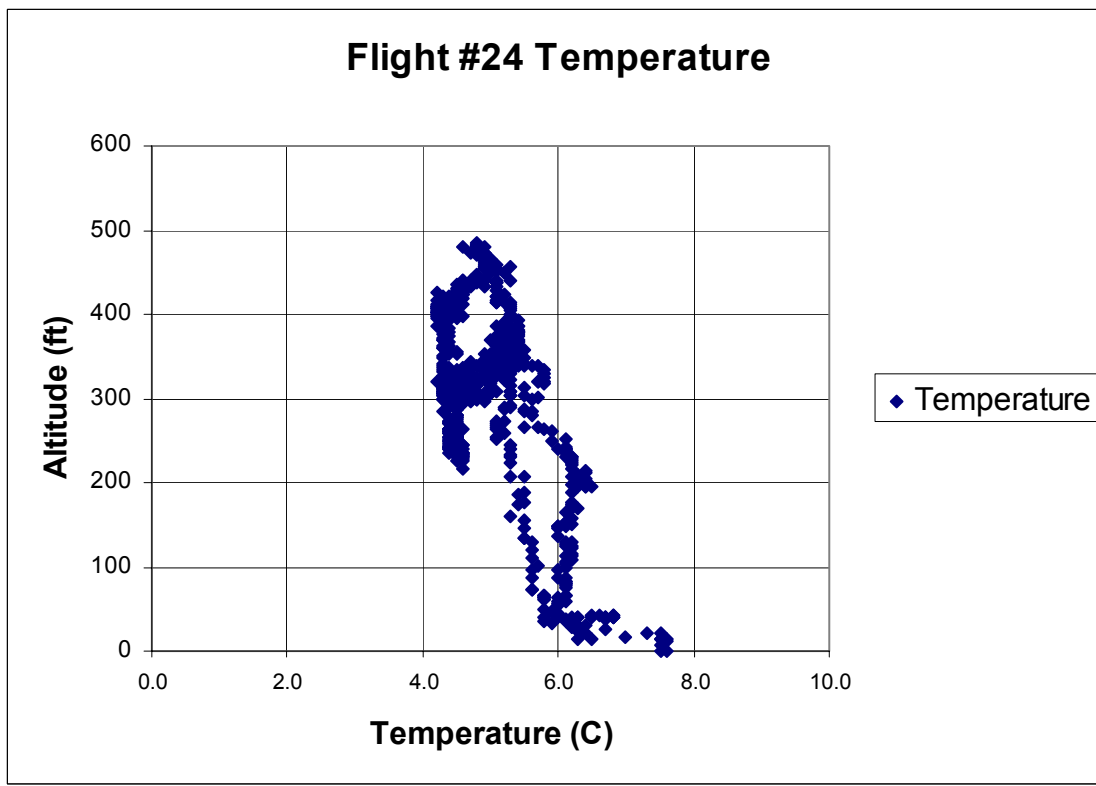
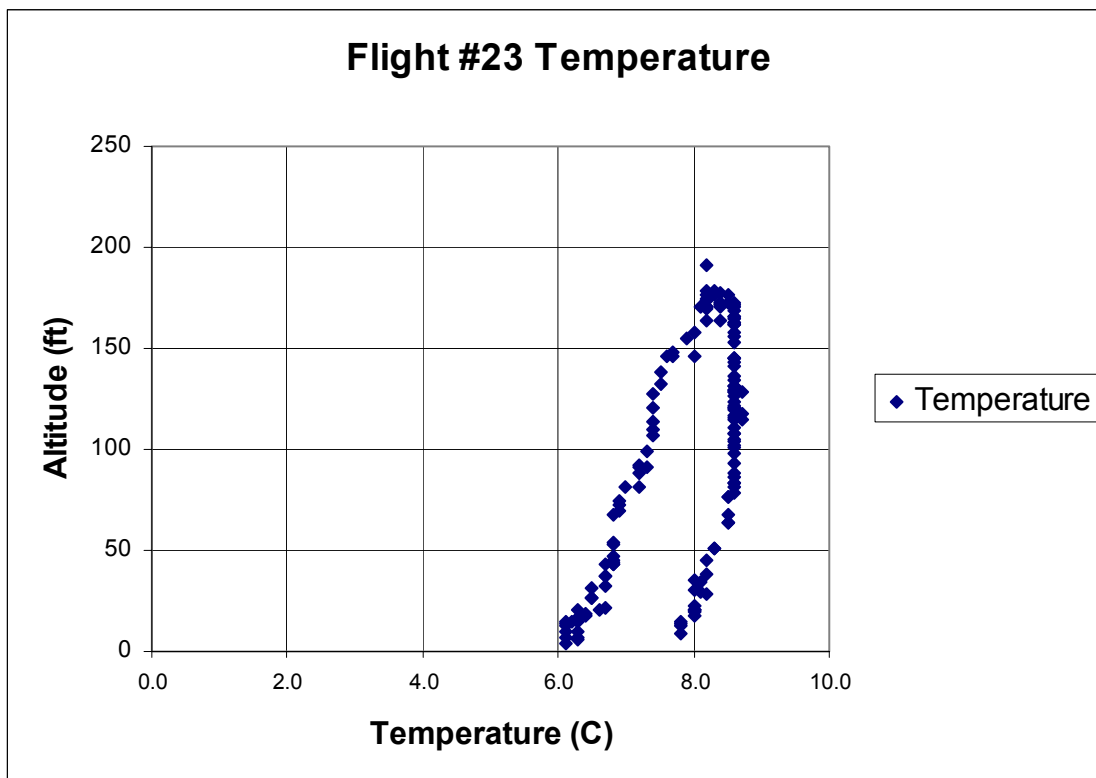


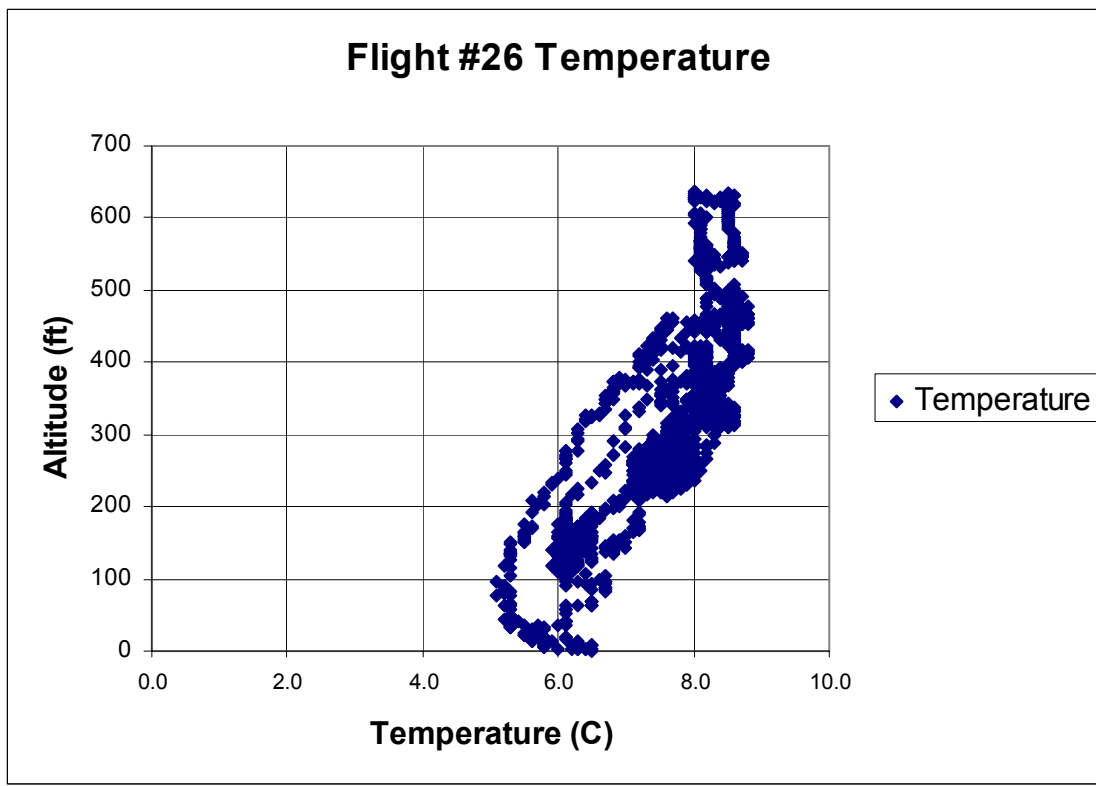
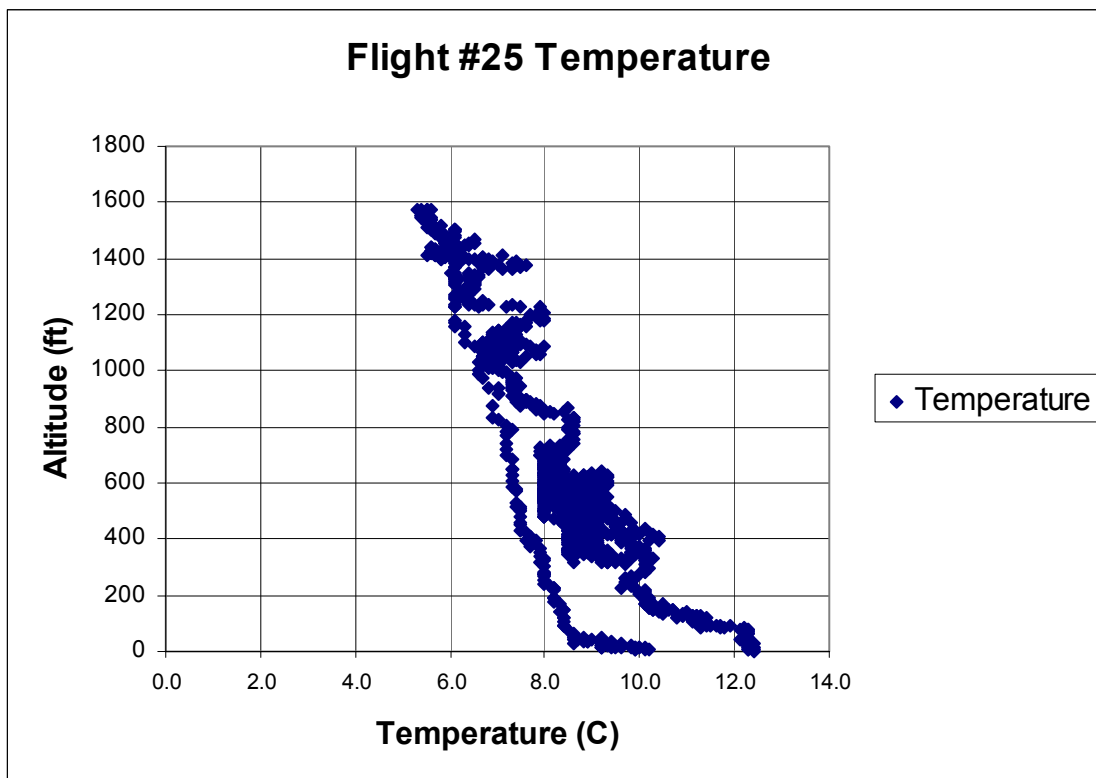


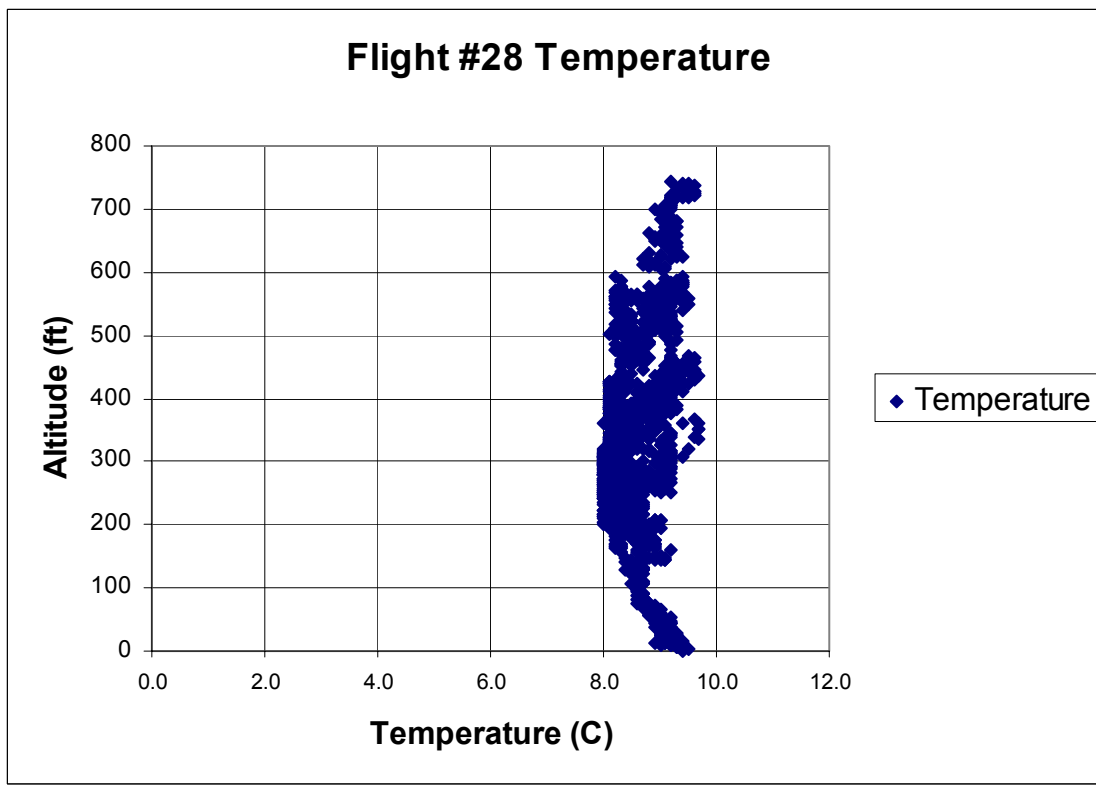
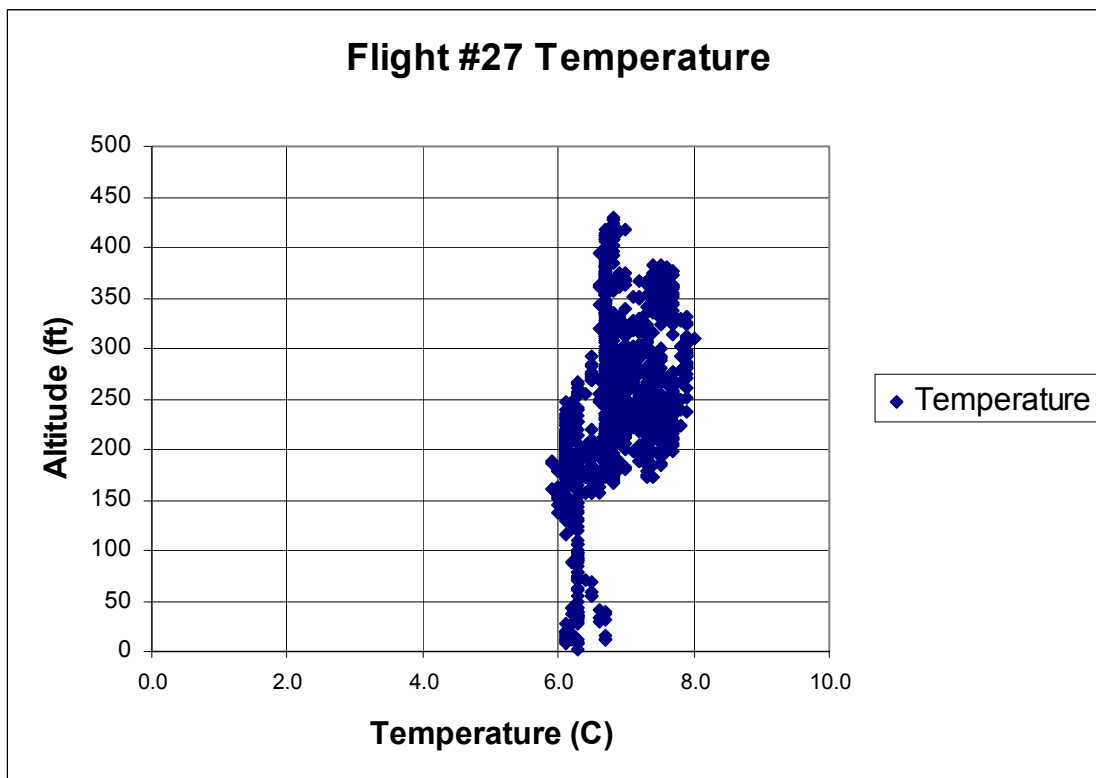




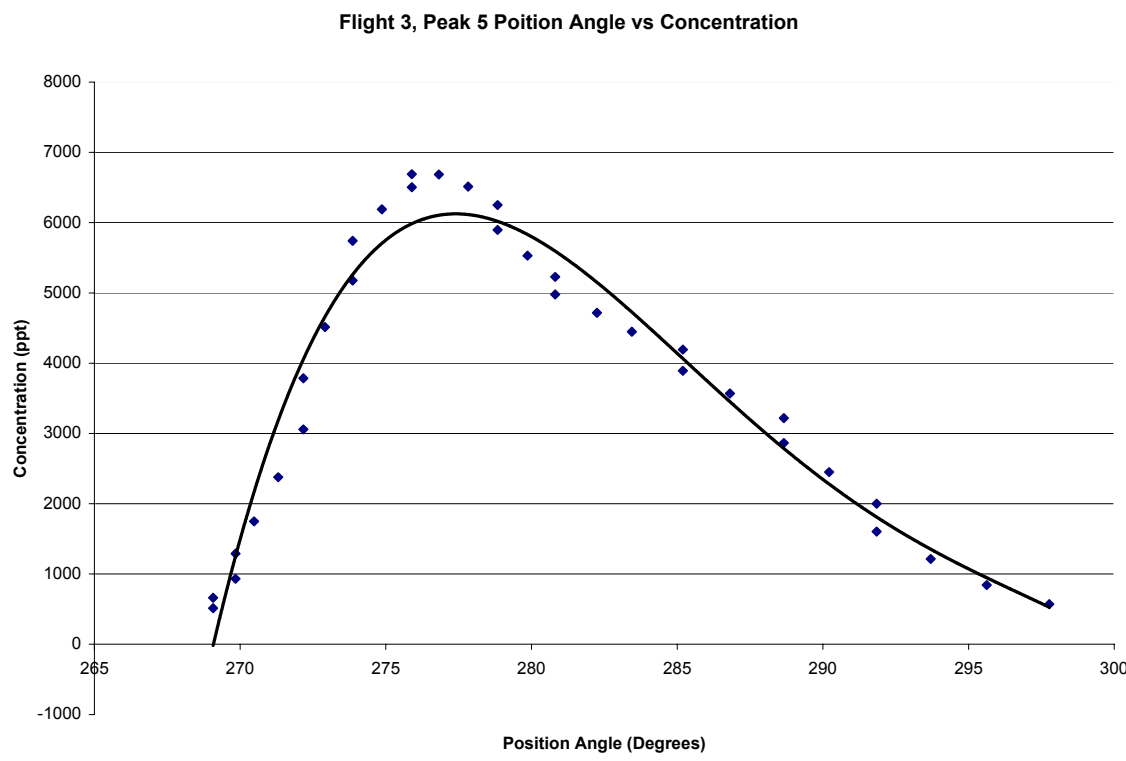
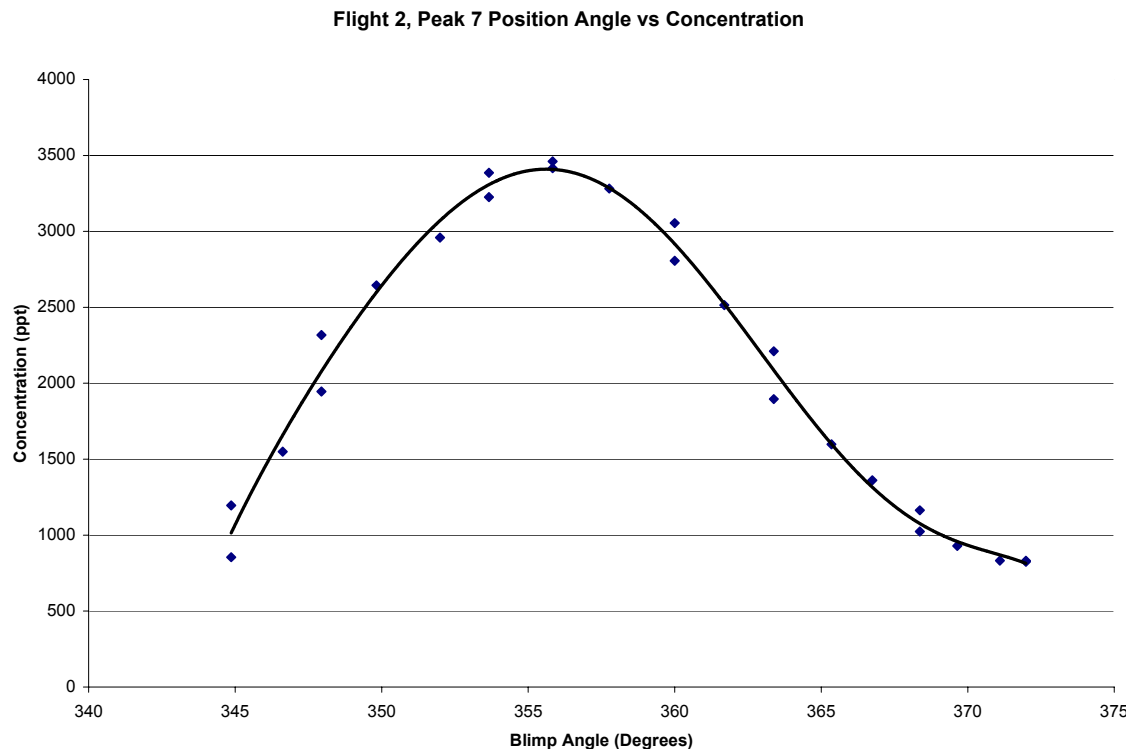


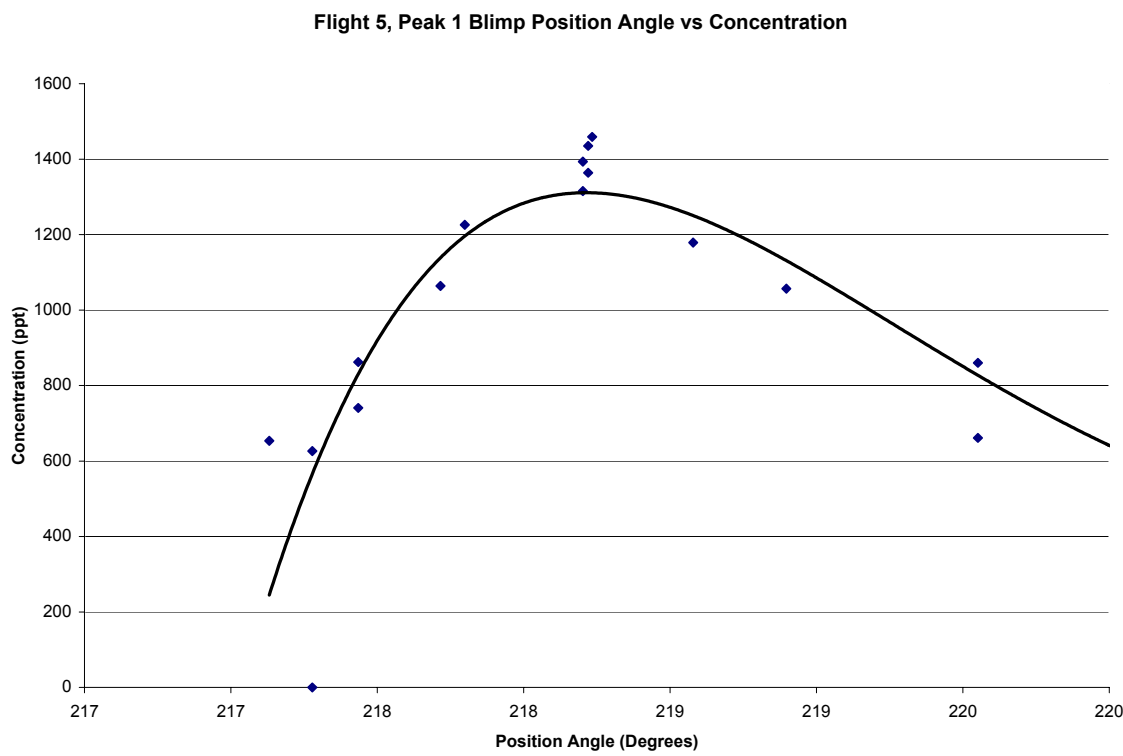
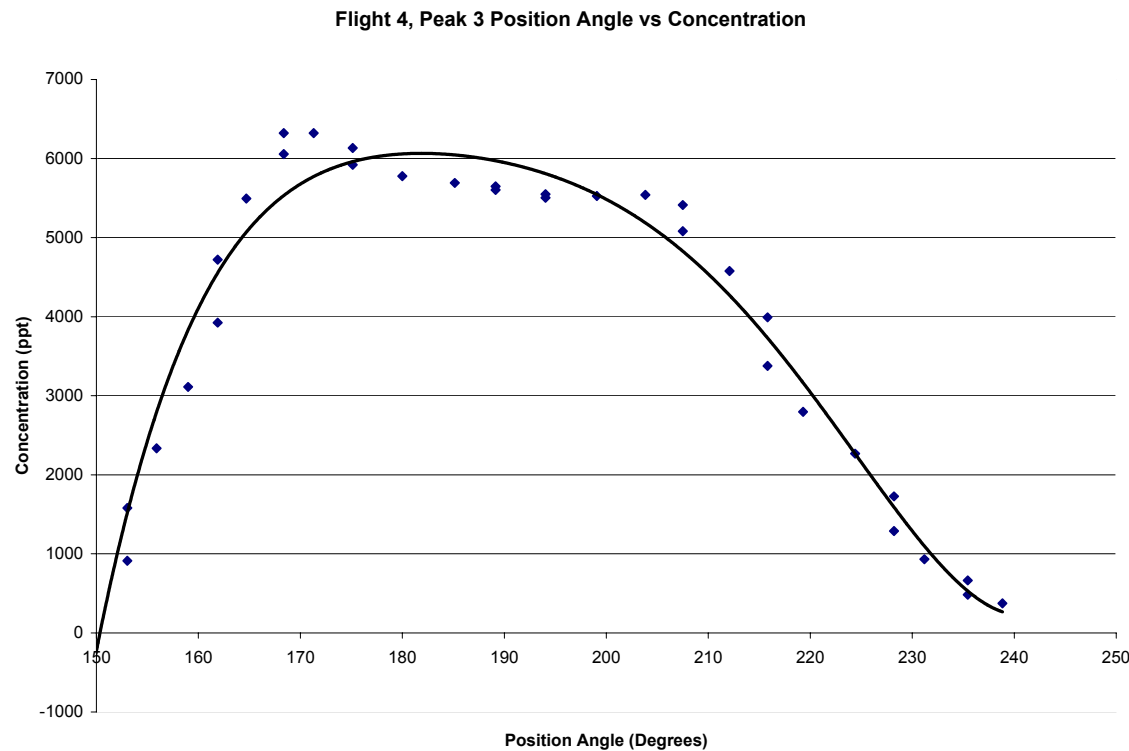


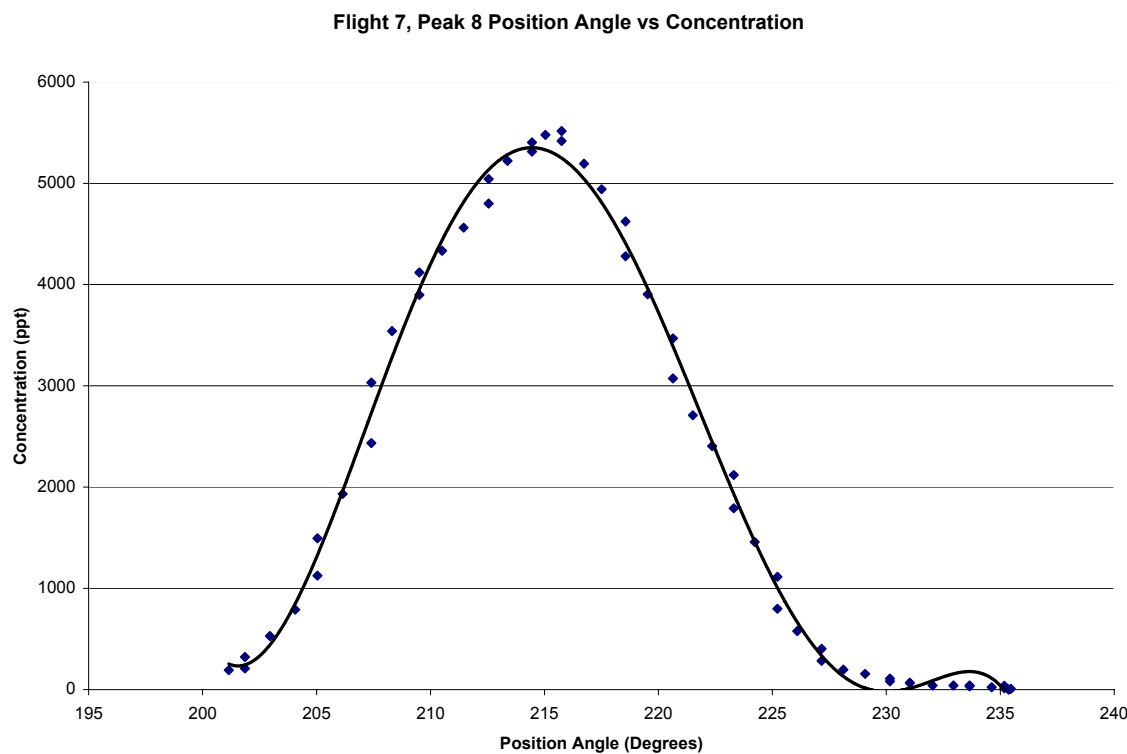
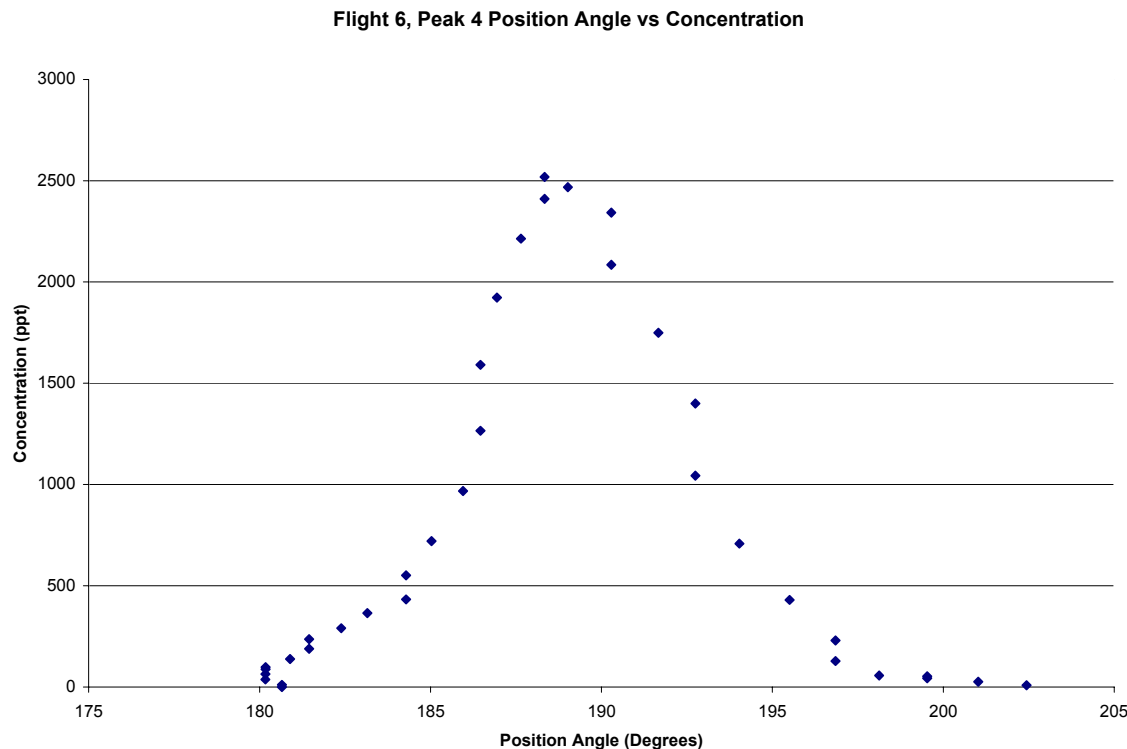


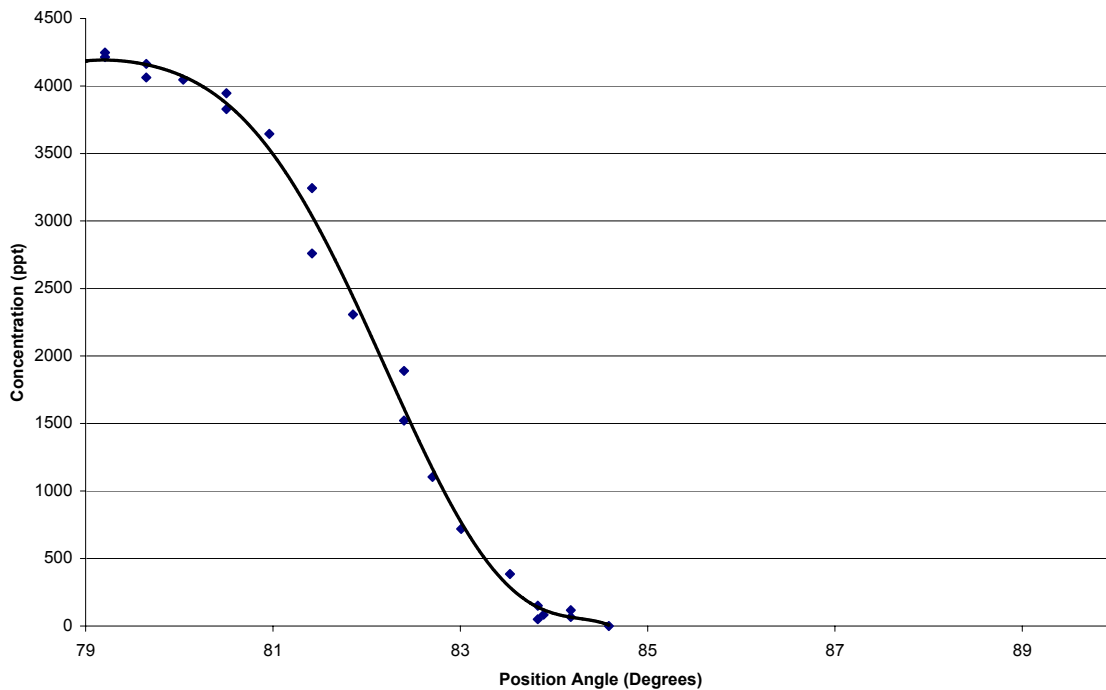
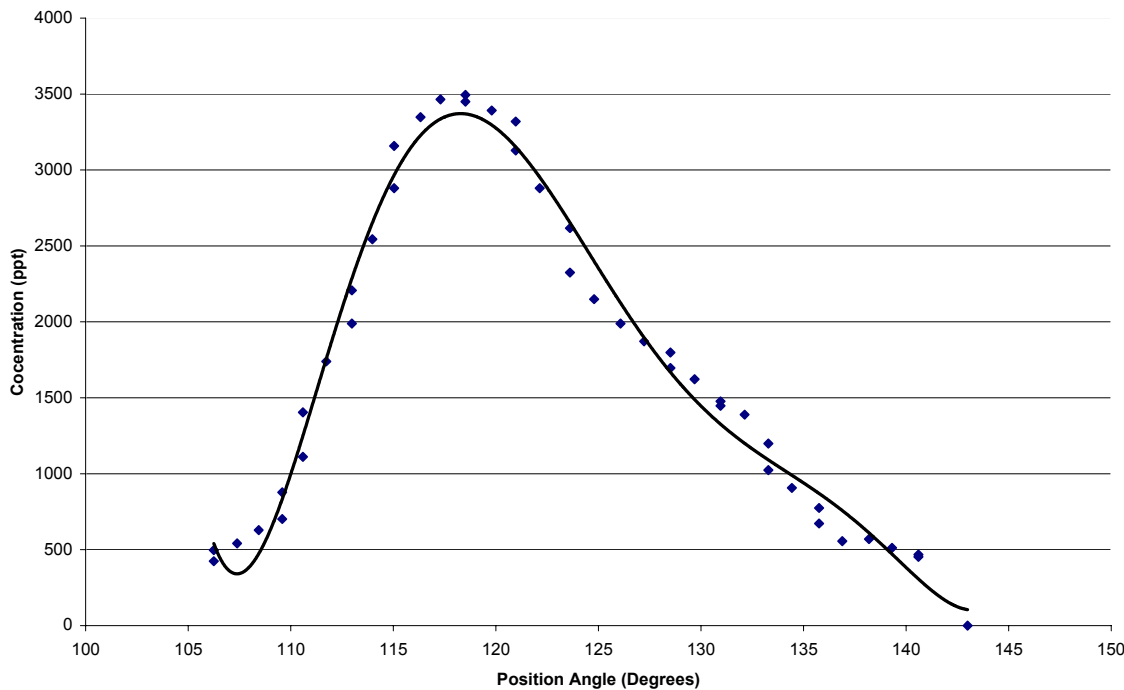


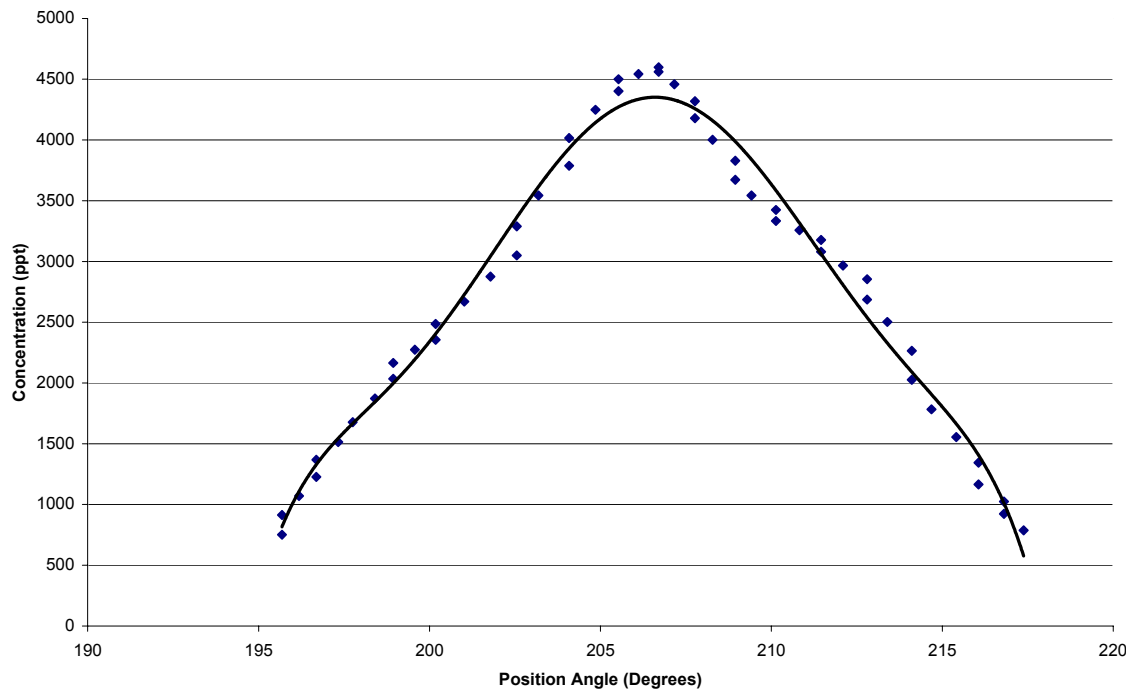
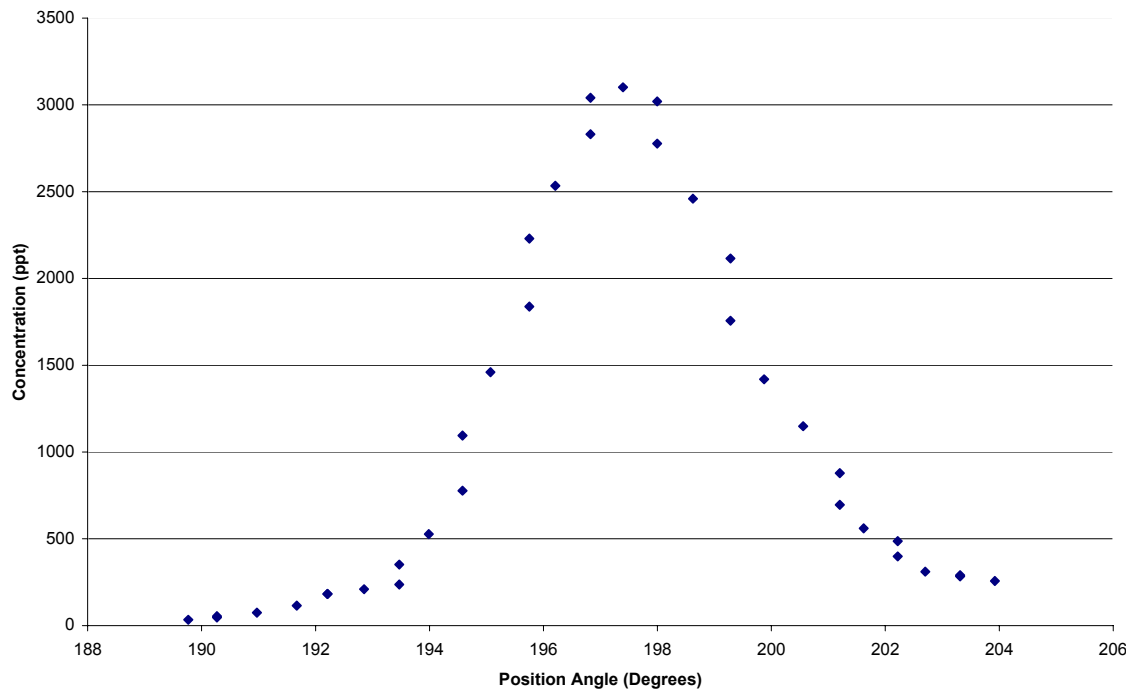
APPENDIX I
SIGMA-Y GRAPHS

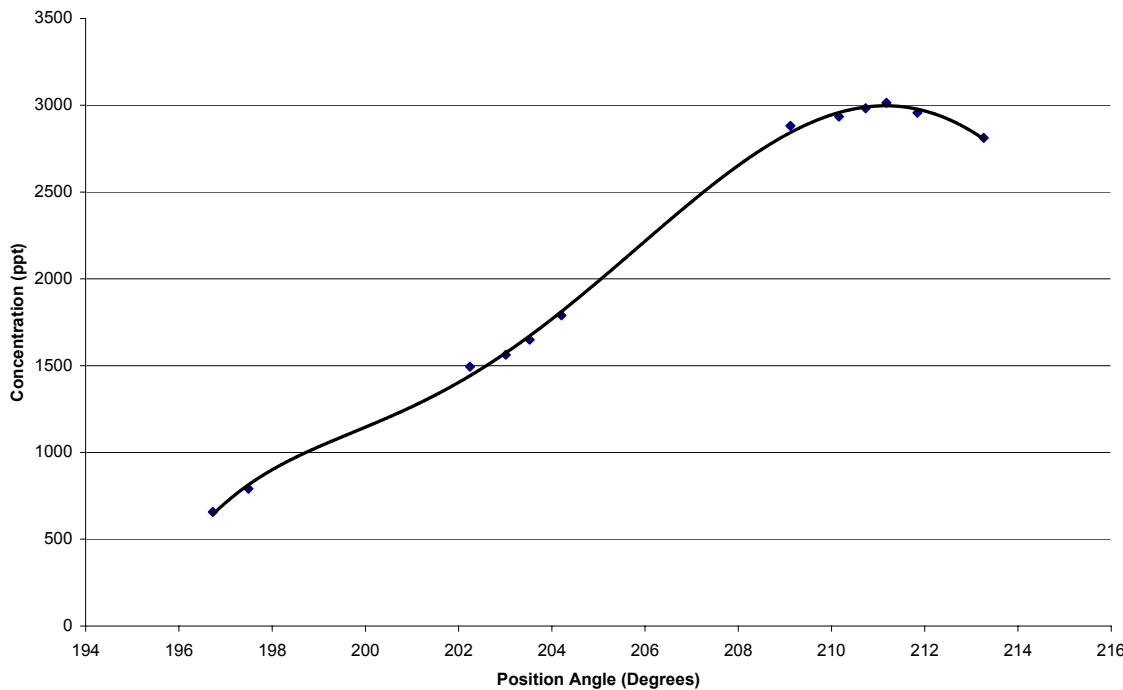
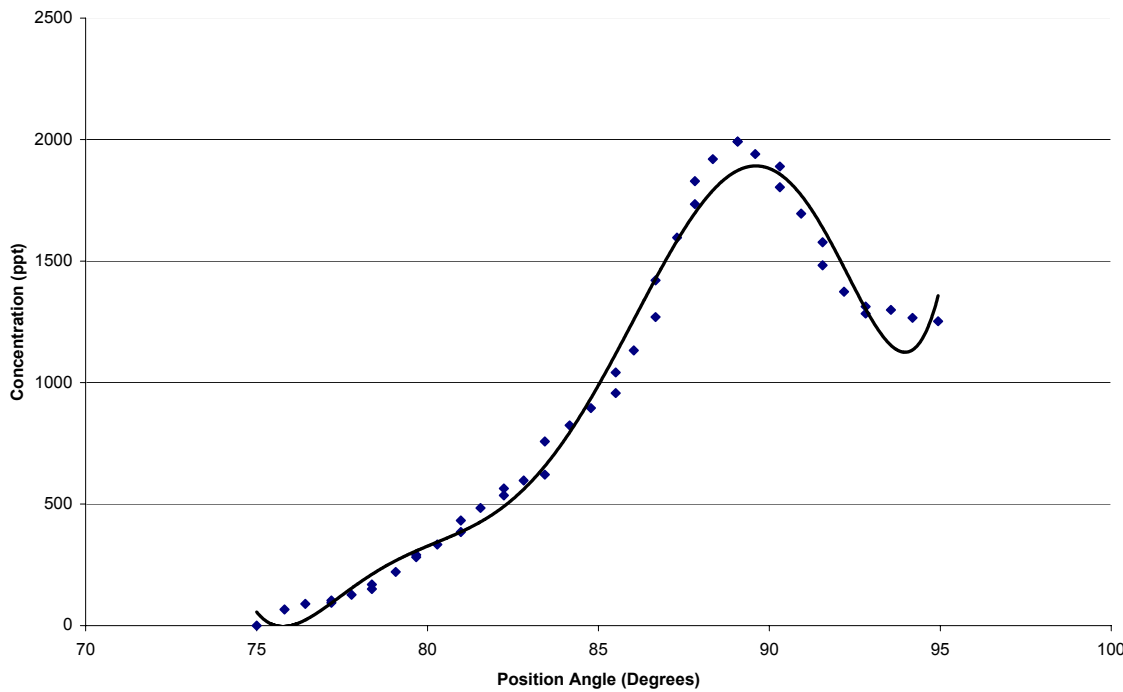


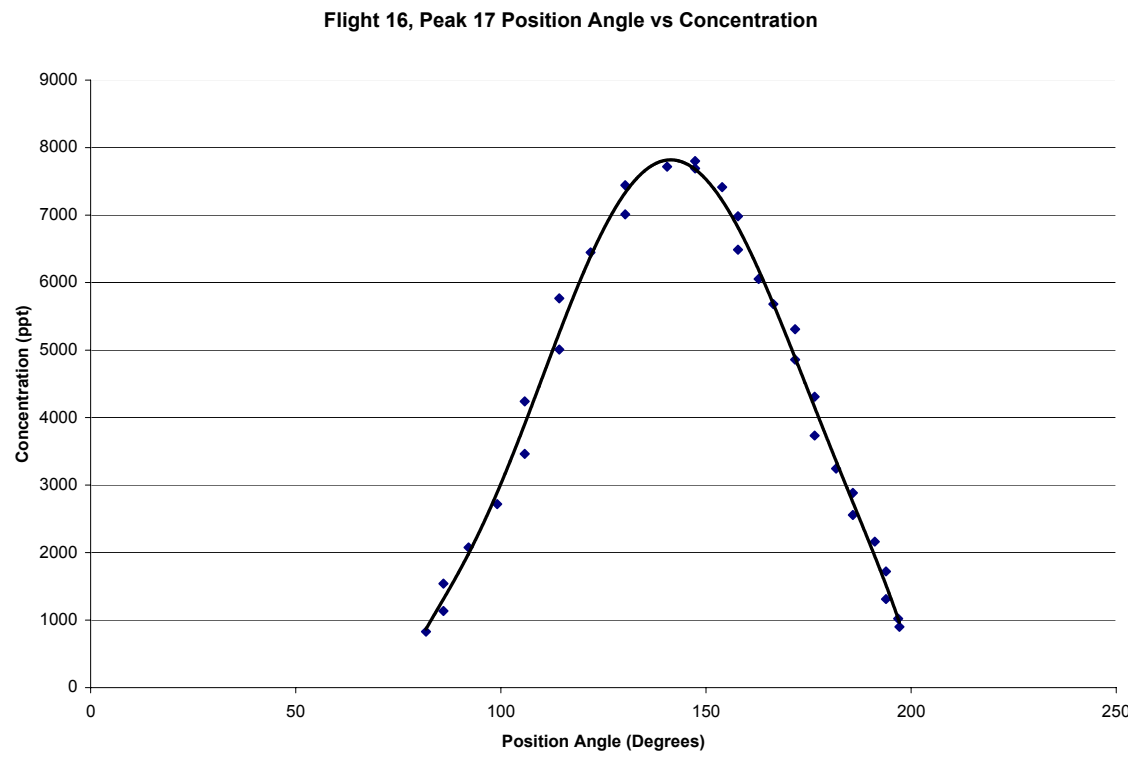
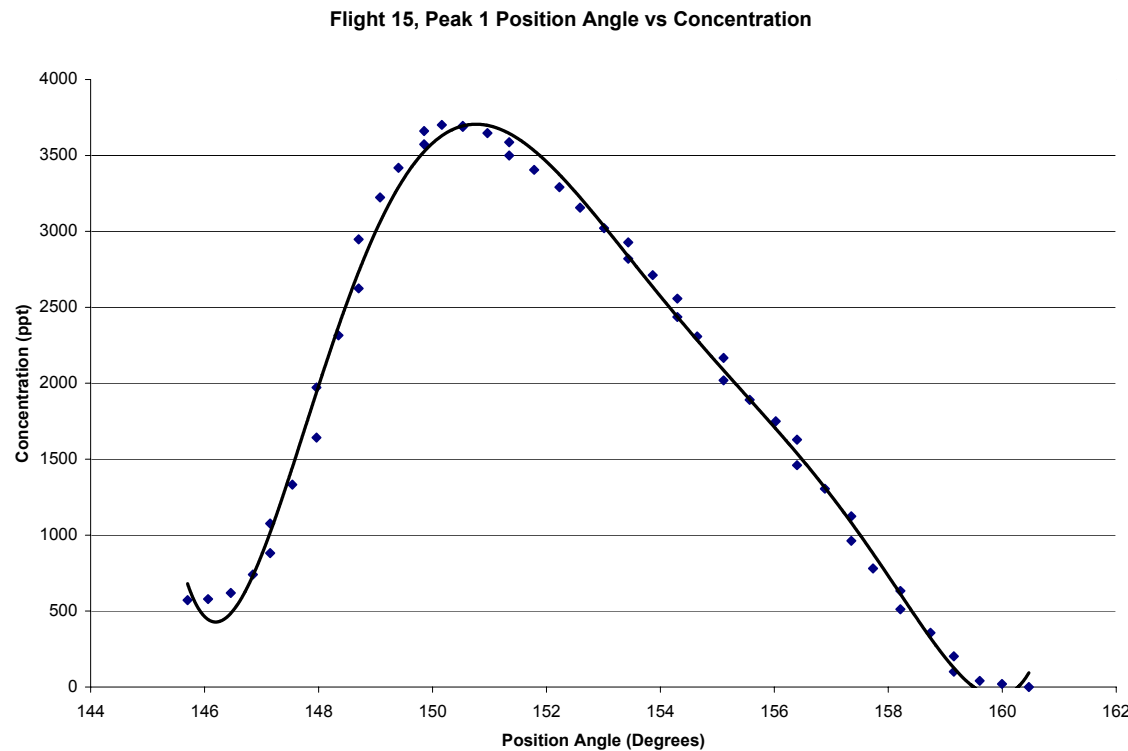


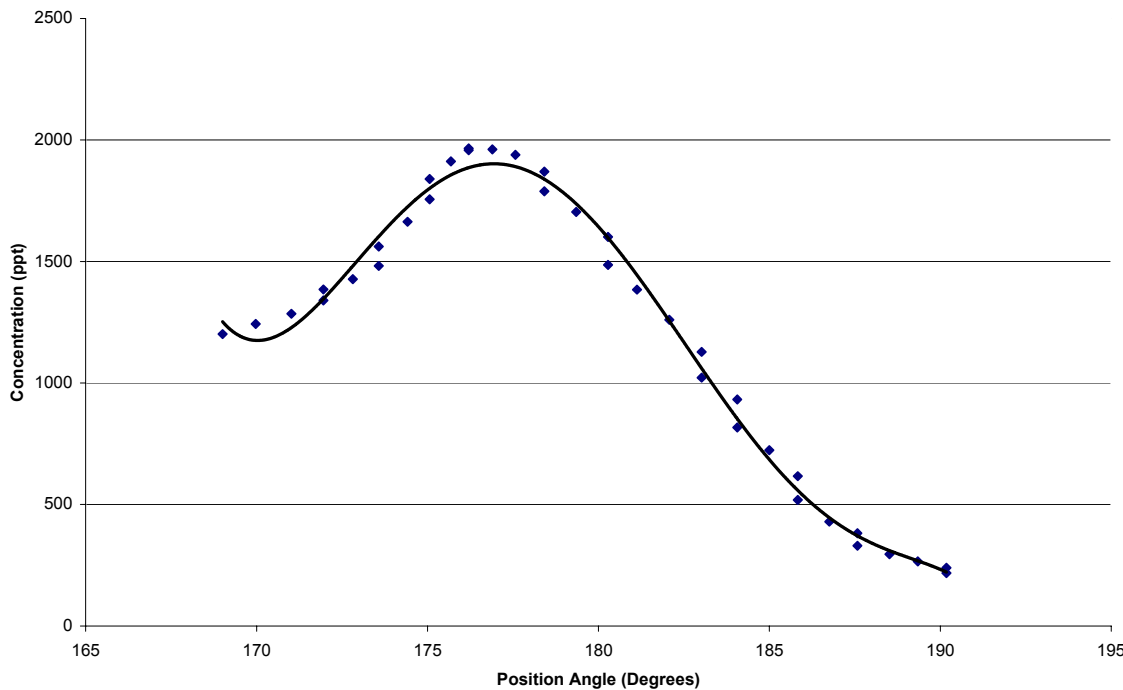
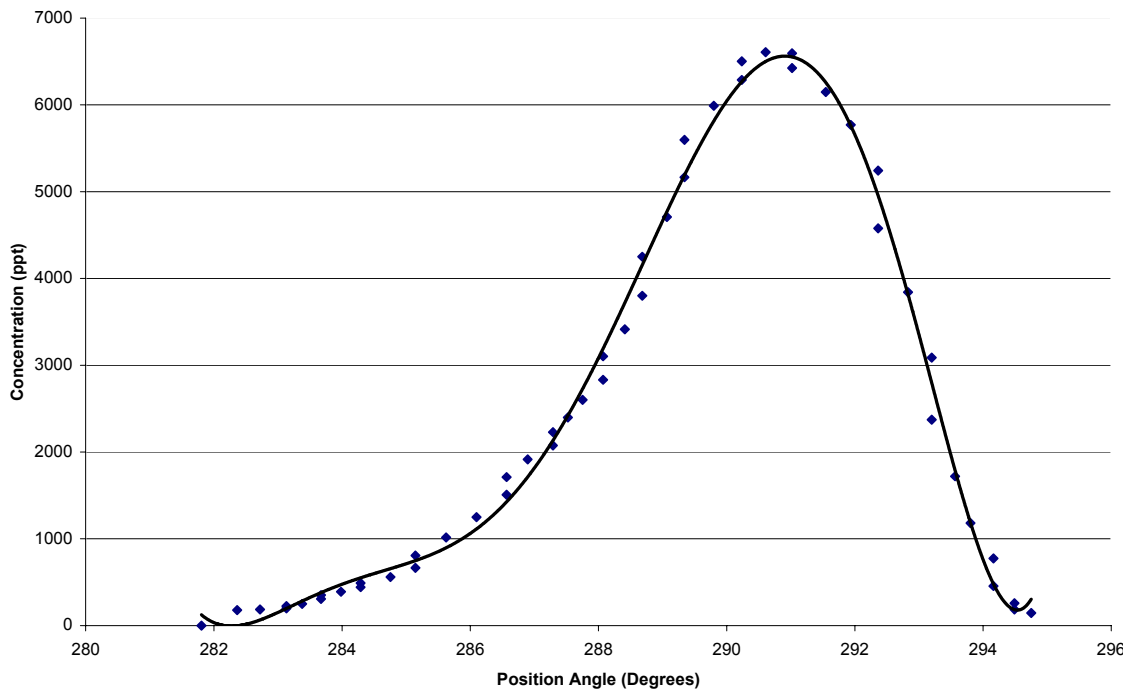


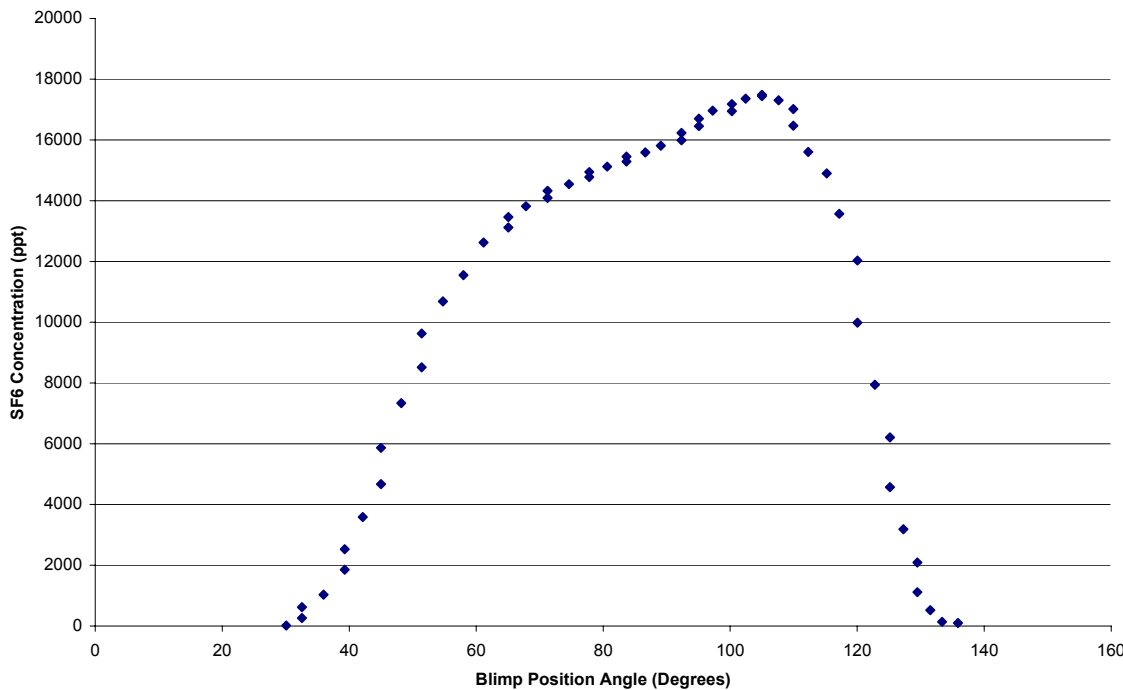
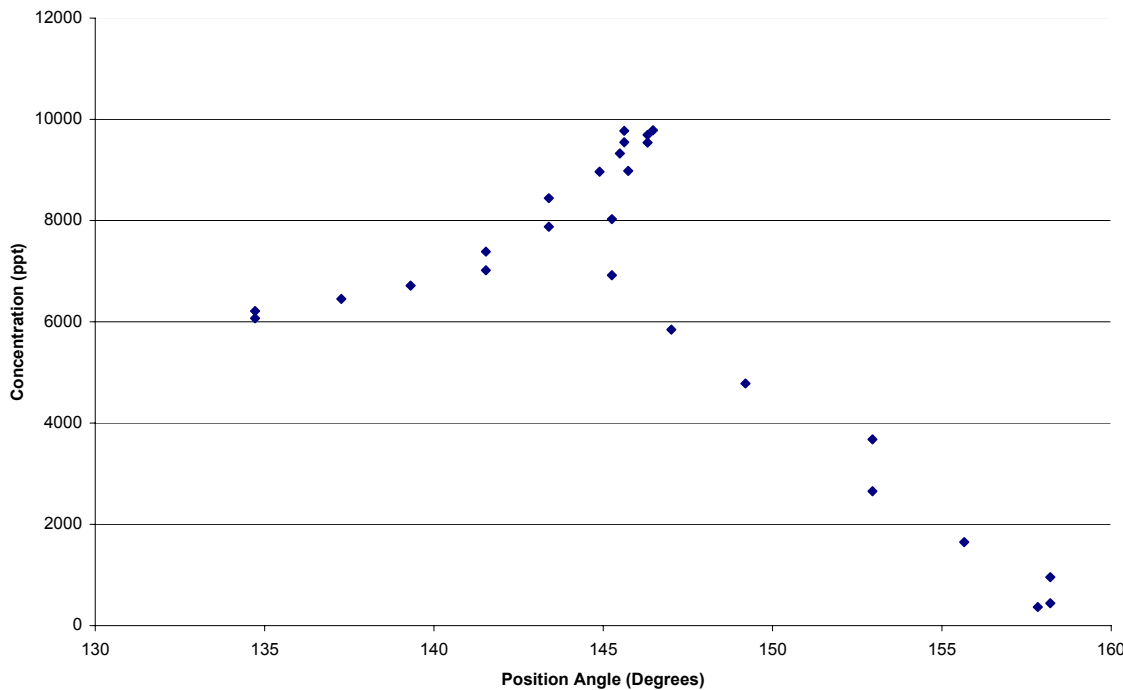
Flight 9, Peak 1 Position Angle vs Concentration**Flight 10, Peak 2 Position Angle vs Concentration**

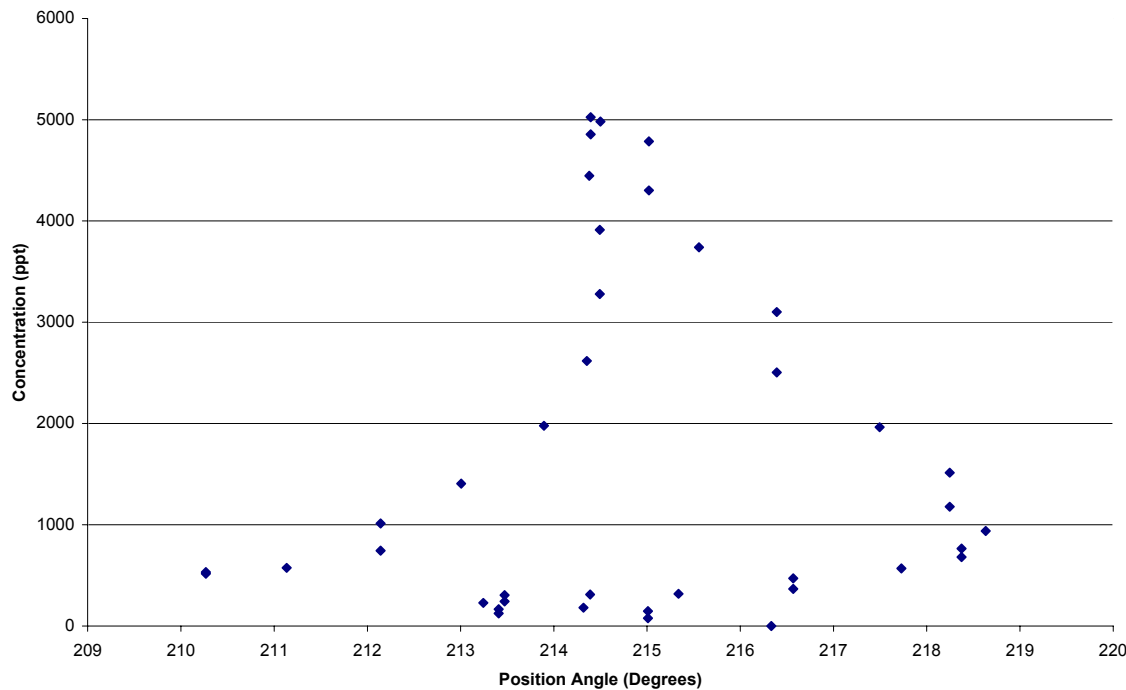
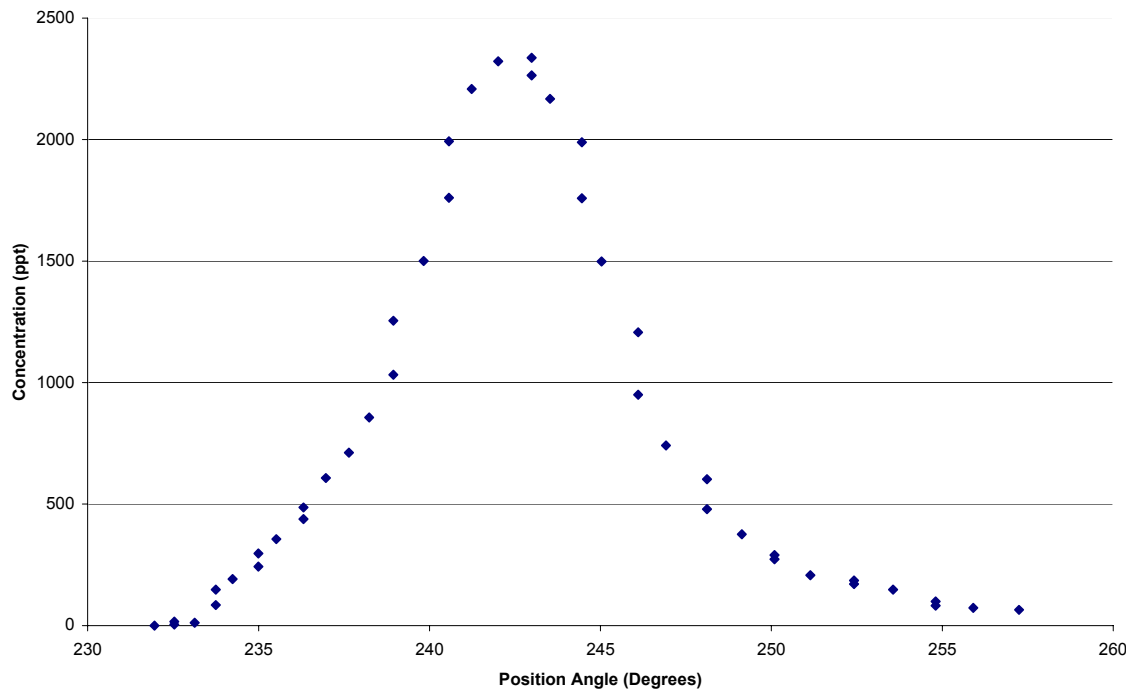
Flight 11, Peak 9 Position Angle vs Concentration**Flight 12, Peak 5 Position Angle vs Concentration**

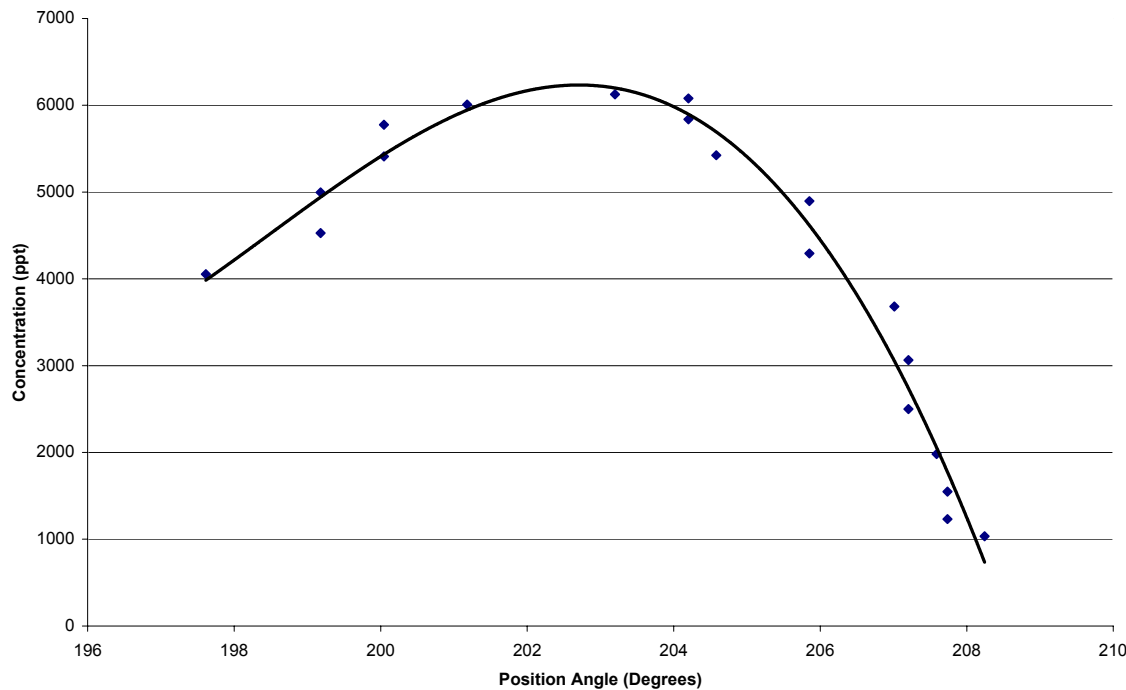
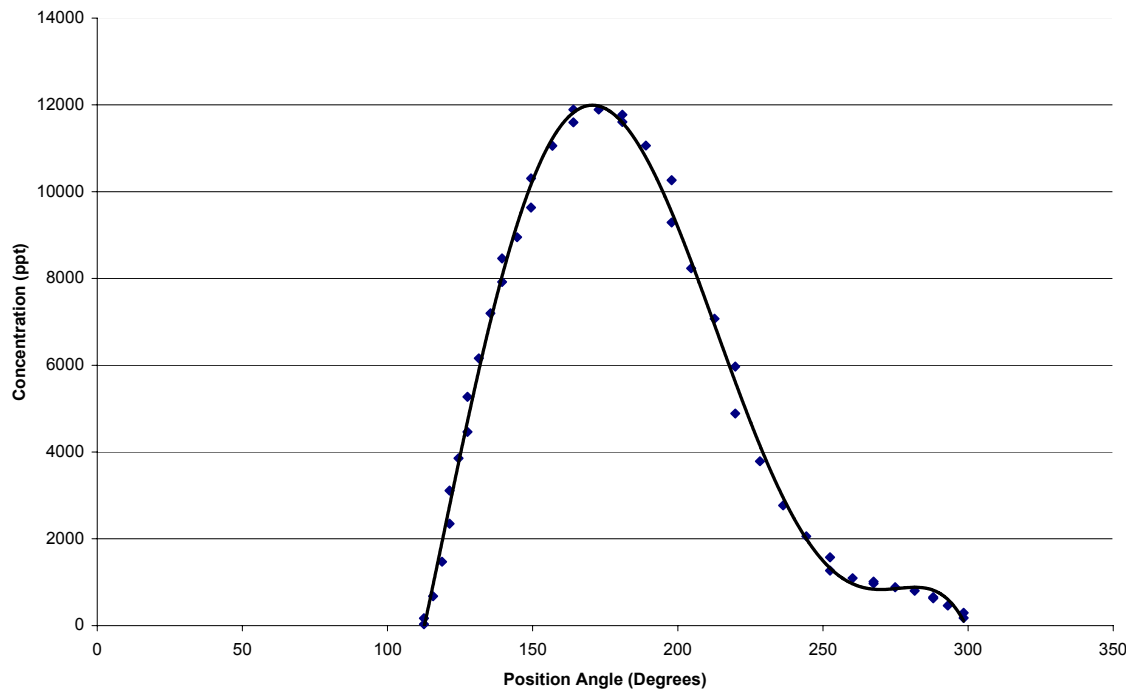
Flight 13, Peak2 Position Angle vs Concentration**Flight 14, Peak 2 Position Angle vs Concentration**

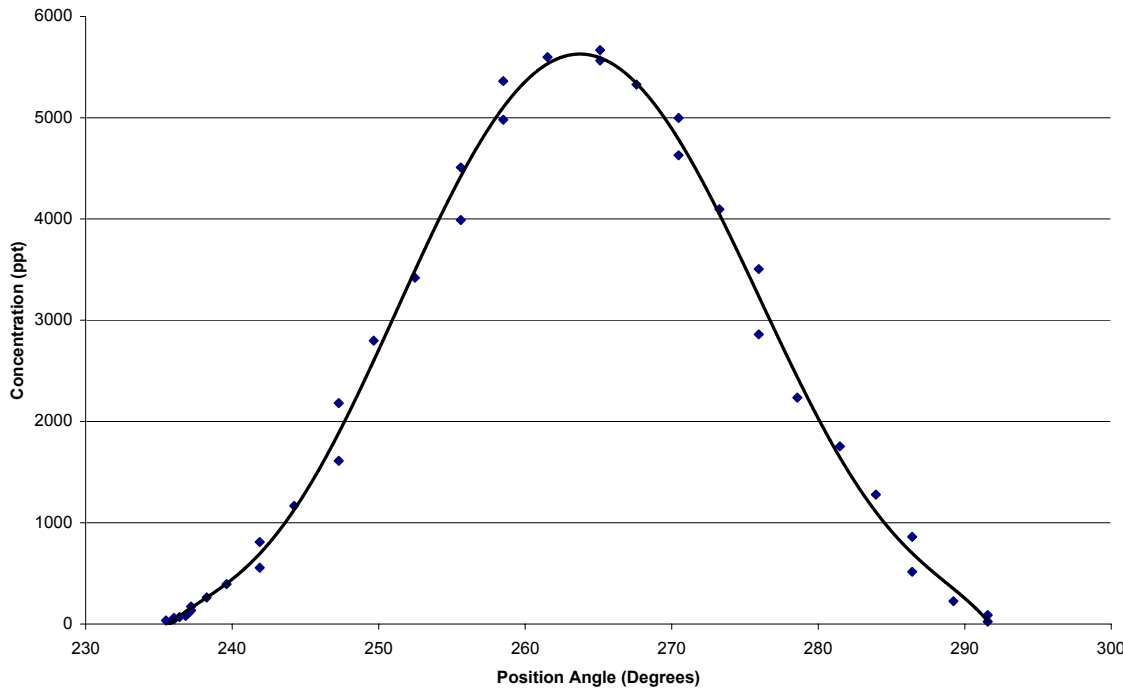
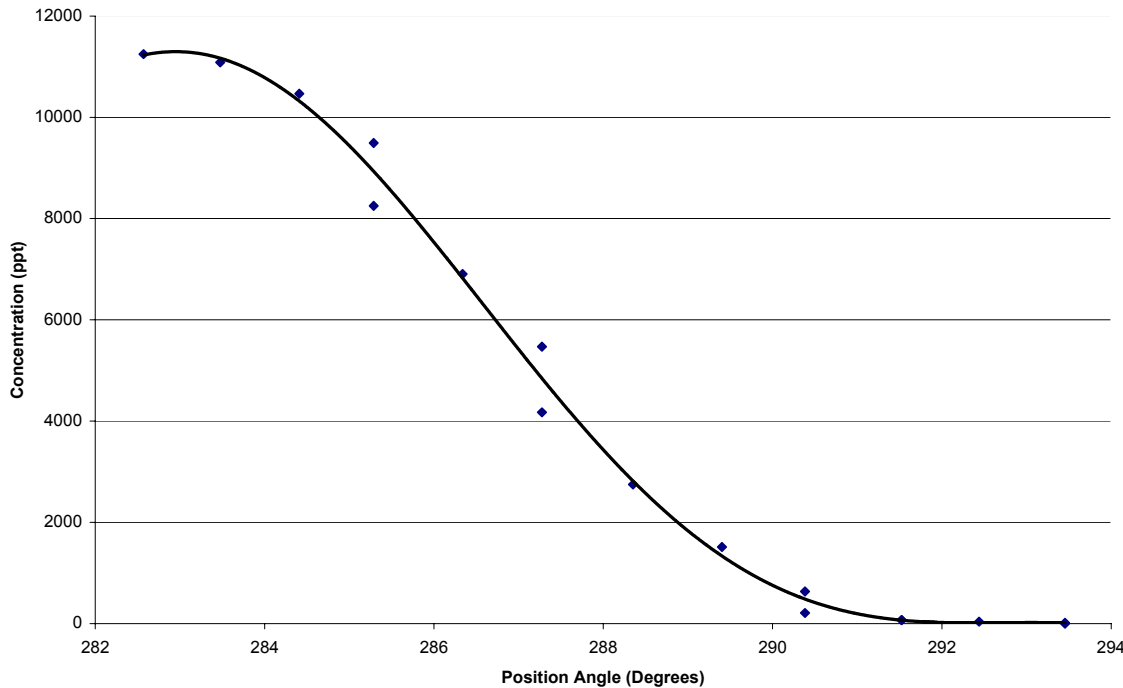


Flight 17, Peak 9 Position Angle vs Concentration**Flight 18, Peak 5 Position Angle vs Concentration**

Flight 19, Peak 1 Blimp Position Angle vs Tracer Concentration**Flight 20, Peak 5 Position Angle vs. Concentration**

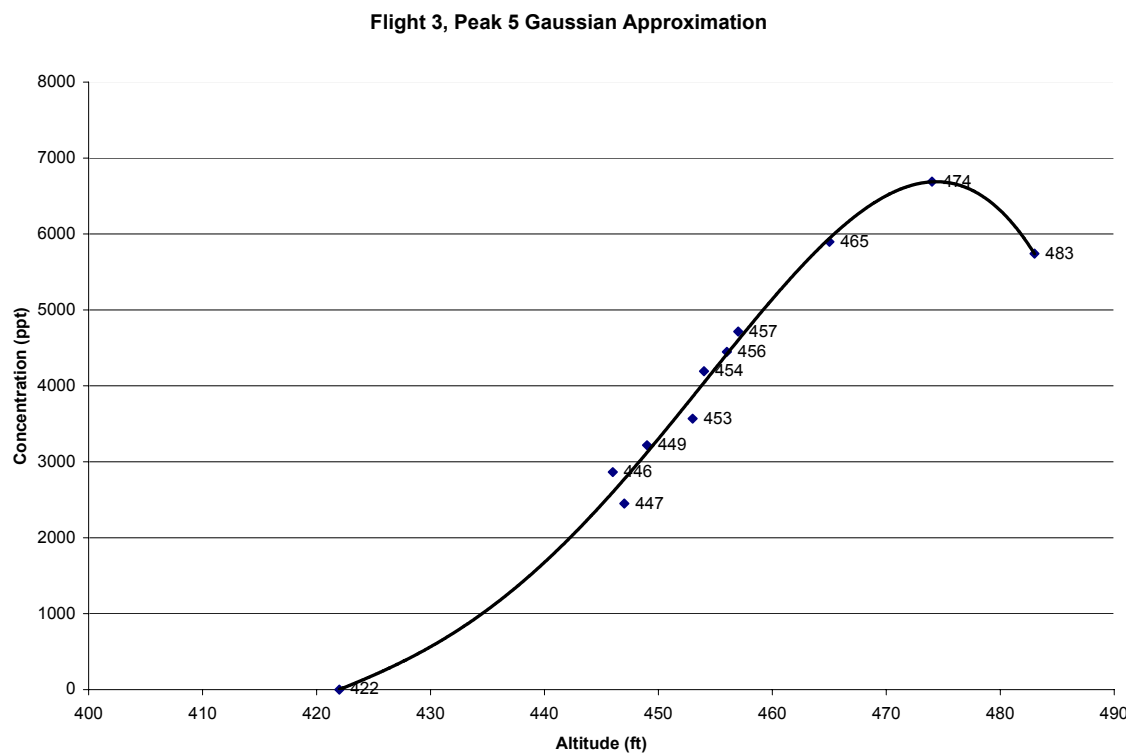
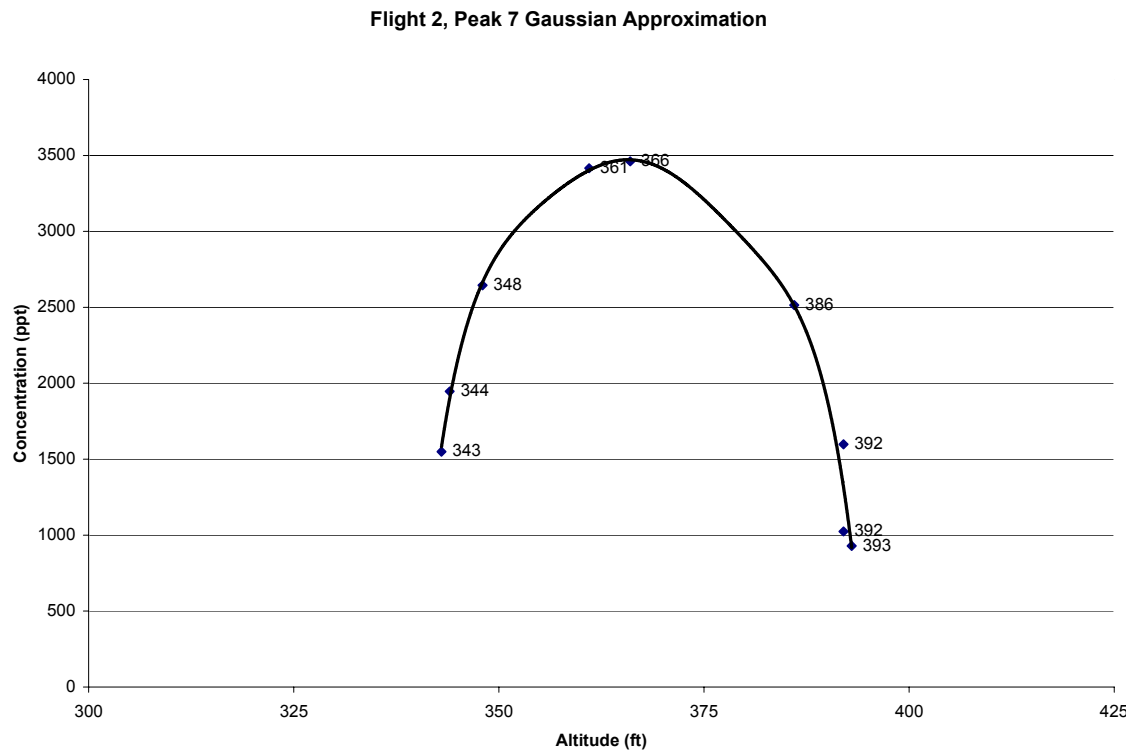
Flight 21, Peak 4 Position Angle vs Concentration**Flight 24, Peak 1 Position Angle vs Concentration**

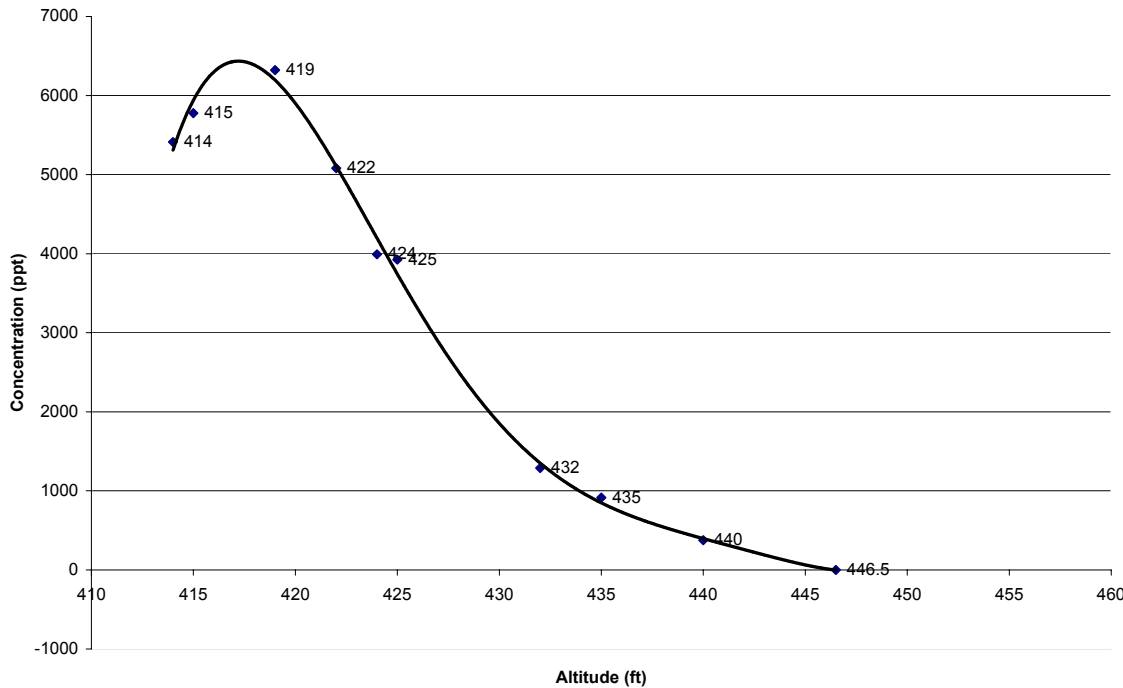
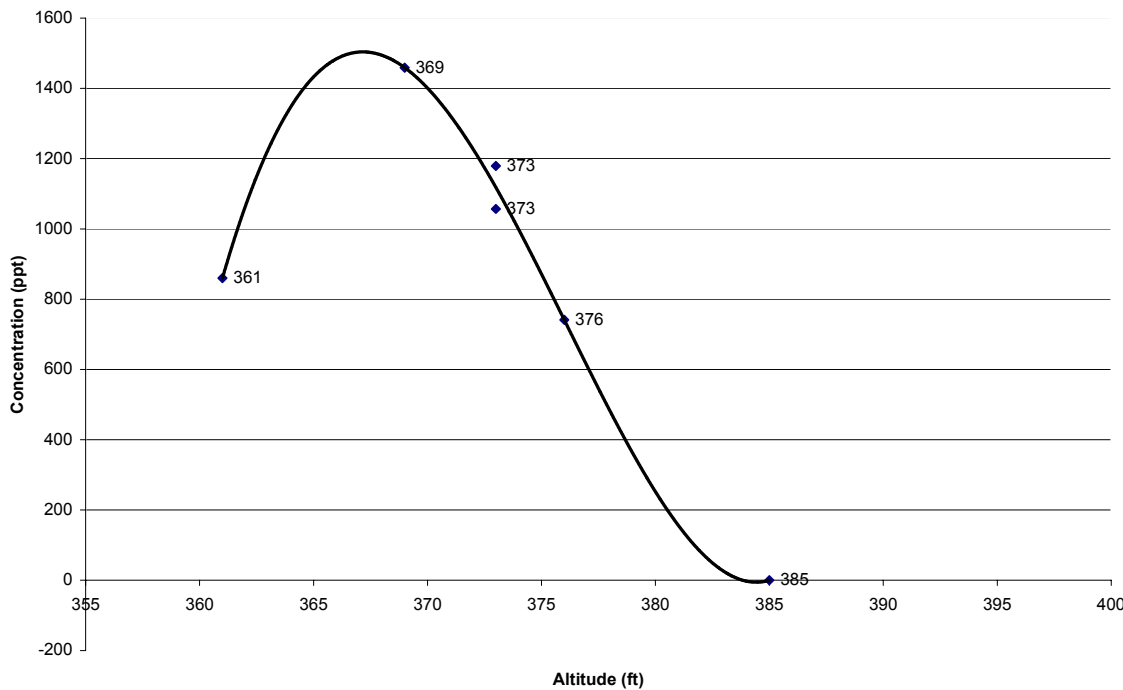
Flight 25, Peak 4 Position Angle vs Concentration**Flight 26, Peak 4 Position Angle vs Concentration**

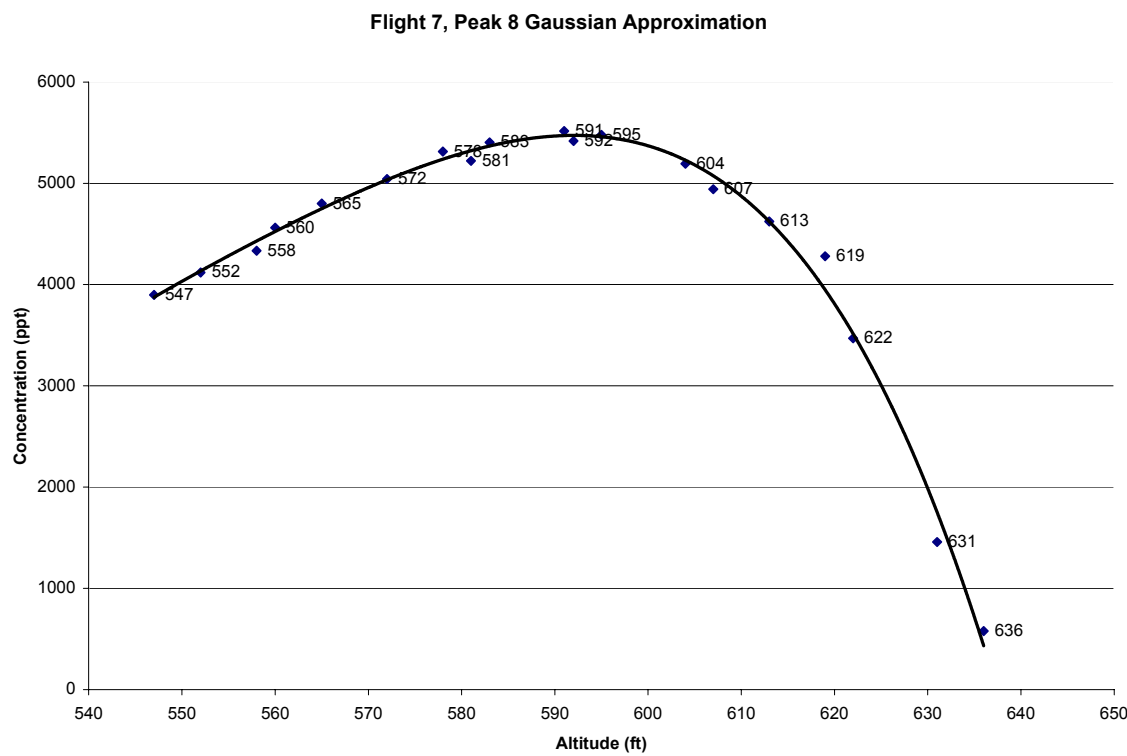
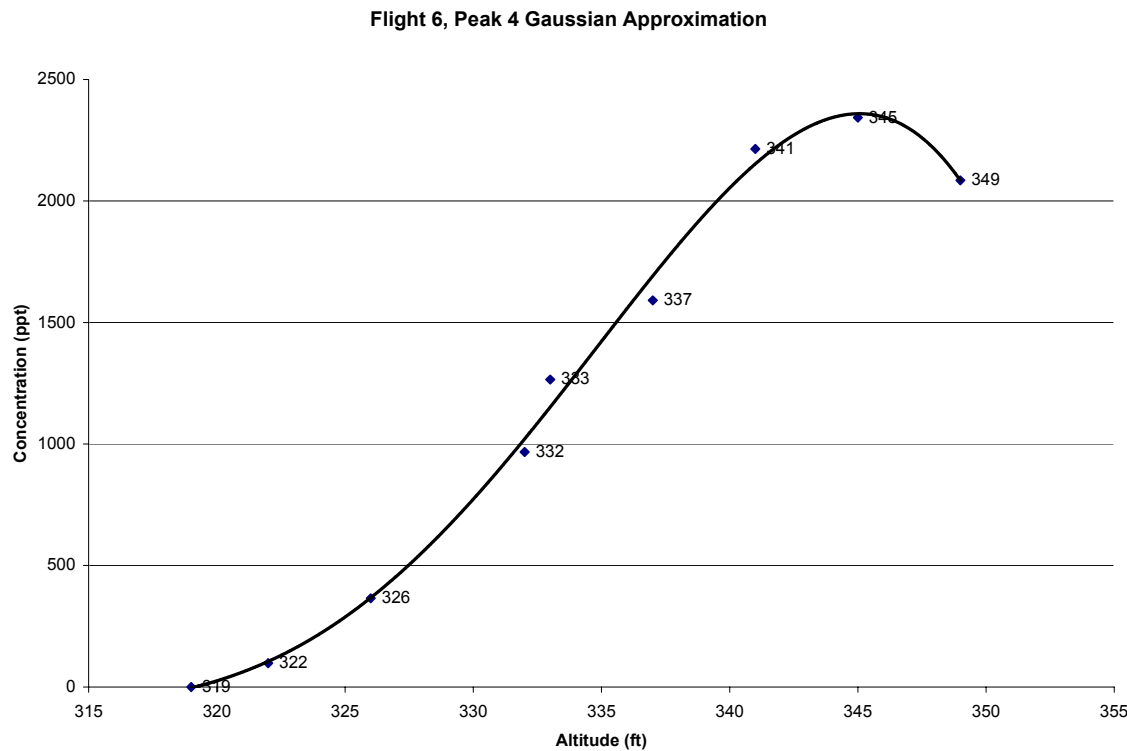
Flight 27, Peak 1 Position Angle vs Concentration**Flight 28, Peak 3 Position Angle vs Concentration**

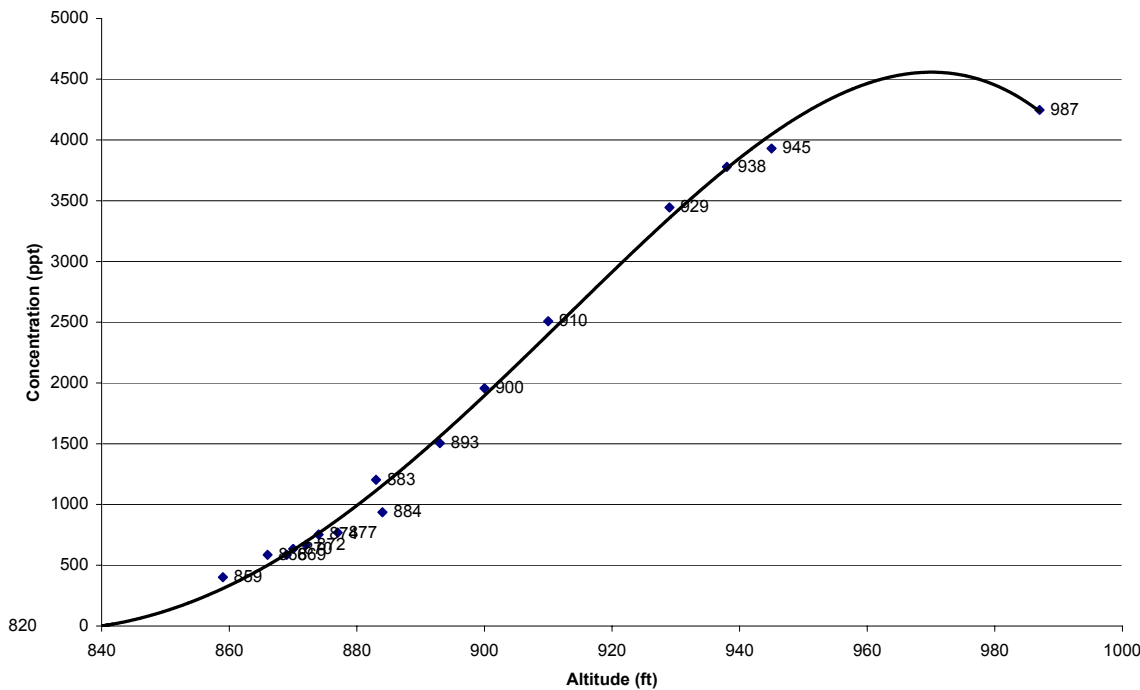
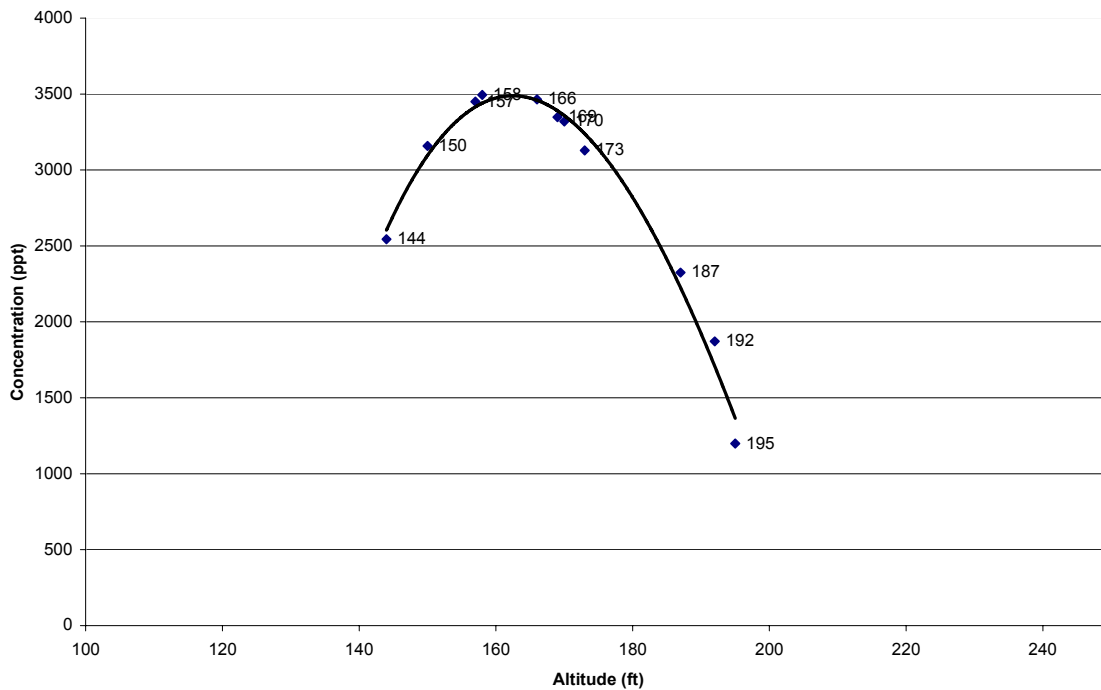
APPENDIX J

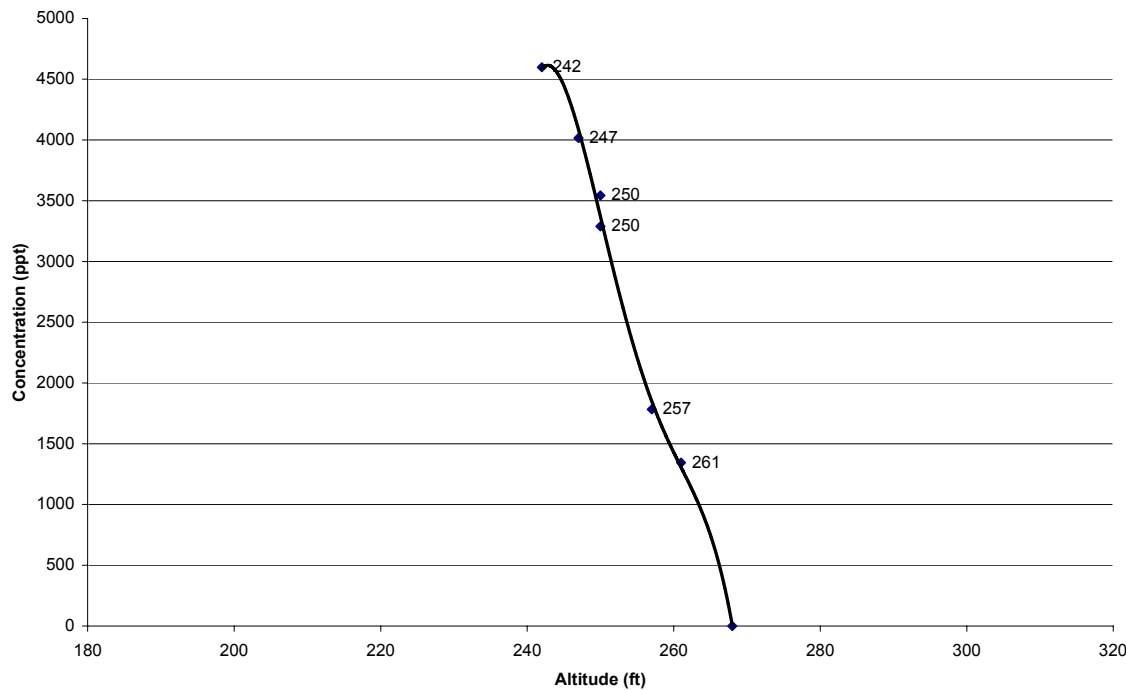
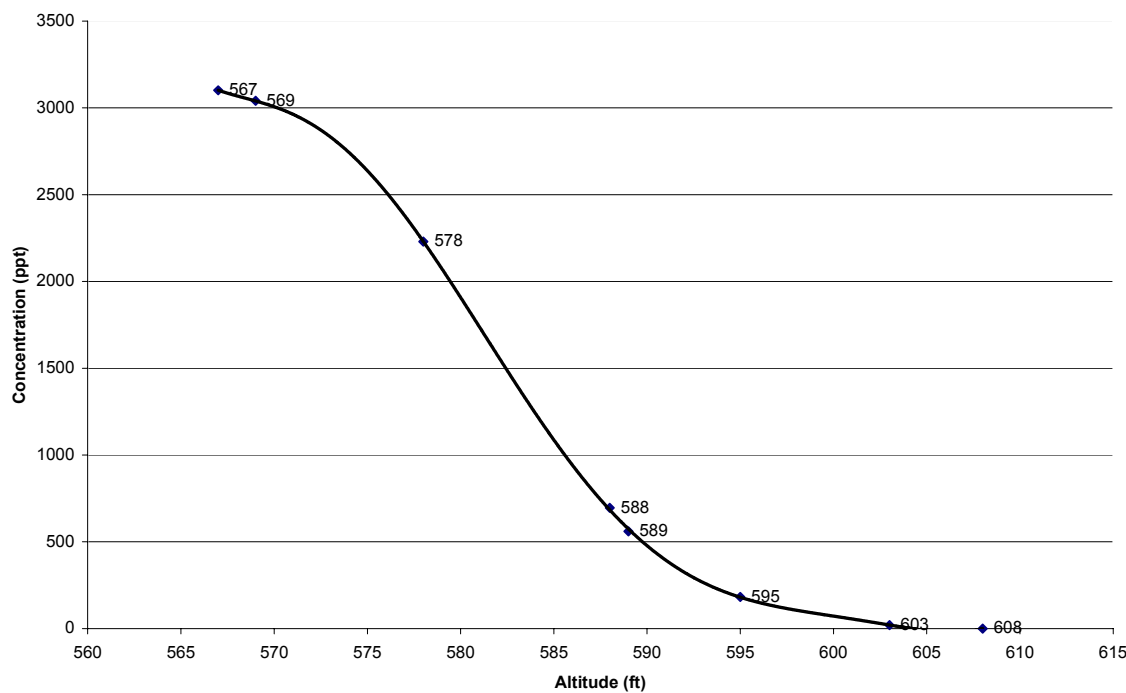
SIGMA-Z GRAPHS



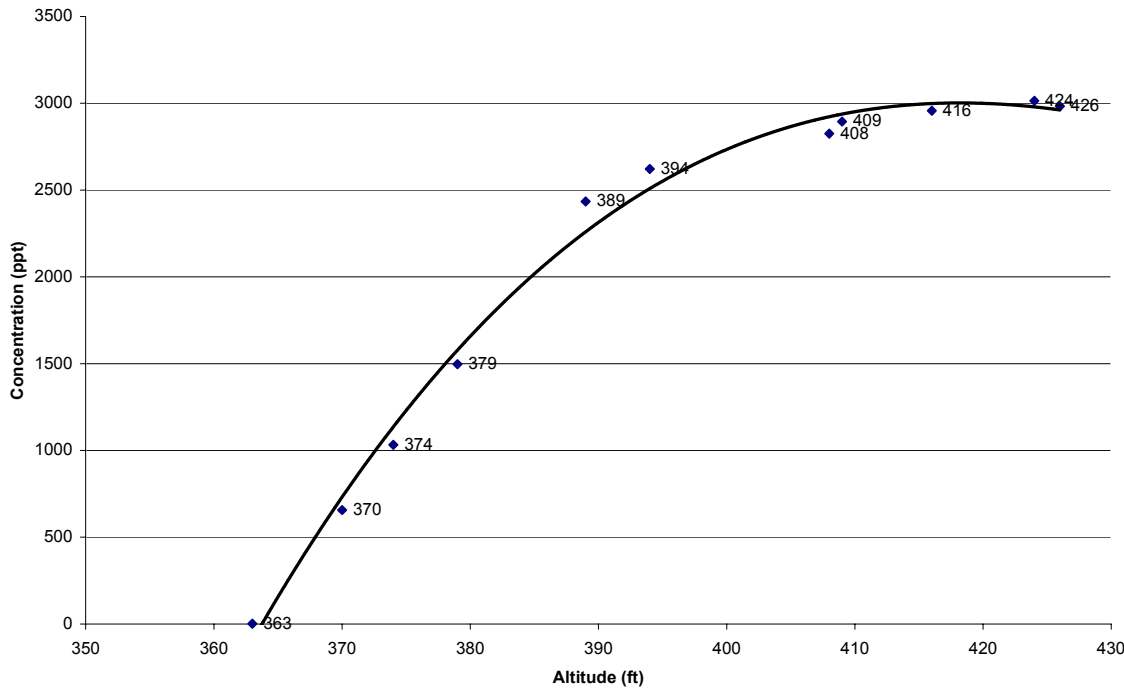
Flight 4, Peak 3 Gaussian Approximation**Flight 5 Peak 1 Gaussian Approximation**



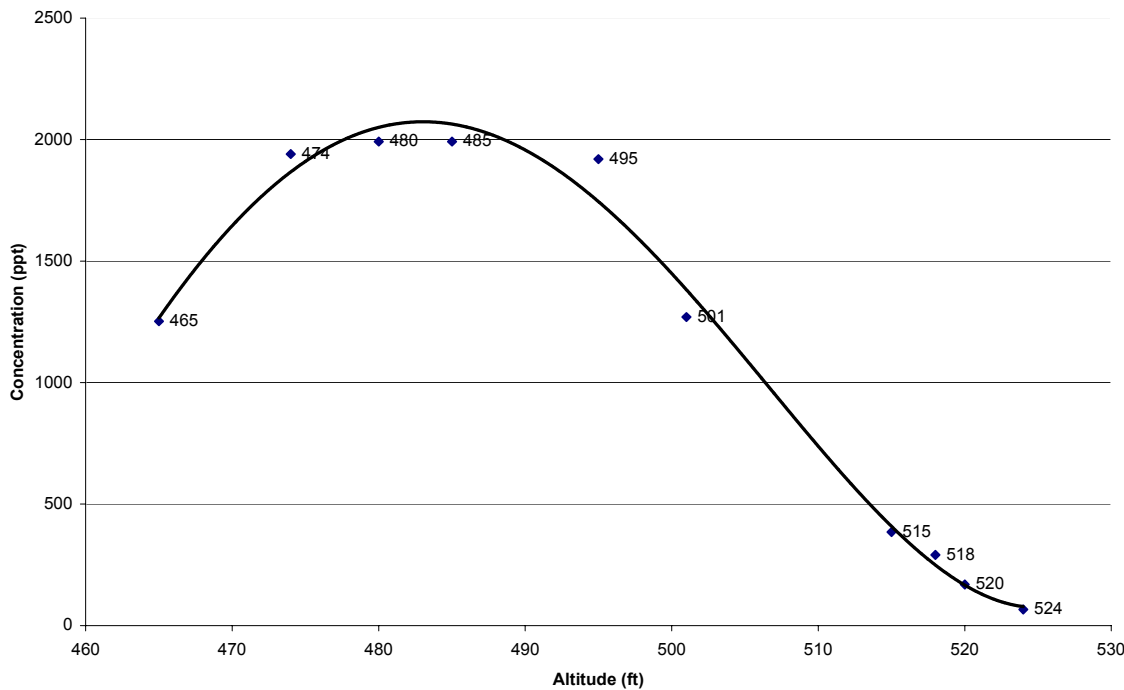
Flight 9, Peak 1 Gaussian Approximation**Flight 10, Peak 2 Gaussian Approximation**

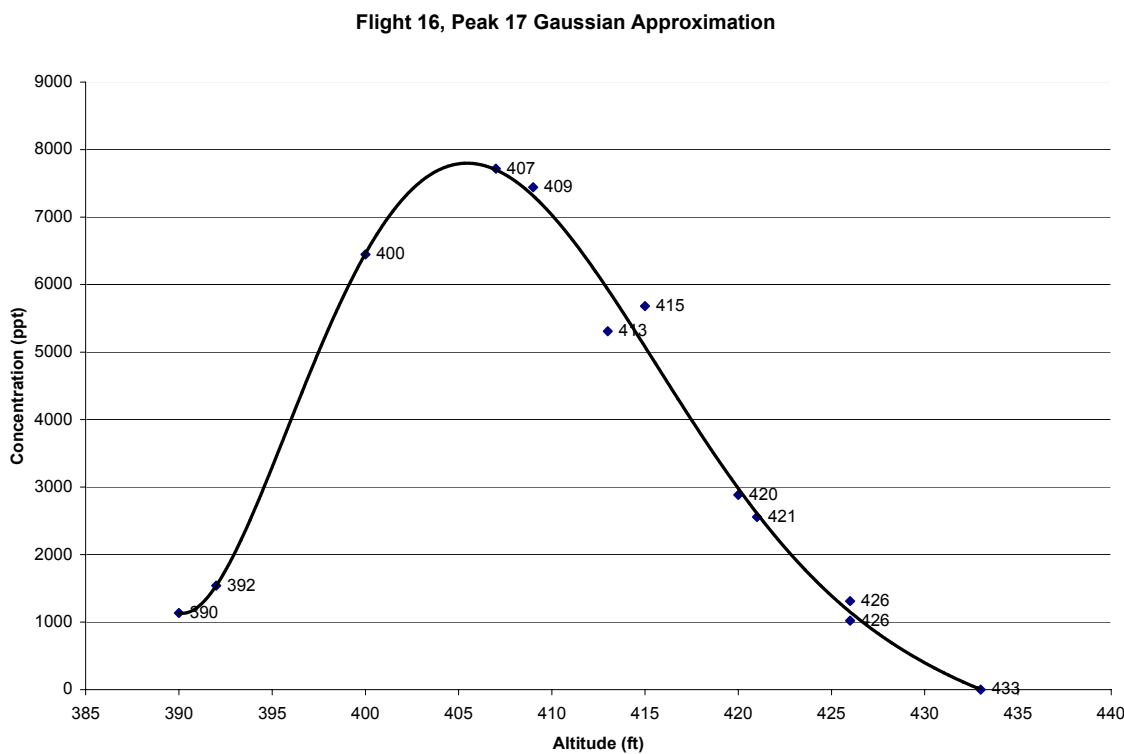
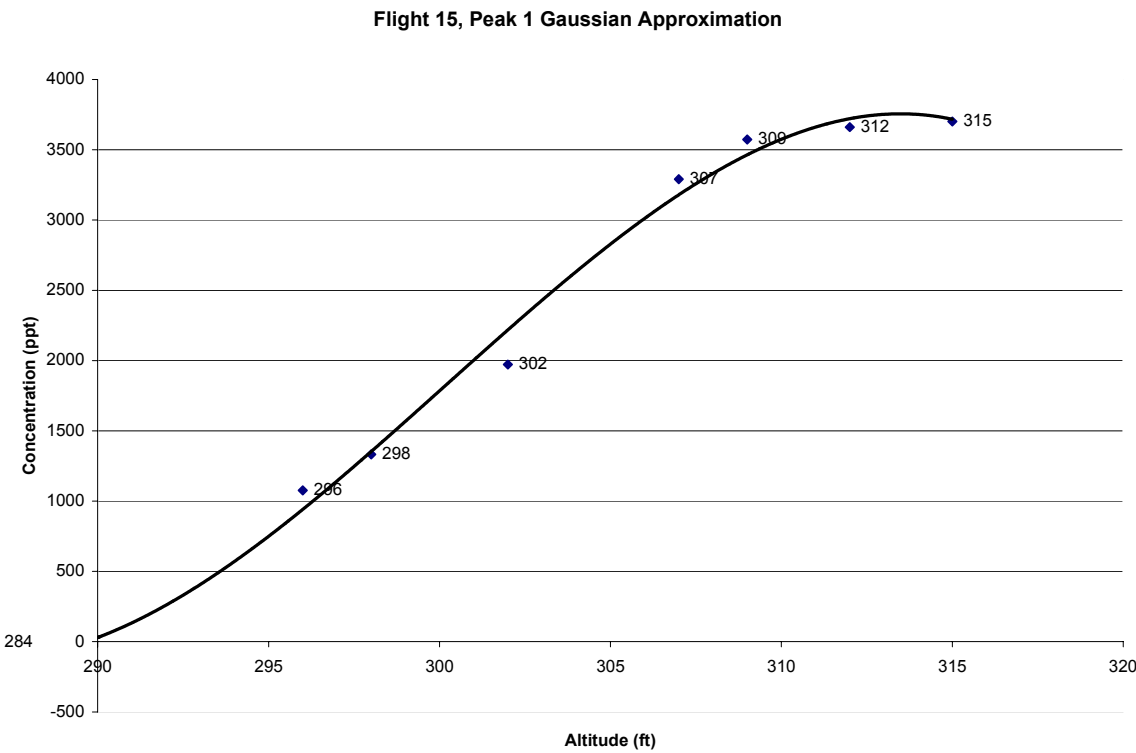
Flight 11, Peak 9 Gaussian Approximation**Flight 12, Peak 5 Gaussian Approximation**

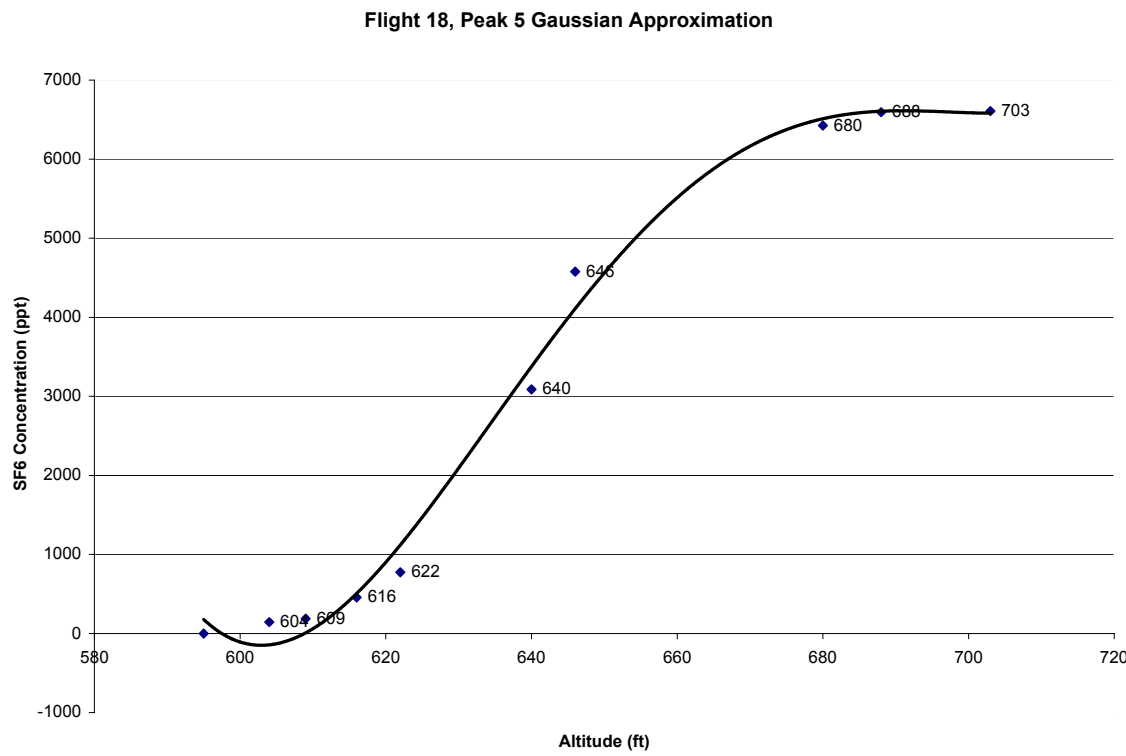
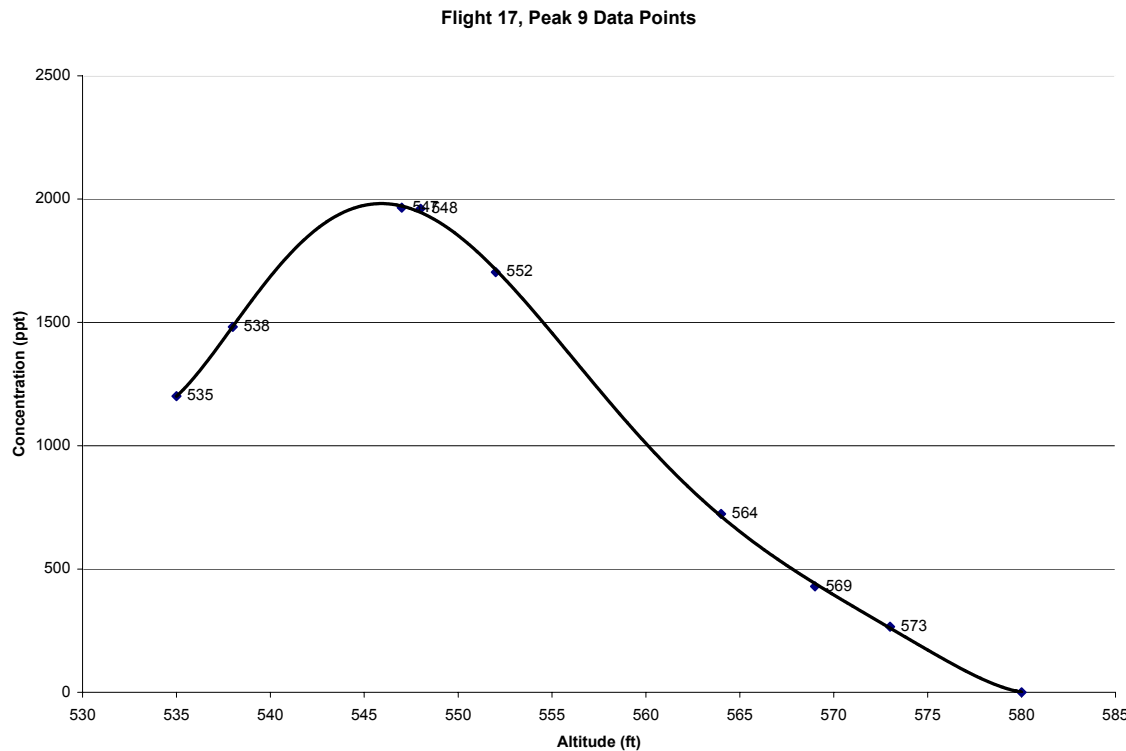
Flight 13, Peak 2 Gaussian Approximation

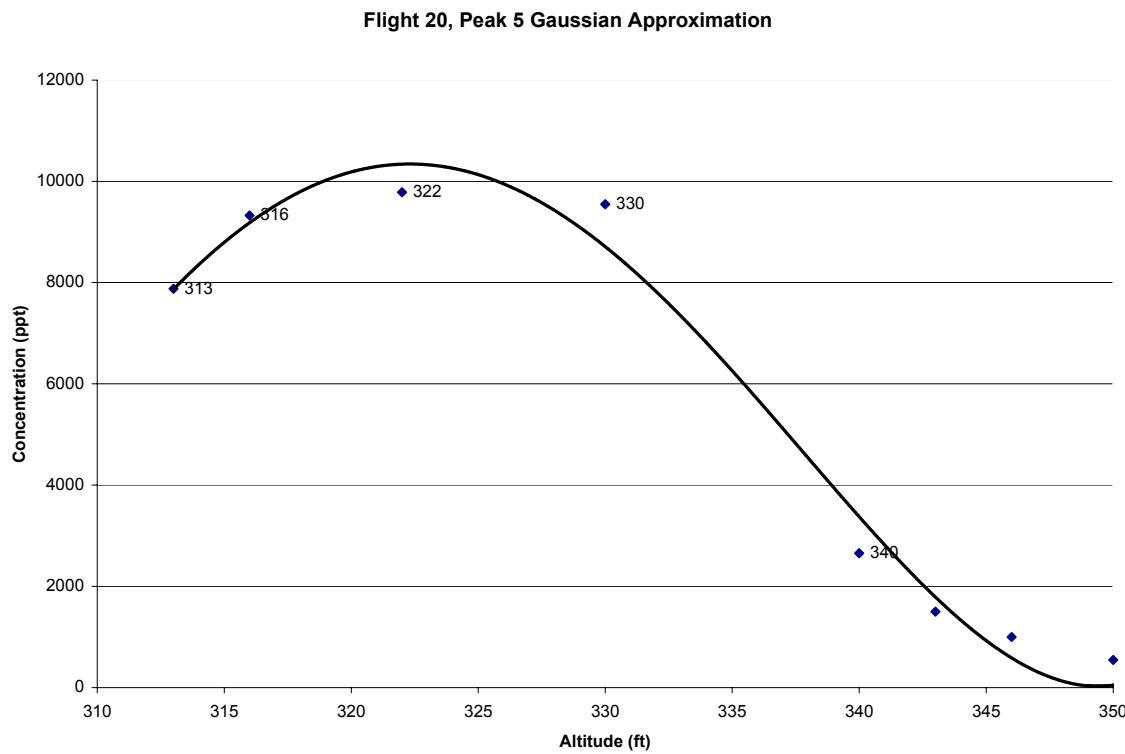
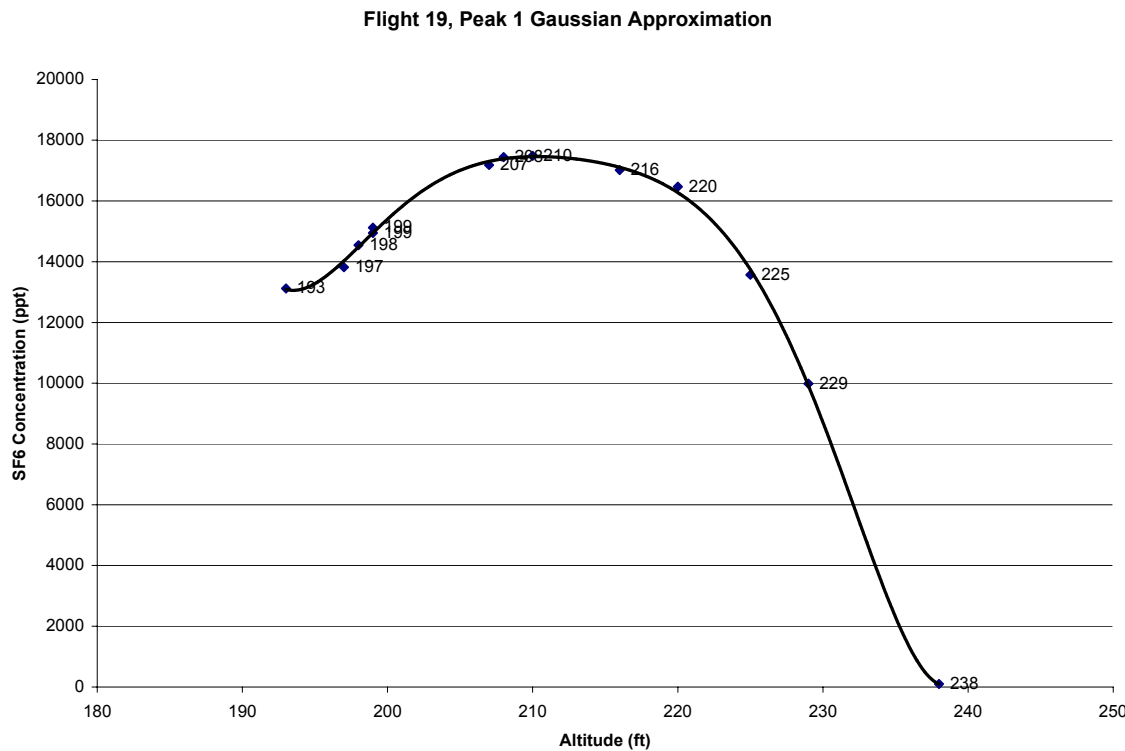


Flight 14, Peak 2 Gaussian Approximation

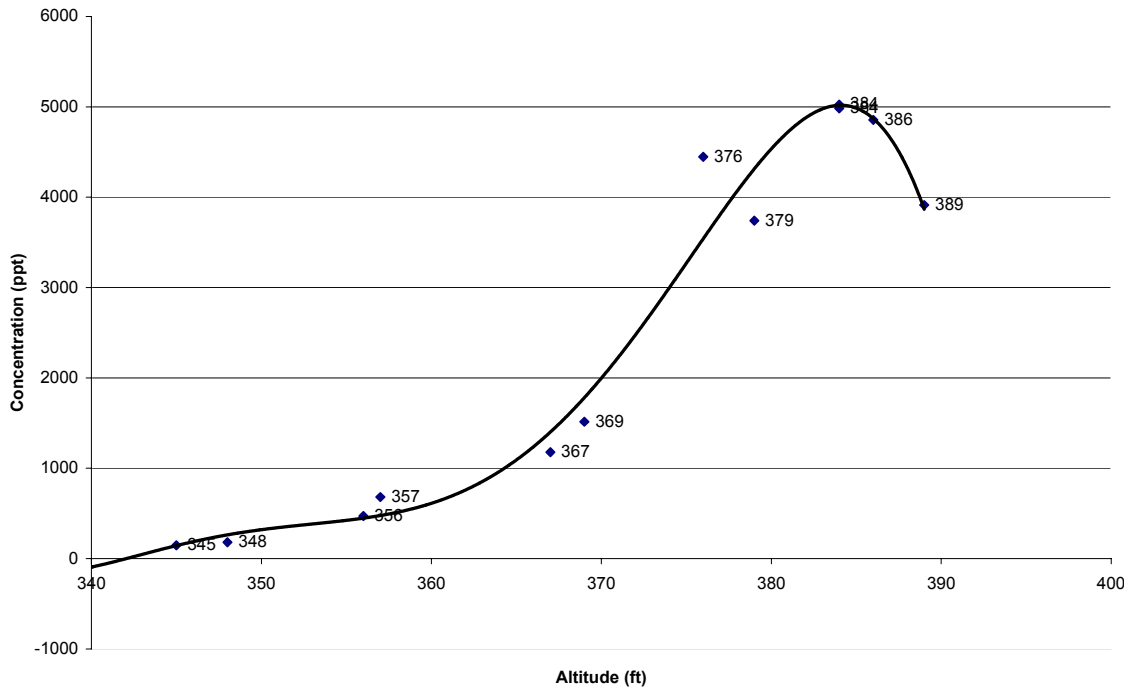




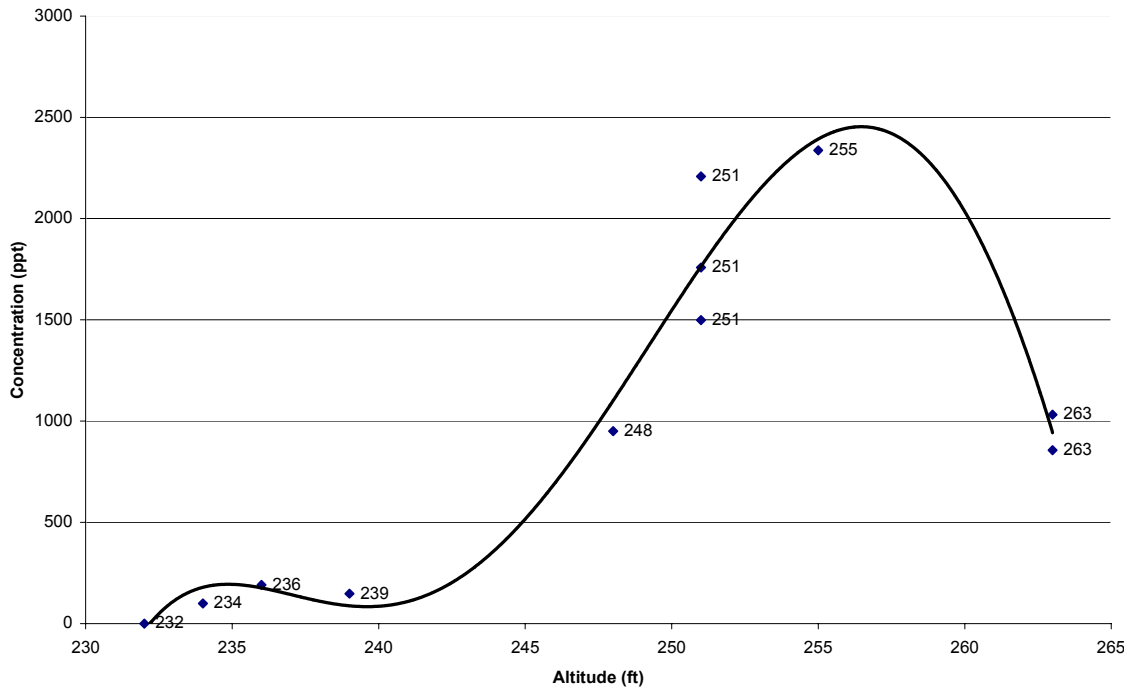


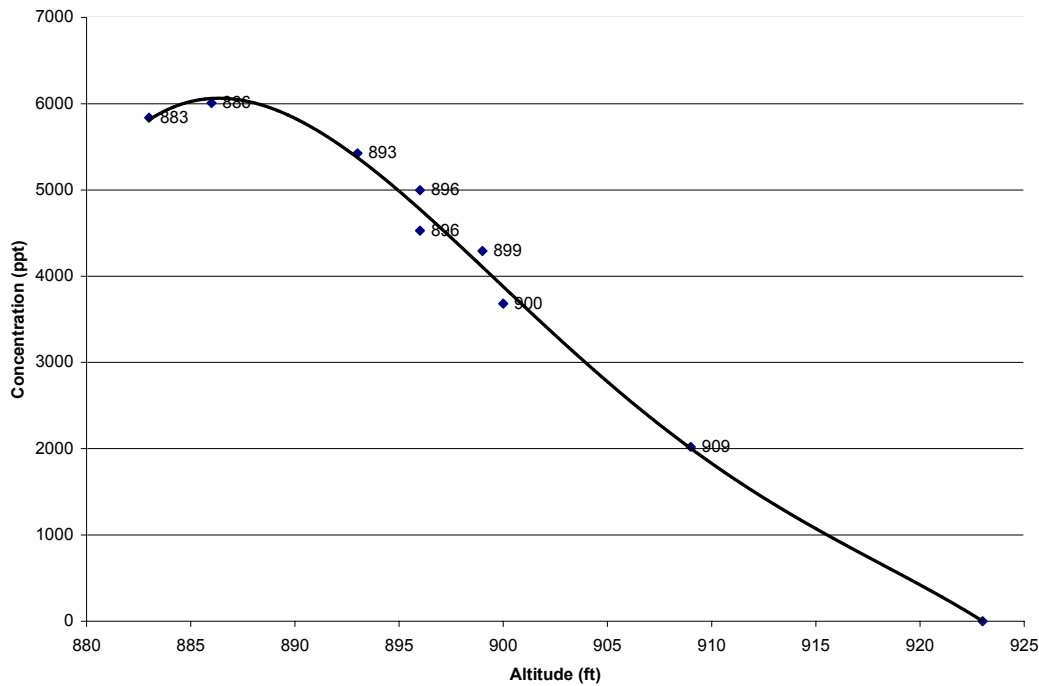
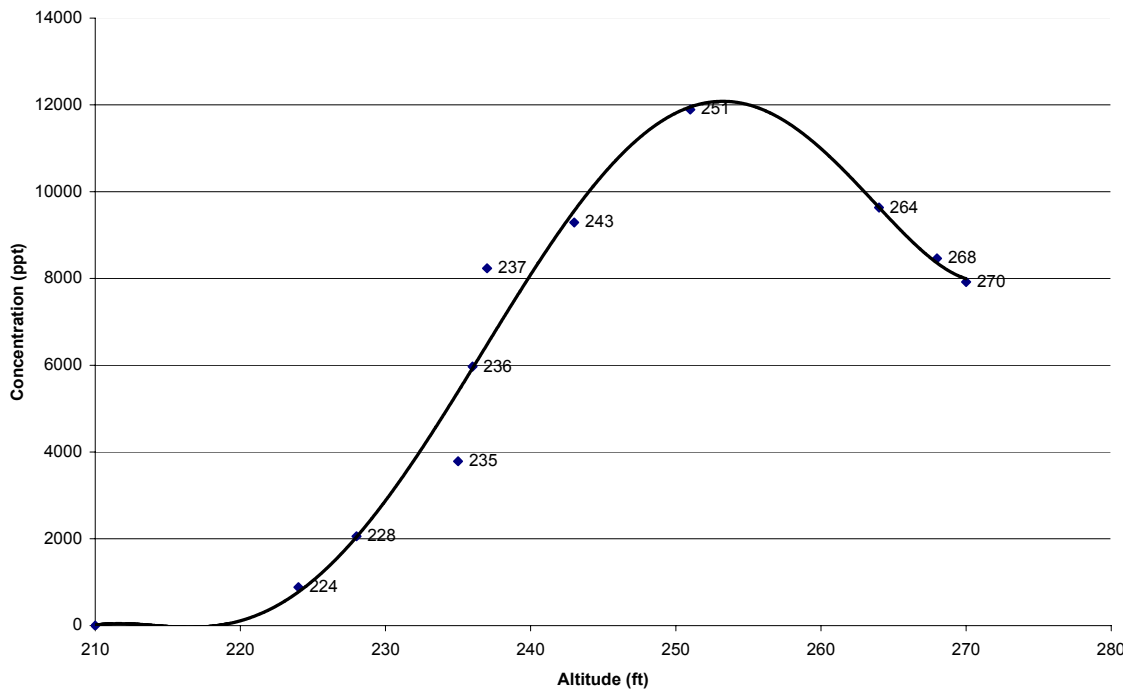


Flight 21, Peak 4 Gaussian Approximation

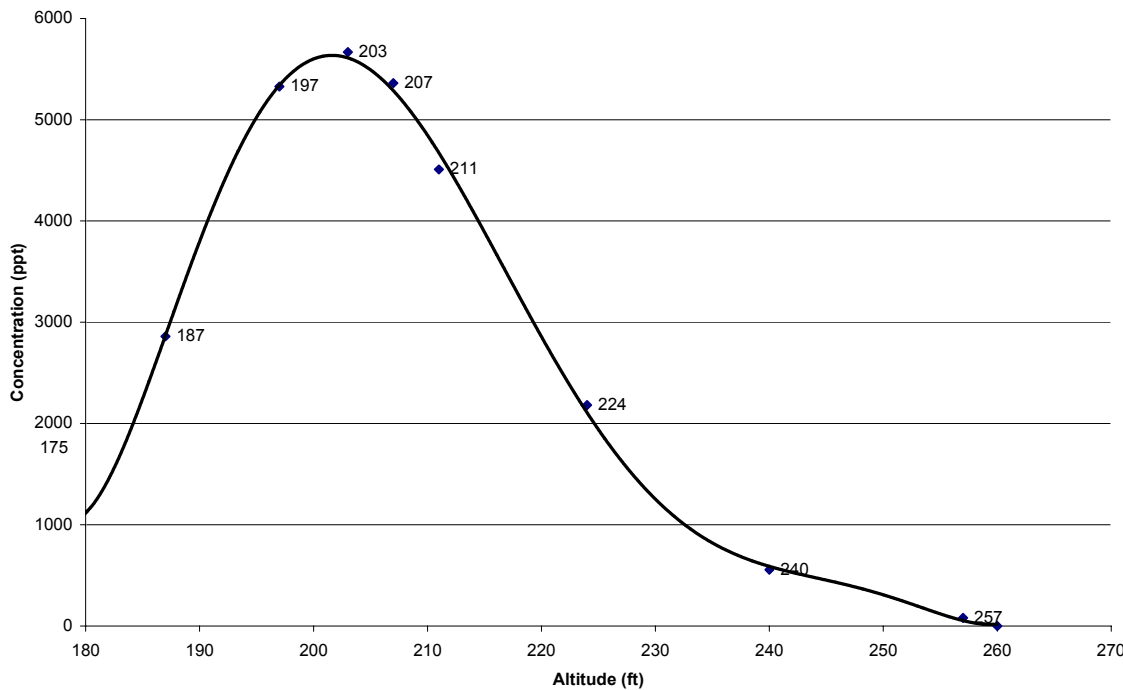


Flight 24, Peak 1 Gaussian Approximation



Flight 25, Peak 4 Gaussian Approximation**Flight 26, Peak 4 Gaussian Approximation**

Flight 27, Peak 1 Gaussian Approximation



Flight 28, Peak 3 Gaussian Approximation

